Studies on the biosynthesis of myxobacterial natural products

–

Untersuchung der Biosynthese myxobakterieller Naturstoffe

DISSERTATION

ZUR ERLANGUNG DES DOKTORS

DER NATURWISSENSCHAFTEN

(DR. RER. NAT.)

DER

NATURWISSENSCHAFTLICH-TECHNISCHEN FAKULTÄT

DER UNIVERSITÄT DES SAARLANDES

VON

ULLRICH SCHEID

SAARBRÜCKEN

2021

Tag des Kolloquiums:	24.03.2022
Dekan:	Prof. Dr. Jörn Walter
Berichterstatter:	Prof. Dr. Rolf Müller
	Prof. Dr. Andriy Luzhetskyy
Vorsitz:	Prof. Dr. Uli Kazmeier
Akad. Mitarbeiterin:	Dr. Angelika Ullrich

Danksagung

Eine Doktorarbeit ist ein langer Weg und manchmal länger als gedacht; dabei ist die Unterstützung derer, die einem helfen und einem lieb sind unersätzlich.

Ich danke meiner Familie, v.a. meinen Eltern, die mir bei allem Rückhalt geben und unterstützen, wo sie können.

Ganz herzlich bedanke ich mich bei Professor Rolf Müller, der mir diese interessanten Projekte in einer großartigen Arbeitsgruppe ermöglicht hat. Auch seine Unterstützung, Ratschläge und Planung rund um meine Projekte weiß ich noch immer sehr zu schätzen

Meinem Supervisor, Dr. Daniel Krug, danke ich herzlich für die Tipps und Hilfe in der Planung und Umsetzung meiner Projekte, sowie seine Unterstützung bei wissenschaftlichen Fragestellungen.

Vielen Dank meinen Kollegen und Freunden in der Gruppe MINS, die mich tatkräftig unterstützt und die mich an die Zeit im Labor stets mit viel Freude erinnern lassen. Besonderen Dank natürlich den Kollegen, die mich in die verschiedenen Bereiche eingearbeitet haben und immer unterstütz haben, ob MS oder NMR, Mikrobiologie, Molekularbiologie oder Proteinbiochemie, da ich davon einfach überhaupt keine Ahnung hatte.

Herzlichen Dank auch an meine Kollegen vom HZI in Braunschweig, Jutta Niggemann und Heinrich Steinmetz, die mir mit Rat und Tat rund um das Myxovalargin Projekt zur Seite gestanden haben. Weiterhin hat mir die Zusammenarbeit und der Austausch mit meinen Projektpartnern vom OCI Hannover (Franziska Gilles), HZI Braunschweig (u.a. Vinay Pawar) und Sanofi Aventis viel Freude bereitet und interessante Ergebnisse hervorgebracht.

Für ihre Unterstützung, Geduld und alles was sie mir gibt und was mich jeden Tag bei allem motiviert danke ich insbesondere meiner Frau Sandra.

Table of contents

Abbreviations

ACN	**acetonitrile**
ACL	**acyl CoA ligase**
ACP	**acyl carrier protein**
A (domain)	**adenylation (domain)**
AT	**acyl transferase**
C (domain)	**condensation (domain)**
cMT	**C- methyltransferase**
CoA	**coenzyme A**
DcL	**condensations domain incorporating D -amino acids**
DH	**dehydratase**
DMSO	**dimethyl sulfoxide**
DNA	**deoxyribonucleic acid**
E (domain)	**epimerization (domain)**
ECH	**enoyl CoA hydrolase**
ER	**enoyl reductase**
EtOH	**ethanol**
HPLC	**high performance liquid chromatography**
HZI	**Helmholtz centre for infection research**
IPTG	**isopropyl-*β*-D-thiogalactopyranosid**
KR	**ketoreductase**
KS	**ketosynthase**
LcL	**condensation domain incorporating L - amino acids**

MeOH	**methanol**
MIC	**minimal inhibitory concentration**
MRSA	**methicillin resistant *Staphylococcus aureus***
MS	**mass spectrometry**
NRPS	**non-ribosomal peptide synthetase**
NMR	**nuclear magnetic resonance**
nMT	**N-mehtyltransferase**
OCI	**Institute for organic chemistry, Hannover**
ORF	**open reading frame**
RNAP	**ribonucleic acid polymerase**
rRNA	**ribosomal ribonucleic acid**
PAGE	**polyacrylamide gel electrophoresis**
PCP	**peptidyl carrier protein**
PCR	**polymerase chain reaction**
PGFE	**pulsed field gel electrophoresis**
PKS	**polyketide synthase**
SDS	**sodium dodecyl sulphate**
TAM	**tyrosine aminomutase**
TE	**thioesterase**
VRSA	**Vancomycin resistant *Staphylococcus aureus***

Abstract

The myxovalargins are natural products from myxobacteria discovered in the course of activity-guided screening in the mid 1980´s, and rediscovered due to anti-biofilm activity. A cooperation project including the Helmholtz Institute for Pharmaceutical Research Saarland (HIPS), the HZI Braunschweig, the OCI Hannover and Sanofi Aventis funded by the Bundesministerium für Bildung und Forschung (BMBF) was issued to investigate this promising compound class in terms of bioactivity, biosynthesis and structural diversity. This thesis therefore includes the structure elucidation of derivatives including a revision of the myxovalargin A stereochemistry and improvment of production, derivatization and biosynthesis elucidation of the myxovalargins. In depth studies of the myxovalargin biosynthesis and genetic manipulation were enabled with focus on achieving a supply for further activity testing, generating and isolating a variety of natural and semisynthetic myxovalargins and developing tools to make derivatization possible according to future needs.

Exploring the myxovalargin-producing myxobacteria led to the identification of additional interesting biosynthesis clusters, which were investigated for their highlights in biosynthesis. Thereby, the phenyl pyruvate dehydrogenase complex was further investigated on its role in the myxobacterial compounds ripostatin, phenalamide and the hyafurone/ hyapyrone/ hyapyrrolidone compound classes.

Zusammenfassung

Die Myxovalargine sind Naturstoffe aus Myxobakterien und wurden im Zuge eines Aktivitätsscrennings Mitte der 80er Jahre identifiziert und schließlich aufgrund ihrer Wirksamkeit gegen Biofilme neu entdeckt. Ein Kooperationsprojekt zwischen dem Helmholtz Institut für Pharmazeutische Forschung im Saarland (HIPS), dem HZI Braunschweig, dem OCI Hannover und Sanofi Aventis gefördert vom Bundesministerium für Bildung und Forschung (BMBF) wurde aufgesetzt, um die vielversprechende Naturstoffklasse im Bezug auf ihre Bioaktivität, Biosynthese und Strukturvarianten zu untersuchen. Diese Doktorarbeit befasst sich mit der Strukturaufklärung der Derivate, einer Revision der Stereochemie des Myxovalargin A und der Verbesserung der Produktion, der Derivatisierung und der Aufklärung der Biosynthese des Myxovalargins. Vertiefende Untersuchungen der Biosynthese und die genetische Manipulation wurden untersucht, um die Durchführung von Bioaktivitätstests zu ermöglichen und die Produktion und Isolierung natürlicher und semisynthetischer Myxovalargine zu erreichen sowie Tools zu entwickeln, um eine Derivatisierung für zukünftige Verwendungszwecke zu ermöglichen.

Im Zuge der Untersuchung von Myxovalargin-Produzenten wurden weitere interessante Biosynthesecluster identifiziert. Hiervon wurde der Phenylpyruvat-Dehydrogenase Komplex auf seine Rolle in der Biosynthese der Myxobakteriellen Klassen der Ripostatine, Phenalamide und der Hyafurone/ Hyapyrone/ Hyapyrrolidone untersucht.

2. Introduction

2.1 Infectious diseases

For a long time infectious diseases have been the major cause of death in human populations.[1,2] Several milestones in research have developed medicine to a status in which a significant number of known infectious diseases can be cured and the pathogen eradicated or at least unharmed. Beside the description of hygiene as prophylaxis for childbed fever from Ignaz Semmelweis[3] and the vaccination[4], a major step forward in the fight against infectious diseases was the discovery of the antibiotics. A fundamental turning point was the identification of microorganisms as pathogens of tuberculosis by Robert Koch[5] supporting Louis Pasteurs theory of microorganisms as source of infectious diseases. The first identification of antibiotic effects of certain fungus goes back to the 19th century. In the early 20th century the introduction of the first synthetic antibiotic arsphenamin by Paul Ehrlich[6] and the description of Penicillin as antibiotic natural product from *Penicillium notatum* by Fleming, Florey and Chain[7] started the golden era of antibiotics, which put forth a vast list of antibiotics especially in the 1950s and 1960´s. (Figure 1) In this time a variety of antibiotics with different mode of actions was determined and brought to the market. Natural products were isolated and partially modified to semisynthetic compounds. On the other hand, fully synthetically derived antiobiotics were developed as potent antiinfectives.

Antibiotics are classified in groups with similar mode of action and range of antibiotic spectrum. Antibiotics can target several morphologic or biosynthetic characteristics which are only present in prokaryotes, but also ubiquitous structures in pro- and eukaryotes (Figure 2). From the 1960´s after the golden era of antibiotics a slack period with few new antibiotic classes discovered followed. Since the 90´s only some antibiotics with enhanced properties, but generated from known antibiotic classes were brought to the market.[8] Moreover, from the 60´s antibiotic therapy began to face an increasing problem with microbial resistance in the upcoming decades[9,10], however just in recent years the slow progress and arising antibiotic resistance arouse interest of public, media and politics.[11,12] Beside activities to reduce expansion of antibiotic resistance, the urgent need to drive antibiotic research and bring putative therapeutic compounds in clinical phase and finally on the pharmaceutical market has become a topic of political, economic and social importance.

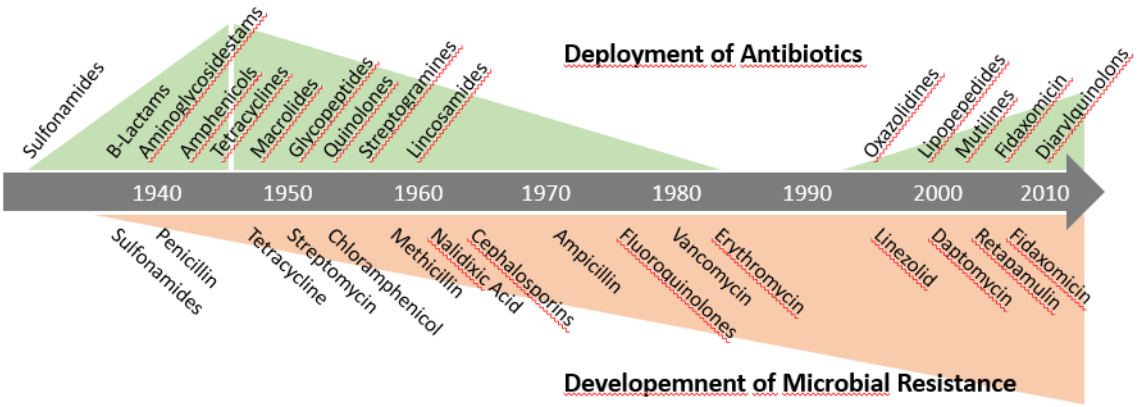

Figure 1: Schematic picture of deployment of antibiotic classes versus deployment of microbial resistance against active compounds

However, the environmental conditions for academic research and the economic benefit for pharmaceutical companies still requires improvement. The “Declaration by the Pharmaceutical, Biotechnology and Diagnostics Industries on Combating Antimicrobial Resistance” [13], aiming to develop alternative market structures and strategies for antibiotics, can be seen as a step forward to overcome such issues.

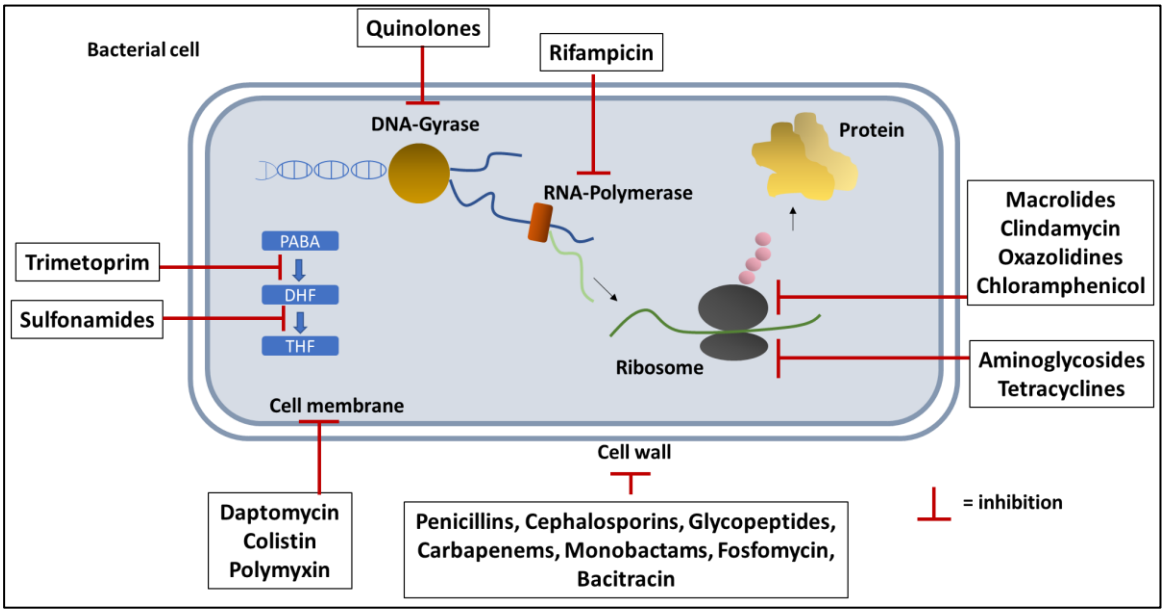

Figure 2: Mode of action of different marketed antibiotics in prokaryotic cells. Trimetoprim and Sulfonamides inhibit at different stages the folic acid metabolism (PABA = paminobenzoic acid, DHF dihydrofolic acid, THF = Tetrahydrofolic acid), while the *β*-lactams and others inhibit cell wall synthesis. Gyrase inhibitors like the quionolones hinder nucleic acid transkription, which in a later step leads to protein synthesis. The protein biosynthesis at the translation level is tackled by inhibitors like macrolides and aminoglycosides inhibiting the ribosome.

2.2 Anti-infectives Resistance

An emerging problem of pathogenic bacteria is the development of resistance against anti-infectives.[14,15] This resistance of bacterial cells can be caused by a naturally missing target like the peptiodglycan only present in gram positive bacteria, which is targeted by most *β*-lactams, or by different forms of adaption to the exposure of anti-infectives and antiseptics. Resistance mechanisms can be modifications of targets in the chemical structure, efflux pumps, alternative biochemical pathways or defusing the drug by metabolization.[16] The development of resistance is a statistical probability, when organisms need to adapt to survive or evolve in a certain environment.

Hence, the appearance of insensitivity is linked to the extensive use of antibiotics. Different factors of excessive or irrational use of antibiotics promote bacterial adaptation to antibiotics. Causes can be found in agricultural overuse for economic reasons as well as a lack of knowledge

or undifferentiated use in human and veterinary medicine. Though in recent times, regulations in these fields try to overcome this problem, a loss of activity against different pathogens and/or diseases has led to an urgent need for the therapy of multiresistant bacteria.

Even reserve antibiotics like the glycopeptide Vancomycin for the treatment of pathogens, as the Methicillin resistant *Staphylococcus aureus* (MRSA) have already led to the development of Vancomycin resistant staphylococcus aureus (VRSA).

Different approaches are already used in the pharmaceutical treatment to diminish the resistance development. A well-known example is the combination of different active pharmaceutical ingredients. A treatment with different antibiotics targeting different targets in the bacterium diminishes the occurrence of resistances.[17] An example is the fix combination of sulfamethoxazole and trimetroprim, named cotrimoxazol. Two antibiotics, which target different enzymes in the folic acid metabolism, thus having a synergistic effect (Figure 2). Combinations of treatments with different antibiotics targeting different pathways can be an indicated approach to tackle different stages of bacterial development and/or to overcome formation of antibiotic resistance. An example of a sophisticated treatment scheme is the standard therapy of tuberculosis, which consists of a combination of isoniazid, rifampicin, ethambutol and pyrazinamide. Also, the therapy with an antibiotic and a non-antibiotic compound has brought an established administration. The *β*-lactamase inhibitors like clavulanic acid and sulbactam are not antibiotics by themselves, but inhibit the *β* –lactamase. By that the *β*-lactam antibiotics like amoxicillin, which have a high potential of resistance development can be efficiently used.[18] For certain applications a broader approach is used, which does not only attack the bacterium itself, but changes the environmental conditions to hinder the bacterial comfort zone and thus enhance therapy. This approach is used for example in the *Helicobacter pylori* eradication therapy,[19] which includes in the triple therapy of three potent antibiotics a proton pump inhibitor to reduce the acidic conditions in the stomach or in the quadruple therapy the proton pump inhibitor and bismuth salts. Though refined pharmaceutical combinations of marketed chemotherapeutics is a practical approach to e.g. reduce resistance development, but also to reduce side effects by dose reduction, the arising of resistance and persistence of certain pathogens cannot be solved by the registered antiinfectives. The continuous research and development of new chemical and biological entities has to be pursed to keep on track in the often proclaimed infectious arms race.[14]

2.3 Biofilms

A chapter of antibiotic resistance and persistence, which raises increasing interest in the fight against infectious diseases is antibiotic insensitivity occurring because of bacteria forming biofilms. In contrast to planktonic cells, targeting bacteria in biofilms is often less efficient, thus drugs tested active against planktonic cells may fail in therapy of biofilms.[20,21] Such colonization can generate problems either in technical applications by clotting e.g. pipes or tubes, but also in human and veterinary medicine by colonizing tissue as organs and wounds[22] or medical devices as for example implants or stents.[23]

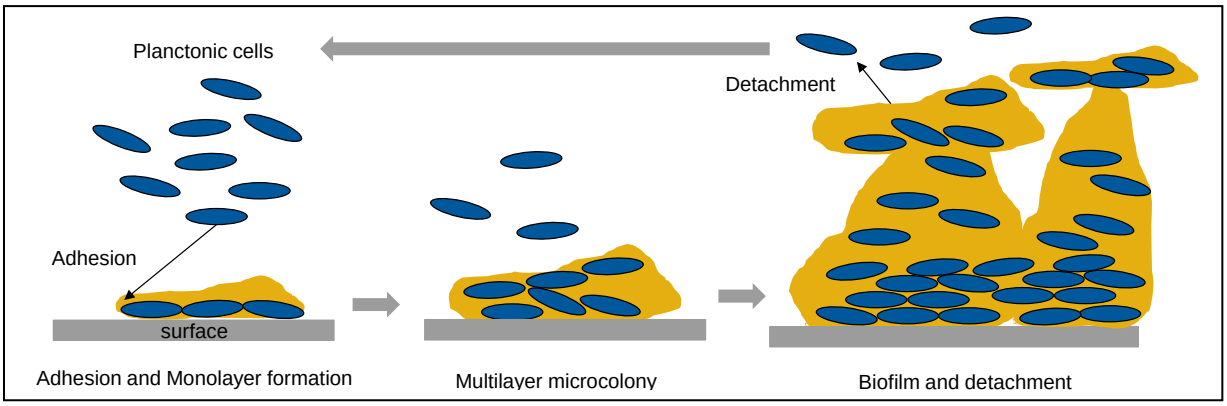

Figure 3: Biofilm formation of microorganisms. Cells attach to surfaces and start building a monolayer and an extracellular matrix of polysaccharides, proteins and nucleic acids. Signalling molecules promote adhesion of additional cells to form multilayer microcolonies. By further cell adhesion and expansion of the extracellular matrix a biofilm is formed. By detachment the cells proceed to planktonic cells again.

A biofilm consists of an accumulation of microorganisms embedded in a self-produced polymer matrix of polysaccharides, proteins, and deoxyribonucleic acid (DNA).[24] The specific reason for bacterial resistance in biofilms is not finally elucidated, but it might be an issue of different factors, including hindering penetration of the intercellular matrix for anti-infectives and functional metabolic transformation of cells inside the biofilm. When single cells start to attach to a surface, they start excreting small molecules, which induce the formation of bacterial cell layers. Beside attachment of further cells, a matrix is formed embedding the cells of the bacterial multilayer. Cells from the mature colony can go back to the planktonic growth. These coatings contain polysaccharides and other macromolecules and might hinder drug components to reach cells enclosed in the biofilm matrix. Furthermore, cells in different layers might have different metabolic functions or decrease their growth and cellular functions, which leads to a loss of

targets for several antibiotic agents, which attack preferentially proliferating cells or cells with high metabolic throughput. The signalling mechanisms for cell to cell communication are investigated and partially unravelled for several bacteria including potent pathogens like *Pseudomonas aeruginosa*.[25] This communication is called Quorum sensing and exhibits an interesting target for inhibition of biofilm formation or other pharmaceutical purposes.[26,27] Nevertheless, the disruption of biofilms as a major aim in antiinfective therapy has not yet been accomplished successfully.

Biofilm disruption may be a promising target to enhance endogenic immune defense mechanisms, but also synergistic use with antibiotics which are potent against planktonic bacterial cells can be feasible.[28] Thus, applications as single drug therapy of biofilm disrupting compounds seems reasonable, but also the combinatorial use to reduce the amount of required single components might be a putative option, thus reducing side effects of other drugs. Furthermore, embedding such agents in matrices of medicinal products or other materials might hinder the formation of biofilms with its variety of technical and medicinal problems.

2.4 Natural products

The term natural products is used for organic molecules of eukaryotic and procaryotic descent, such as bacteria, archeae, plants, fungi, but also animals. Natural products are used in a wide range of pharmaceutical as well as industrial purposes. Besides the role in the field of antiinfectives, they are e.g. used for anti-inflammatory, cardio vascular, analgetic and oncologic purpose. [29,30]

The importance of natural products in antibiotic research has been widely discussed.[31,32] The superior number of natural products and derived drugs in the field of antibiotics demonstrate their dominant role in this therapeutic field.[33,34] Among the main groups of antibiotics only one group is represented solely by synthetic compounds, these are the qhinolones. Nevertheless, their target, the gyrase, can also be tackled by a number of secondary metabolites including those of myxobacterial origin [35,36]. Efforts in driving natural products to pharmaceutical drugs has declined for several years. In this time the focus was set on synthetic small molecules or antibiotic research was neglected at all. The arising need for new chemical entities and the

search for new targets for antiinfective mechanisms to overcome the spreading of resistant pathogens has drawn the focus again on the promising, but tedious research in natural products.

The economic disadvantage of research-intensive natural product discovery, leading in best cases to pharmaceutics, which are used as reserve antibiotics, has become a political issue. The social and political awareness has been sensitized in recent years for this ongoing problem. But still, the conditions to drive science and economic viability needs to be further improved, as research for antibiotics is costly, tedious and long-term commitments[37,38].

Molecules of natural origin were designed evolutionary over billions of years and thereby offer chemistry and complexity, which is optimized to specific targets in organisms and can rarely be covered by synthetic molecules. Figure 4 highlights the chemical variety and complexity of natural products assembled by different bacterial secondary metabolite producers. Several of these intriguing molecules are in therapeutic use since several decades, others are still part of current research for potential anti-infectives.

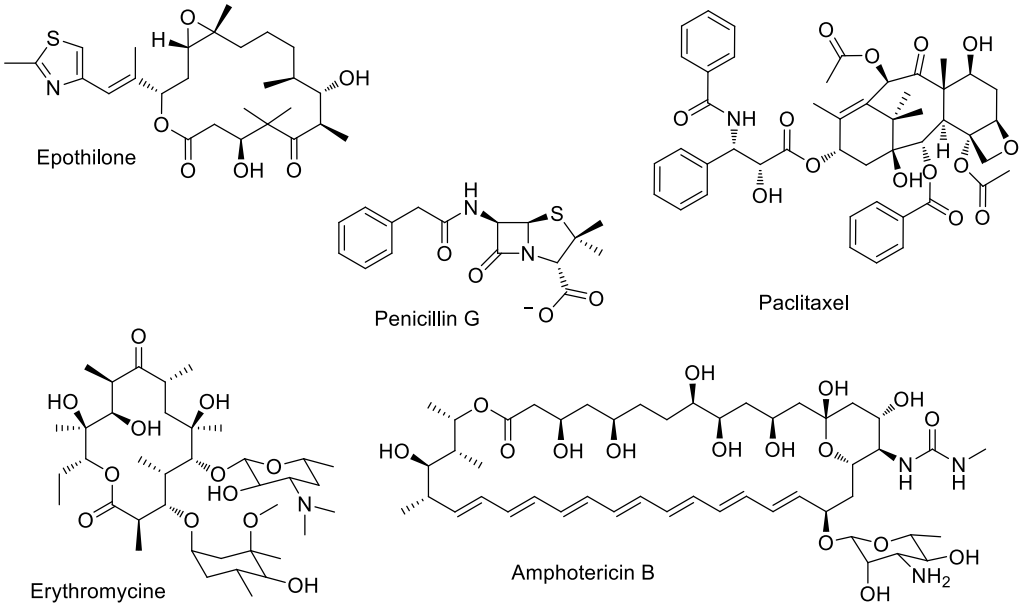

Figure 4: Diversity of chemotherapeutic natural products produced as secondary metabolites from different organisms. A variety of natural products is found in the field of antibiotics as e.g. Penicillin G or the macrolide erythromycin. Other antiinfectives like the polyketide fungicide amphotericin B are also natural products. The myxobacterial compound epothilone is registered as cytostatic and exhibits an analogous mode of action as Paclitaxel from the plant *Taxus* species.

However, they were commonly not designed by evolution to be used as drugs in humans and to target pathogens inside the human body. Therefore, a lot of compounds lack essential physicochemical and pharmacological properties for pharmaceutical use such as low cytotoxicity, stability, solubility in specific solvents, not to mention oral bioavailability. This does however not diminish the role of natural products as lead structures for antibiotic molecules [31,39–41]. The possibility for exploiting an established compound or target system will offer a variety of opportunities in drug design and understanding of biochemical processes. Thus, result two major aims of pharmaceutical purpose in the screening of natural products in the field of antiinfectives: Finding lead structures and identifying unknown modes of action.

The most prominent example for exploitation of lead structures are the *β*-lactams. The *β*-lactam ring as central pharmacophore has been widely adapted to yield a variety of pharmaceutical and physicochemical effects. Different generations of *β*-lactams were classified by their extended antibiotic spectrum and chemical properties.[42] Penicillins, Cephalosporins, Carbapenems and Monobactam offer a wide variety of applications and represent standard therapy for several infectious diseases. Beside the antibiotically active *β*-lactams the *β*-lactam inhibitors were designed corresponding to this core lead structure to overcome the hydrolytic resistance mechanism of the *β*-lactamases.

Identifying new modes of action is another major aim of natural product research. The evolutionary adaption to their habitat stimulated bacteria to evolve compounds aiming at

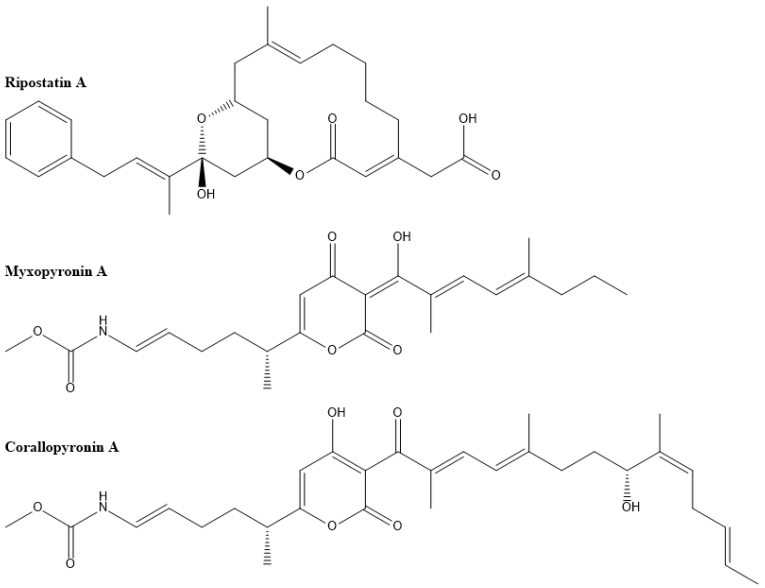

different organisms and targets. An example for recently identified targets is the switch region of RNA-polymerases.[43] While Rifamycin, a first line therapy antibiotic for tuberculosis, binds to the Rifamycin binding region [44], several natural products were identified to bind to the alternative switch region of RNA polymerase.[45] Compounds targeting the switch region are almost exclusively of myxobacterial origin: the corallopyronins, myxopyronins and ripostatins.[46] (Figure 5)

2.5 Secondary metabolite biosynthesis by multimodular enzyme complexes

Natural products with antibacterial activity are usually produced as secondary metabolites. There are several mechanisms known for the production of secondary metabolites in bacteria, fungi and plants. Two intensively studied, yet still in many cases not fully elucidated pathways are the polyketide synthase and the non-ribosomal peptide synthetase. Both pathways comprise a multienzyme complex, in which several enzymes of conserved function are grouped in multimodular, so called, "assembly lines".[47,48] The sum of all genes, which are required to enable production of a natural compound including the "assembly line" as well as genes required for synthesis of incorporated building blocks or enzymes for post-assembly modifications are called biosynthesis gene cluster (BCG).

In principle each module is responsible for the incorporation of a building block into a growing molecule, though of course there are numerous exceptions to the rule. Polyketide synthases use small carboxylic acid building blocks to form polyketide chains, while non-ribosomal peptide synthetases can couple, in contrast to ribosomal peptide synthetases, proteinogenic and non-proteinogenic amino acids into polypeptide chains.[49] In recent years a growing number of hybrid clusters of PKS and NRPS modules were identified and published, combining elements of both pathways, thus resulting in molecules which can harbour chains or single moieties of each production line. During the assembly process the growing molecule is attached via a thioester to a carrier protein while different reactions are performed on the intermediate. The assembled molecule is released after reaching the final module by different mechanisms. A general way is the cleavage of the thioester by a thioesterase as terminal domain. Nevertheless, a variety of different mechanisms is known, which lead to a dissociation of the thioester, like

an intramolecular cyclization or a combined condensation and termination. [50,51] The occurrence of unusual building blocks in natural products is a common motif, which is caused by modifications of structural elements. These mechanisms can occur before, during or after the assembly process. Building blocks can be derived by cluster specific enzymes or as intermediates from primary metabolism. On the other hand, the growing molecule can be modified while tethered to a carrier protein on the assembly line.[52] Specific domains of known functions, but also functionally altered domains can catalyse these reactions. Lastly, a molecule can also be modified after being released from the assembly line. This allows the formation of specific non proteinogenic amino acids and unusual polyketide moieties and is an essential reason of the structural diversity of secondary metabolites from bacteria. Furthermore, it also results in the occurrence of closely related molecules of the same compound class. Incomplete modification, incorporation of closely related building blocks and derivatization caused by environmental or conditions during the purification process can lead to the presence of a variety of structurally related compounds, which can be grouped as a compound class. [53]

Assembly lines can be encoded from short gene clusters like the myxochelin cluster[54] to large BCG (58 kbp) encoding multienzyme complexes like the Myxovalargin NRPS. In recent years, it became possible to annotate whole genomes including detailed information of gene clusters and related open reading frames (ORF) by combining tools with basic sequence alignment and protein identification algorithms for coding sequences and those identifying specific NRPS and PKS properties [55–57]. Thus a variety of bioinformatic tools has been established to specifically highlight domains and characterize their functionality, substrate specificity or further properties.[58,59] Software like Antismash combines a variety of different prediction instruments and has facilitated the identification of NRPS and PKS cluster from whole genomes.[60] As technique to further refine these approaches on the biochemical characteristics and secondary metabolite potency of myxobacteria, e.g. the Microbial Natural Products group of HIPS combines these in silico predictions with laboratory data of biochemical, microbiological and chemical aspects of the target organism and its compounds in the in-house database: myxobase.[61] Furthermore we connect these data with cluster information acquired from annotated myxobacterial biosynthesis pathways, harmonized by a comparative NRPS/ PKS specific annotation program, BiosynML, which in the end offers a direct comparison of cluster and associated information from different myxobacterial genomes to simplify the identification of related cluster and cluster elements. The recent progress and the productivity in elucidation

of secondary metabolite biosynthesis has led to an increasing number of clusters identified and published every year. To harmonize scientific publications and enhance use and benefit for the natural product community a consolidated approach for nomenclature and minimal information of a biosynthesis cluster has been elaborated by an international consortium of scientists.[62]

Beside the above mentioned mechanisms there are several other important pathway types known, for example for lantibiotics [63,64] and bacteriocins[65] in bacteria or terpenoids[66,67] and alkaloids[68] in plants, just to mention a few, but they will not be covered in this work.

In the following the focus is laid on NRPS and the different types of PKS.

2.6 Secondary metabolites – Non-ribosomal peptide synthetase (NRPS)

A major secondary metabolite producing protein assembly line is the non-ribosomal peptide synthetase (NRPS). In contrast to the ribosome, which is responsible for protein biosynthesis, the NRPS is able to condensate not just proteinogenic, but also non-proteinogenic amino acids to form a polypeptide. In order to achieve this, an NRPS consists of a several modules, each responsible for the incorporation of a single amino acid derivative into the growing molecule. The basic elongation step consists of activation and condensation of the new building block with the previously assembled molecule (Figure 6). For this, the non-ribosomal peptide synthetase needs the basic organization of condensation domain (C), adenylation domain (A) and peptide carrier protein (PCP). The adenylation domain activates the amino acids to an adenylate; amid bond formation is performed by the condensation domain, by which the molecule is beeing transferred from the previous PCP domain to the following PCP domain under covalent thioester formation. The substrate of the elongation process is chosen by the adenylation domain. Core motifs of these enzymes indicate building block selectivity for activation of a certain amino acids, which enables the in silico prediction of substrate specificity for an A domain [55,69,70]. Furthermore, condensation domain core motifs allow to distinguish between condensation domains with specificity to linking L-amino acid to the growing polypeptide chain (LcL) and those binding D amino acids (DcL). [71] Bioinformatic tools like the NRPS predictor 2 align the sequence of a domain of interest with known motifs at essential positions in characterized domains and thereby can predict the putative substrate of the adenylation domain. Still, it could be shown that a certain degree of substrate promiscuity of A

domains in many cases facilitates incorporation of chemically similar building blocks [72–75]. Furthermore, prediction limitations can lead to vague statements, which might not always coincide with the building blocks as found in the real molecule. Therefore, it is not yet possible to make structure predictions solely by in-silico analysis and it is necessary to further improve the foundation for comparability by assigning new biosynthesis pathways to know structures.

It exists a known set of additional domains in NRPS pathways, which can catalyse modifications during the assembly process. These domains are named by the reaction they catalyse; some important domains are epimerization domains (E), which convert L-amino acids into D-amino acids, oxidases (Ox) and reductases (Red), which promote the respective modification and can also be found as terminal domains; furthermore cyclases (Cy), which lead to cyclizations of parts of an assembled compound or the whole molecule, methyltransferase (MT), which can be divided into N-methyltransferases and C-methyltransferases, halogenase (Hal) and acyl-CoA ligase (ACL), which are often responsible for the activation of the starter molecule [76] are described elements of the NRPS assembly lines. A variety of different compounds can be obtained as the molecules are not limited to the proteinogenic amino acids, but are products of an increasing set of building blocks of various biosynthetic modifications. Promiscuity of catalysing enzymes, lacking of required precursors or other factors during biosynthesis usually lead to the observation of compound classes. Compound classes of

secondary metabolites are closely related compounds which are biosynthetic by-products or degradation products.

Figure 6: Elongation of a peptide chain by non-ribosomal peptide synthetase (NRPS). The adenylation domain (A) catalyzes the activation of a building block by binding adenosine triphosphate (ATP) to form

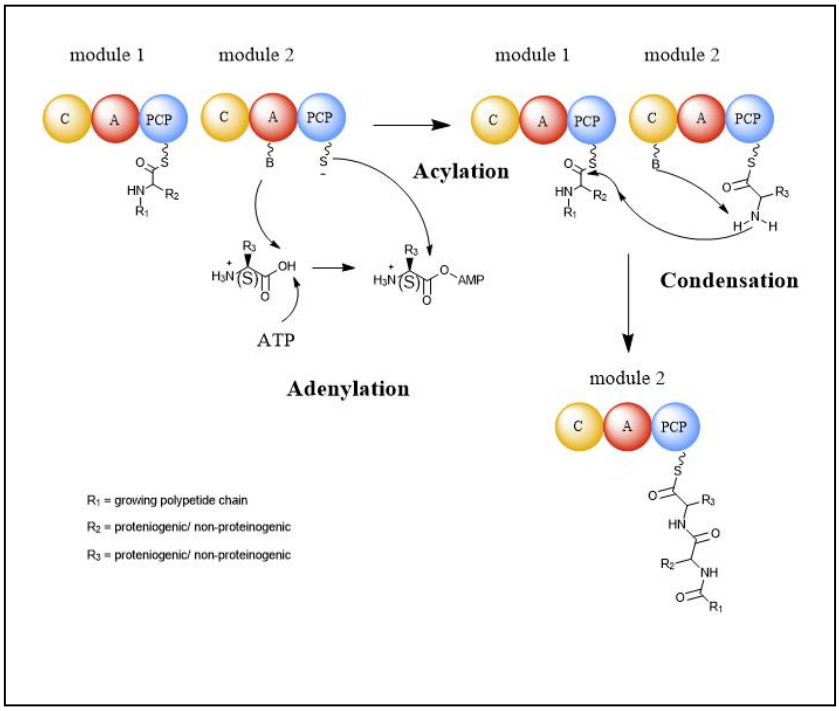

an activated aminoacid with adenosine monophosphate (AMP). The peptide carrier protein (PCP) binds the activated peptide as thioester (Acylation). Subsequently, the condensation domain (C) deprotonates the amino group of the building block, thus enabling the condensation of the aminoacid with the polypeptide chain.

2.7 Secondary metabolites - Polyketide Synthases (PKS)

A second major biosynthetic machinery for the production of antibiotic secondary metabolites is the polyketide synthase (PKS). PKS are the biosynthetic source of a variety of the most important natural products for antibiotic use like erythromycin[77], tetracycline[78] and also the myxobacterial anti tumor class of the epothilones.[79]

The PKS can be divided in three different classes: type-I, type-II and type-III PKS. The basic principle of PKS is comparable to that of the non-ribosomal peptide synthetase (NRPS). Single building blocks are conjugated to form complex molecules. While type I PKS show a comparable multimodular architecture as NRPS, there are PKS which follow a colinearity rule

with non-iterative module organization, but also assembly lines with iterative use of single modules. [80] Type II PKS consist of protein aggregates, which catalyse several iterative elongation steps to yield the final molecule.[81] A third type of PKS lack the acyl carrier protein (ACP) domains, which bind the intermediate during elongation in type I and type II PKS.[82,83] This chapter will focus on type-I PKS, which are commonly found in bacterial secondary metabolite producers. Domains with distinct functions are grouped into assembly lines, which can functionally be separated into modules. Each module can facilitate the incorporation of a building block into the growing polyketide chain. However, the domains in polyketide systems follow a different logic than those in NRPS. Moreover, the polyketide synthases reveal a variety of chemical moieties and structures, which cannot be easily explained by the basic architecture of domains and the predictable elongation steps. In depth domain in vivo and in vitro analysis has increased understanding of certain mechanism but nevertheless, constantly there are new polyketide synthase discovered, which still raise questions on the biosynthesis of the respective natural product.[84,85]

Similar to the NRPS modules, the basic architecture in PKS modules consists of three domains catalysing activation and selection of the substrate, condensation of the substrate with the growing molecule and a carrier protein which binds the intermediate by a thioester. (Figure 7) The acyltransferase (AT) domain selects the particular building block to be incorporated. Acyl-CoA extender units are the chemical precursor, which are selected and activated by the AT domain. The acyl moiety is then covalently bound by a thioester to the acyl carrier protein (ACP) domain at a swinging phosphopantetheinyl arm. The *β*-ketoacylsynthase (KS) domain then catalyzes the conjugation with the intermediate molecule bound to the upstream ACP domain. Interestingly, it was shown by cryo-microscopy that two entrances to the KS domain facilitate that the correct extender unit is channelled from the catalytic chamber while the intermediate accesses from a second entrance, thus ensuring correct elongation.[86] Condensation is catalysed by a decarboxylative claisen reaction resulting in a *β*-ketoester. Three additional domains can further reduce the *β*-keto group. A ketoreductase domain (KR) protonates to a hydroxyester.[87,88] Consecutively a dehydratase (DH) domain can dehydrate the hydroxyl moiety leading to a α,β-double bond[89]. Finally, an enoyl reductase (ER) domain can reduce to the saturated alkane. This process is a stepwise reduction, which requires the three domains in the depicted order. However, if for example the DH domain is not present, the reduction is only performed to the hydroxyester, accordingly a missing ER domain leads to an enoyl residue.

However, cases have been observed, where domains are present, but reaction stops at a certain intermediate, those domains are then marked as putatively inactive. Correspondingly modules were observed, which lack one of these domains, but the final structure implies, that the reductive step is performed. In those cases, it is assumed that domains of other modules might substitute in this position.

A special form of PKS, which does not show the basic module arrangement of AT-KS-ACP are trans-AT clusters.[90] Those clusters have been observed to lack the integrated AT domains in several modules of an assembly line. However, those gene clusters encode AT domains closely to the PKS genes, which act in trans position as AT domain for the respective module. These AT domains are able to take over the function of acylation in more than one module. Interestingly it could be shown, that trans-AT PKS clusters in contrast to cis-AT PKS clusters were not evolutionary developed by gene duplication of single modules, but by horizontal gene transfer leading to a mosaic structure of different modules. [91,92] The trans-AT cluster and their parallel evolutionary development, again highlight the diversity and versatility of these intriguing biosynthetic pathways, which have evolved a variety of natural products with chemotherapeutic potency. Nevertheless, this complexity and unpredictability has also raised a vast number of unsolved questions, but also opprotunities, which will have to be unravelled and tackled in the ongoing natural product research.[93]

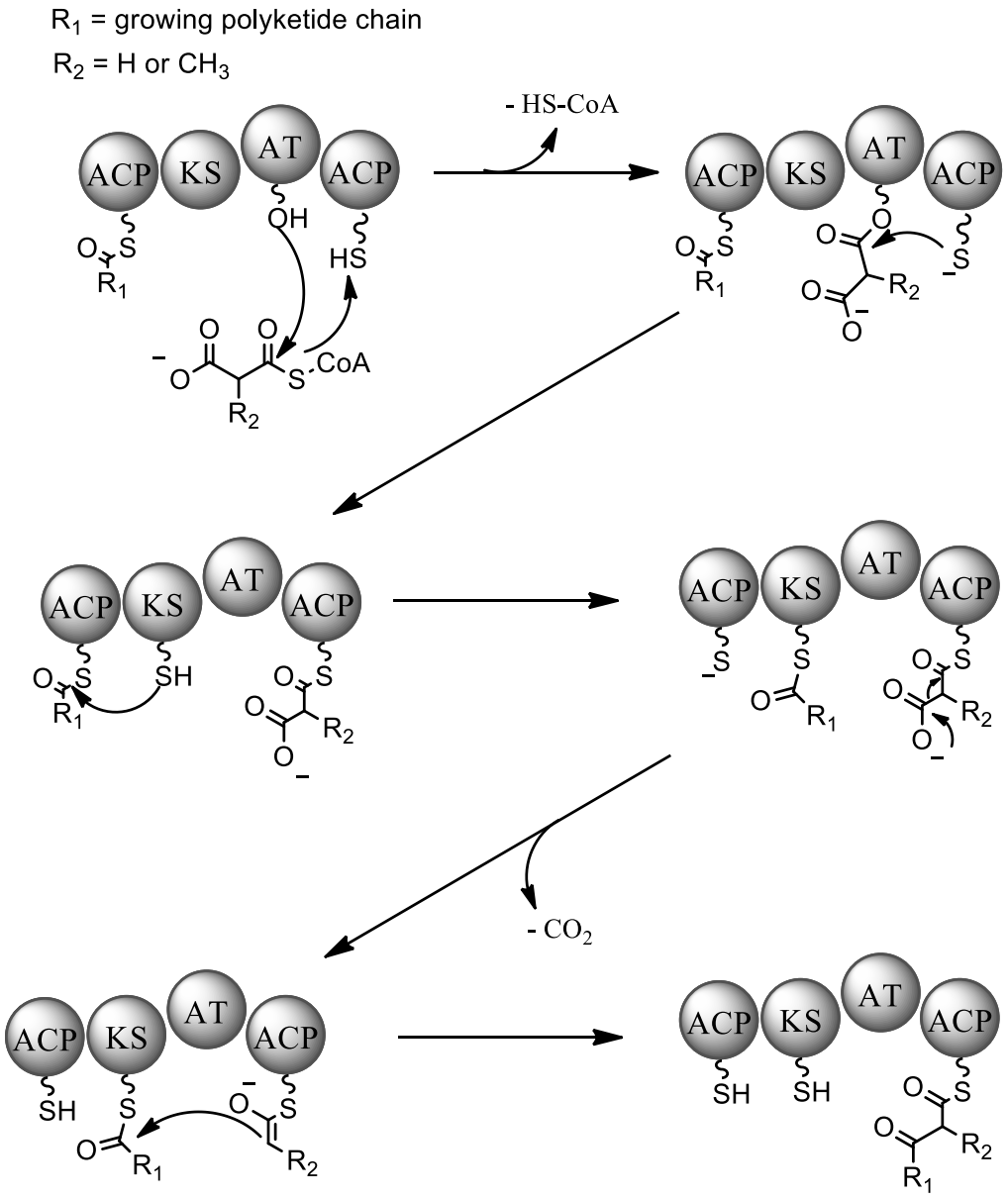

Figure 7: Elongation of a polyketide chain by polyketide synthase (PKS). The acetyltransferase domain (AT) selects the Malonyl-CoA or Methylmalonyl-CoA building block. By transthiolation it binds the building block to the acyl carrier protein (ACP). Polyketide elongation by C-C bond formation then is catalyzed by the ketosynthase (KS) via an enol intermediate.

2.8 Secondary metabolites - Silent gene clusters

A phenomenon, which can be observed for different secondary metabolite producing prokaryotes, is the discrepancy between genes encoding assembly lines for the production of secondary metabolites and the number of isolated natural products of these strains. This allows the assumption, that some clusters are either inactive under applied conditions or functionally incomplete. These genes are therefore called “silent” gene cluster and can be targeted by different biotechnological approaches. Beside the microbiological attempt to trigger production by environmental aspects, as growth conditions, temperature, nutrients, pH, co-cultivation biotechnological methods like heterologous expression, influencing regulatory mechanisms, promotor insertions are potential techniques to trigger the production of unknown metabolites.[94–96] In particular genomes of Streptomycetes, which are producers of several marketed antiobiotics were exploited for their biosynthetic potential. As production under laboratory condition does not represent the actual habitat of those organisms it is likely that some of the silent gene cluster might be active under certain conditions or for a certain purpose in nature.

Beside the streptomycetes similar genetic challenges occur in the broad variety of natural product manufacturing organisms as e.g. cyanobacteria and of course myxobacteria.

2.9 Myxobacteria - Phylogeny

Myxobacteria are prokaryotes of the order of Myxococcales that belong to the class of γ-proteobacteria in the phylum of proteobacteria. Myxococcales, are subdivided in the suborders of *Cystobacterineae*, *Sorangiineae* and *Nannocystineae*. Of main importance for this work are the families of Cystobacteraceae and Myxococcaceae in the suborder of Cystobacterineae.

The myxobacteria were first mentioned by Thaxter et al. [97] and have since been studied for their interesting microbiological characteristics, as well as for their striking secondary metabolite potential [98]. Up to date a myxobacterial genome is the largest published prokaryotic genome with over 14 Mbp [99]. Their large genome size might be a factor, why myxobacteria offer a large number of secondary metabolite clusters in their genome.[100] Their competitive habitat as soil and dung dwelling organisms has led to interesting morphologic and biosynthetic potential of

myxobacteria. Recently the identification by rRNA sequencing of marine myxobacteria in sponge tissue and the cross-link of sponge derived metabolites and terrestrial secondary metabolites from myxobacteria, has shed light on the source of "marine" natural products and expands the potential and importance of myxobacterial natural product diversity. [101,102]

2.10 Myxobacteria - Morphology and Life cycle

Several special morphological and ecological abilities highlight the predatory and competitive lifestyle of myxobacteria and might be closely connected to their terrestrial and marine habitat in large heterogenic bacterial communities. The complex lifecycle (Figure 8) has been well

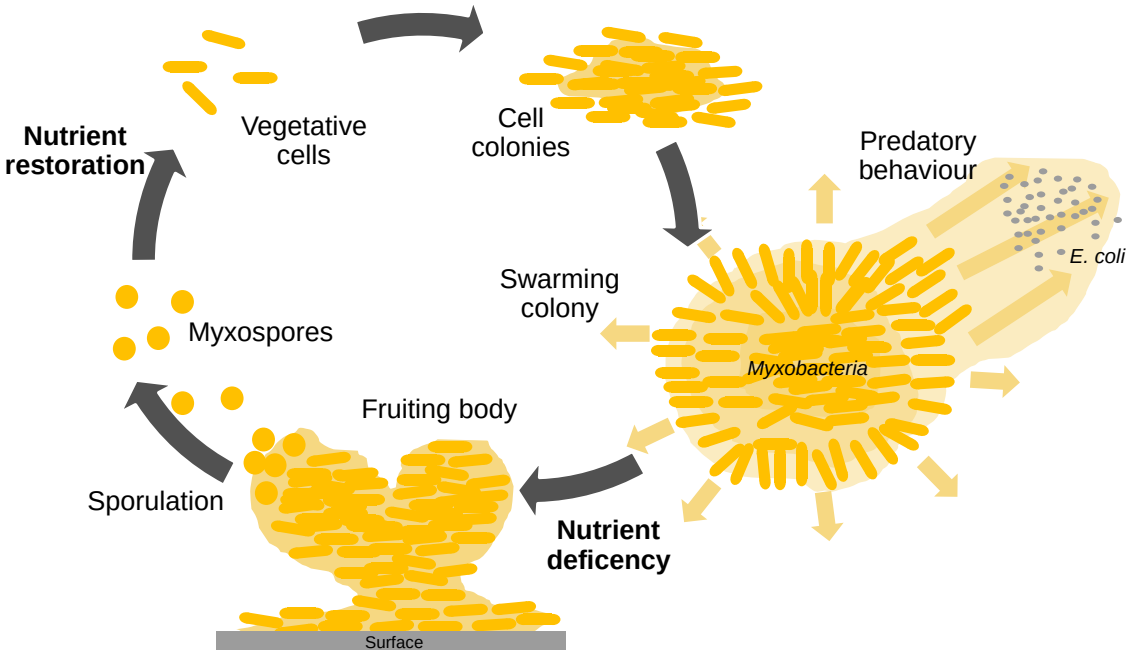

Figure 8: Life cycle of myxobacteria. Vegetative cells group to cell colonies, which can swarm on solid surfaces. This motility can be used to extend to nutrient sources like a predatory behavior to hunt for prey (e.g. E.coli). During starvation periods, myxobacteria decrease motility and aggregate to form fruiting bodies. By sporulation to myxospores harsh conditions and nutrient deficiency can be endured. After nutrient restoration, vegetative cells are build and the life cycle is continued.

studied and shows their adaption to their biological niche[103,104]. Biochemical mechanisms induce changes in motility or aggregation and are the basis of the multicellular behaviour of myxobacteria.[105] On solid surfaces myxobacteria agitate in swarms. Cell colonies swarm in circular directions by sliding on the solid surface. When approaching "prey" cells like *E.coli*, they show a predatory behaviour, which leads to overgrowing of the target organism with lysis

and nutrient uptake from their prey. If nutrients deplete, vegetative cells are able to form fruiting bodies. These fruiting bodies can exhibit different morphologies and can be used as a defining characteristic for taxonomy classification of myxobacterial strains. By sporulation myxobacteria can form myxospores in fruiting bodies, which endure in harsh conditions. Once nutrient levels have been restored myxospores can form vegetative cells again to continue their diversified life cycle.

2.11 Myxobacteria - Secondary metabolites

Myxobacteria are known for their potential to produce a chemical and biological variety of natural products.[106,107] Some of these compounds gained particular interest as they led to discovery of novel bacterial targets.[108] Prominent examples are the RNA-Polymerase (RNAP) inhibtors, which are almost solemnly represented by myxobacterial secondary metabolites. Three myxobacterial compound classes, the corallopyronins, myxopyronines and ripostatins[109], allosterically inhibit the RNAP at the switch region at a different locus than the competitive RNA-Polymerase inhibitors.

One myxobacterial secondary metabolite derived compound has been marketed. Ixabepilon is a semisynthetic derivative of the polyketide Epothilon, which is produced from the myxobacterium *Sorangium cellulosum*. With its Paclitaxel like biological activity it was approved by the FDA on the US market in 2007. (Figure 9)

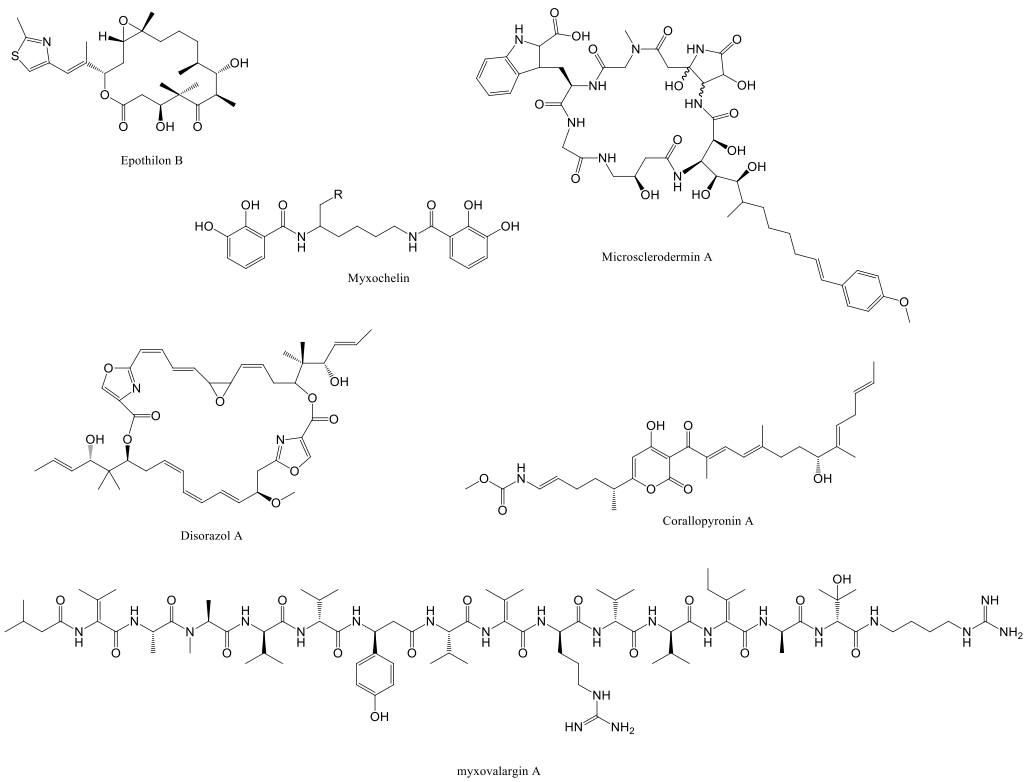

Figure 9: Natural Products from myxobacteria. Epothilone B is the basis for the semi-synthetic derivative Ixabepilone, marketed in 2007 for certain breast cancer indications. The antimitotic Disorazol A acts on tubulin polymerization. Corallopyronin A potent anti-filariasis drug and under developement for treatment of Tsutsugamushi fever. Myxovalargin A performs disruptive on bacterial biofilms and shows activity in antituberculotic assays.

2.12 Aims and Scope of this work

The aim of this work is to foster fundamentals for antiinfective natural products as basis for potential drug candidate development. This includes the identification and characterization of the natural product class of the myxovalargins, optimization of their production and properties using microbiological and biotechnological tools.

In this course the scope of this work includes different stages of natural product development from optimization and upscaling of production yields including purification, structure elucidation and production of derivatives, to identification and manipulation of biosynthesis pathways.

3. Material and Methods

3.1 Strains

strain	short term	source	purpose
Escherichia coli DH10B	(DH10B)	HIPS-MINS	cloning strain
Escherichia coli Rosetta	(Rosetta)	HIPS-MINS	expression strain
Escherichia coli BL21 (DE3)	(BL21)	HIPS-MINS	expression strain
Myxococcus fulvus 65	MCy8286 (Mxf65)	HIPS-MINS	myxovalargin producer
Myxococcus xanthus 113	MCy3592 (Mxx113)	HZI-MWIS	myxovalargin producer
Myxococcus xanthus 136	MCy3578 (Mxx136)	HZI-MWIS	myxovalargin producer
Corallococcus coralloides 1071	MCy6431 (Ccc1071)	HZI-MWIS	myxovalargin producer
Unclassified sp. 983 former Angiococcus sp. 983	MCy5730 (Ang983)	HZI-MWIS	myxovalargin producer
Myxococcus sp. 171	MCy9171 (Mxs171)	HIPS-MINS	myxovalargin producer
Sorangium cellulosum 377	MSr7234 (Soce377)	HIPS-MINS	Ripostatin producer
Hyalangium minutum NOCb10	MCy2730 (NOCb10)	HIPS-MINS	Hyafuron producer
Pyxidicoccus fallax SBCy002	MCy9557 (SBCy002)	HIPS-MINS	Pyxidienon producer

3.2 Kits

Kit	manufacturer	purpose
Gentra® Puregene® Yeast/ Bact. Kit	Qiagen Sciences	Preparation of genomic DNA
NucleoSpin® Gel and PCR cleanup Kit	Machery Nagel	Purification of nucleic acids
GeneJET Plasmid Miniprep Kit	Thermo Scientific	Isolation of plasmids from cells
TOPO TA Cloning® Kit Dual Promotor	Invitrogen	Cloning Kit
CloneJET^{TM} PCR Cloning Kit	Thermo Scientific	Cloning Kit

3.3 Vectors

Plasmid	Origin	resistance	Size (bp)	Use	features
%pCR®2.1-TOPO®	Invitrogen	KanR, AmpR	3931	Transformation	lacPromotor
pJet 1.2	Fermentas/ Thermo Scientific	AmpR	2974	Cloning	-
pET28 (b)	Novagen	KanR	5368	Expression	N-terminal His tag
pSBtn5Kan	pTOPO derived	KanR, AmpR	4000	Transformation	tn5 promotor
pMycoMarKan	-	KanR, TetR	5957	Transformation	Transposase
pET28 (a)	Novagen	KanR	5369	Expression	N-terminal His tag
pCDF1b	Novagen	SpecR	3621	Expression	-

3.4 Enzymes

enzyme	manufacturer	Use
Taq DNA Polymerase (native)	Thermo Scientific	Polymerase chain reaction
Phusion® High Fidelity DNA Polymerase	Thermo Scientific	Polymerase chain reaction
Restriction enzymes	Thermo Scientific	Cloning, restriction analysis
T4 Ligase	Thermo Scientific	Cloning

3.5 Ruler

Ruler	manufacturer	Use
GeneRuler™ 1 kb DNA ladder	Thermo Scientific	Agarose gel
GeneRuler™ 1 kb Plus DNA Ladder	Thermo Scientific	Agarose gel
GeneRuler™ High Range DNA ladder	Thermo Scientific	Agarose gel
CHEF DNA Size Markers – *H.wingei*	Biorad	PFGE
CHEF DNA Size Standard, lambda (λ) ladder	Biorad	PFGE
DNA Size Markers – Yeast Chromosomal	Biorad	PFGE
PageRuler™ Prestained Protein Ladder	Thermo Scientific	PAGE
PageRuler™Unstained Protein Ladder	Thermo Scientific	PAGE
DNA molecular weight marker VII	Roche	Southern Blot
DNA molecular weight marker III	Roche	Southern Blot

3.6 Oligonucleotides

Name	source	Sequence	purpose
1sca3Nfwd	Ccc1071	GACGGAGGGCACCACCTTCAC	Gap bridging
1sca3Nrev	Ccc1071	CCAGCTCGGTCTGCCAGATGG	Gap bridging
1071_Mxv8_fwd	Ccc1071	GACTTCGCCCGCAGGCACAAG	Plasmid recovery – single crossover
1071_Mxv8_rev	Ccc1071	CATGACGTACGCCAGCTGCTCC	Plasmid recovery – single crossover
1071_Mxv8_test_fwd	Ccc1071	GACTACCTCAAGTGGCTCTCC	Plasmid recovery – single crossover verification
1071_Mxv8_test_rev	Ccc1071	CGAAGCCCACGTAGTGCTG	Plasmid recovery – single crossover verification
1071_Mxv10_fwd	Ccc1071	GGTTCGGCAACGAGCTCCTTCC	Plasmid recovery – single crossover
1071_mxv10_rev	Ccc1071	CACCACGCCTTCCATGTCATCCAG	Plasmid recovery – single crossover
1071_Mxv10_test_fwd	Ccc1071	CAGGTGCAGGAGTGGAGC	Plasmid recovery – single crossover verification
1071_Mxv10_test_rev	Ccc1071	CCAACGGTGACCTCGGTG	Plasmid recovery – single crossover verification
Ccc_ABfwd	Ccc1071	GAGTCCGCCACCAGCAGGAC	Knockout *mxvH*
Ccc_ABrev	Ccc1071	CTGCGCAACCCGGAGATGCTG	Knockout *mxvH*
Ccc_ABtestFwd	Ccc1071	CGTAGAGCCAGGACACCGGAG	Verification *mxvH*-KO
Ccc_ABtestRev	Ccc1071	GTCCACTCCTGGTACGCGCAC	Verification *mxvH*-KO
ABC1KO_fwd	Ccc1071	GAATTCCTGCTGCACCTGACGCTCGCTC	Knockout *mxvI*
ABC1KO_rev	Ccc1071	AAGCTTGCAACGTCGTCGCCAAGTGGAG	Knockout *mxvI*
ABC1test_fwd	Ccc1071	CCTGGTCCAGCACGATGATGCG	Verification *mxvI*-KO
ABC1test_rev	Ccc1071	CTCGTGCGCATGCCCATCACC	Verification *mxvI*-KO
Ccc_Tam_TestF	Ccc1071	CAGCCCCATGCTGACGATGTGGATCCC	Knockout *mxvJ*
Ccc_Tam_TestR	Ccc1071	CTGCCTCATGAAGGGCTACTCC	Knockout *mxvJ*
CCC_TAMconF	Ccc1071	GTCAACACCGGCTTCGGCGAG	Verification *mxvJ*-KO
CCC_TAMconR	Ccc1071	CTGACGCAGCTTCTCGTGCAC	Verification *mxvJ*-KO
Ccc_Abc_TestF	Ccc1071	GGAGGTGCTGCTGCTGGACGAG	Knockout *mxvK*
Ccc_Abc_TestR	Ccc1071	CGAGCACCAGCAGCCACACGTG	Knockout *mxvK*
ABCconFwd	Ccc1071	CTCCTGTGCACCCAGTCCGTG	Verification *mxvK*-KO
ABCconRev	Ccc1071	ACGTGCCAGTGCGTCAGGGTG	Verification *mxvK*-KO
Adx_fwd	Ccc1071	CATGCGCGTGAAGCTGTCCACG	Knockout *adc*
Adx_rev	Ccc1071	GCAGGTCGCCCAGAATCTCCTG	Knockout *adc*
Adx_test_fwd	Ccc1071	CTCGACAACGAGGACGCGCTC	Verification *adc*-KO
Adx_test_rev	Ccc1071	GGTGATCTTCCCGTTGCGCAGC	Verification *adc*-KO
CupinKO_fwd	Ccc1071	GATGGTGGCGGCGCTGATTGC	Knockout *ORF2*
CupinKO_rev	Ccc1071	GACGAAGTCGCCCGGTGACAG	Knockout *ORF2*
1071_cupintest_fwd	Ccc1071	CGTCGACATCCAGCAGGTCGTC	Verification *ORF2*-KO

1071_cupintest_rev	Ccc1071	GGTACACGTACCCCGCATACG	Verification *ORF2*-KO
DEH1fwd	Ccc1071	CTCCCGGGAGACGTCGTAGTAG	Knockout *ORF5*
DEH1rev	Ccc1071	GTGGTGATGGCCTCGCGCTC	Knockout *ORF5*
1071_dehtest_fwd	Ccc1071	CGTGATTCGGAGAGAGCGGACC	Verification *ORF5*-KO
1071_dehtest_rev	Ccc1071	GTGGCGGAGCAGGACCTGAAG	Verification *ORF5*-KO
ORFdown1_fwd	Ccc1071	GCGTGCCGGAACTGGTACACG	Knockout *ORF1downstream*
ORFdown1_rev	Ccc1071	CCAGGAGCGGAAGACGCACTC	Knockout *ORF1downstream*
mxvAKOfwd	Ccc1071	CTGCTCCTGTCCTCACGGGAG	Knockout *mxvA*
mxvAKOrev	Ccc1071	GTCCTCCAGCATCAGCGCCAG	Knockout *mxvA*
mxvAKO1kb_test_fwd	Ccc1071	CAGCTACCGCGACTTCGTGCTG	Verification *mxvA*-KO
mxvAKO1kb_test_rev	Ccc1071	GTGGAGCCGGAGGTGTAGATGAG	Verification *mxvA*-KO
MXVApromins_fwd	Ccc1071	CATATGATGAGCGTATCGCCCAACGCCC	Promotor insertion – single crossover
MXVApromins_rev	Ccc1071	GAATTCGTCTCGAGCTCGAACGGCGAG	Promotor insertion – single crossover
Promins_mxvA_test_fwd	Ccc1071	GTGCAGCGATGACACGCGGT	Promotor recovery – single crossover verification
Promins_MxvA_test_rev	Ccc1071	CGAGCGACTCCAGCTCGAG	Promotor recovery – single crossover verification
MXVJpromins_fwd	Ccc1071	GAATTCCGATGCTGAGGTAGTCACAGG	Promotor insertion – single crossover
MXVJpromins_rev	Ccc1071	CATATGATGCTCATCCAGGGACGGAATTTC	Promotor insertion – single crossover
Promins_MxvJ_test_fwd	Ccc1071	CCTCGAAGCCGCAGAACAGG	Promotor recovery – single crossover verification
Promins_MxvJ_test_rev	Ccc1071	GTCCAGGAGACGGGAAACGTC	Promotor recovery – single crossover verification
pJET1.2 - forward seq	pJET1.2	CGACTCACTATAGGGAGAGCGGC	Sequencing amplicons
pJET1.2 - reverse seq	pJET1.2	AAGAACATCGATTTTCCATGGCAG	Sequencing amplicons
pTOPOin	pTOPO 2.1	CCTCTAGATGCATGCTCGAGC	test primer for pTOPO Knock-out mutants
pTOPOout	pTOPO 2.1	TTGGTACCGAGCTCGGATCC	test primer for pTOPO Knock-out mutants
pSBin	pSBtn5Kan	GGCCCTCTAGAGCCCTTTGG	test primer for pSBtn5Kan Knock-out mutants
pSBout	pSBtn5Kan	CACTTTATGCTTCCGGCTCGTATG	test primer for pSBtn5Kan Knock-out mutants

3.7 Media

Name	Ingredients	amount	pH
AMB modified	Starch, soluble Casitone HEPES $MgSO_4$ x 7 H_2O (Grüssing) K_2HPO_4	5 g/l 2.5 g/l 1.19 g/l 0.5 g/l 0.25 g/l	pH 7.0 (KOH)

Soce377-4H	Starch, soluble yeast extract (BD) $MgSO_4$ x 7 H_2O (Grüssing) HEPES Fe-EDTA $CaCl_2$ x 2 H_2O Glucose monohydrate (Applichem) Fructose K_2HPO_4	3 g/l 1.7 g/l 1.5 g/l 4 g/l 8 mg/l 0.1 % 0.1 % 0.1 % 0.1 %	pH 7.4
VY/2	baker's yeast (50g/100mL) $CaCl_2$ x 2 H_2O HEPES vitamin B12 (sterilfiltered)	10 ml/l 1.0 g/l 50mM 0.5mg/l	pH 7.2 (KOH)
A-Medium	glycerol (99,5g/l w/v) soy flour (degreased) HENSEL starch soluble (ROTH) yeast extract (BD) $CaCl_2$ x 2 H_2O $MgSO_4$ x 7 H_2O (Grüssing) HEPES (11.9g/l) Fe-EDTA	4.0 g/l 4.0 g/l 8.0 g/l 2.0 g/l 1.0 g/l 1.0 g/l 50mM 8mg/l	pH 7.4
A/2 –Medium	glycerol (99,5g/l w/v) soy flour (degreased) HENSEL starch soluble (ROTH) yeast extract (BD) $CaCl_2$ x 2 H_2O $MgSO_4$ x 7 H_2O (Grüssing) HEPES (11.9g/l) Fe-EDTA	2.0 g/l 2.0 g/l 4.0 g/l 2.0 g/l 1.0 g/l 1.0 g/l 50mM 8mg/l	pH 7.4
B-Medium	starch soluble (ROTH) glucose monohydrate (Applichem) soy flour (degreased) HENSEL Probion FM582 peptone (Marcor M) $CaCl_2$ x 2 H_2O $MgSO_4$ x 7 H_2O (Grüssing) HEPES (11.9g/l) Fe-EDTA	8.0 g/l 2.0 g/l 4.0 g/l 0.2 g/l 0.2 g/l 1.0 g/l 1.0 g/l 50mM 8mg/l	pH 7.2
CLF-Medium	fructose Glucose monohydrate (Applichem) skim milk yeast extract (BD) $CaCl_2$ x 2 H_2O $MgSO_4$ x 7 H_2O (Grüssing) HEPES (11.9g/l)	4.0 g/l 6.0 g/l 10.0 g/l 2.0 g/l 1.0 g/l 1.0 g/l 50mM	pH 7.0

CLF(sugar free)-Medium	skim milk yeast extract (BD) $CaCl_2$ x 2 H_2O $MgSO_4$ x 7 H_2O (Grüssing) HEPES (11.9g/l)	10.0 g/l 2.0 g/l 1.0 g/l 1.0 g/l 50mM	pH 7.0
CY-Medium	Casitone (Marcor typ M) yeast extract (BD) $CaCl_2$ x 2 H_2O HEPES (11.9g/l)	3.0 g/l 1.0 g/l 1.0 g/l 50mM	pH 7.2
CY+H-Medium	Casitone (MBD) yeast extract (BD) glucose monohydrate (Applichem) soy flour (degreased) HENSEL starch soluble (ROTH) $CaCl_2$ x 2 H_2O $MgSO_4$ x 7 H_2O (Grüssing) Na-Fe-EDTA HEPES (11.9g/l)	1.5 g/l 1.5 g/l 1.0 g/l 1.0 g/l 4.0 g/l 1.0 g/l 0.5 g/l 0.004 g/l 50mM	pH 7.2
E - Medium	skim milk soy flour (degreased) HENSEL yeast extract (BD) starch soluble (ROTH) $MgSO_4$ x 7 H_2O (Grüssing) HEPES (11.9g/l) Fe-EDTA Glycerol (99.5% w/v)	4.0 g/l 4.0 g/l 2.0 g/l 10.0 g/l 1.0 g/l 50mM 8 mg/l 5.0 g/l	pH 7.4
E/2 – Medium	skim milk soy flour (degreased) HENSEL yeast extract (BD) starch soluble (ROTH) $MgSO_4$ x 7 H_2O (Grüssing) HEPES (11.9g/l) Fe-EDTA Glycerol (99.5% w/v)	2.0 g/l 2.0 g/l 1.0 g/l 5.0 g/l 1.0 g/l 50mM 8 mg/l 2.5 g/l	pH 7.4
H-Medium	soy flour (degreased) HENSEL glucose monohydrate (Applichem) starch soluble (ROTH) yeast extract (BD) $CaCl_2$ x 2 H_2O $MgSO_4$ x 7 H_2O (Grüssing) HEPES (11.9g/l) Fe-EDTA	2.0 g/l 2.0 g/l 8.0 g/l 2.0 g/l 1.0 g/l 1.0 g/l 50mM 8 mg/l	pH 7.4
K-Medium (Gerth)	Dextrose Glucose monohydrate (Applichem) Peptone (Marcor Typ S) $(NH_4)_2NO_3$	40.0 g/l 2.0 g/l 2.0 g/l 1.0 g/l	pH 7.2

	KH_2PO_4 K_2HPO_4 $CaCl_2$ x 2 H_2O $MgSO_4$ x 7 H_2O (Grüssing) HEPES (11.9g/l) Fe-EDTA	0.9 g/l 2.3 g/l 1.0 g/l 1.0 g/l 50mM 8 mg/l	
K-Medium (fermentation)	Peptone (Marcor Typ S) Starch, soluble (Roth) Soytone (BD) Phytone (BD) Yeast extract (BD) $CaCl_2$ x 2 H_2O $MgSO_4$ x 7 H_2O (Grüssing) HEPES (23.8g/l) Fe-EDTA	2.0 g/l 8.0 g/l 4.0 g/l 2.0 g/l 2.0 g/l 1.0 g/l 1.0 g/l 100mM 8 mg/l	pH 7.2
M – Medium	Soytone (BD) Maltose Monohydrate (Roth) $CaCl_2$ x 2 H_2O $MgSO_4$ x 7 H_2O (Grüssing) HEPES (11.9 g/l) Fe-EDTA	10.0 g/l 10.0 g/l 1.0 g/l 1.0 g/l 50mM 8 mg/l	pH 7.2
M/2-Medium	Soytone (BD) Maltose Monohydrate (Roth) $CaCl_2$ x 2 H_2O $MgSO_4$ x 7 H_2O (Grüssing) HEPES (11.9 g/l) Fe-EDTA	5.0 g/l 5.0 g/l 1.0 g/l 1.0 g/l 50mM 8 mg/l	pH 7.2
POL - Medium	Probion FM582 Starch, soluble (Roth) $CaCl_2$ x 2 H_2O $MgSO_4$ x 7 H_2O (Grüssing) HEPES (11.9g/l) Vitamin B12	3.0 g/l 3.0 g/l 0.5 g/l 2.0 g/l 50mM 0.5 mg/l	pH 7.2
P - Medium	Peptone (Marcor S) Starch soluble (ROTH) Probion FM582 Yeast extract (BD) $CaCl_2$ x 2 H_2O $MgSO_4$ x 7 H_2O (Grüssing) HEPES (23.8g/l) Fe-EDTA	2.0 g/l 8.0 g/l 4.0 g/l 2.0 g/l 1.0 g/l 1.0 g/l 100mM 8 mg/l	pH 7.5
S-Medium	Soy flour (degreased) HENSEL Glucose monohydrate (Applichem) Starch soluble (ROTH) $CaCl_2$ x 2 H_2O $MgSO_4$ x 7 H_2O (Grüssing)	4.0 g/l 2.0 g/l 8.0 g/l 1.0 g/l 1.0 g/l	pH 7.4

	HEPES (11.9g/l) Fe-EDTA	50mM 8 mg/l	
S/2+V-Medium	soy flour (degreased) HENSEL glucose monohydrate (Applichem) starch soluble (ROTH) $CaCl_2$ x 2 H_2O $MgSO_4$ x 7 H_2O (Grüssing) HEPES (11.9g/l) Fe-EDTA Vitamin solution (Schlegel)	2.0 g/l 1.0 g/l 4.0 g/l 1.0 g/l 1.0 g/l 50mM 8 mg/l 1 ml/l	pH 7.4
Myxovirescin - Medium	Casein Peptone (Marcor typ M) $CaCl_2$ x 2 H_2O $MgSO_4$ x 7 H_2O (Grüssing) $CoCl_2$ HEPES (23.8 g/l)	10.0 g/l 0.05 g/l 0.1 g/l 1 mg/l 100mM	pH 7.0
M7 – Medium	Probion FM582 Starch, soluble (Roth) Glucose monohydrate (Applichem) Yeast extract (BD) $CaCl_2$ x 2 H_2O $MgSO_4$ x 7 H_2O (Grüssing) HEPES	5.0 g/l 5.0 g/l 2.0 g/l 1.0 g/l 1.0 g/l 1.0 g/l 10.0 g/l	pH 7.4
M7P – Medium (adapted)	Soytone (BD) Phytone (BD) Starch, soluble (Roth) Glucose monohydrate (Applichem) Yeast extract (BD) $CaCl_2$ x 2 H_2O HEPES	2.5 g/l 2.5 g/l 5.0 g/l 2.0 g/l 1.0 g/l 1.0 g/l 10.0 g/l	pH 7.4
MD1 – Medium (modified from Behrens et al. 1976)	Peptone (Marcor M) $CaCl_2$ x 2 H_2O $MgSO_4$ x 7 H_2O (Grüssing) HEPES	3.0 g/l 0.5 g/l 0.2 g/l 10.0 g/l	pH 7.2
AMB medium (Ringel et al., 1977)	Starch, soluble (Roth) Casitone (BD) $MgSO_4$ x 7 H_2O (Grüssing) K_2HPO_4	5.0 g/l 2.5 g/l 0.5 g/l 0.25 g/l	pH 7.0
Vitamin solution 1000x (Schlegel)	Biotin Nicotinsäure Thiamin 4-Aminobenzoesäure Pantothenat Pyridoxamin Cyanocobalamin	2.0 g/l 20.0 g/l 10.0 g/l 10.0 g/l 5.0 g/l 50.0 g/l 20.0 g/l	Sterilized by filtration

3.8 General instruments

Instrument	manufacturer	purpose
Mastercycler® Pro	Eppendorf	Thermocycler
peqSTAR 96x	peqlab	Thermocycler
Transferpette® S, 0.1 – 1 µl	Brandt	Single chanel pipette
Transferpette® S, 0.5 – 10 µl	Brandt	Single chanel pipette
Transferpette® S, 2 – 20 µl	Brandt	Single chanel pipette
Transferpette® S, 20 – 200 µl	Single chanel pipette	Single chanel pipette
Transferpette® S, 100 – 1000 µl	Brandt	Single chanel pipette
Transferpette® S - 8	Brandt	Multi chanel pipette
Multipette® Plus pipette	Eppendorf ®	Pipette
Vortex-Genie® 2	Scientific Industries	Vortex
Rotavapor®	Büchi	Rotary evaporator
Rotaphor System 6.0	Biometra	Pulsed field gel electrophoresis
CT15E	Hitachi	centrifuge
CT15RE	Hitachi	Cooled centrifuge
Eppendorf 5810 R	Eppendorf	Cooled centrifuge
Avanti J-25	Beckmann Coulter	Cooled centrifuge

3.9 Protein purification systems

For protein purification an Äkta purifier (affinity chromatography) or Äkta prime (affinity and size exclusion chromatography) from GE Healthcare was used.

3.10 Columns for protein purification

Column	Manufacturer	Purpose
HisTrap™HP 1 mL	GE Healthcare	His-tag affinity chromatography
HisTrap™HP 5 mL	GE Healthcare	His-tag affinity chromatography
HiLoad 16/60 Superdex 200 pg	GE Healthcare	Gel filtration chromatography
Superdex 200 Increase 10/300 GL	GE Healthcare	Size exclusion chromatography
Amicon® Ultra 15 mL 30000 NMWL	Merck Millipore	Spin column concentrator

3.11 Analytical HPLC-MS

Agilent 1260 LC, Bruker amaZon, Waters Acquity C18 BEH 50x2mm, 1.7 um	40 °C, 0.6 mL/min, A: H_2O, B:ACN, with 0.1% formic acid	linear gradient from 1 to 20 min, 5% to 95% B
Dionex RSLC, LTQ-Orbitrap, NanoMate, Waters Acquity C18 BEH 50x2 mm, 1.7 um	45°C, 0.6 mL/min, A: H_2O, B:ACN, with 0.1% formic acid	linear gradient from 1 to 10 min, 5% to 95% B
Dionex RSLC, LTQ-Orbitrap, NanoMate, Waters Acquity C18 BEH 100x2mm, 1.7 um	45°C, 0.55 mL/min, A: H_2O, B:ACN, with 0.1% formic acid	linear gradient from 1 to 19 min, 5% to 95% B
Dionex RSLC, Bruker maXis 4G, Acquity C18 BEH 50x2mm, 1.7 um	45°C, 0.6 mL/min, A: H_2O, B:ACN, with 0.1% formic acid	linear gradient from 1 to 6 min, 5% to 95% B

Dionex RSLC, Bruker maXis 4G, Acquity C18 BEH 100x2mm, 1.7 um	45°C, 0.6 mL/min, A: H_2O, B:ACN, with 0.1% formic acid	linear gradient from 1 to 19 min, 5% to 95% B

3.12 (Semi-)preparative LC

Waters Autopurifier UV/ MS; Phenomenex® Gemini C18 250 x 21.20 mm, 5 µm	RT, 25 mL/ min; A:H_2O, B:ACN, with 0.1% formic acid	MassLynx
Dionex Ultimate® 3000; Bruker HCT; Phenomenex Luna C18, 250 x 4.6 mm, 5 µm	40°C, 0.6 mL/min, A: H_2O, B:ACN, with 0.1% formic acid	Chromeleon
Biotage® Isolera™ Prime , Biotage® SNAP Cartridge KP-Sil	RT, Flow and run time dependend on cartridge size. A: DCM, B: MeOH + 1% Acetic acid or 0.1 % formic acid	Build-in software

3.13 NMR

NMR spectra were obtained on a Bruker Ascend 700 spectrometer with a 5 mm TXI cryoprobe (1H at 700 MHz, 13C at 175 MHz) or on a Bruker Ascend 500 spectrometer. TopSpin software from Bruker Daltonics was used for data analysus, acquisition and processing.

3.14 Fermentation

Fermentation was conducted with an Infors HT Labfors 3 equiped with Mettler Toledo oxygen electrodes. 2L and 7.5 L vessels were chosen for cultivation. For process control and evaluation IRIS 5.2 software was used.

3.15 Media used for growth of myxobacteria

All media components were suspended in highly purified H_2O (Milli-Q Millipore Merck) and then autoclaved.

Agar was produced by adding 16 g/l of agar to the according medium before autoclaving; soft-agar by adding 8 g/l agar.

3.16 Media used for growth of *E.coli* strains

All media components were dissolved in purified H_2O and then autoclaved.

Agar of this media was produced by adding 16 g/l of agar before autoclaving.

LB-medium:	Tryptone	10 g/l
	NaCl	5 g/l
	Yeast extract	5 g/l

3.17 Antibiotics

Antibiotics used as selection marker in liquid and solid media:

Chloramphenicol 25 mg/ mL in EtOH 70% → final concentration 25 µg/ mL

Kanamycin 50 mg/ mL in H_2O_{dest} → final concentration 50 µg/ mL

Hygromycin 50 mg/ mL in H_2O_{dest} → final concentration 100 µg/ mL

Ampicillin 100 mg/ mL in H_2O_{dest} → final concentration 100 µg/ mL

Spectionmycin 100 mg/ mL in H_2O_{dest} → final concentration 100 µg/ mL

3.18 Cultivation of strains

E.coli strains were grown in shake flasks at 37 °C and 180 rpm. Myxobacteria were grown in shake flasks at 30 °C and 200 rpm. Shake flasks were chosen at size of five times media volume.

3.19 Isolation of plasmids

The isolation of plasmid DNA from myxobacteria and E. coli was conducted either by using the GeneJET Plasmid Miniprep Kit from Fermentas/ Thermo Scientific or by alcalic lysis described by Sambrook et al.[4]

3.20 Isolation of genomic DNA from myxobacteria

Isolation of genomic DNA from myxobacteria for PCR was performed by using the Gentra® Puregene® Yeast/ Bact. Kit" by the manufacturer Qiagen Sciences accordingly to the protocol "DNA Purification from Gram- Negative Bacteria.

Genomic DNA for plasmid recovery and sequencing was purified by using the following protocol (adapted from Dr. Shwan, R.):
50 ml (100 ml) of fresh culture were spun down at 8.000 rpm for 10 min at room temperature. Supernatant was discarded and cells washed once with 15 ml TE buffer and then resuspended in a 15 mL Falcon tube by addition of 6 ml TE buffer. 30 µl Proteinase K solution (20 mg/ml in 50 mM Tris-HCl pH 8.0; 1 mM CaCl2) were added, then inverted several times. With 300 µl 10% SDS the tube was inverted until the mixture becomes clear. After incubation in the hybridization of for 2 h at slight rotation, 1 mL 5 M NaCl, then 800 µL of CTAB/NaCl were added and thouroughly mixed. The tube was incubated at 65 °C for 30 min in the hybridization oven.1 volume (= 8 ml) Phenol:Chloroform:Isoamylalcohol (25:24:1) was added and the tube swung for 1 h, then centrifuged at 8.000 rpm for 5 min at room temperature. The upper phase was transferred into a new tube by using an end-cut 1 ml-tip.This step was repeated 3 times. The supernatant was transferred into a new falcon tube by using an end-cut 1 ml-tip. After adding 5 ml Chloroform:Isoamylalcohol (24:1) the tube was swung for 1h, then spun for 10 min at 8000 rpm. 4 mL supernatant was carefully transferred into a new tube using end-cut 1

ml tip. 400 µl of 3 M Na-acetate pH 7.5 were added, then mixed very well, by inverting the tube several times. 11 ml of 100% cold ethanol were poured in and the tube inverted several times, until the appearance of cotton like DNA. The DNA was collected using a Pasteur-pipette by rolling the DNA on the end of the Pasteur-pipette. The pipette-end (with DNA) was immersed into a 2 ml tube containing 70% ethanol for DNA washing. The DNA pellet was dried on the pipette-end by carefully attaching the inner site of a fresh 2 ml tube to remove the ethanol drops and dried over night at room temperature. The genomic DNA was suspended in 0.5-1 ml 10 mM Tris-HCl, pH 8.0).

3.21 Polymerase chain reation (PCR)

For amplification with Phusion® High Fidelity Polymerase kit (New England Biolabs) the denaturation temperature of 98°C was chosen and the elongation temperature of 72°C. The annealing temperature was chosen according to the primer sequence or evaluated by gradient PCR. The elongation time was calculated by using 20 sec. for approximately 1 kbp.

For Taq polymerase (Fermentas) a denaturation temperature of 95°C was chosen and an elongation temperature of 72°C. The annealing temperature was chosen according to the primer sequence or evaluated by gradient PCR. The elongation time was calculated by using 30 sec. for approximately 1 kbp.

PCR with Phusion®	
H_2O purified:	14 µl
HF buffer:	5 µl
dNTPs:	2 µl
DMSO:	1 µl
Primer fwd.	1 µl
Primer rev.	1 µl
Template	1 µl
Phusion®	0.2 µl

PCR with Taq	
H2O purified :	14 µl
MgCl2 buffer:	2.5 µl
Taq buffer + KCl	2.5 µl
dNTPs:	2 µl
DMSO:	1 µl
Primer fwd.	1 µl
Primer rev.	1 µl
Template	1 µl
Taq	0.2 µl

3.22 Electrophoresis

Electrophoresis was performed with gels of 0.8% agarose (Biolabs Agarose) and in gel staining with Roti®Safe. As DNA reference ladder GeneRuler^{TM} 1kb DNA Ladder, GeneRuler^{TM} 1kb Plus DNA Ladder and GeneRuler^{TM} 100 bp by Thermo Scientific were used. Gels were run between 80 to 120 V depending on size of the gel, if not mentioned differently.

3.23 Pulsed field gel electrophoresis

The samples were run in Agarose 1 % in 0.25 % TBE and buffer: 0.25 % TBE in a Biometra Rotaphor System 6.0. The chosen program "2 kb – 800 kb, 24 h" was set to the following parameter: duration: 24 h; temperature: 13°C; interval: 60 sec. to 1sec (log), angle 120°C to 110 °C (lin); voltage 180 V to 120 V (log).

3.24 Nucleic acid purification

Nucleic acids were purified by using the NucleoSpin® Gel and PCR cleanup Kit by Machery-Nagel GmbH Co KG, 52355 Düren, Germany.

3.25 Preparation of competent cells *E.coli* cells

E.coli cells were grown in 500 ml LB medium to an OD_{600} = 0,6-0,8. Then the cell suspension was centrifuged 12 min at 4°C with 6000 x g. The Pellet was washed three times with glycerin 10% 100 ml, 50 ml and 50 ml. The cells were centrifuged each time for 5 min at 4°C with 6000 x g. After the final centrifugation cells were resuspended in 2.5 ml glycerin 10 % and then 50 µl filled in a 1.5 ml Eppendorf tube. Cells were directly shock-frosted in liquid nitrogen and stored at -80°C.

3.26 Transformation of *E.coli*

Competent *E.coli* cells were electroporated at 1250V, 200 Ω, 25 µF in a 1 mm glass cuvette. After electroporation 250 µl LB medium were added and cells incubated at 37 °C for 1 h. Finally they were plated on LB agar by supplementation of the appropriate selection marker.

3.27 Transformation of myxobacteria

Cells were grown to an OD_{600} = 0.6 – 1.0 in 50 ml medium. 2 ml culture were transferred to a 2 ml Eppendorf tube and centrifuged at 8000 rpm for 1 min. The supernatant was discarded and the cells were once washed with 1ml purified water and centrifuged again with 8000 rpm. The cells were resuspended in 50 µl purified water and 5 µl plasmid solution (200 – 600 ng/µL) was added. After mixing the suspension was transferred into a 1 mm glass cuvette and electroporated at 650 V, 200 Ω, 25 µF. 1 ml medium was added and transferred into a 2ml Eppendorf tube and incubated on a 30 °C shaker. After 6 h regeneration time the cells were plated in 10 ml soft-agar on an agar plate, both containing the same selection marker.

3.28 Crude extracts

A 50 ml culture was spun down at 8000 rpm and twice extracted with 30 ml methanol for 20 minutes at a stirring rate of 300 rpm. The solvent was evaporated and the residue resuspended in 1 ml MeOH. This procedure was scaled-up or -down according to the culture volume.

3.29 Heterologous protein expression

Expression strains were grown in 50 ml LB medium at 37°C and 180 rpm on a shaker until an OD_{600} of 0.4-0.6. IPTG was added to a final concentration of 0.1 mM IPTG and incubated either at 30°C for 4 hours or at 37°C for 2h. 1.5 ml culture was centrifuged 5 min at 110 rpm. The pellet was once washed with 500 µl lysis buffer (20mM Tris pH 8.0, 200 mM NaCl, 10% Glycerol), then resuspended in 500 µl lysis buffer. The cells were lysed by ultrasonic (10s) then spun down (5 min, 110 rpm). The supernatant was collected separately and the pellet dissolved in 500 µl lysis buffer. The samples were applied on a discontinuous polyacrylamid gel.

3.30 Polyacrylamid Gel (PAGE)

Reducing and native polyacrylamide electrophoresis was performed according to common protocols.

3.31 Southern Blot

Southern Blot was performed by using 1 -10 µg genomic DNA purified according to 3.20. The probe was labelled with DIG High prime (Roche) according to manufacturer procedure. Blotting, Hybridization and detection was conducted according to common protocols.[110]

4. Results

4.1 Myxovalargin

4.1.1 Introduction and overview

The myxovalargins were discovered in an antibiotic screening of the Gesellschaft für Biotechnologische Forschung (GBF) Braunschweig in 1983 from a crude extract supernatant of *Myxococcus fulvus* Mx f65 (MCy8286) [111]. Their antibacterial potential against gram-negative and gram-positive organisms led to a subsequent investigation of their mode of action. Two general mechanisms were shown to be present in-vitro, which is the blockage of the A-site of ribosomes, thereby inhibition of protein biosynthesis at 1 µg/mL myxovalargin A, and a membrane destruction of cells at 5 µg/mL.[112] The MIC for myxovalargin A, the most prominent derivative in MCy8286, was determined 0.3 - 5 µg/mL for gram-positive, 6 - 100 µg/mL for gram negative bacteria and the LD_{50} as 10 mg/kg s.c. in mice.
Structure elucidation and stereochemical assignment of myxovalargin A was performed using TLC coupled total acidic hydrolysis, Edman degradation and mass spectrometry.[113] Myxovalargin is a linear polypeptide of 1676 Da, which contains sixteen building blocks of mainly non-proteinogenic type derived from eight valines, three alanines, two arginines, an isoleucine and a tyrosine, as well as a 3-mehtyl-butanoic acid starter. [114]

In the course of this work the myxovalargins were in focus of a successfully finished project funded by the Bundesministerium für Bildung und Forschung (BMBF) on biofilm activity, in cooperation with Sanofi Aventis and groups of the TWINCORE Hannover and the HZI Braunschweig. Different issues regarding production, biosynthesis, in-vitro and in-vivo activity, toxicology, pharmacokinetic, pharmacology and mode of action studies were investigated. The role of HIPS was mainly specified on the isolation of natural and semisynthetically derived myxovalargins for activity testing, as well as the elucidation of the biosynthetic machinery of the myxovalargin compound class (Figure 10). In this context several myxovalargins were isolated, purified and their structure elucidated by tandem mass spectrometry (MS-MS) and nuclear magnetic resonance (NMR) spectroscopy. The biosynthesis was investigated by in-silico analysis, gene disruption by mutagenesis and feeding experiments. Production of semisynthetic compounds was performed by precursor directed biosynthesis and

mutasynthesis, up-scaled and followed by purification of the respective compounds. The myxovalargins were sent to various bioactivity testing: in-house at MINS by Dr. Jennifer Hermann,[115] in-vitro biofilm activity assays by Dr. Mathias Müsken (TWINCORE and HZI)[116,117] and in vivo mouse models by Dr. Vinay Pawar at HZI Braunschweig[118,119] as well as tuberculosis screeing at the university of Capetown in South Africa.

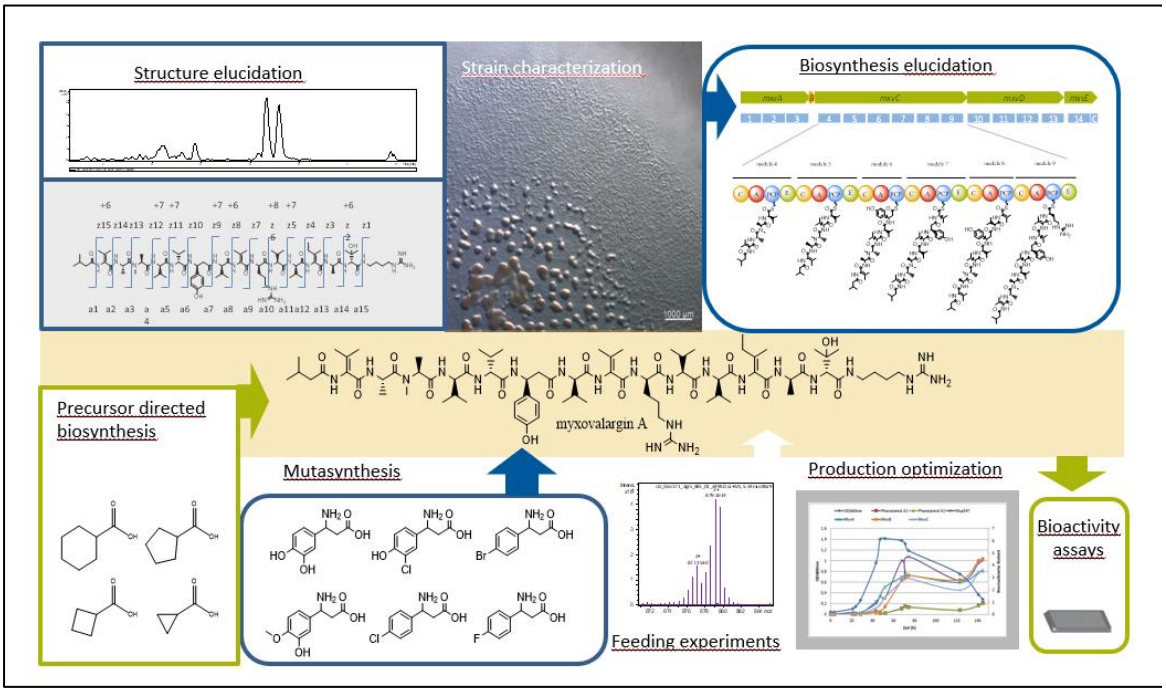

Figure 10: Overview of acitivites and techniques applied for the characterization of the myxovalargins. Structure elucidation and biosynthesis elucidation were conducted in a combined approach of analytical techniques (mass spectrometry, NMR spectroscopy), biotechniological procedures (Precursor directed biosynthesis, mutasynthesis, feeding experiments) and in silico tools (Geneious, Antismash, BiosynML). The overall picture was extended by microbiological characterization, production optimization and bioactivity screening.

4.1.2 Characterization of the Myxovalargin producer

In order to find a suitable myxovalargin producer, screening of myxobacterial LC-MS datasets was performed using a query selective for the mass of myxovalargin A. Besides the known producer *Myxococcus fulvus* Mx f65 [MCy8286], we identified additional strains, all of them belonging to the suborder of *Cystobacterinae*: *Corallococcus coralloides* 1071 (Ccc1071) [MCy6431], *Angiococcus sp.* 983 (Ang983) [MCy5730], *Myxococcus xanthus* 113 (Mxx113)

[MCy3592], *Myxococcus xanthus* 136 (Mxx136) [MCy3578]. An additional producer *Myxococcus sp.* 171 [MCy9171] could be identified in a later project stage by identification of the gene cluster and target analysis of myxovlaragin hits in the extracts of this strain. As in the course of this project and due to new taxonomical characterization techniques strain classification of some myxovalargin producers was revised, the MCy naming will be referred to in this document. All strains were evaluated for their suitability in terms of production, application of genetic tools and growth properties (Table 1). The initial experiments were conducted using Mcy8286 (Mx f65). Therefore, mutagenesis and growth were studied in depth for this strain, although the low frequency of mutants obtained lead to disqualification of this strain for further experiments on the biosynthesis of the myxovalargins. The strain showed fast growth in CTT medium while cells mainly remained planktonic. Random mutagenesis by transposon insertion was possible in high yield, nevertheless site directed mutagenesis was only achieved with one out of 5 constructs in several attempts and only a single mutant was generated, which was verified by PCR to be correct. The method established did not yield further mutants with other constructs.

Growth of MCy3592 (Mxx113) and MCy3578 (Mxx136) was acceptably fast, though these strains grow slower in the chosen CTT medium. A major disadvantage occurred in their formation of aggregates in liquid medium. Though it does not necessarily have impact on production, it hinders proper monitoring of growth stages and properties, thereby impeding upscale processing and process standardization. Transfer of solely planktonic cells or cultivation in baffled shake flasks did only slightly reduce aggregates or induce smaller conglomerates, a complete planktonic growth could not be achieved. Transposon mutagenesis was possible, but only in low yield; site directed mutagenesis was unsuccessful.

MCy5730 (Ang983) and MCy6431 (Ccc1071) showed similar characteristics regarding their growth. Both occur in nutrient-poor VY/2 medium in red roundish cell colonies of up to approximately 0.5 cm, but in AMB medium suspended cultivation is obtained to high cell density ($OD_{600} > 2.0$). Random mutagenesis was successful in both strains; nevertheless single crossover recombination was only achieved in MCy6431. It has to be noted that site directed mutagenesis has not been studied in depth for MCy5730, hence this strain is a putative alternative candidate for biotechnological modification. The production levels of myxovalargin compared relatively against the wildtype, showed a superiority of MCy6431 and MCy5730 over the Myxococci. The strain MCy6431 was chosen as feasible producer for further development (Table 1). A reliable mutasynthesis method was established (Figure 11),

furthermore growth conditions were optimized and production transferred to fermentation scale (4.1.3).

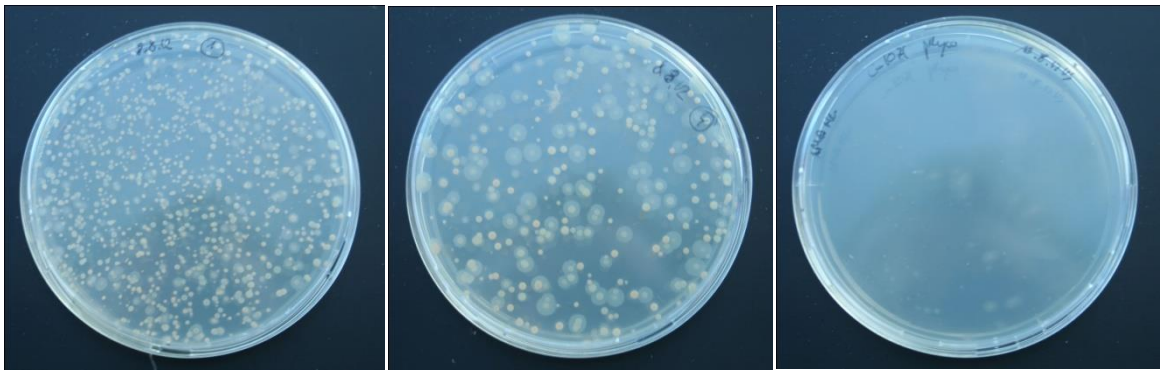

Figure 11: Study of different mutagenesis procedures for MCy6431 by transposon mutagenesis with pMycoMarKan on AMB agar plus 50 µl/ml kanamycin; left panel: 2 ml cells of liquid culture were centrifuged, washed once, resuspended in 50 µl, electroporated and plated out in soft agar; mid panel: cells from agar plate were scratched of and resuspended in 1ml purified water, washed once, resuspended, electroporated and plated out in soft agar; right panel: cells from liquid culture as prepared in left panel were plated out after electroporation with a Drigalski spatula.

Myxococcus sp. 171 (MCy9171) as Myxovvalargin producer was identified in a late stage of this project. Therefore, this strain was not evaluated in-depth. The strain shows fast growth in AMB and CTT medium. Mutagenetic tools were not applied to this strain. The production seems to be less than achieved with MCy5730 and MCy6431. However, its potential was not directly compared to the other myxovalargin producers. The strain was used for reverse feeding experiments due to its growth in nutrient poor medium. For further experiments a fundamental characterization of this strain might offer additional opportunities.

Table 1: comparison of microbiologic and biotechnologic parameters of different myxovalargin producers regarding time span to reach end of exponential growth by comparable cultural conditions, liquid growth characteristics, production of myxovalargin A and applicability of mutagenetic tools.

Strain	Appr. time in liquid until stationary phase	Liquid growth characteristics	Production of Myxovalargin A	mutagenesis
MCY8286	TS (2d) CTT (2-3d) AMB (3-4d)	planktonic planktonic planktonic	+ + +	Transposon +++ Site directed +
MCy6431	AMB (4d) VY/2 (>4d)	planktonic aggregated	++ +	Transposon +++ Site directed +++
MCy5730	AMB (4d) VY/2 (>4d)	planktonic aggregated	++ +	Transposon ++ Site directed -
MCy3592	CTT (4d)	aggregated	+	Transposon + Site directed -
MCy3578	CTT (4d)	aggregated	+	Transposon ++ Site directed -
MCy9171	CTT ((4d) AMB (4d)	planktonic	+ +	Not evaluated

4.1.3 Characterization of MCy6431

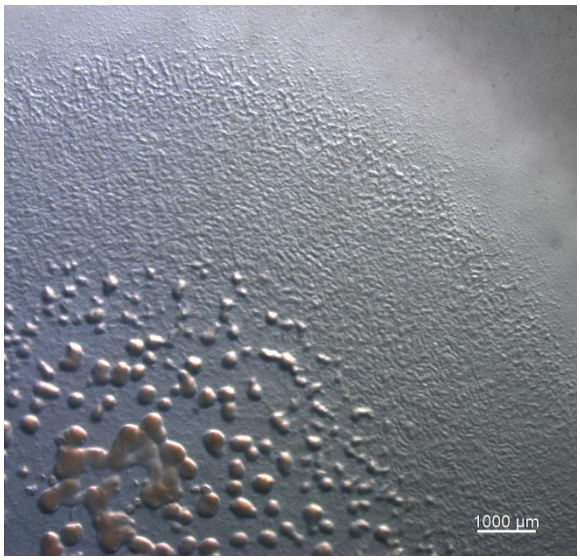

Figure 12: MCy6431 on VY2 agar. The colony shows formation of fruiting bodies in the left lower corner. Around the fruiting bodies, swarming cells of MCy6431 are visible.

Taxonomy

Formerly *Corallococcus coralloides* 1071 (MCy6431) as most promising candidate for further optimization of biotechnological manipulation, but also for production enhancement, was further studied and characterized. Due to its production profile and its genetic accessibility the former classification of this strain in the family of Myxococcaceae[120] was questioned. 16 S rRNA comparison in cooperation with Dr. Ronald Garcia revealed a close relationship to *Pyxidococcus fallax* DSM14698^{T} [121], rather than the Corallococci (Figure 13). This clade is also closely related to the Myxococci, which exhibit a similar production profile. The myxoprincomides[73] are predominantly found in *Myxococcus* strains as well as the myxovalargins, which are produced by four additional Myxococci (4.1.2). Also 16 s rRNA of the unclassified strain *Angiococcus* sp. 983 (MCy5730) groups with the *Pyxidicocci*, as well as *Myxococcus* sp.171 (MCy9171), which correlates with similar growth characteristics like MCy6431. Further investigation of morphology and fatty acid profile will shed light on a correct taxonomic classification.

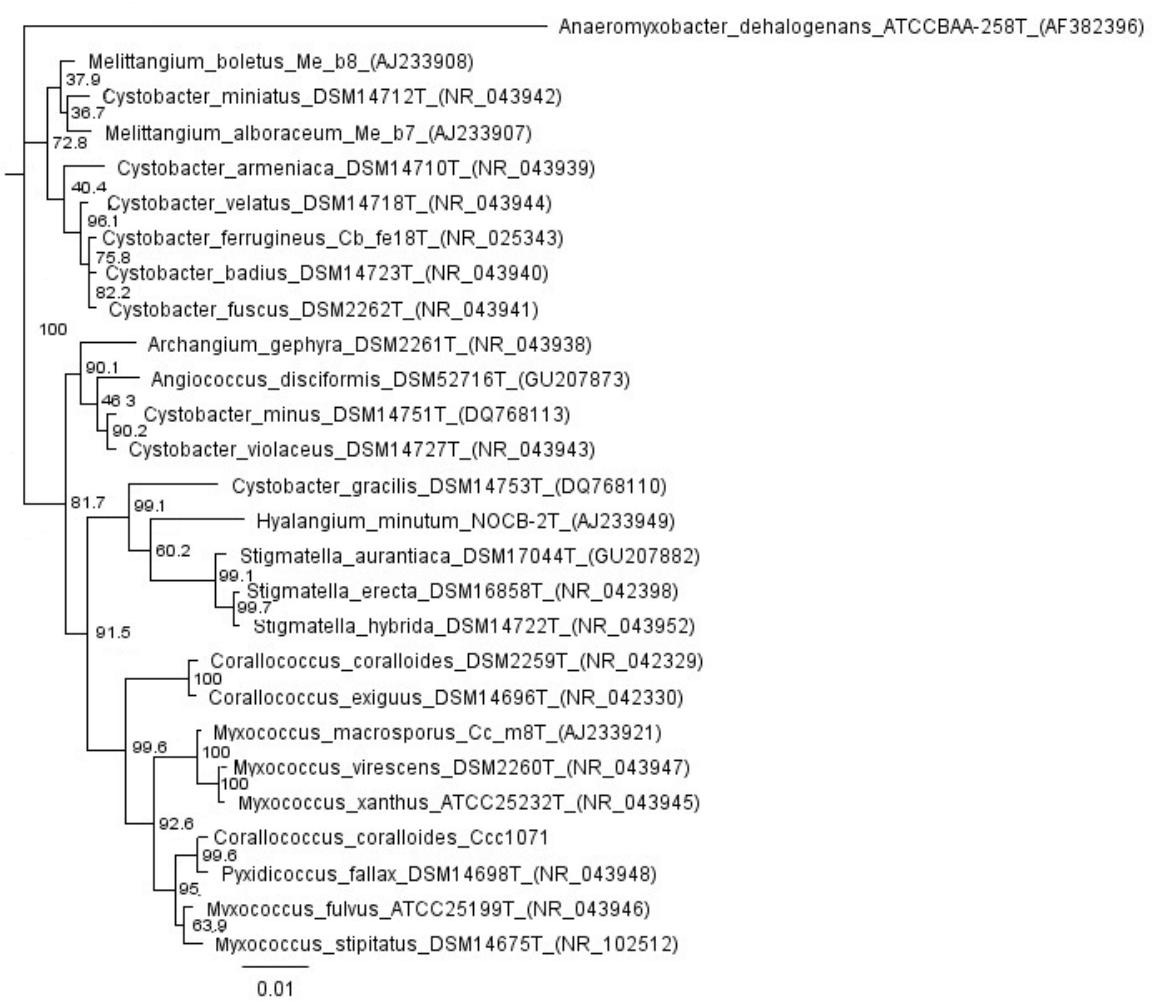

Figure 13: 16S rRNA comparison of the strain MCy6431 (Ccc1071), formerly characterized as *Corallococcus coralloides* strain. The comparison shows the affiliation of MCy6431 (Ccc1071) to the group of Pyxidicocci, highlighted in green, instead of the Corallococci, marked in red.

Genome sequencing

The Ccc1071 strain was sequenced by Illumina, Roche 454 and Pacific Bioscience at the DSMZ.[122,123] For the latter, in house protocols for myxobacteria were combined with commonly used techniques to yield high quality genomic DNA. Quality of genomic DNA was assessed by pulsed field gel electrophoresis. Comparative assembly of Pacbio data was performed by combining Pacbio and Illumina data and by using solely Pacbio scaffolds. This comparison was conducted due to putative miss-assembly and repetitive regions in the myxovalargin cluster. Nevertheless, both sequences showed an equal circular genome. The sequence was optimized and assembled by Dr. Nestor Zaburannyi resulting in a 13,193,010 bp genome without gaps in

the nucleic acid sequence (Figure 14). The genome holds approximately 25 PKS and NRPS clusters, interestingly several NRPS cluster in the size of the myxoprincomide and myxovalargin assembly lines are present, although these belong to the largest NRPS BGCs reported to date. Furthermore, though they show typical NRPS domains and modules encoded, there are no homologies to known NRPS clusters except of the myxovalargin, myxochelin and myxoprincomide genes indicating potential for a variety of unknown complex natural products.

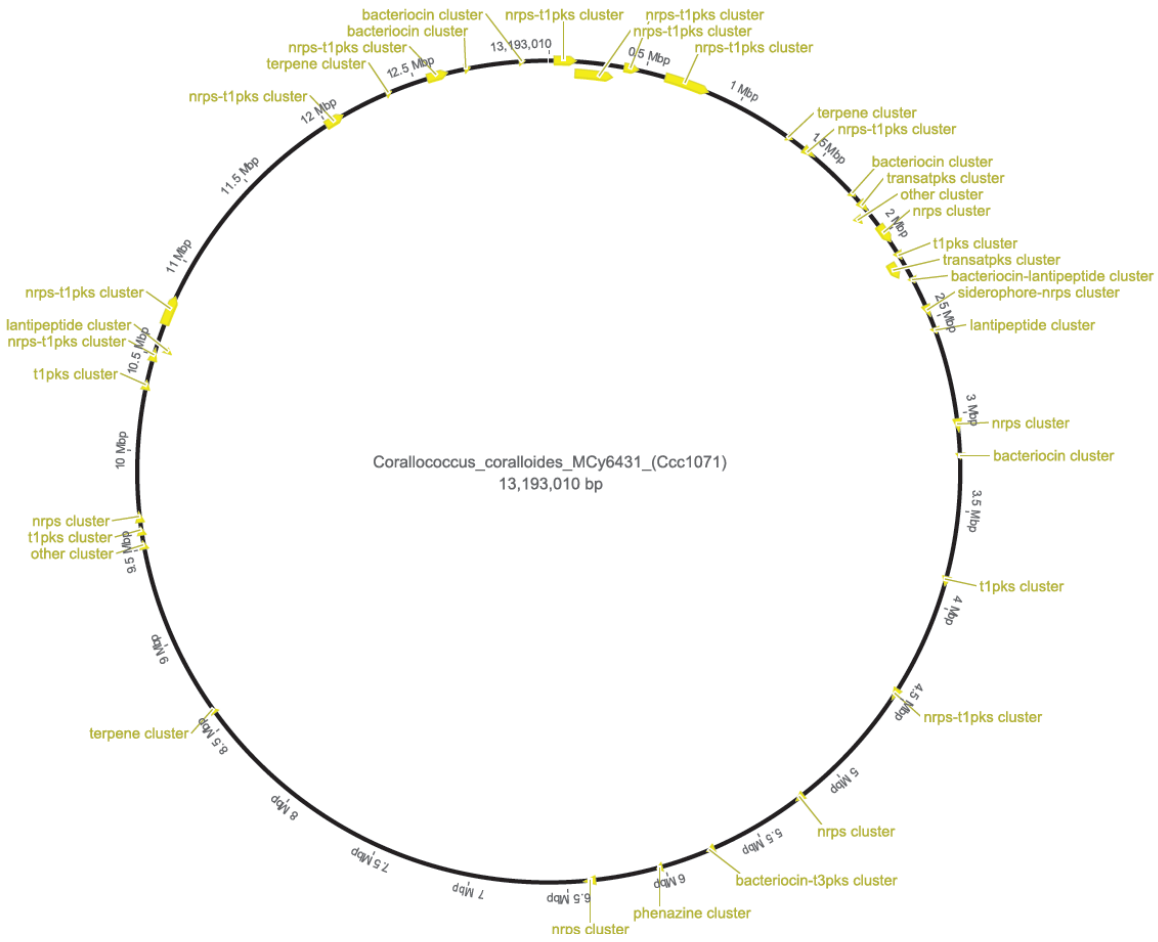

Figure 14: The complete genome of *Corallococcus coralloides* MCy6431 is approximately 13.2 Mbp in size. It holds approximately 25 PKS and NRPS gene clusters, furthermore several other secondary metabolite biosynthesis pathways.

Media optimization

General modifications on media components were conducted to find optimal production conditions. Since the siderophore myxochelin [124] is produced in high amounts and thereby might influence the production profile of other secondary metabolites, a suppression by supplementation of iron in form of FeEDTA was performed. A total loss of myxochelin production by supplementation with 8 mg/L FeEDTA could be achieved. Production levels of myxovalargin A were slightly increased, whereas myxovalargin B yield was raised about 10-fold (Figure 15). Further increase of FeEDTA concentration did alter the ratio between myxovalargin A and B in favor of the latter.

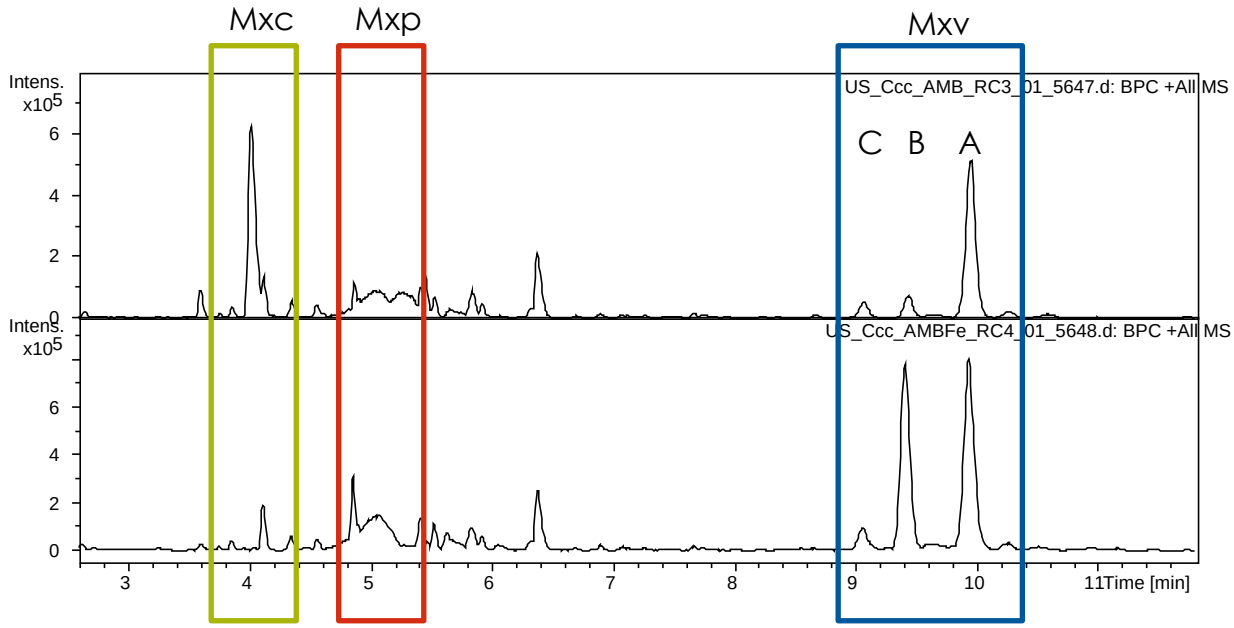

Figure 15: Chromatograms of Cc1071 grown in AMB medium without FeEDTA (upper chromatogram) and with 8 mg/L FeEDTA (lower chromatogram). The production of the iron chelator myxochelin (Mxc; green box) diminishes under FeEDTA supplementation, whereas the myxovalargin production (Mxv; blue box) is increased, especially of myxovalargin B. The production of the myxoprincomides (Mxp; red box) is also influenced by this change.

Further studies were conducted to specify a suitable pH range for MCy6431 (Figure 16). The general pH of AMB medium is set at pH 6.8, therefore the strain was cultivated ranging from pH 5 to 10. All cultures were harvested simultaneously, when no additional growth could be observed in the cultures. Growth and production in pH 5 and 6 were not detectable. The standard pH 6.8 as reference yielded reasonable growth and production. Nevertheless, at pH 8 a twofold production increase could be achieved compared to pH 6.8. At pH 9 production decreased and pH 10 showed minimal growth and production. Therefore, a pH of 8.0 was determined as optimal production condition with a fast growth of cells. These results were underlined by pH monitoring in shake flask versus fermenter, where an increasing of pH from 7.0 to a stable 8.0 during cultivation was observed. However as with pH 8.0 other growth challenges occurred during fermentation, the pH 7.0 which allows almost equal growth properties, was used for all described experiments.

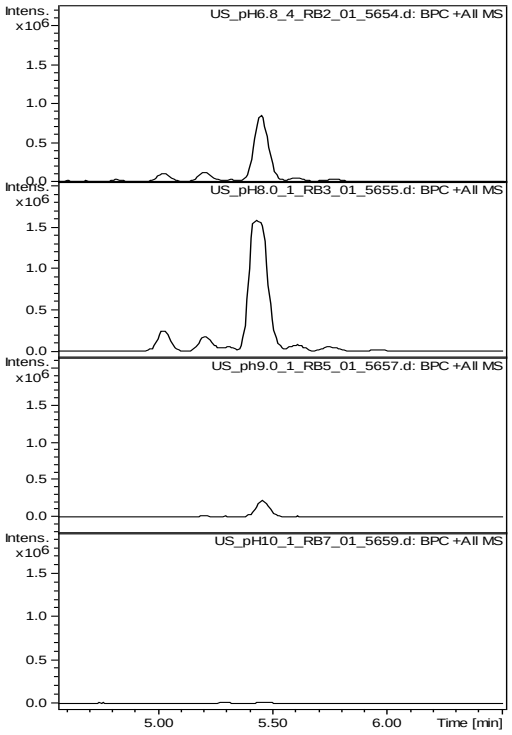

Figure 16: production of myxovalargin A could be observed in a range of pH-6.8 – 10. A maximum of production was observed at pH 8.0

By cultivation in different media using the 24 deep-well Duetz systems (Kuhner shaker) [125] additional information on suitable media combinations could be determined (Figure 17). Several commonly used media for myxobacteria were used at 8 mL each. In addition of XAD 16 the strain was grown for several days at 30 °C and 180 rpm. Extracts were harvested, extracted und compared. In general, a superiority of media containing larger amounts of nitrogen source yielded in an increased production of myxovalargin. Probion containing media were shown to be a suitable nitrogen source, as well as other peptones. Nevertheless, in several media, the strain showed conglomerates, which reduced their suitability for further upscale development. As this phenomenon was observed for strains with high production yields, a putative reason could be the fast growth with the nutrient rich media, which leads to local high cell densities resulting in agglomeration. Cultivation in P-medium, a nutrient rich medium with high production yields in Duetz cultivation and small scale, in the MWIS group of the HZI Braunschweig, support these findings, since strong aggregation was reported, which led to foam formation in the cultivation process and clogging of filters in the downstream process.

Therefore, adapted AMB medium still seems to be reasonable for microbiological and biotechnological improvement of growth. However, the low nutrient supply of 2.5 g/l Casitone can be optimized by adding additional nitrogen sources or replacing the nitrogen. Preliminary experiments suggest a concentration of 5 g/l or the substitution of casitone by other nitrogen rich peptones, but this was not studied into detail. Using these further optimizations with casitone increase and pH adjustment cultivation was transferred to small scale fermentation.
Cultivation was repeated with the second potent myxovalargin producer, Ang983. Results for MCy5730 are comparable to MCy6431 (Figure 45). The cultivation of MCy5730 also shows its high production yields of myxovalargins in different media. For high throughput production of myxovalargins MCy5730 seems to be superior to MCy6431. Fermentation of MCy5730 was also conducted at the HZI Braunschweig. However, due to the biotechnological achievements with MCy6431, this strain was used for further experiments.

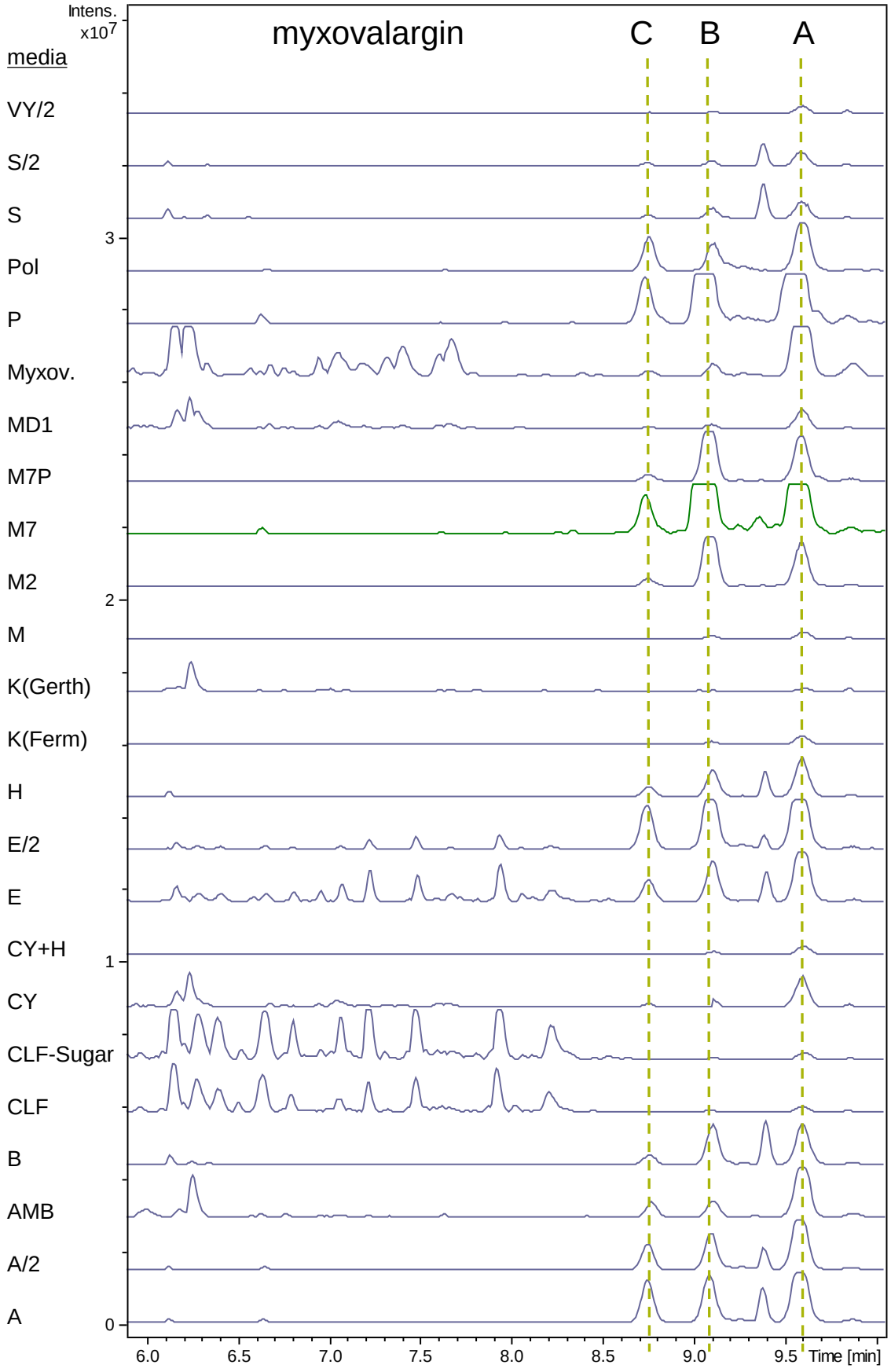

Figure 17: 25 deep-well cultivation of MCy6431. Nitrogen rich media show increased production of the myxovalargins.

Fermentation and growth specification

To allow large scale production of myxovalargins and mutaynthesis studies, cultivation was transferred to fermentation scale. Results of these experiments were reported to MWIS in Braunschweig to facilitate up-scaling fermentation and downstream process development for MCy6431. First cultivation experiments in 1 L fermentation vessels led to massive aggregation on steel surfaces like baffle, electrodes and air tubing. This problem was overcome completely by removal of baffles, which lead to a turbulent flow and shear stress, a putative reason for the strong agglomeration. Cultivation was conducted as batch culture and in preliminary experiments compared to shake flask cultivation. As it was shown that production and growth were optimized by pH adjustment, pH trend was analysed in shake flask, since during fermentation this parameter can be hold steady. A pH adjustment could be detected, leading from pH 7.0 to a pH of 8.0 during cultivation process. When comparing growth rates between shake flask and fermenter, only slight differences could be detected 0.081 h^{-1} versus 0.076 h^{-1}, respectively. In a following experiment in 1 L scale cultivation with XAD 16 was compared versus no XAD addition. Results showed only small difference in growth rates of 0.076 h^{-1} for the XAD culture versus 0.084 h^{-1} without XAD. Nevertheless, in shake flask it could be shown that lower cell density is achieved, when cultivating without XAD 16.

To analyse growth and metabolite production, samples of supernatant and cell extract were taken separately from the broth of fermenter and shake flasks (Figure 18). OD_{600} measurements were taken in triplicates at each time point. Log phase was reached after 20h, while stationary phase followed after approximately 40h. Stationary phase quickly fades off into die-off phase within about 20 h. Maximal cell density of about OD_{600}: 2.2 (see fermentation and determined from previous experiments) was not reached in the shake flask experiment since XAD was not added in this experiment, as a reproducible amount of XAD cannot be taken from the cultivation broth especially in case of the fermenter vessel. Nevertheless, a dependency of secondary metabolite production and cell growth could be determined. Amounts are given relatively in normalized units. Three main compound classes were analysed: phenalamides (A1 and A2), myxoprincomides (mxp547) and the myxovalargins (A-C). Phenalamides can be found in cell extracts and supernatant, while myxoprincomides and myxovalargins mainly occur in the supernatant. In the shake flask experiment phenalamides are primarily accumulated in the cells. In the fermenter phenalamides are produced during log-phase and decrease in die-off phase, which is also true for the myxoprincomides. A similar production trend for the myxoprincomide

can be seen in the shake flask, though with a time delay of approximately 20 h. Myxovalargins on the other hand are constantly excreted in the supernatant. Even during die-off phase the myxovalargin concentration increases in the broth. Nevertheless, the fastest increase in production rate is achieved during log phase.

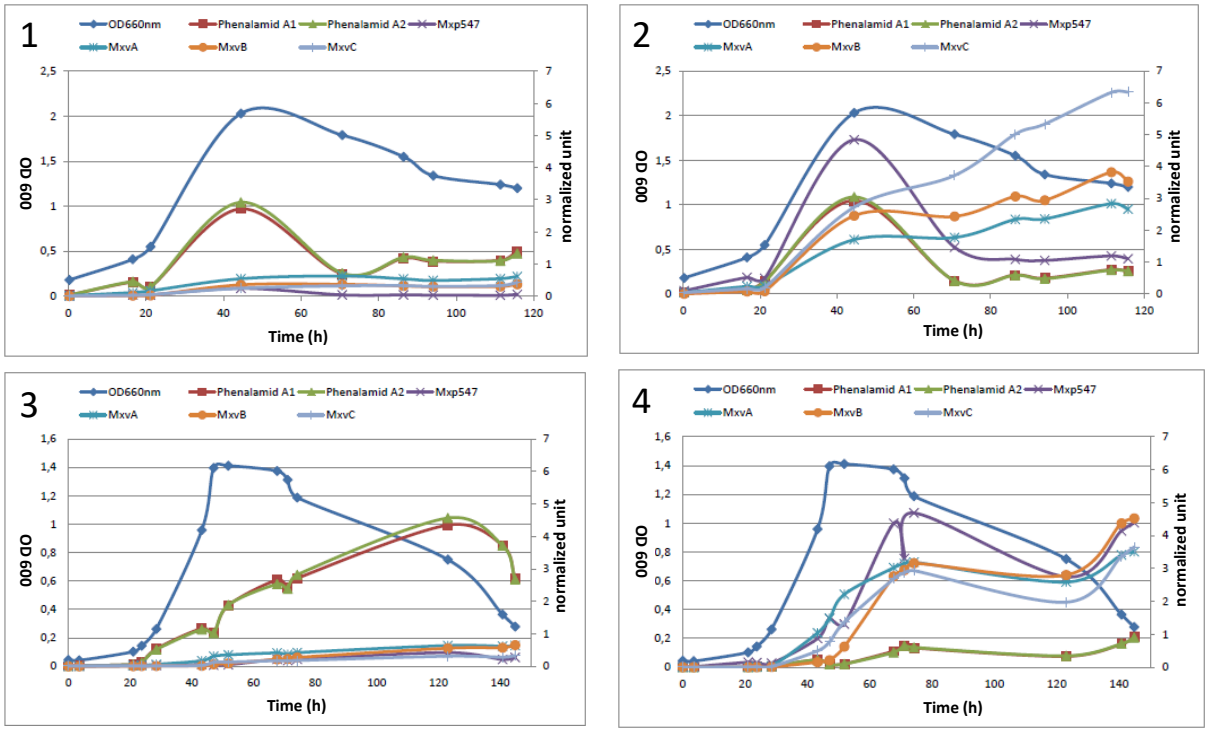

Figure 18: Comparison of fermentation and shake flask cultivation. [1] **The upper panels (1, 2) show cultivation in shake flasks, while panel 3 and 4 show fermenter cultivation. Samples of cell extract (left panels) and supernatant (right panels) were taken separately and extracted. Production levels of major secondary metabolites are given in normalized units as factor compared to the internal standard sulfadimethoxin (6,75 mg/L), allowing a relative comparison, since pure standards of the compounds were not available for the experiment. Prodcution of the myxovalargins is constant, although the main increase takes place during log and stationary phase. Myxoprincomide and phenalamide production on the other hand decreases in die off phase.**

[1] Experiments were partially carried out and compiled within internship by A.Lis under supervision of U.Scheid. Graphs taken from intership report.

4.1.4 Secondary metabolite profiling

Using the established mutagenesis method, biosynthetic gene clusters (BGCs) of the most abundant metabolites in the chromatographic profile of MCy6431 were knocked out. The mutants of the phenalamide, myxoprincomide and myxovalargin BGC knock-outs were genetically confirmed and showed the expected loss of the compound family in their chromatograms. Comparison between the knockout mutants and against the wildtype showed no prominent difference in their antibiotic profile against chosen gram negative and positive bacteria except for the myxovalargin knock-out, which led to almost a total loss of antibiotic activity of the crude extract. The supression of the metabolites of the phenalamid and myxoprincomide compound classes, therefore, did not increase the crude extract activity. However, this results confirms again the prominent antibiotic activity of the myxovalargins.

4.1.5 Myxovalargin biosynthetic gene cluster

All chapters referring to genetic information from the myxovalargin BGC relate to sequences from MCy6431, if not mentioned otherwise.

By knockout experiments, the core region of the myxovalargin cluster could be narrowed down to a sequence of almost 70 kbp. The genetic sequence encoding the domains of the fourteen modules of the myxovalargin BGC comprises approximately 58 kbp and an upstream region of appr. 8 kbp encoding additional proteins participating in the myxovalargin production. The NRPS domains encoding region is subdivided in 5 genes (*mxvA – E*), while the upstream part covers additional 6 genes (*mxvF – K*) (Figure 19). With 58 kbp the myxovalargin BGC is one of the largest reported and functionally assigned NRPS-type gene clusters up-to-date. A detailed overview of the respective genes and conducted knockout experiments is given in Figure 20 and Table 2. Beside most of the core genes, several adjacent genes were knocked out to narrow down the cluster boundaries. Furthermore, putative genes or pathways, which could be responsible for production of myxovalargin precursors, were targeted for knockout experiments like the arginine decarboxylase or the branched chain ketoacid dehydrogenase complex.

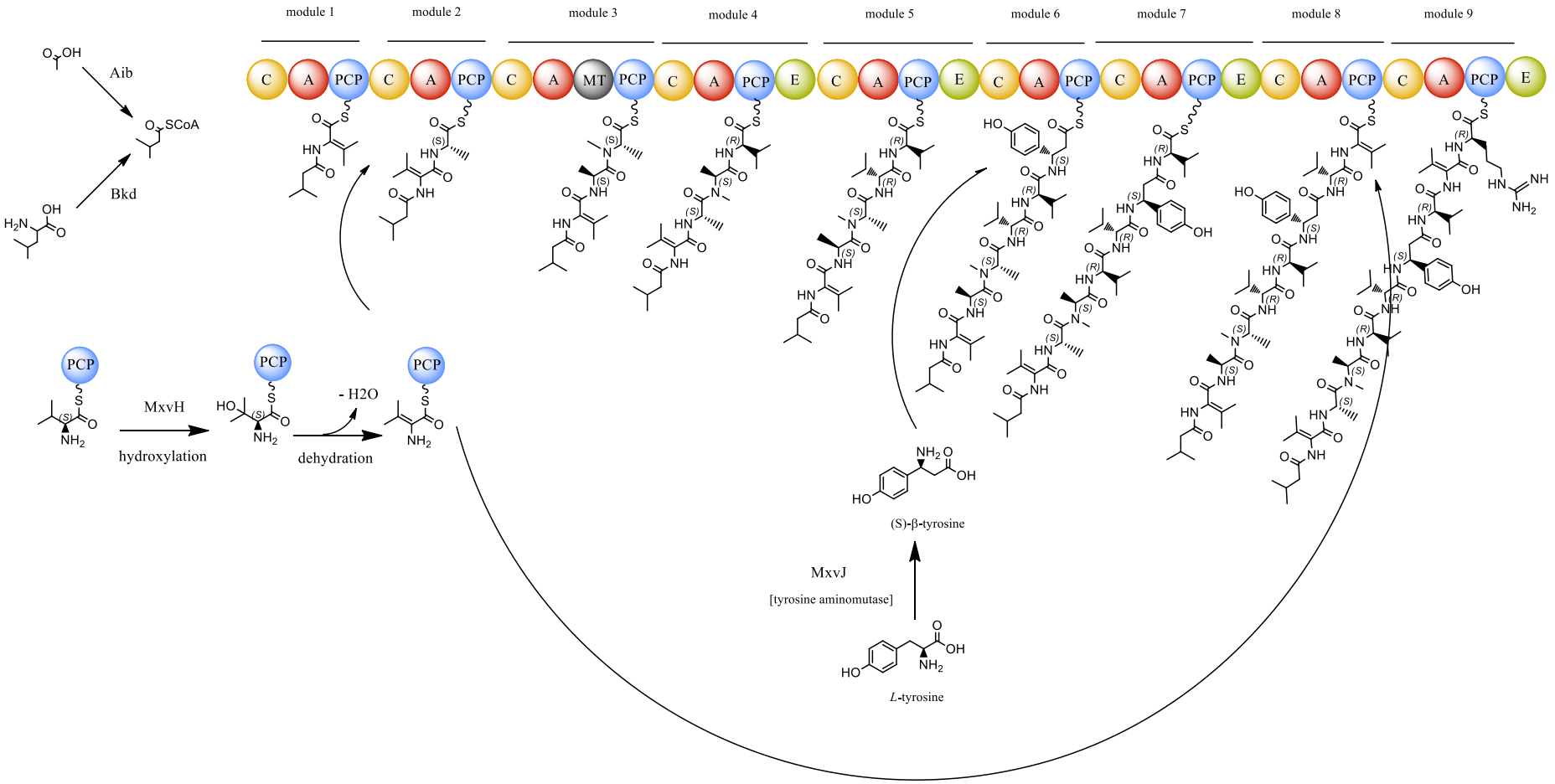

Figure 19a: Myxovalargin biosynthesis. The enzymes of the 14 modules spanning non-ribosomal peptide synthase of Myxovalaring A are encoded on genes *mxvA, C, D, E*. The synthesis starts with the Isovaleryl-CoA starter putatively generated from the branched chain ketoacid dehydrogenase (Bkd*)* and/or alternative IV-CoA biosynthesis (Aib) . The nine following modules catalyze beside the incorporation of L-amino acids, also the formation of D-amino acids, the incorporation of (S)-*β*-tyrosine generated by the tyorsine aminomutase and the formation of dehydro amino acids. (continuation on next page)

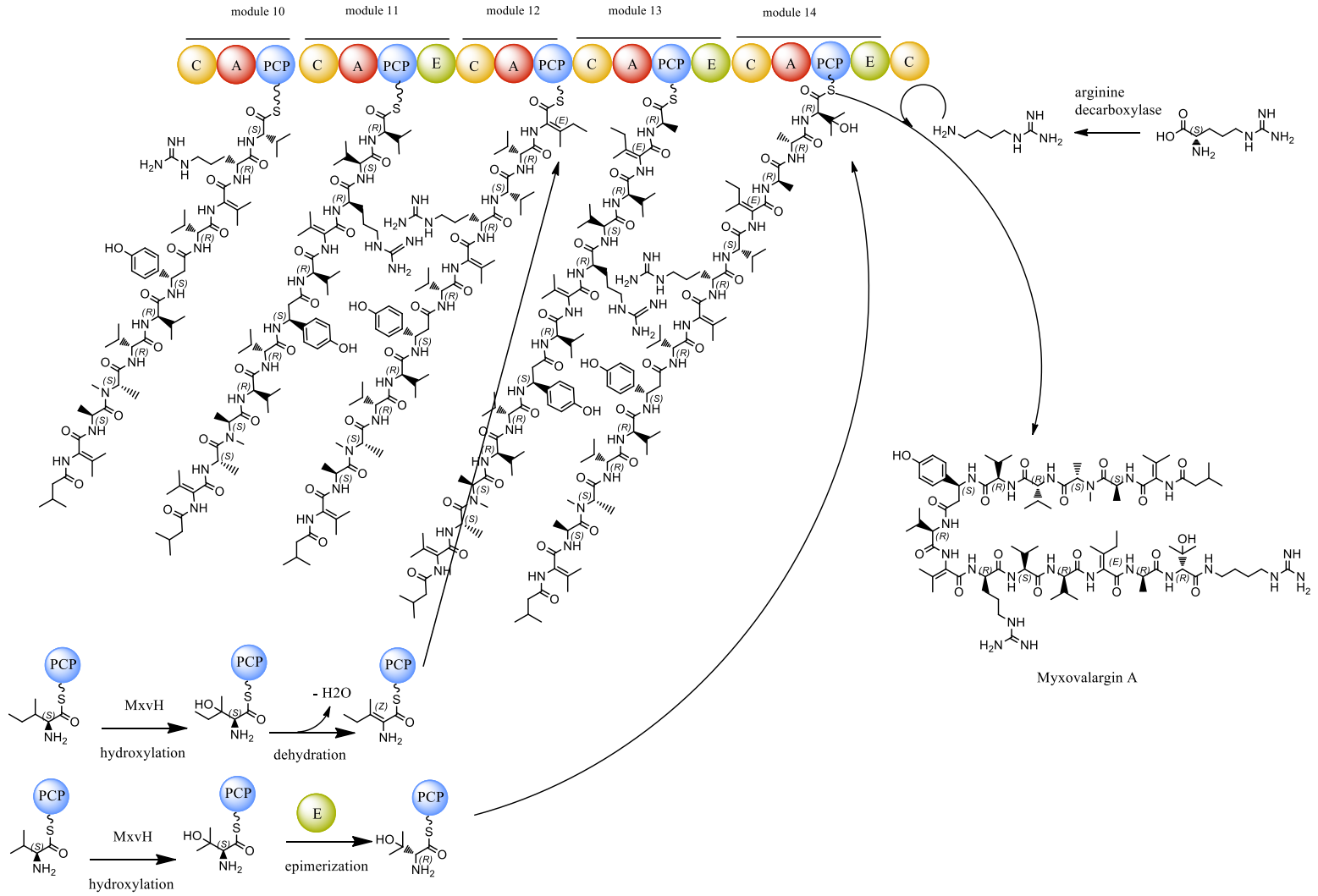

Figure 19b: Myxovalargin biosynthesis. The following modules 10 – 14 catalyze the formation of dehydro isoleucine as well as the formation of hydroxy valine formed by the putative *β*-hydroxylase encoded on *mxvH*. Finally, the incorporation of agmatine by the final condensation domain catalyzes the release from the assembly line.

Figure 20: Genetic organisation of genes assigned to the myxovalargin biosynthesis cluster (*mxvA - K*). *mxvA, C, D* compressed for visibility.

Table 2: List of genes of the myxovalargin biosynthesis cluster, adjacent genes or putatively associated genes.

ORF	similarities	Proposed function	Knockout/production	Distance from NRPS start
mxvA	NRPS	module 1 – 3	yes/ no	1 – 10854 bp
mxvB	NRPS	PCP domain	Not achieved	10866 – 11378 bp
mxvC	NRPS	module 4 – 9	yes/ no	11375 – 36451 bp
mxvD	NRPS	module 10 – 13	yes/ no	36454 – 52122
mxvE	NRPS	module 14	Not achieved	52128 – 58064 bp
mxvF	Microcystin synthetase associated protein	TE II function	-	79-903 bp (up)
mxvG	MbtH like domain containing protein	MbtH function	-	1506 – 1721 bp (up)
mxvH	Antibiotic biosynthesis protein	Val-/Ile-*β* hydroxylase	yes/ no	1798 – 3381 bp (up)
mxvI	ABC transporter related protein	ABC transporter – Permease	yes/ yes	3394 – 5232 bp (up)
mxvJ	Tyrosine 2,3 aminomutase	Tyrosine aminomutase	yes/ no	5304 – 6914 bp (up)

mxvK	ABC transporter related protein	ABC transporter – ATPase	yes/ yes	6911 – 8431 bp (up)
ORF 1	UPF0059 membrane protein	unknown	-	8625 – 9218 bp (up)
ORF 2	Cupin	Unknown	yes/ yes	9237 – 10364 bp (up)
ORF 3	Transcriptonal regulator, LysR family	Unknown	Not achieved	10478 – 11365 bp (up)
ORF 4	DNA alkylation repair enzyme	Unknown	-	11376 – 12119 bp (up)
ORF 5	Dehydrogenase/ reductase SDR family member	dehydrogenase	Yes/yes	12277 – 13179 bp (up)
ORFdown1	Adenylate cyclase	Unknown	Yes/ yes	76 – 4259 bp (dn)
ORFdown2	Hypothetical protein	Unknown	-	4400 – 4802 bp (dn)
ORFdown3	Multicopper oxidase domain containing protein	Unknown	Yes/yes	5002 – 6463 bp (dn)
ORFdown4	Hypothetical protein	Unknown	-	6559 – 6712 bp (dn)
ORFdown5	Deoxyhypusine synthase	Unknown	Yes/ yes	6753 – 7722 bp (dn)
ORFdown6	Long chain fatty acid CoA ligase	Unknown	Not achieved	7963 – 9787 bp (dn)
adc	Arginine decarboxylase	Agmatine biosynthesis	Not achieved	Distant
gct	Glutaconate transferase	Isovaleryl biosynthesis	Yes/ yes	~ 30 kbp (dn)
bkd	Branched chain ketoacid dehydrogenase	Isovaleryl biosynthesis	Yes/ yes	~ 90 kbp (dn)

4.1.6 Proteins MxvABCDE

The NRPS assembly line is located on genes *mxvA – E*. The total assembly line spans fourteen modules, which are located on *mxvA, C, D* and *E*. All modules are organized in linear order from *mxv*A modules 1 – 3, *mxvC* modules 4 – 9, *mxvD* modules 10 – 13 and *mxvE* module 14 (Table 3).

Table 3: Predicted domain specificity in the myxovalargin gene cluster. C = condensation domain, A = adenylation domain, PCP = peptide carrier protein, MT = methyltransferase; DcL = condensation of upstream D amino acid with downstream L amino acid. LcL = condensation of upstream L amino acid with downstream L amino acid

Gene	Module	Domain order	Domain specificity	Phenotype in Myxovalargin A
mxvA	Module 1	C-A-PCP	C domain: LcL A domain: Val	dehydro - valine
	Module 2	C-A-PCP	C domain: DcL A domain: Ala	l-alanine
	Module 3	C-A-MT-PCP	C domain: LcL A domain: Ala	N-methyl-L-alanine
mxvB	-	PCP	-	-
mxvC	Module 4	C-A-PCP-E	C domain: LcL A domain:Val	D-valine
	Module 5	C-A-PCP-E	C domain: DcL A domain: Val	D-valine
	Module 6	C-A-PCP	C domain: DcL A domain: β-tyrosine	(S)-β -tyrosine
	Module 7	C-A-PCP-E	C domain: LcL A domain:Val	D-valine
	Module 8	C-A-PCP	C domain: DcL A domain: Val	dehydro - valine
	Module 9	C-A-PCP-E	C domain: DcL A domain: (Gln)	D-arginine
mxvD	Module 10	C-A-PCP	C domain: DcL A domain: Val	L-valine
	Module 11	C-A-PCP-E	C domain: LcL A domain: Val	D-valine
	Module 12	C-A-PCP	C domain: DcL A domain: Ile	dehydro-isoleucine
	Module 13	C-A-PCP-E	C domain: DcL A domain: Ala	D-alanine
mxvE	Module 14	C-A-PCP-E	C domain: DcL A domain: Val	hydroxy-valine
	-	C	C domain: DcL	-

Modules 1 – 3 (MxvA) encoded on *mxvA*

MxvA has a size of 10854 bp. Module 1 consists of the domain order C-A-PCP, module 2 of C-A-PCP and module 3 of C-A-MT-PCP. Thus, all necessary basic domains for each module are present. A domain specificity (accoding to NRPS-predictor 2) of module 1 shows similarity to valine incorporating domains, module 2 for alanine and module 3 again for alanine. All predictions for A domain specificity fit with the amino acid order in myxovalargin A. Module 1 shows LcL reaction specificity, nevertheless the module is closely related to condensation domains, which catalyse condensation with starter units, which fits to the function module 1. Module 2 interestingly shows DcL reaction specificity though module 1 incorporates L-valine and does not contain an epimerization, thus LcL reaction would be expected. However, the valine incorporated by module 1 in the final molecule is present as dehydro-valine. While the modules reveal no hint on the biosynthesis of the dehydro amino acid, the C-domain specificity can be seen as a hint on the timing of this modification. Comparison with the two other condensation domains (module 9 and 13) catalysing condensation with the dehydro-amino acid building block, show the same specificity. Moreover, these domains group together in a separate clade (Figure 37). This indicates that the condensation performed by C domains of module 2, 9 and 13 conjugate an amino acid on the previous module, which is not in the L-form. As the dehydro amino acids show no stereocenter, the grouping of the condensation domains imply that the modification of the L-amino acids is performed before the condensation. Considering that a hydroxy moiety is present in myxovalargin A as well as the presence of dehydro amino acids in parallel with hydroxy moieties in other molecules like the yaku´amides, the proposed mechanism is a hydroxylation followed by a dehydration (see chapter 4.1.8). Module 3 again exhibits the expected LcL specificity. The N-methyltransferase (MT) in module 3 is responsible for the N-methylation of the alanine as described for the structure. Additional information on the origin of the starter unit 3-methylbutyryl is not present on this gene.

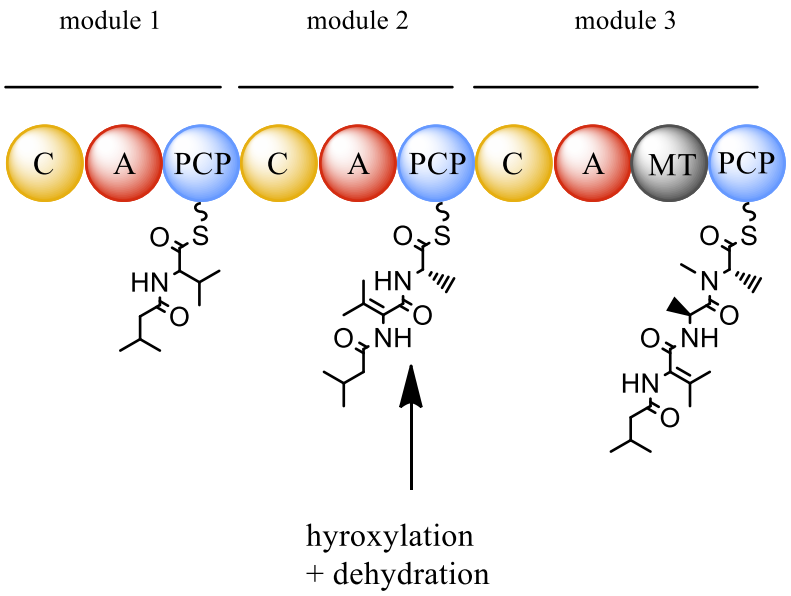

Figure 21: Domain organization of MxvA. Module 1 incorporates the valine building block, which is tethered to the 3-methylbutyryl starter. The proposed mechanism is a hydroxylation followed by a dehydration of the valine, thus, forming the dehydro-valine moiety. The second elongation step by module 2 adds an alanine, while module 3 adds the second alanine. The methyltransferase in module 3 performs the respective N-methylation as present in myxovalargin A.

Single PCP domain encoded on *mxvB*

MxvB is a short reading frame of appr. 600 bp. It encodes a PCP domain in the downstream part of the sequence, while the upstream region shows similarities to an A domain terminus. The function of this PCP domain is unclear. Due to its small size it was not possible to knockout this gene. A double crossover approach was not successful. A rudimentary function could be assumed, yet the gene is conserved in all accessible myxovalargin BGCs. Thus, it is postulated that the gene holds a function during incorporation of precursors.

Modules 4 – 9 (MxvC) encoded on *mxvC*

MxvC encodes module 4 (C-A-PCP-E), module 5 (C-A-PCP-E), module 6 (C-A-PCP), module 7 (C-A-PCP-E), module 8 (C-A-PCP) and module 9 (C-A-PCP-E). A domain specificity in order of modules is valine, valine, *β*-tyrosine, valine, valine and arginine. Module 4 and 5 contain an epimerization domain, which forms the D-amino acids as expected by the chemical structure of myxovalargin A. The A-domain of module 6 incorporates the unusual *β*-tyrosine building block, which is derived from tyrosine by the tyrosine aminomutase of *mxvJ*, which was characterized and described by Krug et al. [126]. In contrast to the assigned stereochemistry of valine in myxovalargin A, module 7 shows an epimerization domain. This discrepancy to the

described stereochemistry of myxovalargin A is discussed in chapter 4.1.12.. Module 8 incorporates valine. While module 9 must incorporate arginine, domain specificity by NRPS predictor 2 indicates glutamic acid (80% similarity). Several examples like the myxoprincomide cluster exhibit discrepancies between A domain prediction and actual substrate[127], this inaccuracy can be due to e.g. substrate promiscuity[128] or closely related building blocks due to similar chemical or stereochemical properties. The A domain region is conserved in all sequenced myxovalargin BGCs. The module exhibits the epimerization domain, which is required to form the D-amino acid. Module 4 connects L-Alanine of module 3 with valine and shows LcL specificity. Module 5 and 6 C-domains connect DcL which is in alignment with the epimerization domain in module 4 and 5. Module 7 conjugates LcL in accordance with L-Valine of module 6, while module 8 connects DcL caused by the epimerization domain in module 7. As module 9 couples the dehydro amino acid with valine, the C-domain specificity fits with the predicted model as described for module 2 in MxvA. Thus, C-domain reaction predictions fit with the module order and epimerization domain organization.

Modules 10 – 13 (MxvD) encoded on *mxv*D

MxvD encodes modules 10 – 13. Module 10 is organized of C-A-PCP. The A domain specificity for module 10 is weak. The condensation domain specification for DcL matches the incorporation of D-Arginine in module 9. Module 10 does not show an epimerization domain; this discrepancy to the described stereochemistry of myxovalargin A is discussed in chapter 4.1.12. Module 11 with C-A-PCP-E order and A domain specificity for valine fits with the chemical structure. Also, the LcL specificity supports the missing epimerization domain in module 10. Module 12 consists of C-A-PCP and A domain specificity for isoleucine. Condensation domain specification for DcL is in accordance with module 11. Isoleucine is present as dehydro amino acid. The module gives no hint on the modification reaction, wheareas module 13 again shows C-domain specificity for a DcL reaction as noted for module 2 in MxvA and 9 of MxvD. Furthermore, module 13 is organized of C-A-PCP-E, where the A-domain has an alanine specificity. The epimerization domain catalyzes the formation of the D-alanine.

Terminal module 14 (MxvE) encoded on *mxvE*

MxvE encodes module 14, which consists of C-A-PCP-E with an A domain specificity for valine. The specificity of Valine matches with the appearance of the hydroxy valine in this position. However, there is no particular hint on the hydroxylation process. The epimerization

domain in module 14 shows no abnormalities in sequence alignment and is thereby regarded as functional epimerization domain. The condensation domain catalyzes the expected DcL reaction. After module 14 a single C domain follows as last domain of the open reading frame and thus of the myxovalargin NRPS cluster. The C domain also does not show any noticeable difference to regular C domains and groups in the C-domain alignment with DcL domains, which supports the functionality of the E-domain in module 14. The *mxvE* region including the stop codon after the terminal C-domain could be identified as highly conserved over all myxovalargin producers sequenced. A thioesterase domain I (TEI) is not present in the protein. The role of the C-domain in the termination mechanism and incorporation of agmatine is discussed in 4.1.10.

4.1.7 Thioesterase and MbtH like protein – Genes *mxvF* and *mxvG*

Two short genes are located upstream of the NRPS assembly line. *MxvF* encodes a single thioesterase (TE) of ~850 bp. Thioesterases type I are responsible for the cleavage of the thioester between the pPant arm of the PCP domain from the terminal module and the molecule assembled. [129] Thioesterase II domains on the other hand cleave intermediates from the assembly line, when blocked by false assembly or other issues. Since a TEI is not present in the terminal NRPS module of myxovalargin, the thioesterase on *mxvF* was analysed in-silico to specify its putative function. [130] The comparison shows, that *mxvF* clearly groups with thioesterases type II (TE II; Figure 22) and therefore the above described function as defined for other TE II is assumed.

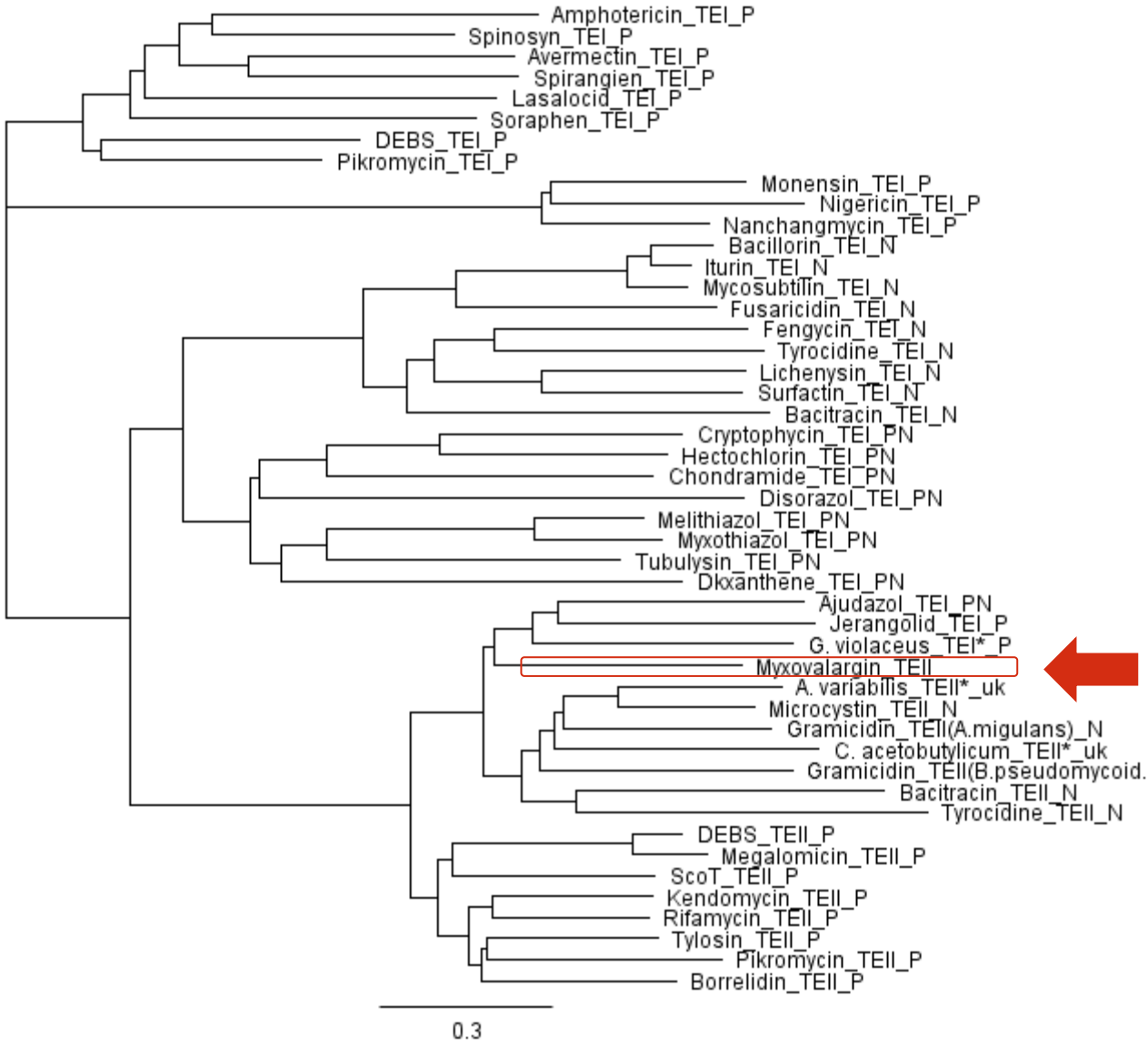

Figure 22: Thioesterase type I (TEI) and type II (TEII) were aligned and their elation visualized in a tree diagram. The gene *mxvF*, marked in red, clearly groups with other TEII domains and is therefore proposed to have the function of cleaving intermediaties from blocked PCP domains, as described in literature.

MxvG (~230 bp) the second ORF upstream of *mxvA* shows similarity with MbtH-like proteins. [131] Those proteins were shown in several cases to facilitate activation by the adenylation domain in NRPS assembly lines. [132–134] Thus their activity correlates with the production rate of a secondary metabolite, but they are not essential. *MxvG* might therefore be relevant for yield optimization by biotechnological tools.

4.1.8 putative β-hydroxylase - *MxvH*

The 1632 bp ORF *mxvH* is located ~1800 bp downstream of the myxovalargin NRPS assembly line. Blastp search did not yield significant hits to known enzymes. Nevertheless, a knockout of this gene resulted in total loss of myxovalargin production. To rule out a polar effect on the consecutive genes, including the essential tyrosine aminomutase (*mxvJ*), feeding of *β*-tyrosine to the *mxvH* knockout mutant was analysed, but did not lead to a restoration of myxovalargin production in contrast to a supplementation of *β*-tyrosine to the *mxvJ* mutant. Furthermore, does the knockout of the following gene *mxvI*, not lead to production abolishment and thereby no polar effect exists between *mxvH* and *mxvI* on *mxvJ*. As mentioned above, blastp search does not yield significant results on the similarity of *mxvH* with described enzymes. Thus, a 3D model of the final protein using Phyre 2, which showed 100 % confidence in modelling prediction, was compared to proteins of the protein data bank (PDB).[135] The *β*-hydroxylase of the chloramphenicol biosynthesis, CmlA, showed 39% similarity. This enzyme catalyzes the hydroxylation of 4-aminophenlyalanine in *β*-position during the assembly process (Figure 23).[136] Thus, a functional relationship is postulated, implying that *mxvH* is the central enzyme in *β*-hydroxylation of the amino acid building blocks in myxovalargin. Furthermore, two structural elements might be derived by this enzyme, which were not yet described in the literature. This is the hydroxy-valine and the dehydro building blocks of valine and isoleucine, which we assume to be synthesized by hydroxylation and subsequent dehydration. Different observations support this hypothesis. Another large polypeptide which was identified from the marine sponge *Ceratopsion* sp. are the yaku´amides. [137,138,138] These large putative NRPS products exhibit concurrent presence of dehyro as well as hydroxy valine and isoleucine moieties in their primary sequence. To date, only few examples of either hydroxy valine/ isoleucine or dehydro valine/ isoleucine are known. The antrimycins [139] and pyridomycin [140] are examples of dehydro-isoleucine in secondary metabolites. Examples of hydroxy valine can be found in the myxoprincomides [127], as well as the coramycins [141]. Nevertheless, none of these compounds show a simultaneous occurrence of dehydro and hydroxy amino acids, as known for the myxovalargins and yaku´amides. Thus, it seems likely that the biosynthesis mechanism in the myxovalargins and the yaku´amides differs from the other mentioned metabolites. Hence, it explains the lack of *mxvH* in the cluster of pyridomycin, coramycin or myxoprincomide, which was determined by alignment with *mxvH*. Two closely located putative dehydrogenases, appr. 15 kbp and 30 kbp upstream of *mxvA*, were knocked out in separate mutants by gene disruption, but a loss or alteration of myxovalargin production did not appear. To determine the exact

precursor and get hints on the mechanistic timing of the hydroxylation, d6-hydroxy valine was supplemented to a wildtype strain, as well as the *mxvH* knockout mutant. Additionally, d6-hydroxy valine was supplemented together with *β*-tyrosine to rule out any effect on the tyrosine aminomutase. An incorporation of a hydroxy valine precursor was not observed. Thus, it is assumed, that the PCP bound valine intermediate is hydroxyled, which is in accordance to the mechanism described for CmlA, which might be another indication of their substantial biological similarity.

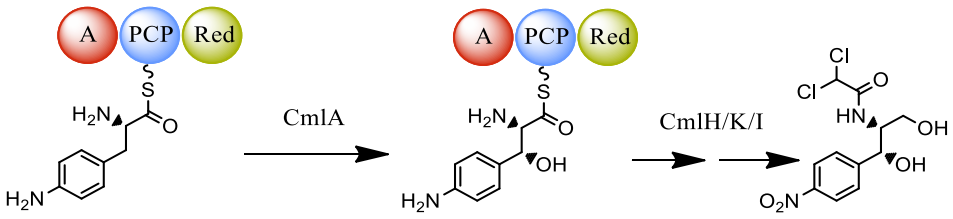

Figure 23: CmlA catalyzes the *β*-hydroxylation of 4-aminophenylalanine in chloramphenicol biosynthesis. Due to structural homology, MxvH is assumed to catalyse the *β*-hydroxylation of valine in the case of myxovalargins by a similar reaction mechanism.

4.1.9 Tyrosine aminomutase - *mxvJ*

The gene *mxvJ* encodes a tyrosine aminomutase, which has been in vitro characterized previously for its product specificity, identifying selectivity for (S)-*β*-tyrosine in comparison to the tyrosine aminomutase of the chondramides, which generates (R)-*β*-tyrosine. [126,142,143] A knockout of *mxvJ* led to a loss of myxovalargin production. As it could be shown in vitro that the reaction is independent from the assembly line, it was possible to restore production by supplementation of *β*-tyrosine (Figure 25). Though the production yield of myxovalargin in the knockout mutant by addition of synthesized (S)-*β*-tyrosine was not 100% compared to the wildtype, a production of 60% denotes the possibility to use this approach for mutasynthesis studies. Further feeding of *β*-tyrosine like molecules in a mutasynthesis approach, led to their incorporation in the *mxvJ* deficient mutant (Figure 24). Due to material availability, racemates were used for the feeding experiments except for the native (S)-*β*-tyrosine.

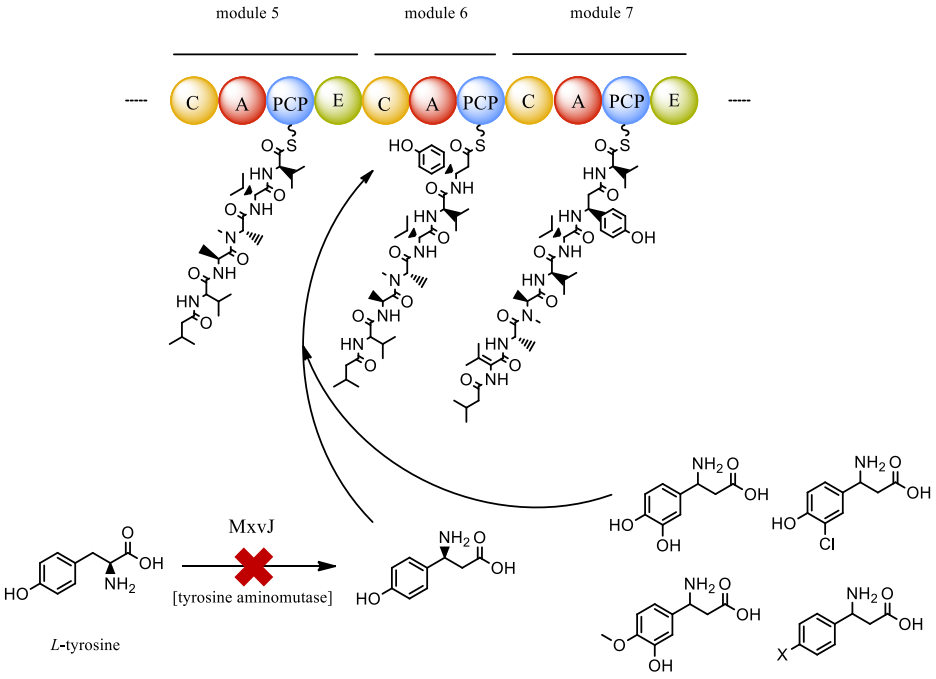

Figure 24: (S)-*β*-tyrosine is stereospecifically generated from *L*-tyrosine by the tyrosine aminomutase (*mxvJ*). The building block is incorporated in the growing polypeptide by module 6 of the NRPS assembly line. The A domain in this module shows specificity for (S)- *β* -tyrosine. By knockout of *mxvJ* myxovalargin production is abolished, but can be restored by supplementation of (S)- *β*-tyrosine. Furthermore, closely related building blocks are accepted and lead to the production of the respective mutasynthetically derived myxovalargins.

Different mutasynthons were fed at 0.2 mM concentration. The incorporation was mainly dependent on the size of the substituent replacing the hydroxy group. Halogens thereby showed incorporation levels F > Cl > Br. Also, larger substituents as a methoxy group showed significant decrease in incorporation. Furthermore, the size of the substituent in para position relative to the hydroxy group is important for incorporation. A chlorination in this position shows better acceptance compared to a hydroxy group. However, the at the para position chlorinated derivative shows a similar incorporation as the native *β* -tyrosine derivative. In general, the yields allow a sufficient purification of derivatives for assays, but could be also used for large scale production. Furthermore, mutasynthons were not enantiomerically pure available for the experiments, since they were synthesized and purified without enantioselectivity. Hence, though a high concentration was fed, the respective enantiopure mustasynthons might yield even higher amounts even comparable to the wildtype. An

evaluation of an optimized feeding protocol regarding frequency, concentration, environmental conditions and broth culture could further increase the production levels.

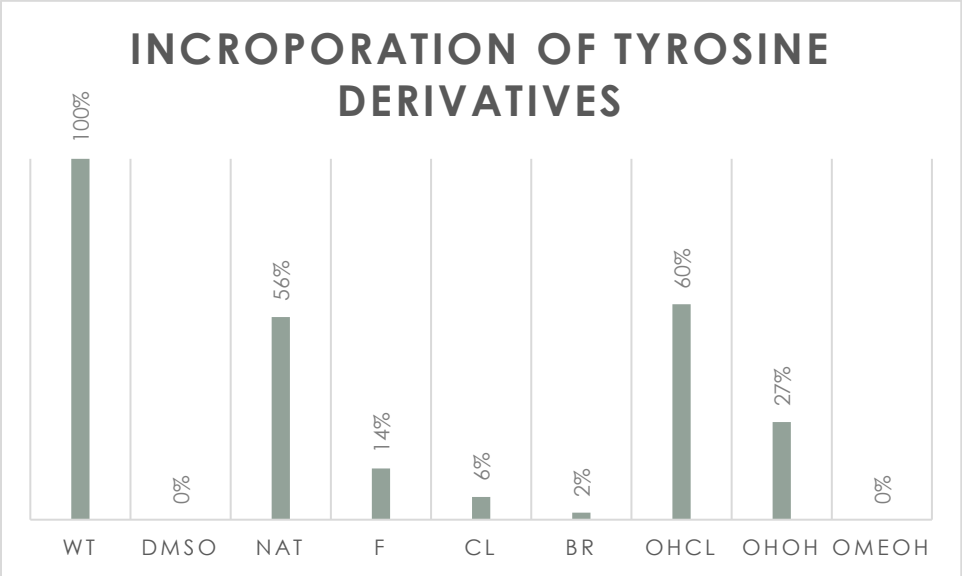

Figure 25: Yields of myxovalargin A after supplementation of different *β*-tyrosine derivatives in the *β*-tyrosine aminomutase knockout mutant relative to the production of the wildtype mutant. DMSO as solvent of the mutasynthons was used as negative control. A decrease in production levels could be observed with an increase of substituent size at the benzol ring. WT: wildtype; DMSO: Dimethylsulfoxide; NAT: 2-amino-3-(4-hydroxyphenyl)propanoic acid (*β*-tyrosine); F: 2-amino-3-(4-fluorophenyl)propanoic acid; Cl: 2-amino-3-(4-chlorophenyl)propanoic acid; Br: 2-amino-3-(4-bromophenyl)propanoic acid; OHCl: 2-amino-3-(3-chloro-4-hydroxyphenyl)propanoic acid; OHOH: 2-amino-3-(3,4-dihydroxyphenyl)propanoic acid; OMeOH: 2-amino-3-(3-hydroxy-4-methoxyphenyl)propanoic acid.

The 2-amino-3-(3,4-dihyroxyphenyl)propanic acid mutasynthon derived compounds were purified by scale up to 5 L and purification by normal phase silica gel, followed by reverse phase preparative and semipreparative purification steps. Activity of all purified compounds revealed a loss in activity especially of the *Pseudomonas aeruginosa* activity (Table 4). The activity difference against *Micrococcus luteus*, showing the expected highest activity for the myxovalargin A derivative > myxovalargin B derivative > myxovalargin C derivative nevertheless can serve as a positive control for the activity assay. Though the activity could not be increased by this experiment, the total loss of activity especially against *Pseudomonas aeruginosa* indicates the structural importance of the *β* -tyrosine moiety in the pharmacophore. Nevertheless, additional mutasynthetically derived myxovalargins should be evaluated including chemical and structural considerations.

Table 4: Activity of the mutasynthetically derived myxovalargins from 3-amino-3-(3,4-dihydroxyphenyl)propanoic acid (OHOH).

	MIC [µg/ml]				IC50	In vitro biofilm inhibition
strain	**M.luteus DSM 1790**	**S.aureus Newman**	**PA01**	**PA14**	**CHOK1**	**PA14**
OHOH_mxvD	> 64	> 64	> 64	> 64	> 111,1	no
OHOH_mxvC	16	64	> 64	> 64	> 111,1	no
OHOH _mxvB	8	64	> 64	> 64	> 111,1	no
OHOH _mxvB2	64	> 64	> 64	> 64	> 111,1	no
OHOH _mxvA	4	32	> 64	> 64	> 111,1	yes
OHOH _mxvE	64	> 64	> 64	> 64	> 111,1	no

4.1.10 Agmatine

Agmatine is the biogenic amine of arginine and is generated via decarboxylation by the arginine decarboxylase (adc).[144,145] It functions as intermediate of the putrescine biosynthesis (Figure 26).

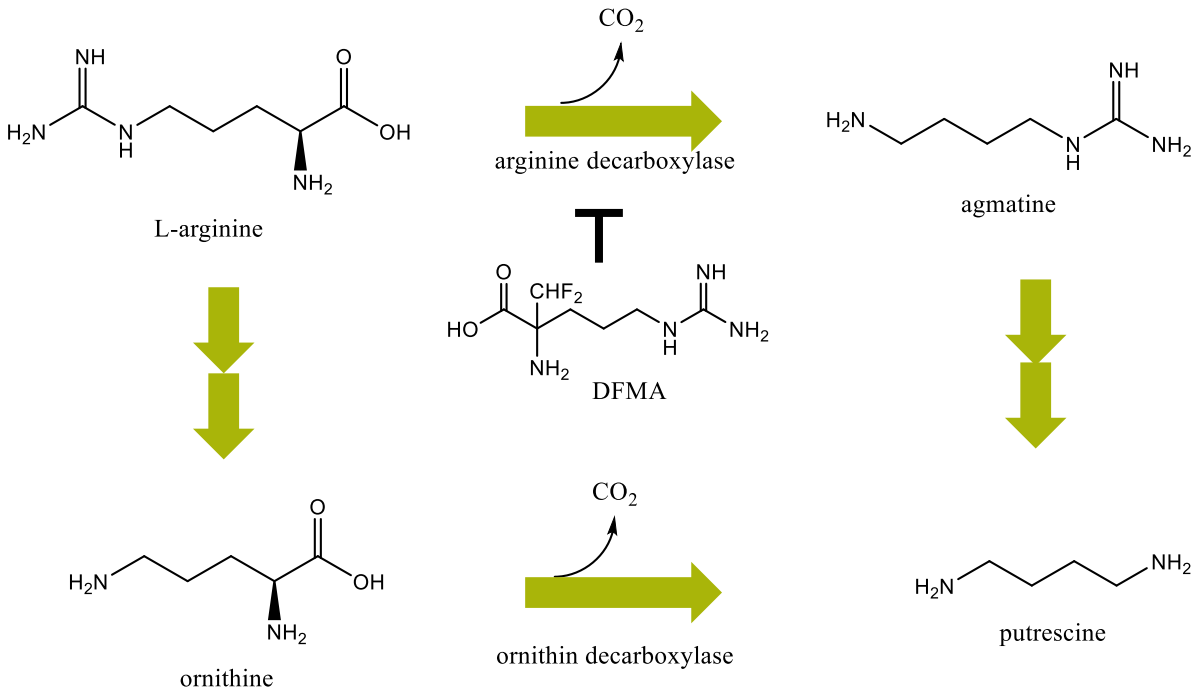

Figure 26: The role of Agmatine in primary metabolism. Agmatine is generated from arginine, catalysed by the arginine decarboxylase. In further steps, it can be transformed into putrescine, which can also be produced from arginine via ornithine by the ornithine decarboxylase. Difluoromethyl arginine (DFMA) irreversibly blocks the arginine decarboxylase by competitive inhibition.

Only one second natural product is known so far, which exhibits an agmatine moiety. The NRPS assembly line of this compound, called aeruginoside B, shows a terminal C- and PCP-domain following the final module. [146] The PCP domain was postulated to be inactive and the dissociation to be facilitated by condensation of the agmatine residue with the polypeptide chain catalysed by the C-domain, thus offering no carboxy group to form a thioester with the consecutive PCP domain. [146] The actual incorporation of agmatine instead of an incorporation of arginine followed by decarboxylation could, however, not be proven. The compound class of aeruginosides is produced by several Planktothrix and Microcystis strains. Interestingly also the presence of argininol and argininal, instead of agmatine was shown for certain Mycrocystis strains, but not for Planktothrix. Yet, these producers harbour a complete module (C-A-PCP-Red) instead of the rudimentary C-PCP domains. [147] Also the spumigins, which are structurally related to the aeruginosides offer argininal, argininol and even complete arginine C-terminal residues. [148] Hence, these biosynthesis mechanisms seem to vary from the mechanism of aeruginoside B from Planktothrix and the myxovalargins from Myxobacteria. A terminal condensation domain, which does not belong to a complete module does also occur in case of the myxovalargins located on *mxvE*, and is assumed to catalyse the condensation of the free agmatine with the polypeptide chain (Figure 27). Hence an in-silico analysis was conducted, which did not provide evidence for inactivity, any unusual features or grouping to condensation domain-like proteins, which are able to catalyse thioesterase reactions, as known for e.g. CroK from the crocacin pathway in Myxobacteria. [51]

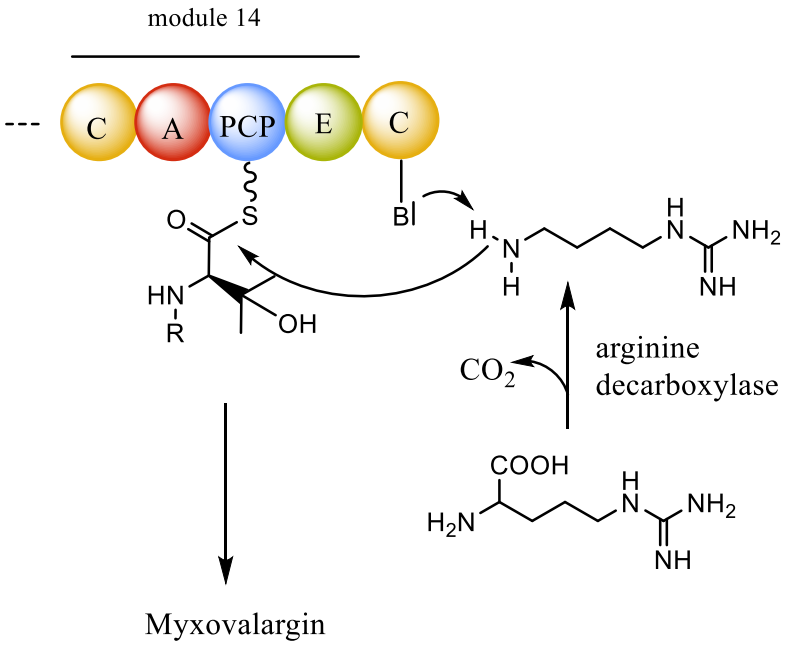

Figure 27 Suggested mechanism of the incorporation of agmatine in the polypeptide chain by the terminal condensation domain. The lack of a carboxy group in the terminal agmatine residue results in a dissociation of the assembly line. The enzyme arginine decarboxylase (Adc) was shown to catalyse the synthesis of arginine from agmatine and thus is assumed to be the precursor building protein.

By blast comparison the arginine decarboxylase gene could be found in most myxobacterial genomes, thus underpinning its central biosynthetic role. Site-directed mutagenesis was carried out, leading to numerous mutant colonies in several attempts, nevertheless none were shown to be interrupting the gene of interest. Furthermore, extracts of these mutants did not show a loss of myxovalargin production. Since the single crossover construct was shown to be correct by SANGER sequencing, the knockout of this enzyme seems to be impossible in these organisms. From literature a variety of reversible and irreversible inhibitors of the arginine decarboxylase are known. [149] The most potent irreversible inhibitor 2-amino-2-(difluoromethyl)-5-quanidinopentanoic acid was fed at 0.2 mM to inhibit adc. Neither production loss, nor growth inhibition could be observed.

Since the chemical synthesis of agmatine was achieved in the total synthesis project of myxovalargin A at the OCI Hannover, it seemed possible to synthesize, supplement and detect the isotope labelled and incorporated agmatine by mass spectrometry. Unfortunately, the synthesis of ^{13}C, ^{14}N-labelled agmatine was not successful. Therefore, a more sophisticated approach by reverse feeding was pursued.

From a pilot scale project, yeast consisting of 95% ^{13}C: 5% ^{12}C was available in low amount and was used to conduct a reverse feeding experiment. [150] To minimize ^{12}Ccontamination VY2 medium, containing yeast as only carbon source, was used and the strain was transferred in two steps from its unlabelled broth culture to the ^{13}C VY/2 medium. After supplementation of ^{12}C agmatine (0.2 mM), the culture was harvested and extracted. The isotope pattern of myxovalargin A shows a broad distribution caused by the ^{12}C-^{13}C mixture. By overlay of the agmatine supplemented myxovalargin A pattern with the one, acquired from the negative control (addition of water instead of agmatine), it is possible to see a mass shift to a lower mass in the ^{13}C medium. Due to the low mass shift of 2.5 Da (5 m/z) for $[M+2H]^{2+}$, and the competitive incorporation versus the unlabelled yeast derived ^{12}C arginine, which is converted by the myxobacterium to form ^{12}C agmatine, the shift appears to be very small, nevertheless, present (Figure 28). Due to the small batch size of modified yeast this experiment could not be repeated.

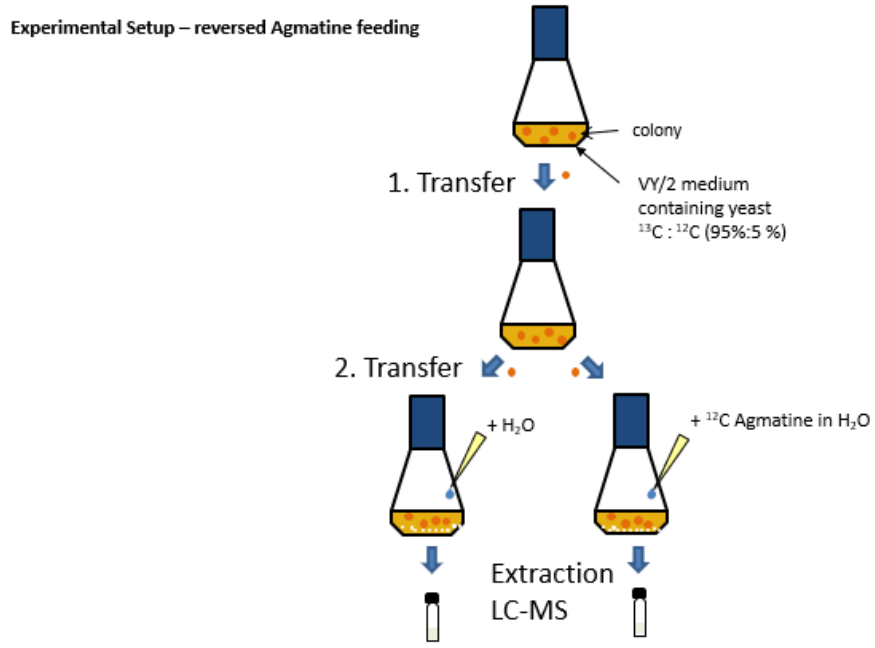

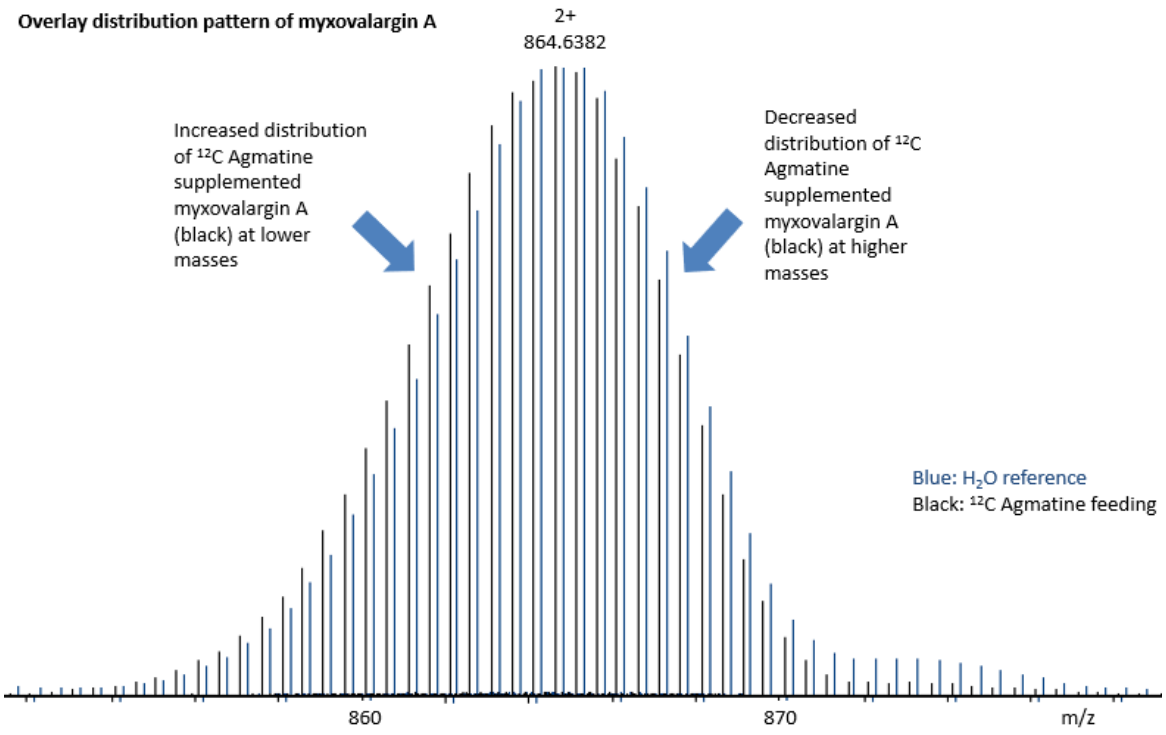

Figure 28: In the reverse feeding experiment cells of MCy6431 were cultivated in VY/2 medium containing yeast of ^{13}C: ^{12}C (95:5 %) as only carbon source. Cells were twice transferred to reduce ^{12}C contamination. One sample was fed with ^{12}C agmatine, the other wirh H2O as reference. After Extraction of the adsorber resin, the isotope distribution pattern of myxovalargin taken by LC-MS was compared as overlay. The sample fed with ^{12}C agmatine (black) shows an increased distribution of lower mass variants compared to the rederence control. This indicates the incorporation of agmatine.

A consecutive experiment was conducted in Isogro®-^{13}C Powder- Growth medium (99 atom % ^{13}C). Strain MCy9171 and MCy6431 were transferred from agar plate directly in the labelled medium to reduce contamination with ^{12}C. Supplementation of either agmatine, β-tyrosine (pos. control) or water (neg. control) at 0.2 mM or at equivolume, respectively, lead to a detectable incorporation of agmatine and of the positive control *β* -tyrosine, thus confirming in a second experiment the incorporation of agmatine as precursor for the terminal building block (Figure 29).

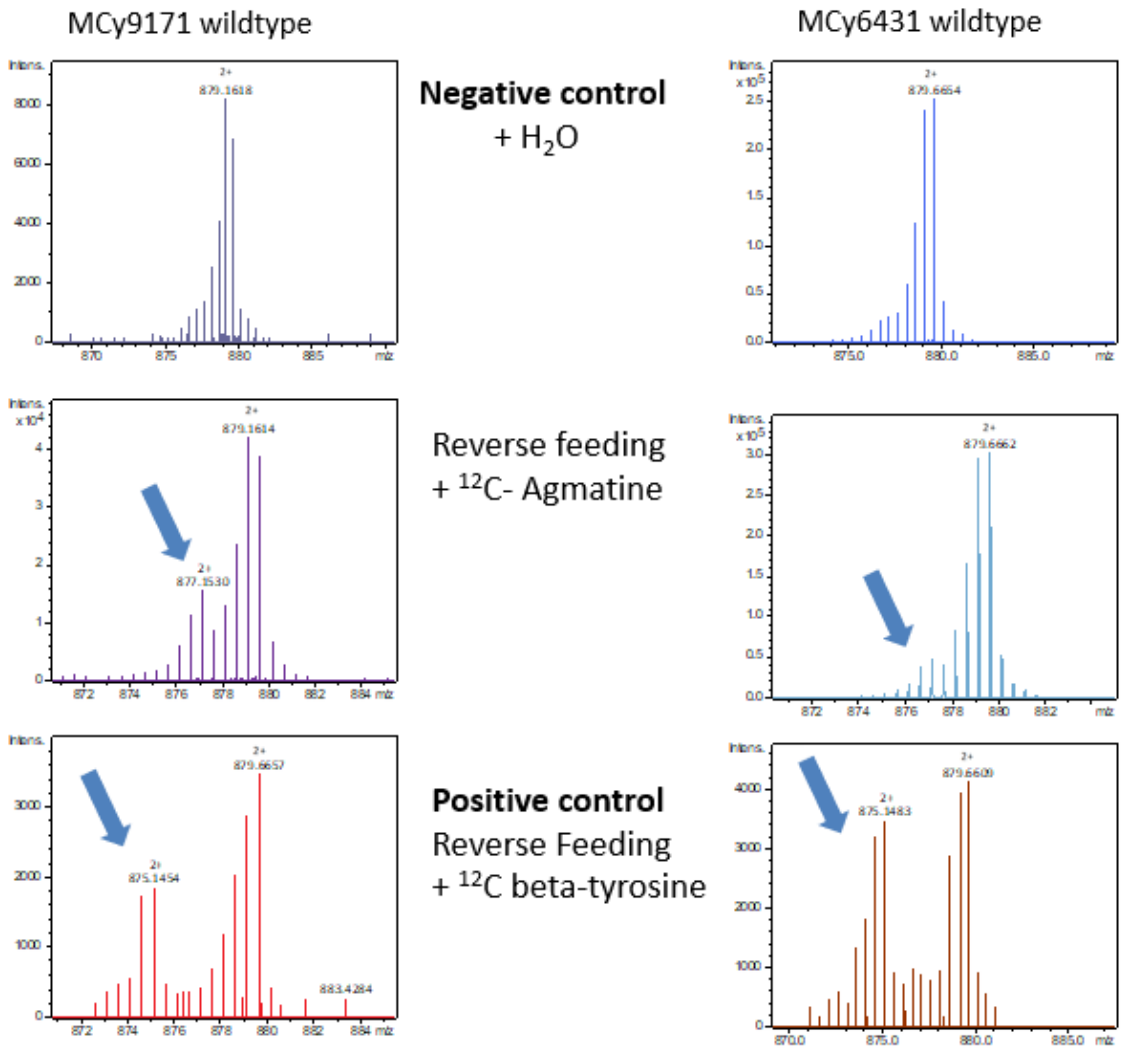

Figure 29: A reverse feeding experiment in 99% ^{13}C Isogro® medium showing the incorporation of different ^{12}C precursor in ^{12}C labelled myxovalargin A in the wildtype. Left panels were acquired from wildtype strain MCy9171, while right panels belong to wildtype strain MCy6431. The upper row shows the wildtype with blank solution (H_2O) and a myxovalargin a mass of 879 m/z. The second row demonstrates the incorporation of ^{12}C-agmatine resulting in a mass 877 Da, which leads to a mass shift of 5 m/z, thus showing a 2.5 Da mass shift for the $[M+H]^{2+}$ ion in both strains. The positive control with C^{12}-*β*-tyrosine in the bottom panel exhibits the expected mass shift for its incorporation, proving the suitability of the experimental setup with ^{12}C precursor reverse feeding in ^{13}C Isogro® medium.

4.1.11 The starting precursor: Isovaleryl-CoA

The described 3-methyl butyric acid starter unit is commonly found in different myxobacterial secondary metabolites like the myxalamids, myxothiazol and aurafuron. The origin of the starter as isovaleryl-CoA (IV-CoA) has been studied in detail and lead to the description of two different mechanism in myxobacteria.[151] Beside the decarboxylation of leucine by a branched chain ketoacid dehydrogenase complex (see also 4.5.3), an alternative IV-CoA biosynthesis (Aib) has been described in myxobacteria (Figure 30). [152–155] Both gene complexes can potentially provide the precursor for the myxovalargins.

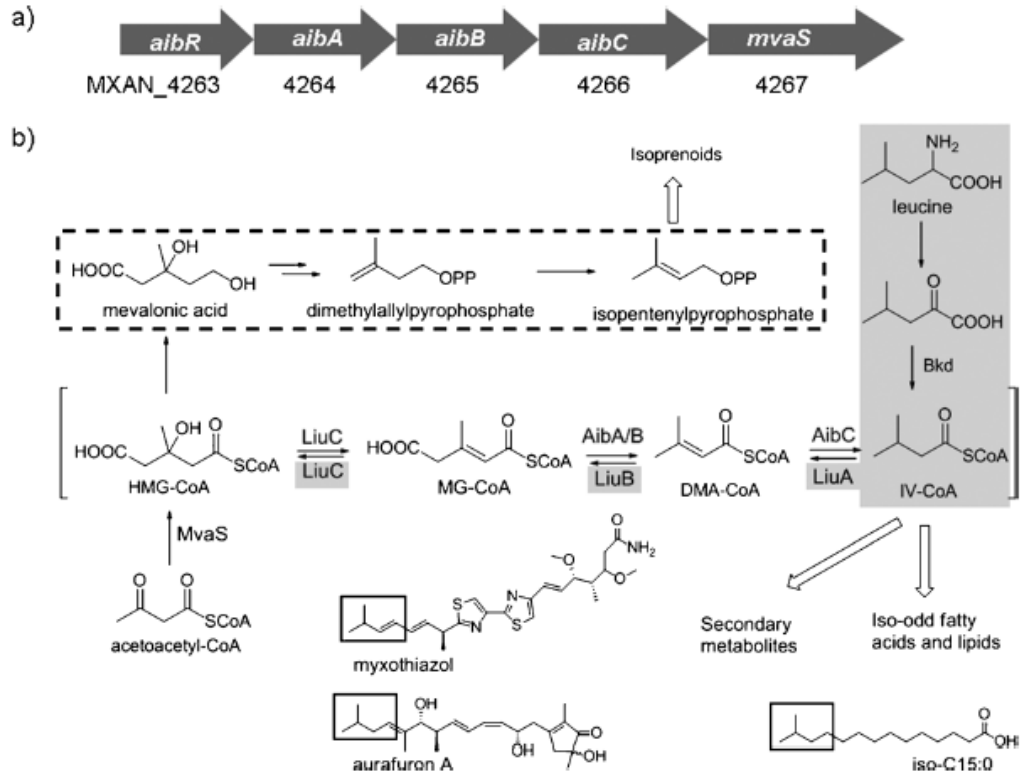

Figure 30: Pathways, which lead to the production of the Isovaleryl-CoA starter, which was shown to be involved in the myxothiazol and aurafuron A biosynthesis. Since neither a knockout of genes encoding the branched chain ketoacid dehydrogenase complex nor the Hydroxymethylglutaryl-Coenzyme A (HMG-CoA) pathway by disruption of *aibA/B* led to loss of myxovalargin A production, it is assumed that both pathways can provide the starter for myxovalargin A production (picture taken from Li et al.[153]).

To confirm leucine as precursor for the isovaleryl starter unit, d10-leucine was supplemented to the myxovalargin producer. Incorporation could be detected by a mass shift of 9 Da, due to

the loss of one α –deuterium. As expected derivatives with the starter of myxovalargin A show the respective mass shift, while myxovalargin B and C do not integrate leucine. Also myxovalargin E with the dehydrated starter unit is incorporating leucine as building block (Table 5).

Table 5: The incorporation of d10-leucine in different myxovalargins.

Myxovalargin	M_r	incorporation
Mxv A	1676	Yes
MxvB	1662	No
MxvC	1648	No
MxvE	1674	Yes
MxvG	1690	Yes
MxvH	1660	Yes

For myxovalargins with the isobutyryl starter like myxovalargin B and C, it is postulated to originate from valine. The incorporation of valine as precursor for the isobutyryl starter could be demonstrated by the determination of valines incorporated in the completely d8-valine labelled myxovalargin (described in 4.1.12). Myxovalargin B shows an additional mass shift regarding to one valine, while myxovalargin C incorporates two additional valines (Figure 31). By fragmentation patterns, in both myxovalargins the starter can be determined as valine derived. Myxovalargin B shows a mass shift of minus 7 Da compared to myxovalargin A though the unlabelled myxovalargin B shows a difference of minus 14 Da due to its missing CH_2 in the starter unit. Therefore, an additional valine with + 7 Da, is incorporated. Myxovalargin C on the other hand, which holds an additional valine in the starter plus an additional valine instead of the isoleucine shows a mass shift of only +14 Da compared to its unlabelled form, which is 28 Da smaller than myxovalargin A. Thus the difference between labelled myxovalargin C to myxovalargin A is 14 Da.

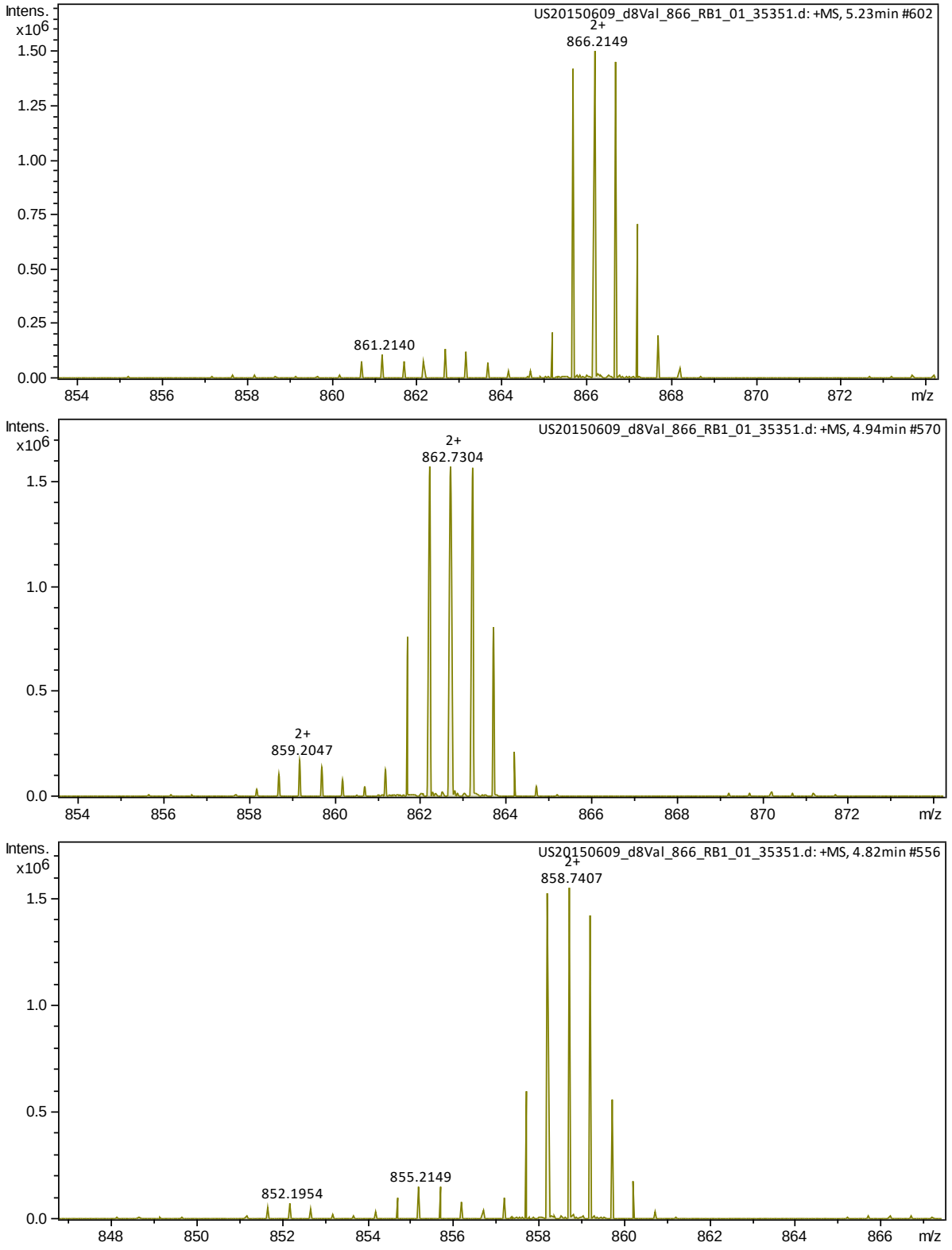

Figure 31: Isotope pattern of myxovalargins, produced by Ccc1071 cultivated in C^{13} medium. The upper panel shows myxovalargin A with a mass of $[M+2H]^{2+}$ 866.2 m/z . Myxovalargin B in the second channel shows a shift of 7 Da (3.5 m/z), which is due to its lower mass of minus 14 Da, but on the other hand an additional valine incorporated (+ 7 Da). Myxovalargin C incorporates two additional valine (+ 14 Da), but is 28 Da smaller than myxovalargin A, thus a mass shift of approximately 13 Da (6.5 m/z) appears.

Since valine and leucine could be identified to server as precursor for branched chain ketoacid starter, which are incorporated in high yields, it was reasonable to test the incorporation of Isoleucine as alternative precursor. Isoleucine-d10 was feed to the wildtype strain and compared to the wildtype. The incorporation experiment also corroborates structural assignments of myxovalargin derivatives: A single isoleucine integration was visible in case of all myxovalargins except of myxovalargin C, which obtains no isoleucine moiety but valine, proving the position of the additional valine in myxovalargin C. On the other hand myxovalargin G shows an additional shift for a second isoleucine moiety, which was found by MS fragmentation to be a hydroxy isoleucine instead of a hydroxy valine. Furthermore, within the myxovalargin A peak with a tendency to a shorter retention time, an additional pattern for a second incorporated isoleucine can be observed. Thus, this compounds´ peak overlaps completely with the actual myxovalargin A. They are isobaric under usual conditions, as both starter exhibit the same atomic composition. Since the second isoleucine is not dehydrogenated it leads to a mass shift of + 9 Da, whereas the regular isoleucine at the dehydro-isoleucine position gives a shift of + 8 Da. In summary this myxovalargin derivative named myxovalargin K shows a mass shift of + 16 Da in the double labelled compound. Incorporation of a second isoleucine therefore can be observed for the appearance of the mass $[M+2H]^{2+}$ 847.5770 m/z, but also by the shift and yield increase of the single labeled myxovalargin incorporating only the + 9 Da isoleucine as starter leading to a mass of $[M+2H]^{2+}$ 843.5542 m/z compared to $[M+2H]^{2+}$ 843.0506 m/z for the + 8 Da dehydro isoleucine incorporation (Figure 32). These findings led to the identification of myxovalargin K with the isoleucine starter instead of the leucine derived isovaleryl starter. It has to be noted that this concludes a mixture of myxovalargin A and K, when they are purified. Due to their chromatographic comparable behavior and the same mass at a assumed same stereochemistry, these compounds can only be distinguished by this feeding experiment.

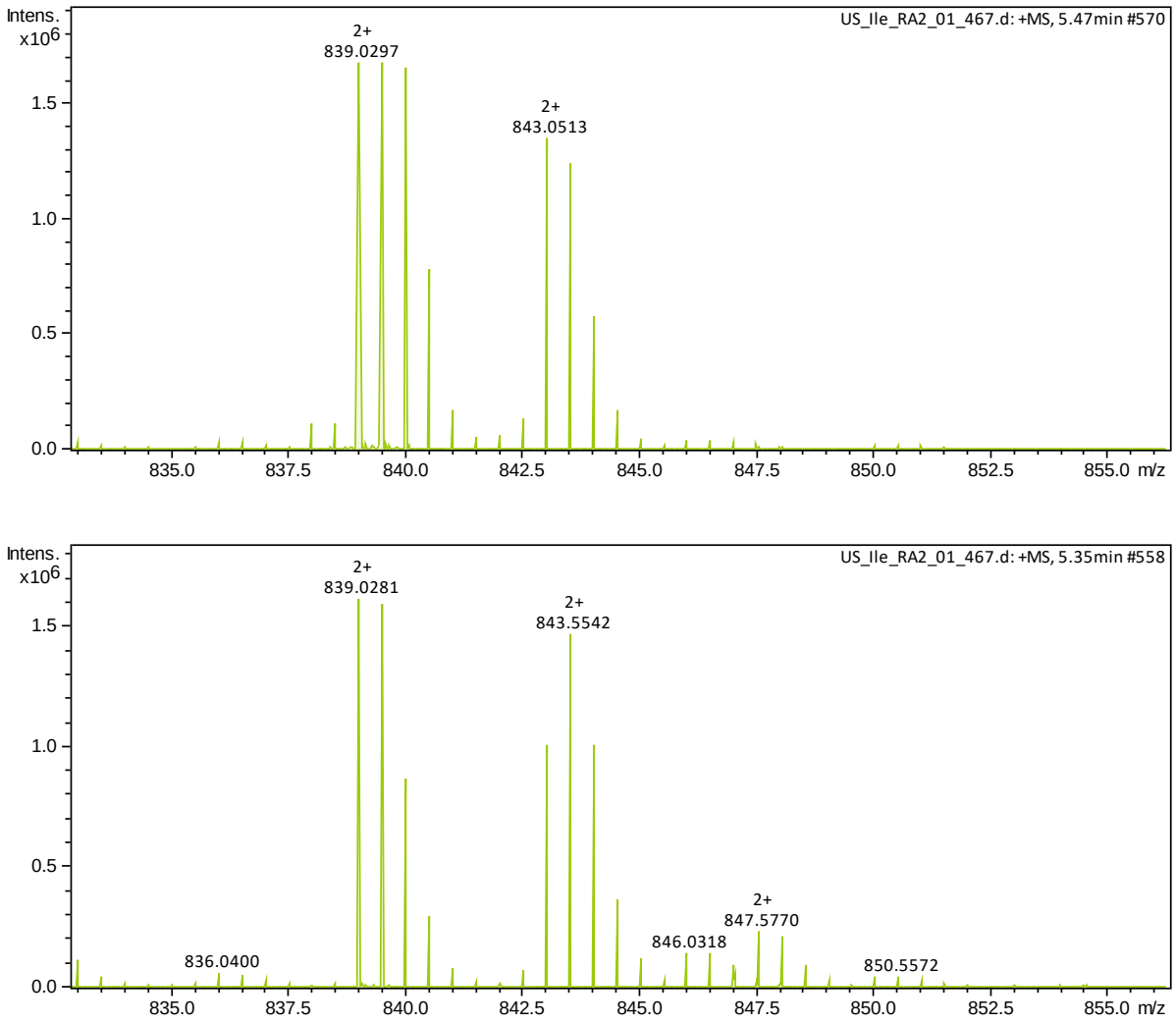

Figure 32: The upper panel shows the distribution pattern of Myxovalargin A at a retention time of 5.47 min, while the lower panel shows the pattern at 5.35 min. The additional incorporation of a second isoleucine with $[M+2H]^{2+}$ 847.5770 m/z, + 9 Da or 4.5 m/z compared to single labelled myxovalargin A (843.0514 m/z), can be observed. Furthermore, the mono labeled myxovalargin shows primarily a mass of $[M+2H]^{2+}$ 843.5542 m/z, which corresponds to the mass shift of + 9 Da (4.5 m/z), when integrating isoleucine as starter unit and not as dehydro isoleucine (+ 8 Da; 4 m/z).

This promiscuity of incorporation of different branched chained keto acids partially explains the vast amount of different myxvovalargins and the appearance of several peaks with comparable or identical chemical masses throughout the chromatographic region, where the myxovalargins elute. However, the results of bioactivity screening showed the superiority of myxovalargin A against all other derivatives. The substitution of branched chain amino acids with their counterparts in the structure of myxovalargin A shows that this promiscuity is not only limited to the starter unit, but also to other building blocks in the myxovalargin structure.

A targeted approach using valine rich medium to suppress other myxovalargin derivatives and increase myxovalargin A production could yield a favorable shift towards the most active myxovalargin derivative.

The promiscuous incorporation of starter units was used to pursue a precursor directed biosynthesis. This approach uses an excess of chemically similar derivatives to yield a competitive incorporation of the fed precursor instead of the natural occurring building block. According to the mutasynthesis experiments of Bode et al. [156] cyclic carboxylic acids were supplemented to the cell broth at 0.2 mM (Figure 33). Small cyclic carboxylic acids like cyclopentane and cyclobutane rings were incorporated with high efficacy. With increasing size of the cyclic carboxylic acid, the incorporation decreases. Sophisticated feeding schemes and media optimization to reduce the natively occurring competitor could further increase the production. The precursor directed biosynthesis of the starter unit offers a variety of modifications to achieve different physicochemical properties.

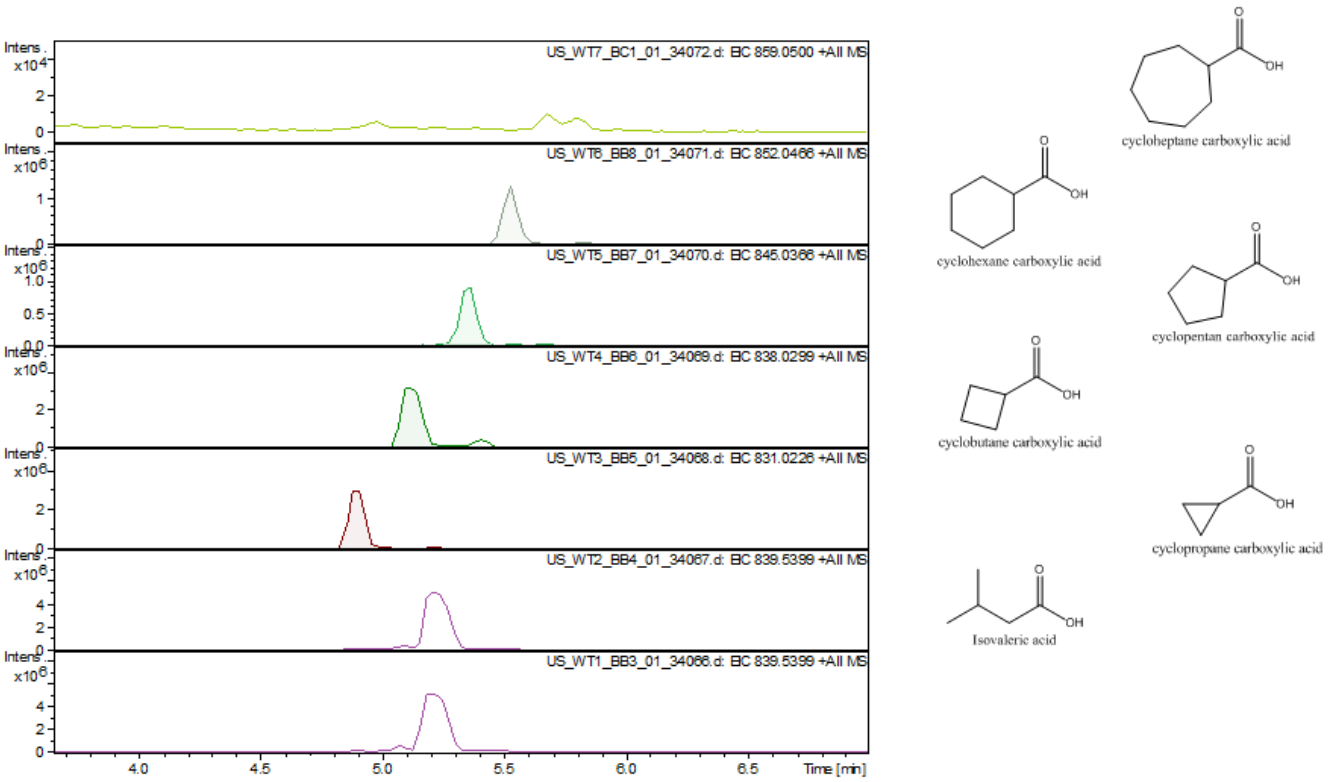

Figure 33: Precursor directed biosynthesis using different cyclic carboxylic acids as competitive building blocks for incorporation in the myxovalargins. Compared to the WT in lane 7 the isovaleric acid (lane 6) does not influence production. The carboxylic acids of cyclopropane (lane 5) and cyclobutane (lane 4) are still incorporated with approximately half yield compared to myxovalargin A. Cyclopentane (lane 3) and Cyclohexane carboxylic acid (lane 2) only yield about a quarter of the myxovalargin A production, while cycloheptane carboxylic acid incorporation (lane 1) is reduced to a minimum.

4.1.12 Elucidating the stereochemistry of Myxovalargin A

A major discrepancy between the results and the interpretation of the initial stereochemical structure determination of myxovalargin bei Steinmetz et al [114] and the genetic analysis of the biosynthetic gene cluster became evident, when the sequence of the myxovalargin biosynthesis cluster was fully identified. Module 7, which should incorporate L-valine according to the initial stereochemical assignment exhibits an epimerization domain while module 10, which should

result in D-valine did not contain an epimerization domain. Epimerization domains are common enzymes in NRPS assembly lines changing stereocenters of carrier protein coupled proteinogenic L amino acids to a D-comfiguration during the assembly process. Therefore, these domains are present as expected in modules 4, 5, 6, 9, 11, 13, 14. Modules 1, 2, 3, 8, 12, which lead to L or dehydro amino acids do not contain an E domain. Sequence alignment of all E domains did not show any unusual signs, which would suggest an inactivity of the enzymes.

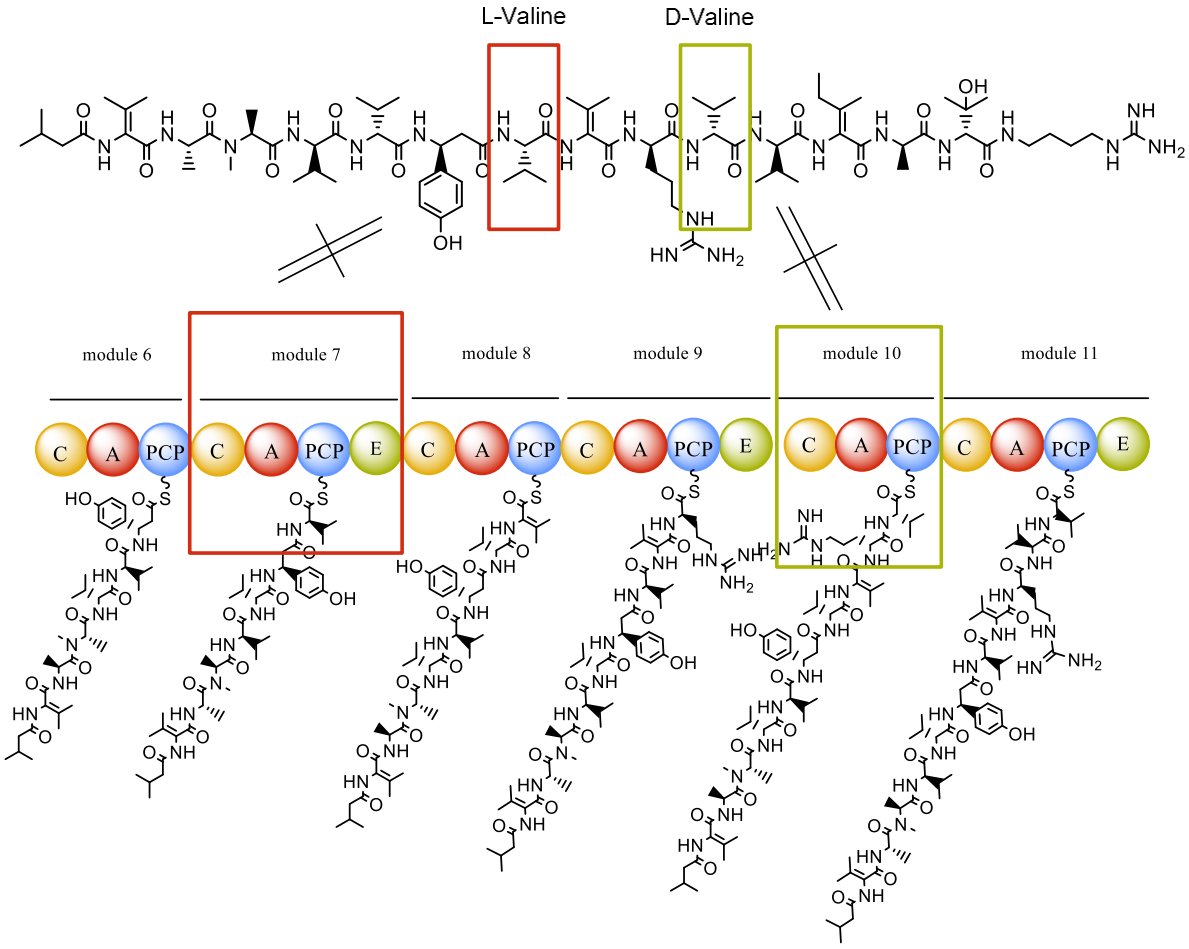

Figure 34: Discrepancy between assigned stereochemistry of myxovalargin A in literature and the sequence of the myxovalargin cluster at module 7 and module 10. Module 7 exhibits an epimerization domain, which suggests a D-Valine at Valine in position 7, while module 10 lacks an epimerization domain, which is contrary to the assigned D-Valine in position 10 of myxovalargin A

Nevertheless, since the region of module 8 – 10 has shown to impede assembly due to its repetitive sequence sections, a verification of these scaffolds was challenging. Assembly of Illumina and Roche454 sequencing data already showed the final domain organization, but still

appeared to leave two gaps in highly repetitive regions. The final sequence was achieved after Pacific Bioscience sequencing, which spans the repetitive regions. Because of the described assembly difficulties, gene clusters identified in strains MCy8286, MCy9171 and MCy5730 showed gaps at similar positions, nevertheless assembly of MCy9171 scaffolds suggests the same domain organization. Due to highly repetitive regions in module 7 and module 11, alignments of Illumina sequencing and Roche 454 sequencing were not unequivocally indicating the genomic sequence of the myxovalargin cluster. Roche 454 and especially Illumina sequencing are techniques, which both yield relatively short sequence scaffolds that need to be aligned to result in a consecutive sequence compared to PacBio sequencing. The repetitive regions left a rest of uncertainty about a correct alignment, especially with regards to the observed inconsistency. Though PacBio sequencing provided a high quality end-to-end sequence, southern blot experiments were carried out to verify the correct alignment. Probes within the regions of module 7 (probe E) and module 10 (probe 10) were chosen (Figure 35). Due to the size of an epimerization domain of approximately 2000 bp, the presence or absence of this domain can be clearly identified by this technique. Nevertheless, the repetitive regions limit the suitability of different restriction enzymes. Three enzymes were chosen to yield suitable scaffolds to underline the sequence alignment: NotI, KpnI, EcoRI. Southern Blot experiments of module 10 with probe 10 and 3 different restiriction digests were successfully performed and confirm the lack of an epimerization domain in module 10 in the genome of the producer. The results for Probe E binding to the epimerization domain in module 7 confirm with two digests the expected scaffolds. The third digest with the restriction enzyme NotI, which would yield a large scaffold of larger than 35 kbp only gives a weak signal above the 8576 bp marker band. Due to the large expected scaffold and the competitive binding of probe E in the repetitive homolog in module 11, this result is plausible. As this result also does not support the presence of an E domain in module 7 by these results, it does not disagree with the sequence alignment. Overall the southern blot experiments support the sequence assembly in this region as described in this thesis.

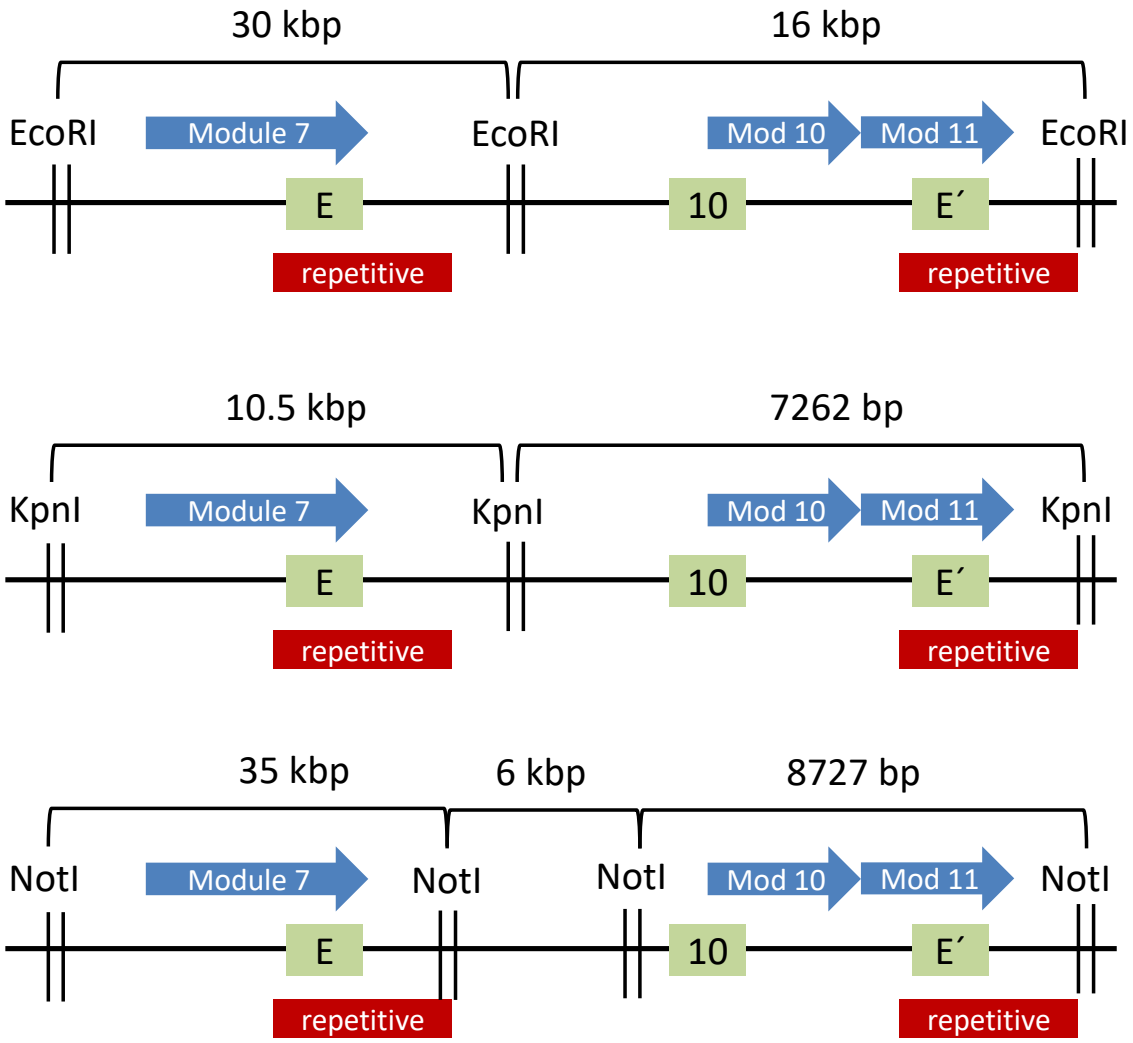

Figure 35: Restriction digest of genomic DNA from Ccc1071. The green squares show the binding region of the probes E and 10. E´ is a putative second binding region for E, due to high sequence similarity, marked in red as repetitive region. The blue arrows show the affected modules, while the discrepancy between sequence and stereochemistry is appearing in module 7 (sequence has E domain, though stereochemistry is L-Valine) and module 10 (sequence lacks E domain, though stereochemistry is D-Valine). The cutting sites of the chosen restriction enzymes and the expected scaffolds are given.

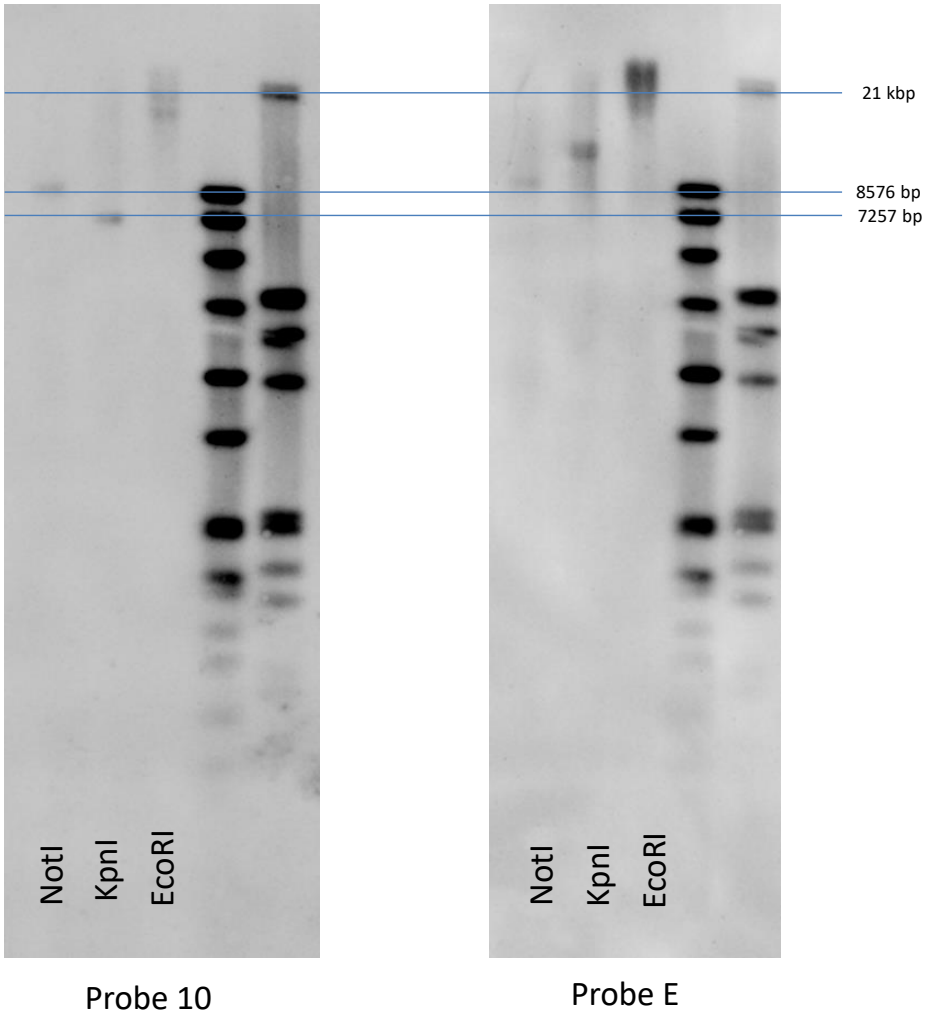

Figure 36: Southern Blot of Probe 10 and Probe E to confirm the sequence assembly of the regions between module 7 and 10. The pattern for Probe 10 fits with the estimated scaffolds: NotI: 8727 bp, KpnI: 7262 bp, EcoRI: 16 kbp (Figure 35). The pattern for probe E fits for KpnI: 7262 bp, EcoRI 35 kbp, but not for NotI appr. 8800 bp. This can be explained by binding to the repetitive region in module 11. All digests support the sequence assembly.

As the sequence by PacBio sequencing and additional Southern Blot was confirmed, the condensation domains in this region were further investigated. It was shown that condensation domains are related regarding their specificity for educts they condensate. [71] This investigation was in particular interesting, since it has been reported that condensation and epimerization domains are closely related and even bifunctional enzymes (C/E domains) exist. However, all C domains present in the myxovalargin assembly line belong to the DcL and the LcL groups (Figure 37). DcL domains condensate D amino acids from the previous module with the L amino

acid attached at the PCP domain of the same module the C domain is located in; LcL domains analogously condensate L amino acids with L amino acids. Thus no unusual C/E mechanism is expected. The C domain of module 1, though grouping to LcL, is closely related to starter incorporating domains, which is reasonable, since this domain condensates the precursor to the first building block in module 1. Furthermore all other C domains except of module 8 and 11 fit with the stereochemical assignments of the original structure elucidation. On the other hand all C domain functionalities concur with the presence of epimerization domains in the cluster sequence. The critical C domain of module 8 belongs to the DcL clade, indicating that module 7 must form a D amino acid, while C domain of module 11 groups with LcL domains suggesting module 10 to build a L-amino acid. While the C-domain of module 8 is located in a the repetitive sequence section, the latter finding is of major importance, since the C domain of module 11 belongs to a conserved region apart of the repetitive, questionable sequence parts. Thus, the C domain comparison supports the revision of the stereochemistry.

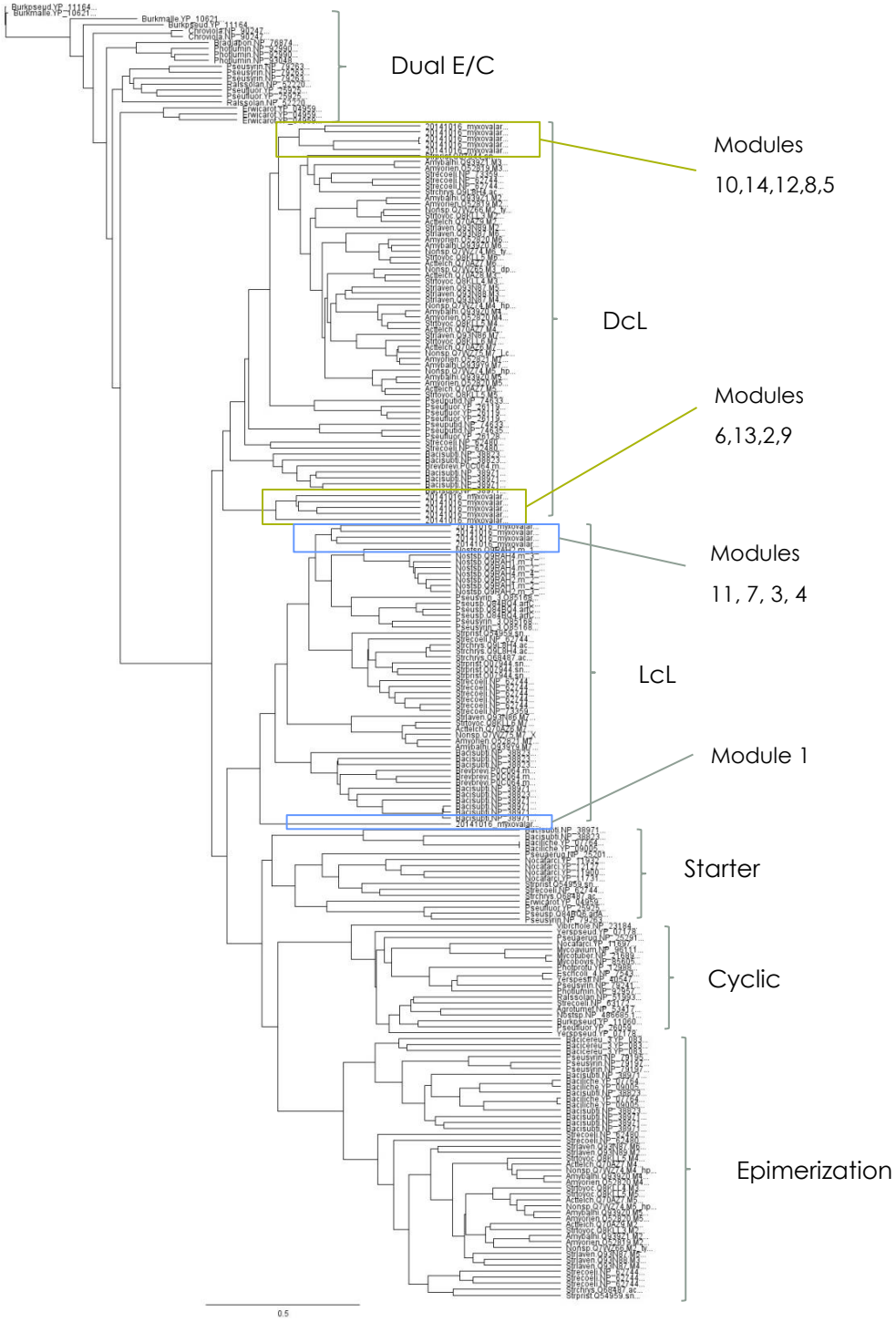

Figure 37: Tree of C domains in the myxovalargin biosynthesis cluster. All C-domains group to the DcL and LcL group which condensate D with L or L with L amino acids, respectively. The predictions correspond to functional reactions, anticipated by the chemical structure. Only exceptions are module

The confirmation of the myxovalargin cluster sequence and its discrepancy with the stereochemical assignment, which was demonstrated by in silico characterization, was further underlined by combined approaches of chemical and biological tools on the actual molecule.

The conversion of the stereocenter at the α-carbon by the Epimerization domain is composed of an elimination of the hydrogen atom leading to a sp2 hybridization, followed by an addition of a hydrogen atom stereochemically directed by the epimerization domain to form the D-amino acid. This elimination-addition reaction leads to the substitution of the hydrogen atom at the stereocenter. Therefore, it is possible to detect the difference of an incorporated amino acid, which is labelled by deuterium at the α-carbon, in terms of their D or L-configuration after epimerization.[157] The elimination of deuterium and subsequent addition of hydrogen results in a 1 Da mass shift. In case of myxovalargin the presence of 8 -10 valine (depending on myxovalargin derivatives, see 4.1.13) made a direct approach by feeding of labeled valine to the culture in regular medium with a full set of amino acids in the nitrogen source impossible. Though the calculated fully labelled myxovalargin could be detected, it was overlaid by isotope peaks of less labelled molecules, which hinders an assignment of labelling to the structural moieties. Therefore, a sophisticated minimal medium was composed where valine was solely substituted as d8- valine on basis of a reported minimal medium for *Myxococcus xanthus* [158] and by including results from microbiological experiments (Figure 38). Hence, fully labelled myxovalargin derivatives could be produced. By MS-MS fragmentation and known detectable fragments from previous high resolution MS data acquired by Orbitrap direct infusion experiments with unlabeled myxovalargin derivatives, it was possible to directly compare fully labelled and unlabeled derivatives. Beside the identification and confirmation of structural assignments by detection of incorporated valines at e.g. the starter positions (see **Fehler! Verweisquelle konnte nicht g efunden werden.**, 4.1.13), additional confirmation of the stereochemical configuration could be achieved.

US_TPM17

100 mM L-Arginine
100 mM L-Alanine
100 mM L.-Asparagine
50 mM L-Cystine
50 mM L-Glycine
50 mM L-Histidine
100 mM L-Isoleucine
500 mM L-Leucine
100 mM L-Lysine
100 mM L-Methionine
100 mm L-Phenylalanine
100 mM L-Serine
100 mM L-Threonine
100 mM L-Tryptophane
200 mM L-Tyrosine
100 mM d8-Valine
10 mM Tris-HCl (pH 7.6)
1 mM KH_2PO_4-K_2PO_4 (pH 7.6)
0.8 mM $MgSO_4$
1 mg/mL $(NH_4)_2SO_4$
8 µg/mL FeEDTA
pH 7.0

Figure 38: US_TPM17 medium with 100 mM d8-valine replacing L-valine.

Feeding of the deuterium labelled valine leads to a mass increase of +8 Da for L-valine, while D-valine results in a +7 Da mass shift caused by substitution of the deuterium ion at the α-carbon by hydrogen. The dehydrogenated valines show a difference of + 6 Da due to their loss of two deuterium ions. Though not all scaffolds of a linear fragmentation by peptide bond

opening can be observed, most of the z and a fragments are typically observed. The difference of L-valine compared to D-valine at the critical positions val7 and val10 can therefore be observed by the fragments z8, z7 and z6, which contain val10, but not val7 and by the fragments a10, a9, a8 harboring val7, but not val10. As a9 and a8 are not observed for myxovalargins, the especially a10, z8, z7, z6 were investigated. Those fragments confirm the stereochemical revision of val7 and val10. Furthermore the correct identification of all other listed a and z fragments shows the suitability of this approach and supports the stereochemical as well as the structural assignment of the other valine building blocks.

The comparison of fully d8-valine labeled myxovalargin A (Figure 39) as well as myxovalargin B (Figure 40) and myxovalargin C (Figure 41) against the respective unlabeled natural occurring myxovalargin A unequivocally confirms the stereochemical assignment of D-valine in position val7 and L-valine in position val10. Thus, the stereochemistry of myxovalargin A-C needs to be revised as suggested by the genomic sequence based approach and as confirmed by the chemical determination.

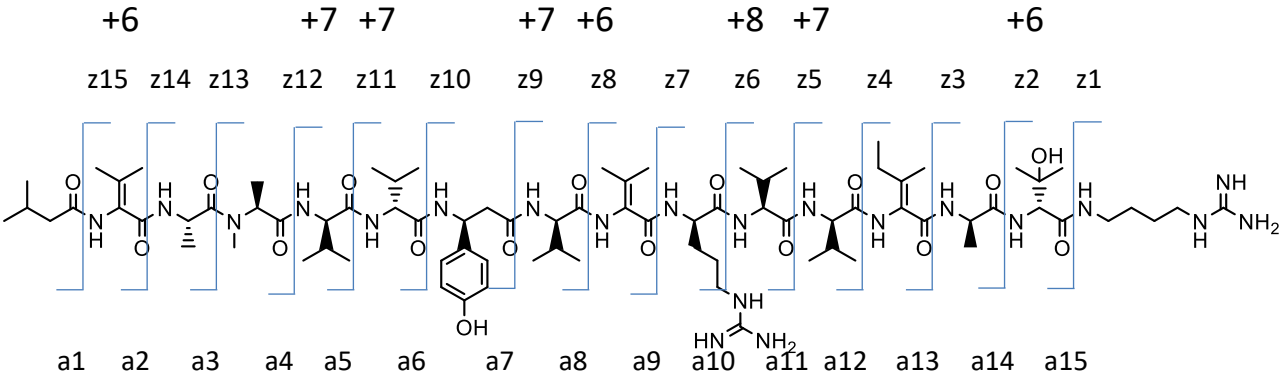

fragment	MxvA (m/z)	d8 Val (m/z)	mass shift	fragment	MxvA (m/z)	d8 Val (m/z)	mass shift
a1	nd	nd	nd	z15	810.00996	nd	nd
a2	nd	nd	nd	z14	1496.94739	nd	nd
a3	253.15433	259.1931	6	z13	1424.9093	nd	nd
a4	338.20697	344.2462	6	z12	1339.85632	1388.1685	48
a5	437.27594	450.3584	13	z11	1240.78943	1282.0391	41
a6	536.3429	556.4700	20	z10	1141.72009	1175.9459	34
a7	nd	nd	nd	z9	nd	nd	nd
a8	nd	nd	nd	z8	879.58759	906.7569	27
a9	nd	nd	nd	z7	782.53497	803.6676	21
a10	1051.62927	1084.8395	33	z6	626.43378	647.5637	21
a11	1150.69629	1191.8191	41	z5	527.36523	540.4480	13
a12	1249.76611	1298.1736	48	z4	428.28727	434.3373	6
a13	1360.83398	1409.1454	48	z3	317.22919	323.2676	6
a14	1431.8723	nd	nd	z2	246.99221	nd	nd
a15	nd	nd	nd	z1	nd	nd	nd

Figure 39: Fragmentation pattern of Myxovalargin A and detected corresponding fragments of the fully labelled myxovalargin A by d8-Valine feeding. Myxovalargin A incorporates 8 valines, thereby showing an overall mass shift of 54 Da. The expected mass shifts (Da) for deuterium labelled valine incorporation are shown above the molecule. The fragments of a10, z6, z7 and z8 which only obtain val7 or val10, respectively confirm the stereochemical revision. All other listed fragments fit with the expected shifts and highlight the suitability of the approach; nd = not detected

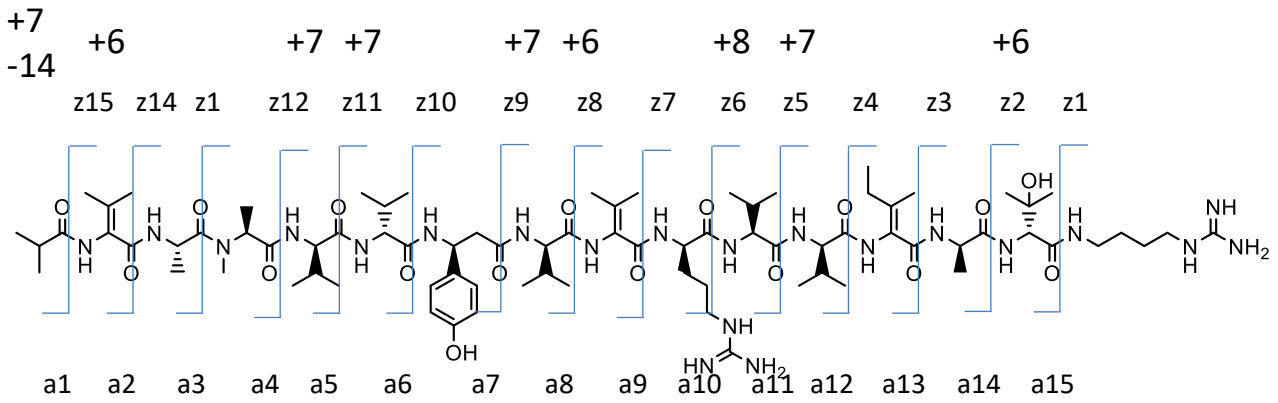

fragment	MxvA (m/z)	d8 Val (m/z)	mass shift	fragment	MxvA (m/z)	d8 Val (m/z)	mass shift
a1	nd	nd	nd	z15	810.00996	nd	nd
a2	nd	nd	nd	z14	1496.94739	nd	nd
a3	253.15433	252.2224	-1	z13	1424.9093	nd	nd
a4	338.20697	337.2751	-1	z12	1339.85632	1388.1695	+48
a5	437.27594	nd	nd	z11	1240.78943	1282.0556	+41
a6	536.3429	548.5170	+12	z10	1141.72009	1175.9398	+34
a7	nd	nd	nd	z9	nd	nd	nd
a8	nd	nd	nd	z8	879.58759	906.7613	+27
a9	nd	nd	nd	z7	782.53497	803.6677	+21
a10	1051.62927	1084.8395	+33	z6	626.43378	647.5680	+21
a11	1150.69629	1191.8191	+41	z5	527.36523	540.4517	+13
a12	1249.76611	1291.1083	+41	z4	428.28727	434.3355	+6
a13	1360.83398	1401.1738	+41	z3	317.22919	323.2685	+6
a14	1431.8723	nd	nd	z2	246.99221	nd	nd
a15	nd	nd	nd	z1	nd	nd	nd

Figure 40: Fragmentation pattern of Myxovalargin A and detected corresponding fragments of the fully labelled myxovalargin B by d8-Valine feeding. Myxovalargin B incorporates 9 Valine caused by an additional valine as starter, thereby showing an overall mass shift of 61 Da. The expected mass shifts (Da) for each incorporated d8-valine against myxovalargin A are indicated above the molecule. The shifts of a3 – z13 show a difference of -7 Da compared to the shifts of myxovalargin A due to one additional valine incorporated (+7 Da) and subtracting the mass loss for a starter with one CH2 extender unit less (- 14 Da). The fragments of a10, z6, z7 and z8 which only obtain val7 or val10, respectively confirm the stereochemical revision. All other listed fragments fit with the expected shifts and highlight the suitability; nd = not detected

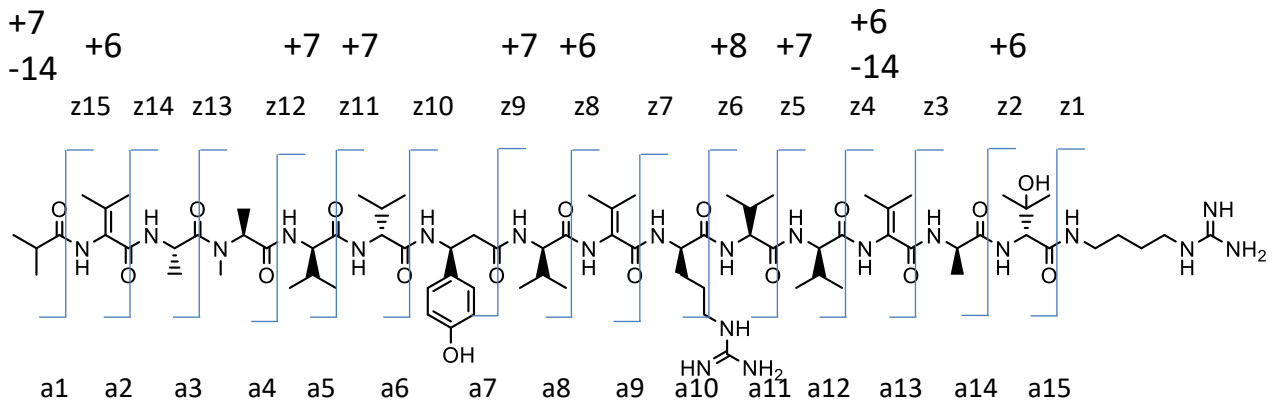

fragment	MxvA (m/z)	d8 Val (m/z)	mass shift	fragment	MxvA (m/z)	d8 Val (m/z)	mass shift
a1	nd	nd	nd	z15	810.00996	nd	nd
a2	nd	nd	nd	z14	1496.94739	nd	nd
a3	253.15433	252.2223	-1	z13	1424.9093	nd	nd
a4	338.20697	337.2742	-1	z12	1339.85632	nd	nd
a5	437.27594	443.2178	+6	z11	1240.78943	nd	nd
a6	536.3429	556.4700		z10	1141.72009	nd	nd
a7	nd	nd	nd	z9	nd	nd	nd
a8	nd	nd	nd	z8	879.58759	898.7832	+19
a9	nd	nd	nd	z7	782.53497	795.6867	+13
a10	1051.62927	1084.8395	+33	z6	626.43378	639.5884	+13
a11	1150.69629	1191.8191	+41	z5	527.36523	532.4694	+5
a12	1249.76611	1298.1736	+48	z4	428.28727	426.3593	-2
a13	1360.83398	1409.1454	+48	z3	317.22919	323.2684	+6
a14	1431.8723	nd	nd	z2	246.99221	nd	nd

Figure 41: Fragmentation pattern of Myxovalargin A and detected corresponding fragments of the fully +labelled myxovalargin C by d8-Valine feeding. Myxovalargin C incorporates 10 Valine, an additional valine as starter and an additional valine instead of isoleucine, thereby showing an overall mass shift of 67 Da. The expected mass shifts (Da) for each incorporated d8-valine against myxovalargin A are indicated above the molecule. The shifts of z4 – z8 show a difference -8 Da compared to the shifts of myxovalargin A due to one additional dehydro valine incorporated (+6 Da) and subtracting the mass loss for substituting dehydro isoleucine (- 14 Da). For a fragments the same shifts as described for myxovalargin B apply. The fragments of a10, z6, z7 and z8 which only obtain val7 or val10, respectively confirm the stereochemical revision. All other listed fragments fit with the expected shifts and highlight the suitability of this approach; nd = not detected

4.1.13 Myxovalargin - structural variants

The myxovalargins are a predominant compound class in the chromatogram of MCy6431 as well as in other myxovalargin producers (Figure 42). The peptide structure of all identified myxovalargins is highly preserved. Few substitutions by similar building blocks could be observed. The interchange of isoleucine or leucine by valine in several positions is the most prevalent observation (Figure 43). Especially the starter unit offers a certain flexibility for different substrates, this is supported by the precursor directed feeding experiments, which allowed the incorporation of different chemically related substrates.

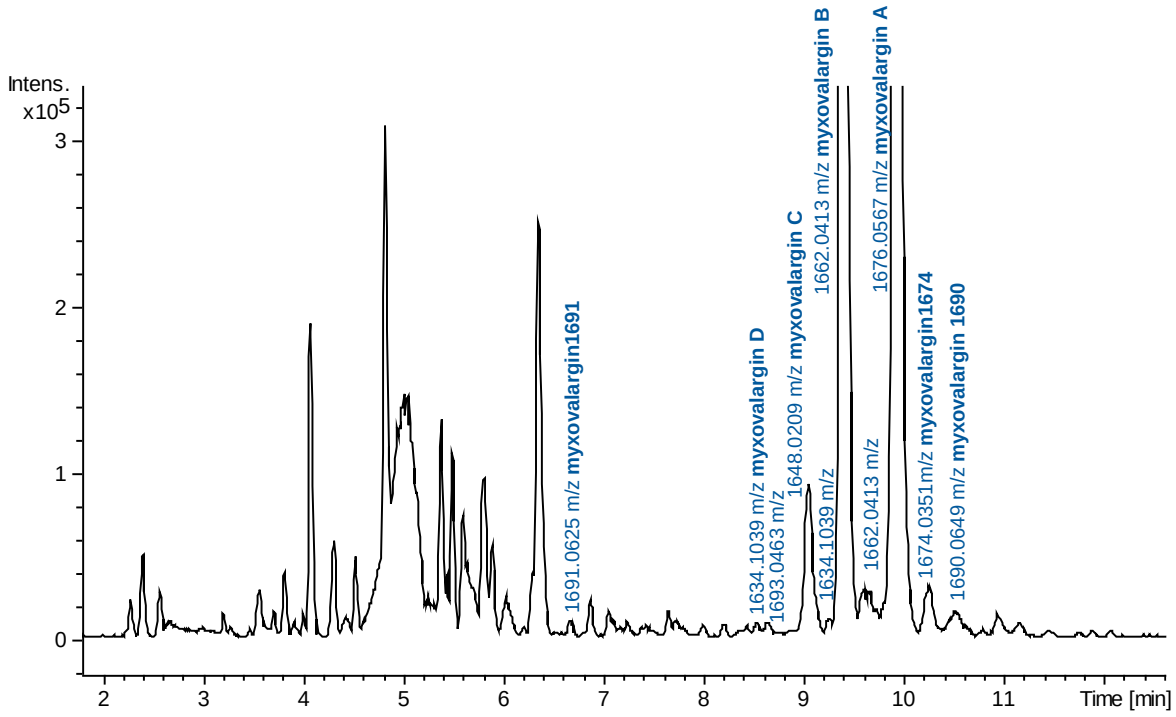

Figure 42: Chromatoram of MCy6431 in AMB + FeEDTA Medium on a xy system. The myxovalargins elute in a time frame of approximately 6.5 – 11 minutes.

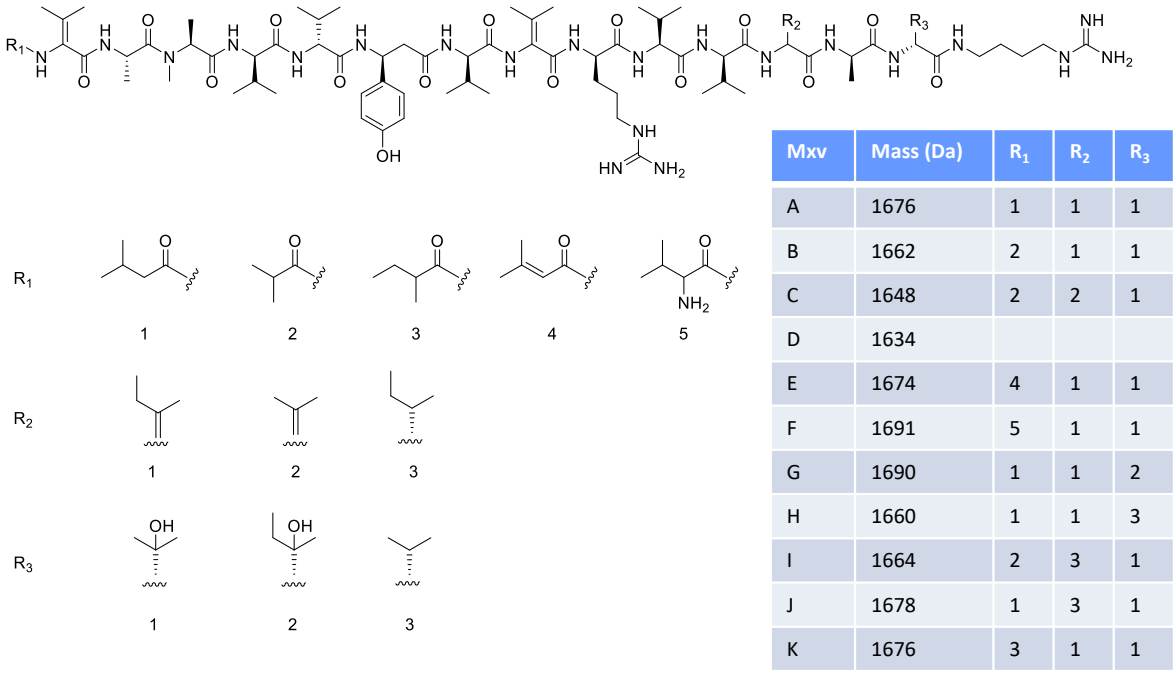

Mxv	Mass (Da)	R_1	R_2	R_3
A	1676	1	1	1
B	1662	2	1	1
C	1648	2	2	1
D	1634			
E	1674	4	1	1
F	1691	5	1	1
G	1690	1	1	2
H	1660	1	1	3
I	1664	2	3	1
J	1678	1	3	1
K	1676	3	1	1

Figure 43: The myxovalargin compound class. Three building blocks were observed to be interchangeable in the most abundant myxovalargins. This is the starter unit, which is present in different forms of short branched chain ketoacids, the Isoleucine moiety and the hydroxyvaline moiety, which show substitution with by valine or isoleucine respectively, and incomplete modification by tailoring enzymes.

4.1.13.1 Myxovalargin A

Myxovalargin A with a mass of 1676 Da is the predominant myxovalargin in all myxobacterial strains. The mass 1676 can be found throughout the whole region, where myxovalargins elute in the chromatogram (Figure 42). Some could be determined to have the same fragmentation pattern, therefore most of them are postulated to be stereoisomers, but also constitutional isomers as myxovalargin K occur (). The structure of myxovalargin A was elucidated and confirmed by MS and NMR. The stereochemistry is determined and confirmed.

4.1.13.2 Myxovalargin B

Myxovalargin B is the second most dominant derivative in all myxobacterial strains eluting prior to myxovalargin A. Cultivation parameters allow a direct influence on the production rate of myxovalargin B, allowing to achieve a comparable yield as A. With a mass of 1662 Da it

lacks 14 Da compared to myxovalargin A. By MS fragmentation the mass loss could be identified at the starter unit. By feeding experiments and MS fragmentation the incorporation of valine could be identified in this position. Using this experimental evidence and biosynthesis considerations the myxovalargin B structure is elucidated. Though a full stereochemical characterization was not performed for myxovalargin B, the abundant occurrence and biosynthesis considerations imply that myxovalargin B shows the same stereochemistry as myxovalargin A.

4.1.13.3 Myxovalargin C

Myxovalargin C is another common myxovalargin eluting prior to A and B. With a mass of 1448 it lacks 28 Da to A and 14 Da to B. MS fragmentation narrows 14 Da mass lost to the starter unit and 14 Da mass loss to the dehydro-isoleucine moiety in myxovalargin A. By feeding experiments with valine also here the incorporation at the starter unit could be confirmed. Furthermore a valine incorporation instead of the isoleucine could be verified. Thus, the constitution of myxovalargin C is determined. Though also for myxovalargin C a full stereochemical characterization was not performed, the abundant occurrence and biosynthesis considerations imply that myxovalargin C shows the same stereochemistry as myxovalargin A.

4.1.13.4 Myxvoalargin D

While myxovalargin D was one of the first identified myxovalargins and was found in sufficient amount in *Myxococcus fulvus* Mxf65 (MCy8286) eluting prior to myxovalargin C, it is a minor derivative in MCy6431 and only produced in very low amounts. Myxovalargin D with a mass of 1434 Da shows a loss of 32 Da compared to Myxovalargin A. This is equal to 3 CH_2 extender units. MS fragmentation indicates a loss of 28 Da at the starter unit and 14 Da at the dehydro isoleucine moiety. Myxovalargin D therefore is assumed to contain a dehydro valine moiety at the isoleucine position. However, the starter unit of myxovalargin D remains unclear. Though the loss of 28 Da suggests a loss of 2 CH_2 extender, as the starter could not be determined, any assumption on the putative starter is theoretical.

4.1.13.5 Myxovalargin E

Myxovalargin E is one of few identified myxovalargins, which elutes after myxovalargin A. With 1674 Da it only misses 2 Da compared to myxovalargin A. The mass difference was determined at the starter unit. Myxovalargin E like myxovalargin A showed an incorporation of isoleucine as starter. Implementing isoleucine as structural basis and considering the dehydrogenation of isoleucine and valine in the myxovalargins, the only reasonable starter is a 2-methyl-but-2-enyl starter.

4.1.13.6 Myxovalargin F

Myxovalargin F is a myxovalargin, which elutes as one of the first myxovalargins in the extract of different myxovalargin producers. While myxovalargin is only produced in small amounts in MCy6431, MCy8286 produces F in larger quantities. F shows a mass shift of 15 Da, which could be allocated to the starter unit. The mass shift, chromatographic behavior of the compound and the information of the other myxovalargin derivatives imply the presence of an amino group in the starter molecule, suggesting the incorporation of valine instead of the deaminated branched chain ketoacid.

4.1.13.7 Myxovalargin G

Myxovalargin G is a commonly found derivative in MCy6431. Its additional mass of 14 Da corresponds to a CH_2 extender. By MS-MS fragmentation the mass shift could be determined at the β-hydroxy moiety, implying a β-isoleucine in this position. Feeding studies with Ile-d10 corroborate this assumption by showing a mass shift for an additional ile incorporated, compared to myxovalargin A (**Figure 44**)

This isoleucine was determined to be integrated in the position of the β-hydroxy amino acid. Myxovalargin G therefore is another example of substrate promiscuity for the hydroxylation mechanism.

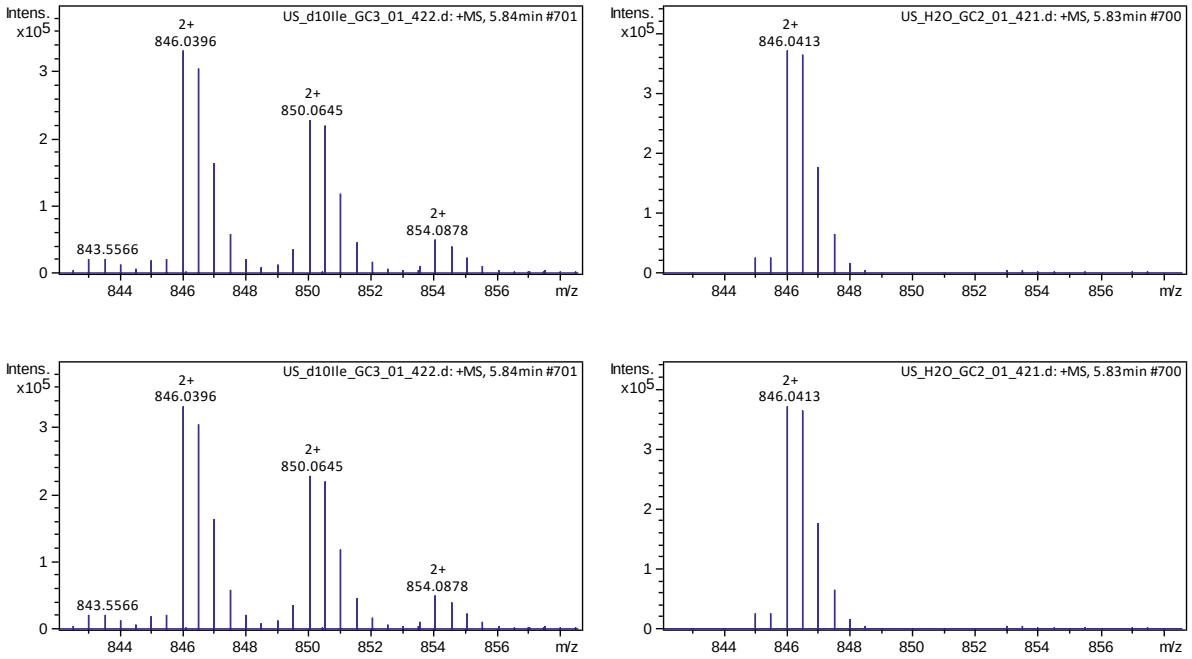

Figure 44: Myxvalargin G exhibits a mass shift of two incorporated isoleucine-d10 precursor. In comparison to myxovalargin A, which has one isoleucine (ile) moiety, myxovalargin G integrates another ile instead of valine in the *β*-hydroxy moiety.

4.1.13.8 Myxovalargin H

Myxovalargin H is a very interesting compound for the elucidation of the biosynthesis mechanisms. The compound is produced in very low yields, nevertheless it was possible to conduct MS fragmentation and determine the chemical constitution of the molecule. With 1660 Da myxovalargin H has a loss of 16 Da compared to myxovalargin A. By MS fragmentation the mass shift could be allocated to the hydroxyl valine moiety of myxovalargin A. As 16 Da correspond exactly to the loss of a hydroxy function, myxovalargin H is assumed to exhibit a non-hydroxylated valine in this position. This mnyxovalargin derivative allows speculation on the hydroxylation mechanism in this position. Two possible reasons lead to the unhydroxylated valine, either a dehydration of the hydroxy valine or a missing hydroxylation of the valine. As a dehydration would imply a doubled bond formation as present in the numerous dehydro amino acids in myxovalargin, an incomplete hydroxylation is reasonable. As the missing hydroxyl moiety did not lead to blockage of the NRPS assembly line and consecutive chain disruption by cleavage by the TEII domain, this modification does not necessarily occur during assembly. Hydroxylation by a tailoring enzyme and not by the NRPS assembly line itself is a feasible

explanation for this observation. The low occurrence of unhydroxylated valine in this position on the other hand implies a high specificity and effectiveness of the tailoring enzyme.

4.1.13.9 Myxovalargin I

Myxovalargin I exhibits a molecular mass of 1664 Da. The occurrence of mass shifts identifies the starter unit as well as the isoleucine moiety as affected moieties. The 14 Da mass loss at the starter indicates the incorporation of valine in this position.

4.1.13.10 Myxovalargin J

Myxovalargin J with a mass of 1678 shows an increase of 2 Da compared to myxovalargin A. This mass difference was attributed to the dehydro-isoleucine moiety of myxovalargin A, indicating a hydrogenation of the isoleucine.

4.1.13.11 Myxovalargin K

Myxovlaragin K was identified by d10-isoleucine supplementation. Similar to myxovalargin G it shows the incorporation of two isoleucine precursors. Myxovlaragin K however, does not show a higher mass as myxovalargin, moreover it elutes approximately at the same time as myxovalargin A and could only be observed by the d10-isoleucine feeding. The mass shift of incorporated d10-isoleucine was determined at the starter position, indicating the incorporation of isoleucine instead of leucine in this position.

4.1.13.12 Myxovalargin L

Myxovalargin L shows a mass shift of – 12 Da compared to myxovalargin A. A plus 2 Da mass shift was observed between fragments z7 and z8 indicating a valine instead of a dehydro-valine in this position. Furthermore indicate the a fragments a mass shift at the starter position as observed for myxovalargin B and C.

4.2 Summary of the myxovlaragin project

During this project it was possible to identify and characterize several myxovalargin producing strains and to establish a reproducible and robust transformation method for the most suitable myxovalargin producer in terms of production and cultivation. The technique was used to elucidate the biosynthesis and apply mutasynthesis. The myxovalargin cluster was partially assembled and identified from several strains and completely assembled for one producer. Most parts of the biosynthesis were elucidated. The cluster borders were determined and the cluster sequence finalized. The origin of the starter was confirmed and a hypothesis for its biosynthesis established. The NRPS cluster was in depth investigated and the assembly process identified. Myxovalargin is the first reported case, where the incorporation of agmatine was proven, supporting the postulated termination mechanism. Though the dehydrogenation and hydroxylation could not be finally elucidated, the gene *mxvH* could be identified, which could unequivocally be shown to be essential in the biosynthesis and which is proposed to catalyse the hydroxylation. Using the biosynthesis knowledge, mutasynthesis by replacing the β -tyrosine moiety and precursor directed biosynthesis by substituting the starter unit was sufficiently performed. Production optimization and up-scaling to of MCy was established to yield mutasynthesis derivatives and natural derivatives for in vivo and in vitro assays. Futhermore, a variety of myxovalargin derivatives could be structurally identified and the myxovalargin A structure was stereochemically revised and structurally confirmed.

4.3 Supplemental information (Myxovalargin)

4.3.1 24 deep-well cultivation of MCy9171

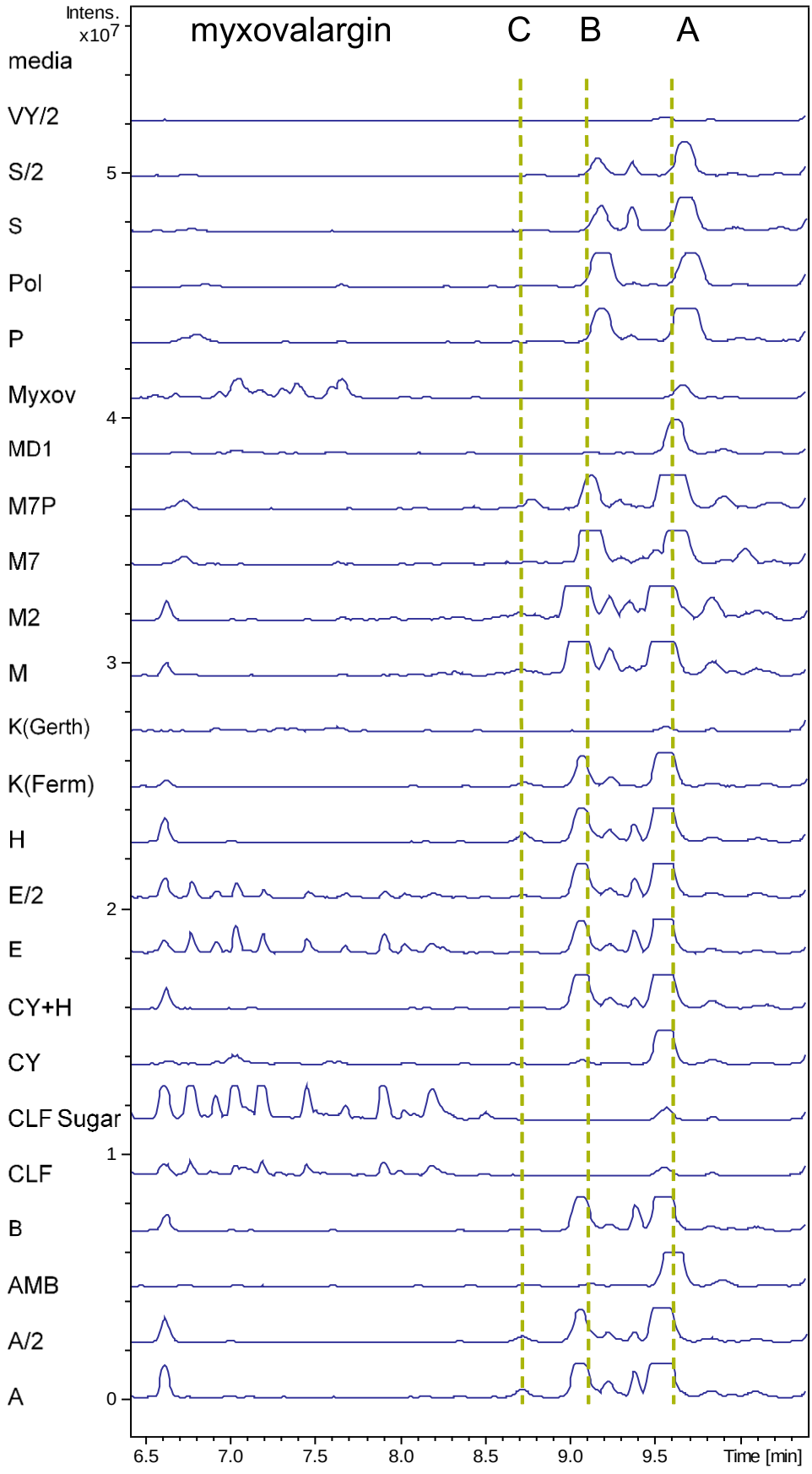

Figure 45: 24 deep-well cultivation of MCy5730 in different media. Results are comparable to cultivation of MCy6431 (Figure 17)

4.3.2 High resolution MS fragmentation of myxovalargins

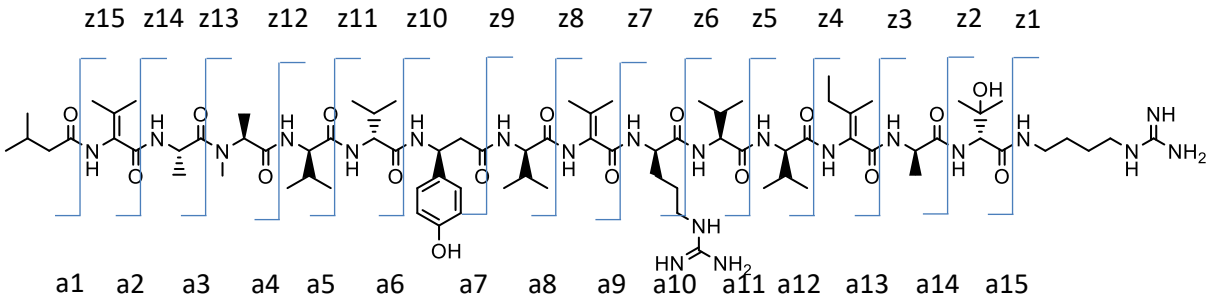

Figure 46: expected a and z fragments according to a linear fragmentation of the peptide by cleavage of the terminal amino acid from C-terminus and N-terminus, respectively.

Table 6: Detected fragments by high resolution MS fragmentation of the myxovalargin derivatives Myxovalargin B (MxvB) to Myxovalargin K (MxvK) and their shift in comparison to the fragments of Myxovalargin A (MxvA). [nd = not detected]

fragment	MxvA	MxvB	shift	MxvC	Shift	MxvD	Shift
a1	nd	nd	nd	nd	nd	nd	nd
a2	nd	nd	nd	nd	nd	nd	nd
a3	253.15433	239.13837	-14	239.13852	-14	225.1235	-28
a4	338.20697	324.19119	-14	324.19086	-14	310.1763	-28
a5	437.27594	429.25961	-14	n.d.	/	n.d.	/
a6	536.3429	522.32703	-14	522.32672	-14	nd	nd
a7	nd	nd	nd	nd	nd	nd	nd
a8	nd	nd	nd	nd	nd	nd	nd
a9	nd	nd	nd	nd	nd	nd	nd
a10	1051.62927	1037.61243	-14	1037.61121	-14	1023.6000	-28
a11	1150.69629	1136.69944	14	nd	nd	nd	nd
a12	1249.76611	1235.74915	14	1235.75256	14	1221.7441	-28
a13	1360.83398	1346.81775	14	1332.80225	28	1318.7933	nd
a14	1431.8723	1417.854149	14	1403.83630	28	nd	nd
a15	nd	nd	nd	nd	nd	nd	nd
z15	810.00996	nd	nd	nd	nd	nd	nd
z14	1495.94739	1495.94519	0	nd	nd	1481.9351	-14
z13	1424.9093	1424.94519	0	nd	nd	1410.9010	-14
z12	1339.85632	1339.85535	0	1325.83887	-14	1325.8468	-14
z11	1240.78943	1240.78821	0	1226.78015	-14	1226.7731	-14
z10	1141.72009	1141.71899	0	1127.70557	-14	1127.7063	-14
z9	nd	nd	0	nd	nd	nd	nd
z8	879.58759	879.58728	0	nd	nd	nd	nd
z7	782.53497	782.55467	0	768.51855	-14	768.5183	-14
z6	626.43378	626.43347	0	612.41718	-14	626.4272	-14
z5	527.36523	527.36493	0	513.34844	-14	513.3496	-14
z4	428.28727	428.29727	0	414.28125	-14	428.2811	-14
z3	317.22919	317.22897	0	nd	nd	317.2301	-14
z2	246.99221	246.64648	0	nd	nd	nd	nd
z1	nd	nd	nd	nd	nd	nd	nd

fragment	MxvA	MxvE	shift	MxvF	Shift	MxvG	Shift
a1	nd	nd	nd	nd	nd	nd	nd
a2	nd	nd	nd	nd	nd	nd	nd
a3	253.15433	251.1379	-2	268.1640	+15	253.1123	0
a4	338.20697	336.1905	-2	353.2170	+15	338.1306	0
a5	437.27594	nd	nd	nd	nd	nd	nd
a6	536.3429	nd	nd	551.3549	+15	536.2454	0
a7	nd	nd	nd	714.4139	nd	nd	nd
a8	nd	nd	nd	nd	nd	nd	nd
a9	nd	nd	nd	910.53925	nd	nd	nd
a10	1051.62927	1049.6122	-2	1066.6398	+15	1051.4943	0
a11	1150.69629	1148.6792	-2	n.d.	nd	1150.7410	0
a12	1249.76611	1247.7469	-2	1264.7818	+15	1249.7610	0
a13	1360.83398	1358.8165	-2	1375.8418	+15	1360.7780	0
a14	1431.8723	1429.8544	-2	1446.3789	+15	1431.5782	0
a15	nd	nd	nd	nd	nd	1560.7540	+14
z15	810.00996	nd	nd	nd	nd	nd	nd
z14	1495.94739	1495.9439	0	1495.94348	0	1509.9647	+14
z13	1424.9093	1424.9072	0	1424.9055	0	1438.6038	+14
z12	1339.85632	1339.8546	0	1339.8538	0	1353.8084	+14
z11	1240.78943	1240.7882	0	1240.7850	0	1254.8623	+14
z10	1141.72009	1141.7188	0	1141.7198	0	1155.7403	+14
z9	nd	nd	nd	nd	nd	nd	nd
z8	879.58759	879.5867	0	879.5880	0	893.6996	+14
z7	782.53497	782.5334	0	782.5341	0	796.5099	+14
z6	626.43378	626.4330	0	626.4330	0	640.3928	+14
z5	527.36523	527.6942	0	527.3642	0	546.3624	+14
z4	428.28727	428.2965	0	428.2958	0	442.3987	+14
z3	317.22919	317.2283	0	317.2287	0	331.3264	+14
z2	246.99221	nd	nd	246.2593	0	nd	nd
z1	nd	nd	nd	nd	nd	nd	nd

fragment	MxvA	MxvH	shift	MxvI	Shift	MxvJ	Shift
a1	nd	nd	nd	nd	nd	nd	nd
a2	nd	nd	nd	nd	nd	nd	nd
a3	253.15433	nd	nd	239.2185	-14	253.1449	0
a4	338.20697	338.2091	0	324.1295	-14	338.0612	0
a5	437.27594	437.2779	0	nd	nd	nd	nd
a6	536.3429	536.3476	0	522.0714	-14	nd	nd
a7	nd	nd	nd	nd	nd	nd	nd
a8	nd	nd	nd	nd	nd	nd	nd
a9	nd	nd	nd	nd	nd	nd	nd
a10	1051.62927	1051.6382	0	1037.4348	-14	1051.4927	0
a11	1150.69629	1150.7068	0	1136.6009	-14	1150.6816	0
a12	1249.76611	1249.7763	0	1233.7118	-14	1249.5070	0
a13	1360.83398	1360.8458	0	1348.4648	-12	1362.9725	+2
a14	1431.8723	nd	nd	1419.9084	-12	1433.2811	+2
a15	nd	nd	nd	nd	nd	nd	nd
z15	810.00996	nd	nd	nd	nd	nd	nd
z14	1495.94739	1479.9643	-16	1497.8822	+2	1497.7963	+2
z13	1424.9093	1408.9255	-16	1426.7817	+2	1426.7006	+2
z12	1339.85632	1323.8726	-16	1341.8357	+2	1341.8364	+2
z11	1240.78943	1224.8035	-16	1242.7562	+2	1242.6579	+2
z10	1141.72009	1125.7340	-16	1143.8298	+2	1143.6873	+2
z9	nd	nd	nd	nd	nd	nd	nd
z8	879.58759	nd	nd	881.5538	+2	881.513373	+2
z7	782.53497	766.5467	-16	784.5770	+2	784.5289	+2
z6	626.43378	nd	nd	628.4280	+2	628.5396	+2
z5	527.36523	511.3750	-16	529.4816	+2	529.3279	+2
z4	428.28727	412.3086	-16	430.1964	+2	430.47510	+2
z3	317.22919	301.2360	-16	317.4724	0	317.2895	0
z2	246.99221	nd	nd	nd	nd	nd	nd
z1	nd	nd	nd	nd	nd	nd	nd

fragment	MxvA	MxvL	shift
a1	nd	nd	nd
a2	nd	nd	nd
a3	253.15433	239.0288	-14
a4	338.20697	324.1874	-14
a5	437.27594	nd	nd
a6	536.3429	522.1089	-14
a7	nd	nd	nd
a8	nd	nd	nd
a9	nd	nd	nd
a10	1051.62927	1039.1877	-12
a11	1150.69629	1138.5553	-12
a12	1249.76611	1237.7727	-12
a13	1360.83398	1348.6334	-12
a14	1431.8723	1419.7814	-12
a15	nd	nd	nd
z15	810.00996	nd	nd
z14	1495.94739	1497.9204	+2
z13	1424.9093	1426.8767	+2
z12	1339.85632	1341.7972	+2
z11	1240.78943	1242.9379	+2
z10	1141.72009	1143.5996	+2
z9	nd	nd	nd
z8	879.58759	881.1407	+2
z7	782.53497	782.4567	0
z6	626.43378	626.3668	0
z5	527.36523	527.4862	0
z4	428.28727	428.3771	0
z3	317.22919	317.2504	0
z2	246.99221	nd	nd
z1	nd	nd	nd

4.5 The Pyruvate dehydrogenase complex

4.5.1 Introduction

The first building block employed in the assembly of a secondary metabolites is called the starter unit. These starter units can be amino acids, metabolites from primary metabolism or they can be specifically synthesized by specialized enzymes as encoded in a secondary metabolite biosynthesis cluster.

In the field of bacterial natural products, a variety of compounds exhibit a starter building block derived from phenyl acetic acid. Examples are the Crypotphycins from Nostoc species, [159] Microcycstins from cyanobacteria [160] and the Thailandamides from Burkholderia thailandensis, [161] but also the Microsclerodermins, [101] produced from different myxobacterial strains, hold this interesting moiety. However, the known mechanisms for phenylacetate formation were not encoded in the strains producing phenalamids, ripostatins and the *Hyalangium* metabolites (Hyafurone, Hyapyron, Hyapyrrolidone), while a different mechanism was postulated: a specialized myxobacterial form of the pyruvate dehydrogenase complex from primary metabolism.

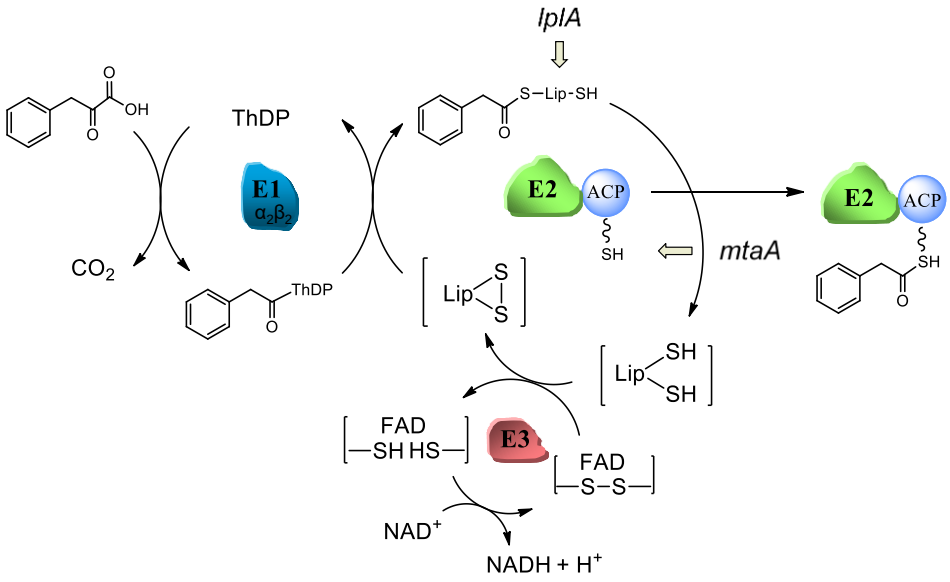

Figure 47: PPDHC complex (U. Scheid modified from Y.Li). The PPDHC in secondary metabolites of myxobacteria catalyzes a similar reaction as the 2-Oxoacid dehydrogenase complexes in primary metabolism. In contrast to primary metabolism, the reaction product ist conjugated to an ACP domain, thus making the precursor accessible for the secondary metabolite production via a polyketide synthase.

4.5.2 Occurrence in myxobacteria

Beside the Microsclerodermins, a putative phenylacetate starter is found in three myxobacterial natural products. The ripostatins [162,163], the phenalamids [164] and the polyketides from *Hyalangium minutum*, hyafurone, hyapyrrolines and hyapyrones. [165] For the phenalamides and the ripostatins it was experimentally shown, that the starter originates from L-phenylalanine. [165] In between the genes encoding the ripostatin biosynthesis, three ORFs were identified showing similarity to genes encoding E1α and β subunit (*ripF*, *ripG*), as well as E2 (*ripH*) of the pyruvate dehydrogenase complex known from primary metabolism in prokaryotes and eukaryotes. [166] To analyse the origin of the phenylacetate starter in the phenalamids and *Hyalangium* polyketides, their gene clusters were identified, the genetic sequence completed and a biosynthesis hypothesis proclaimed. Homologues of E1α, E1β and E2 were found in both clusters (Figure 48).

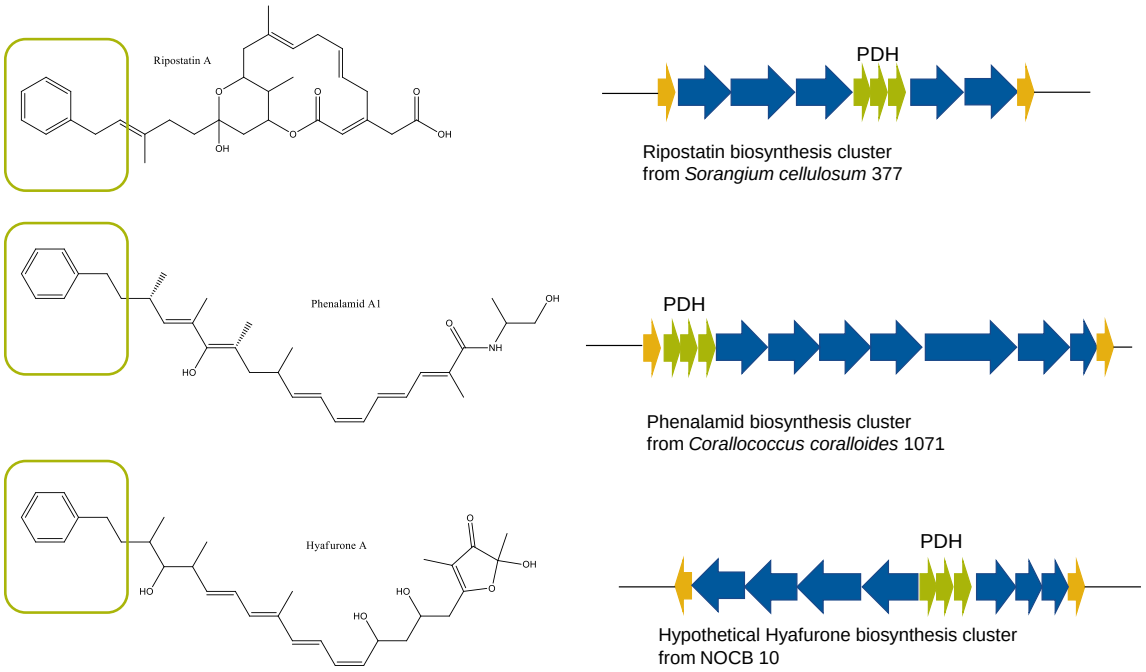

Figure 48: Three myxobacterial compound classes , exemplarily ripostatin A, phenalamid A1 and hyafurone A, combine the presence of the phenylacetate starter (green box) with the presence of three genes (green arrows) encoding proteins similar to E1α, E1β and E2 of the pyruvate dehydrogenase complex, which is known from primary metabolism. These genes are located closely to the respective PKS assembly line (blue arrows).

4.5.3 2-Oxoacid dehydrogenase complexes (OADHC)

A family of catalytic multienzyme complexes with similar proteinogenic character and catalytic function is the family of 2-Oxoacid dehydrogenase complexes. This group comprises the branched chain 2-oxoacid dehydrogenase complex (BCOADHC), pyruvate dehydrogenase complex (PDHC) and the 2-oxoglutarate dehydrogenase complex (OGDHC).[167] Those enzyme complexes play central roles in primary metabolism (Figure 49).

The BCOADC occurs in eukaryotes and prokaryotes. Its substrates are valine, isoleucine, leucine and derivatives. Interestingly, besides its predominant role in primary metabolism, it could be shown that the BCOADC is also responsible for the biosynthesis of precursors for the Myxalamids. This knowledge was used to sucessfully apply mutagenesis experiments, yielding a variety of mutasynthetic derivatives. [156] Also for the myxovalargins a branched chain ketoacid dehydrogenase complex (bkd) is supposed to provide the leucine derived precursor for myxovalargin A and the isoleucine derived starter unit for myxovalargin B (**Fehler! V erweisquelle konnte nicht gefunden werden.**). The same producer seems to use another OADHC related complex in secondary metabolism, which is responsible for the biosynthesis of precursors for the phenalamids. However, this complex is related to the pyruvate dehydrogenase complex.

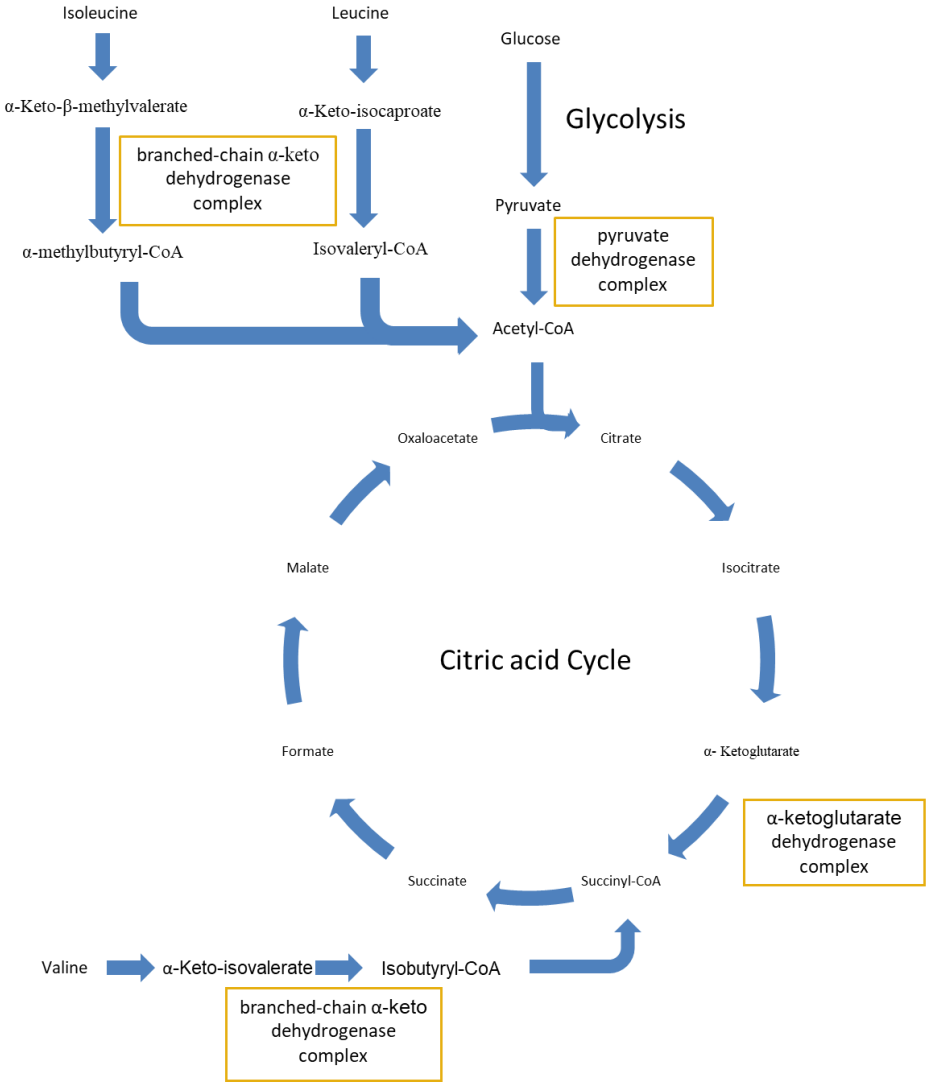

Figure 49: The 2-Oxoacid dehydrogenase complexes play central roles in primary metabolism and in particular the glycolysis and citric acid cycle. The pyruvate dehydrogenase complex catalyzes the formation of acetyl-CoA from pyruvate linking glycolysis and citric cycle. 2-oxoacid dehydrogenase complexes, furthermore, catalyse the formation of different precursor (α-methylbutyryl-CoA, Isobutyryl-CoA and Isovaleryl -CoA) and intermediates (Succinyl-CoA) of the citric acid cycle.

The pyruvate dehydrogenase complex (PDC) also is a central part of primary metabolism in eukaryotes and prokaryotes. Its essential role abounds in case of malefaction in humans leading to metabolic acidosis and neurological deficiency which can cause in e.g. microcephaly and blindness.[168] The PDH holds its central function is the linkage of glycolysis and citric acid cycle by catalysing the conversion of pyruvate to acetyl-CoA. Due to its importance it has been well studied in vivo and in vitro. The complex consists of three enzymes: the pyruvate decarboxylase (E1), the dihydrolipoyl transacetylase (E2) and the lipoamide dehydrogenase

(E3). The numeric distribution of the enzymes differ in eukaryotes and prokaryotes in the PDHC multienzyme complex. In Gram-negative bacteria, E2 monomers build trimers, which form the heart of the complex, the 24 mer cubic core. 24 E1 enzymes and 12 E3 enzymes are attached to the core forming the approximately $5*10^6$ Da assembled multienzyme complex. The E2 core of eukaryotes and Gam-positive bacteria, on the other hand, consists of 60 E2 enzymes. The complex catalyses two modifications of the substrate by the E1 and E2 proteins, while E3 restores the functionality of the E2 catalytic domains.

In a first step the pyruvate decarboxylase E1 enables the decarboxylation of the substrate by elimination of the carboxylic acid. For this it needs thiamine pyrophosphate (TPP) as cofactor, which attacks the carbonyl carbon. The TPP is released, when the swinging lipoyl arm of E2 forms a thioacetate. This lipoyl arm is derived from the cofactor dihydrolipoamide and can translocate the acetyl from the E1 catalytic center to the active site of the E2 unit. Here the acetyl moiety is transferred to CoA by transacylation. The remaining dihidrolipoate is oxidized by the E3 unit to restore the disulfide. For this FAD is reduced to $FADH_2$, which then is oxidized again by reduction of NAD^+ to NADH. The Acetyl-CoA product can undergo a variety of reactions primary metabolism like in the citric cycle or fatty acid biosynthesis.

4.5.4 The Phenyl pyruvate complex (PPDHC)

In contrast to the BCKODAC, which uses multiple substrates of similar chemical structure in primary and secondary metabolism, the pyruvate dehydrogenase complex has a strong specificity for pyruvate. Close to the PKS assembly line of different myxobacteria it was possible to identify another OADHC, which is closely relate to the PDHC. We call this cluster phenyl pyruvate dehydrogenase complex (PPDHC) as it is closely related to the PDHC, but is assumed to have a high specificity for phenyl pyruvate. The compound classes of ripostatins, phenalamids and Hyalangium metabolites contain a phenylacetate starter. As phenylacetate has already been discovered in other secondary metabolites, the genomes were screened for central genes responsible for phenylacetate formation in thalandamides, microcystins and microsclerodermins, giving no hits of similar encoded machineries. Therefore, the PPDHC related genes were further investigated. The three genes show strong homology to E1 subunit α and E1 subunit β as well as E2 of known PDHC complexes. However, a closely located E3 encoding gene could not be identified in any of the producers. E3 genes allocated near E1 and E2 genes of the putative PDHC complex of primary metabolism remote to the secondary metabolite clusters were found by the screening. While the E1 subunit α and β show a

comparable length of the genes compared to PDHC genes, the E2 encoding open reading frame shows additional ~ 200 bp at the downstream region. These additional base pairs are present in E2 genes of all three PPDHC of myxobacterial cluster, but not in genes of putative PDHC cluster in different bacteria including myxobacteria (Figure 50). Sequence alignments of this region show strong homology to acyl carrier proteins.

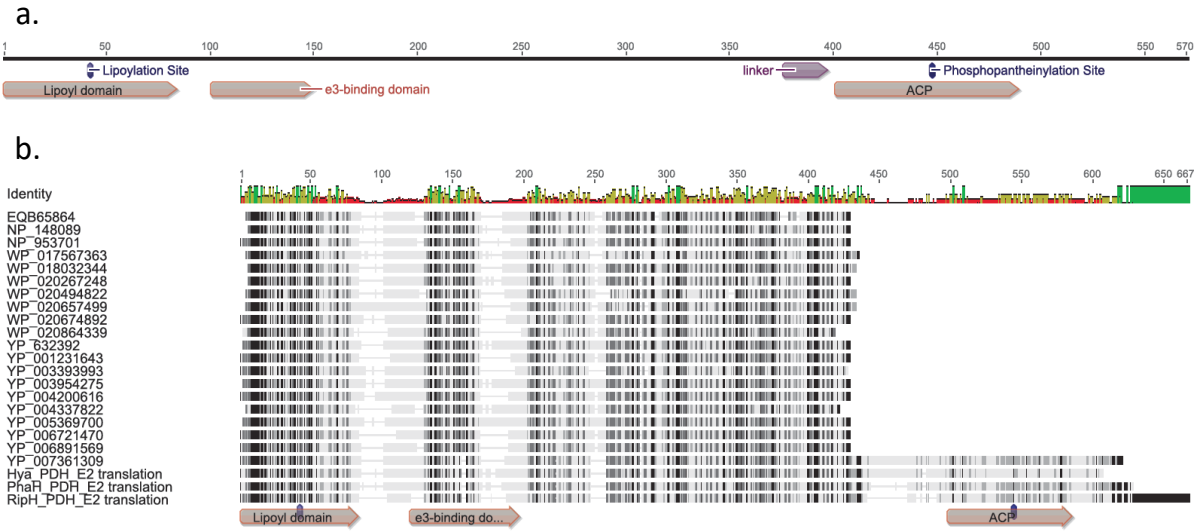

Figure 50: a. *ripH* encoding the dihydrolipoyl transacetylase (E2) and an additional carrier protein. b. In contrast to several E2 proteins from primary metabolism of pyruvate dehydrogenase complexes (PDHC) in several different bacteria (including myxobacteria), the phenyl pyruvate dehydrogenase E2 protein of secondary metabolism in myxobacteria has a sequence elongation for the carrier protein. The myxobacterial secondary metabolite sequences are *ripH* of the ripostatin cluster, *phaH* of the phenalamid cluster, and the gene encoding E2 of the Hyafurone cluster (hya) as well as YP_007361309 from the stipiamids of *Myxococcus stipitatus*, a phenalamid derivative.

Therefore, we proposed that those genes encode the PPDHC, which catalyzes the decarboxylation of phenyl pyruvate to form phenyl acetate, which gets conjugated to an acyl carrier protein (ACP). (Figure 47) The ACP domain pPant bound Phenyl acetate intermediate offers the unit for consecutive PKS assembly of the respective clusters. By the pPant arm in this case the phenyl acetyl can be transacetylated from the swinging lipoyl arm, which translocates the phenyl acetate from the E1 active center to the E2 active center, to the ACP domain forming the pPant thioester. The swinging pPant arm furthermore is able to translocate the phenyl acetate from the E2 active center to the AT domain for the first module. Weather the ACP domain dispatches from the PPDHC multienzyme complex or the PPDHC complex allocates to the PKS multienzyme complex, needs to be determined. Gene expression and in

vitro and in vivo experiments were performed to support this hypothesis. The final confirmation of the proposed biosynthesis was achieved bei Chengzhang Fu, David Auerbach et al.[169]

4.5.5 Expression of the PPDHC

Espression of the phenyl pyruvate dehydrogenase complex enzymes was performed using pet28b vector system. Beside constructs with the genetic regions of MSr7234 from the ripostatin cluster, also the encoding region of MCy6431 in the phenalamid cluster was used. All constructs showed similar properties regarding expression and purification.

The expression of E1α and E1β was executed in different setups using different expression strains, constructs and work up procedures. The yield of soluble protein in all cases was low. Nevertheless, a certain amount of soluble protein could be expressed using BL21 with a pet28b construct. The subunit E2 was expressed in BL21 using a pet28b vector. The protein could be overexpressed and purified by His-tag affinity chromatography using an Äkta prime system. The respective fractions show a protein of ~ 65 kDa in SDS-PAGE. The respective fractions were analysed by high resolution mass spectrometry to identify the exact mass. The expected mass of the protein by peptide sequence of E2 minus the starter L-Methionin and plus the His-tag of 62445 Da was detected. (**Figure 51**). Consecutively co-expression with different vectors carrying the required cofactors was carried out to yield in vivo the full functional enzyme. By co-expression with *lpl*A under supplementation of lipoic acid at 0.2 mM the respective mass shift of + 189 Da was observerd. Furthermore, by coexpression of E2 with MtaA the mass shift of +340 corresponding to the pPant arm was observed. Also co-expression with two plasmid harboring *mta*A and *lpl*A yielded a mass of 62974 close to the expected size of 62978 Da. Attempts to perform an in vitro assay using the in vivo generated holo enzyme and E1 and E3 according to reported assay set-ups[170,171] was not successful. Also trying to load solely on the enzyme linked ACP domain with substrate or product of the E2 reaction step did not yield a mass shift compared to the negative control under the used conditions.

Considering the proposed hypothesis and results of the carried out trials, the project was then successfully finalized by collaborators Fu et al., using an in vitro approach to reconstitute the holo enzyme and finally to confirm the proposed reaction mechanism. [169]

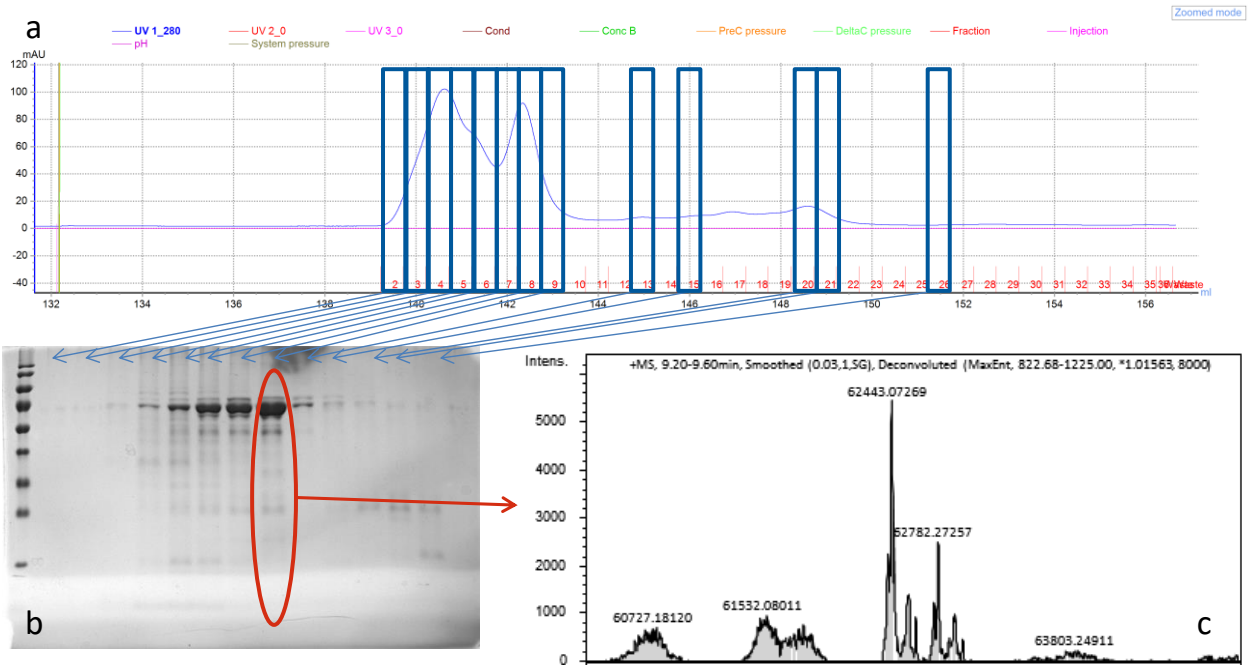

Figure 51: a. Gelfiltration of the in BL21 expressed E2 protein of the phenyl pyruvate dehydrogenase complex after His-tag affinity chromatography. b. SDS-PAGE of gel filtration fractions shows a protein about 60 to 70 kDa. c. HRESIMS measurements of fraction 9 show a mass of the expected size of 62443 Da.

4.5.6 Ripostatin

The Ripostatins belong to an intensively studied group of RNA-Polymerase (RNAP) inhibitors binding to the switch region of RNAPs. [45] This target is of particular interest since it does not collocate with the Rifampicin (Rif) binding site, a standard therapeutic drug in *Mycobacterium tuberculosis* therapy. [172] Furthermore, molecules targeting this region do not show cross resistance with Rifampicin like drugs. [173] Since resistance development limits tuberculosis (TB) therapy, even though a sophisticated treatment regime is required, new drugs, especially those overcoming the problem of Rifampicin resistance are urgently needed. [174] Since the RNAP has been extensively studied, detailed binding modes can be identified with modern techniques. [175] Interestingly, myxobacteria produce beside the ripostatins, two additional natural products addressing this target, the myxopyronins [176] and the corallopyronins. [177] Knowledge of the biosynthesis of myxopyronin was used to make it accessible for mutasynthesis derivatization. [178,179]

The biosynthesis cluster of the ripostatins was identified from Yanyan Li (HIPS-MINS) from the genomic sequence of *Sorangium cellulosum* 377. Random transposon mutagenesis led to a direct link of the Ripostatin genotype (*rpo*) with the phenotype of the ripostatin compounds. [180] Though a hypothesis for the phenylpyruvate dehydrogenase complex was set up, the assembly of the ripostatins remained unclear. Since understanding in trans-PKS biosynthesis has proceeded in recent years, [92] it was here possible to summarize a plausible hypothesis for the production of the ripostatins (Figure 18).

The ripostatin biosynthesis starts with the generation of phenylacetate from L-phenylalanine by the phenyl pyruvate dehydrogenase complex (PPDC), encoded on *ripF-H*. The phenylacetate intermediate is bound to the PCP domain which is encoded on *ripH* together with the E2 protein of the PPDC. The polyketide is assembled by nine modules encoded on six genes in the order *ripI, J, B, C, D, E*. Only module 1 shows an AT domain, while other modules lack this essential domain. Therefore, two AT domains are located on genes *ripM* and *ripN*, as known for trans-AT polyketide cluster.[181] In silico alignment revealed substrate specificity for methyl malonyl-CoA by the AT domain of module 1, while the trans-AT *ripM* recruits malonyl-CoA, leading to incorporation of malonyl-CoA in all other modules.

Two side chains in beta position occur. This is catalysed by a beta branching cassette, whose proteins are encoded on *ripA* (HMG CoA Synthase), *ripK* (Enoyl-CoA Hyrolase), *ripL* (Enoyl-CoA-Hydrolase), *ripR* (Ketosynthase), *ripQ* (acyl carrier protein). This enzymatic cascade adds the *β*-branches in module 6 and 9. The catalytic reactions of the beta branching cassette were investigated, demonstrating a HMG-CoA synthase catalysed beta branching in polyketide trans-AT clusters. [181,182] Furthermore, the gene *ripO* shows homology to trans acting enoyl reductase.[183] The trans-enoyl reductase substitutes the missing ER domain in module 7 leading to a saturated extender unit. The biosynthesis including the interaction with the pheny pyruvate dehydrogenase complex was published by Fu et al. [169]

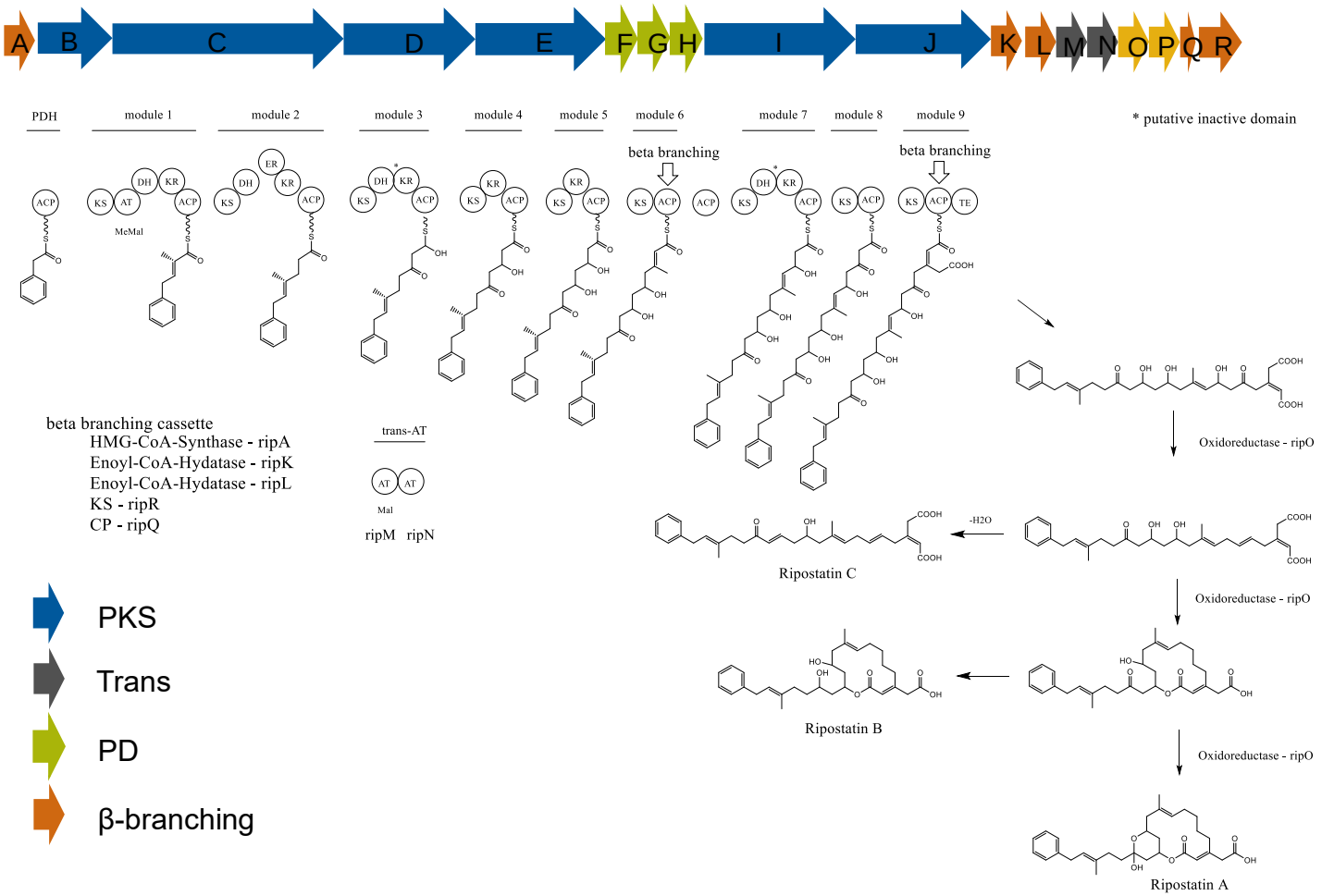

Figure 52: The biosynthesis cluster of ripostatin holds 18 genes. The PKS part in order of the modules in the assembly line is encoded on genes *ripI, J, B, C, D, E*. The phenyl pyruvate dehydrogenase complex (PDH), which generates the PCP bound starter phenyl acetate is located on genes *ripF-H*. Two beta-branching steps are facilitated by a respective protein cassette from genes *ripA* (HMG-CoA-Synthase), *ripK* and *L* (Enoyl-CoA-Hydratase), *ripR* (Ketosynthase) and *ripQ* (carrier protein). The trans-AT domains are encoded on *ripM* and N. *RipO*, an enoylreductase, might play a role in reduction of the keto moiety between module 6 and 7.

4.5.7 Phenalamide

The phenalamides are a class of compounds with antiretroviral activity[10,11]. Recently the phenalamides revealed beside other myxobacterial compoungs high activity by suppressing HIV-1-mediated cell death in the MT-4 cell assay. [184] These compounds arouse interest during this work as they were identified in extracts of MCy6431. The main focus of this project is set on the biosynthesis, in particular on the biosynthesis of the starter unit, derived from phenylalanine. Furthermore the two closely related biosynthesis pathways from the myxalamids[12] and the phenalamides might offer interesting aspects for evolutionary approaches on secondary metabolism development.

The assembly line of the phenalamid cluster could be completed leading to a nine modules spanning assembly line (Figure 53) As a starter unit phenylalanine is incorporated after conversion to phenyl acetate and loading on a carrier protein encoded on the gene of the E2 protein of the phenylpyruvate dehydrogenase complex.

.

I. 1.1.1. Assembly line

A comparison with the myxalamid cluster shows the close similarity which is already obvious in their chemical structures. The difference in the first two building blocks can be explained by the proposed model of the PDH complex and the, for the incorporation necessary, module *phaG,* as well as an additional module *phaF* for the first extender unit (Figure 54).

Beside the difference in the first two modules the phenalamide cluster encodes the phenyl pyruvate dehydrogenase complex on genes *ripH*, *ripI* and *ripJ*. (Figure 53).

The gene cluster was identified during the experimental part of this project in 2014. The phenalamide cluster in *Myxococcus stipitatus* DSM14675 was published by Park et al. in 2016, but without elucidation of the phenyl pyruvate dehydrogenase complex.[185]

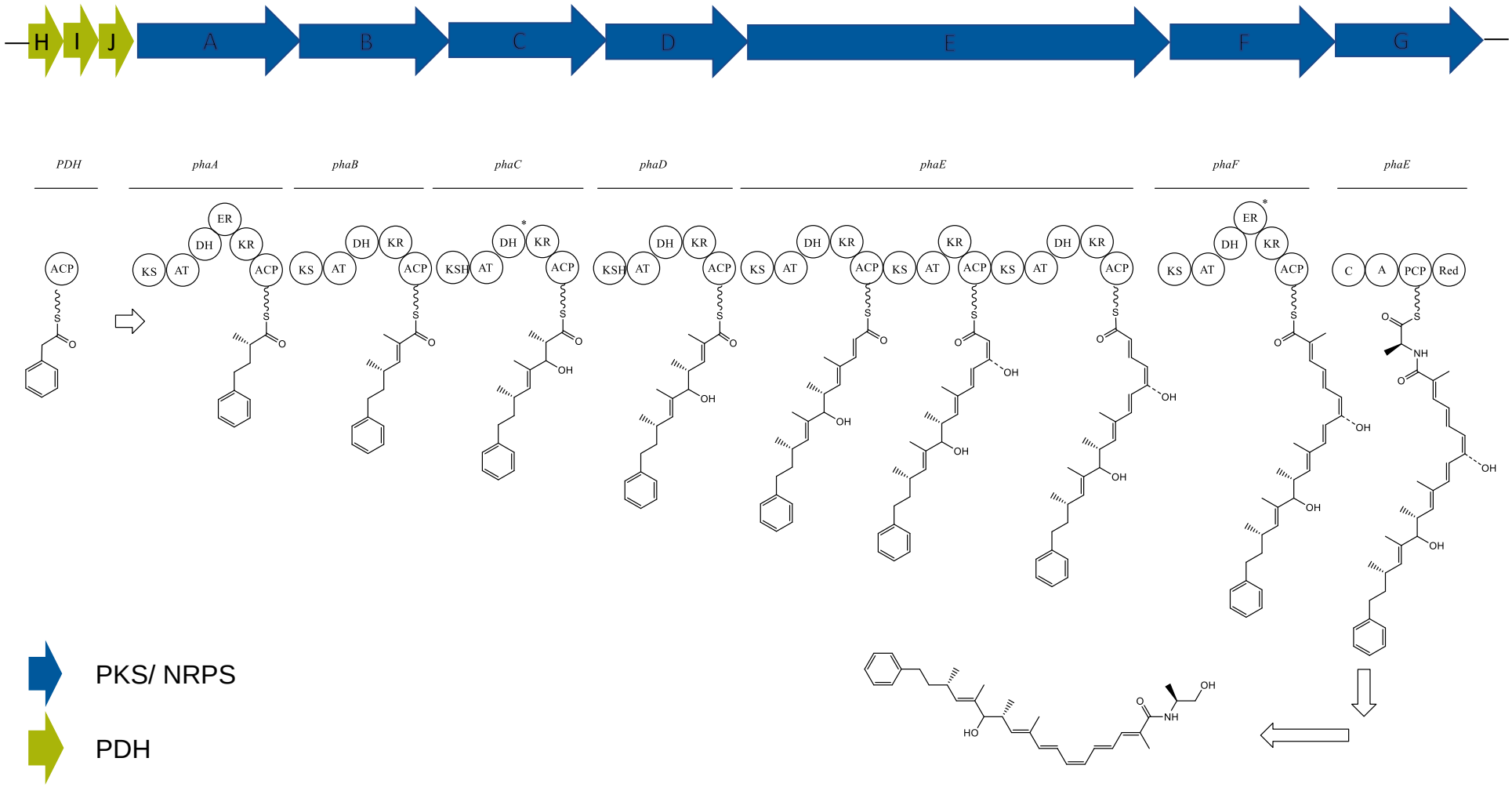

Figure 53: Phenalamide biosynthesis cluster. The cluster consists of seven genes *phaA* to *phaE* encoding the PKS assembly line. *Pha*H – *phaJ* encode the phenyl pyruvate dehydrogenase complex, which generates the phenyl acetate starter moiety.

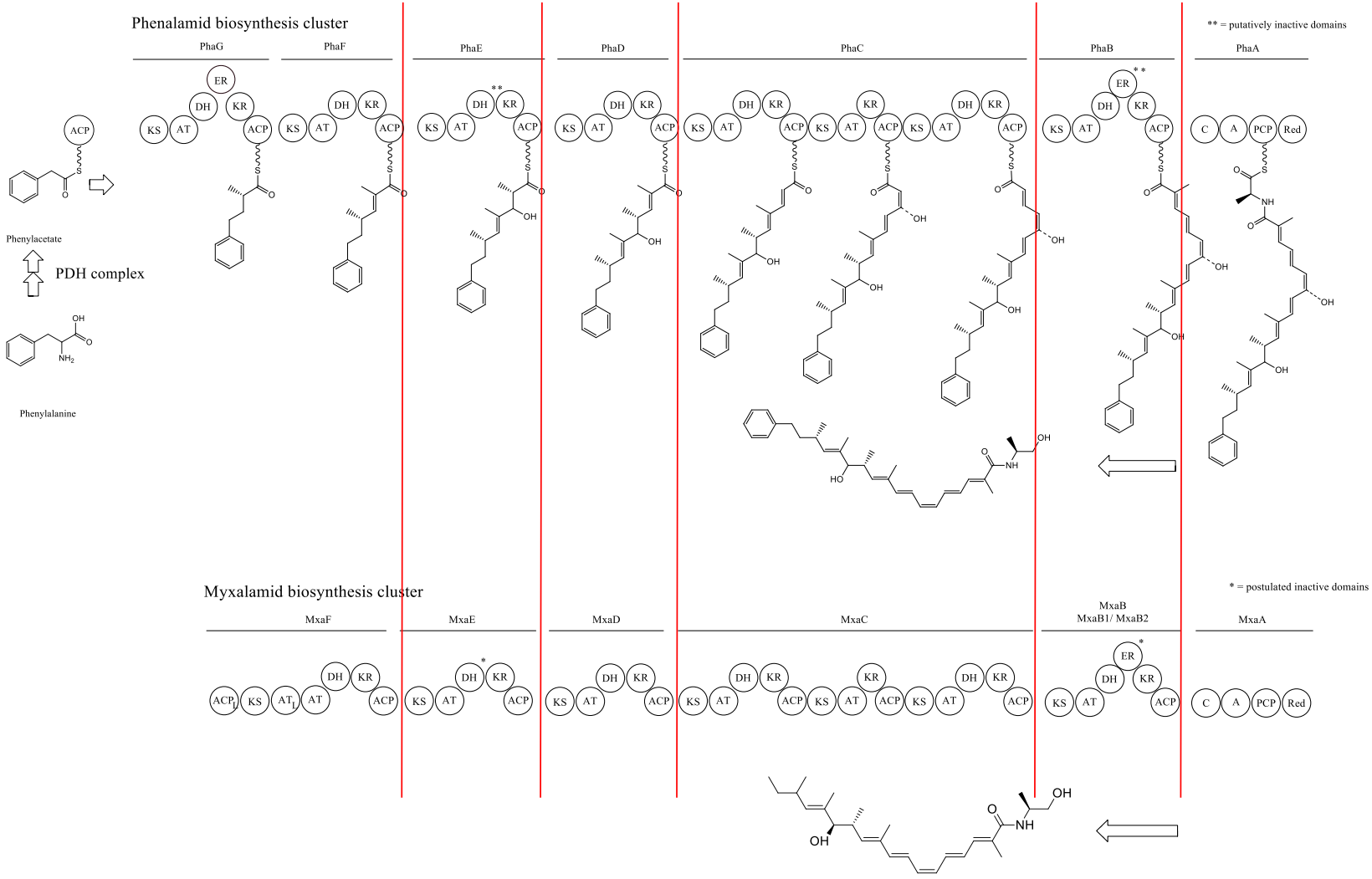

Figure 54: comparison of the phenalamid and myxalamid assembly line. Genes *mxaA – mxaE* are identical to *phaA – phaE*. Instead of *mxaF*, the phenalamid cluster has to additional genes, *phaF* and *phaG* to incorporate the starter unit produced by the phenyl pyruvate dehydrogenase complex.

4.5.8 The polyketides from *Hyalangium minutum* – hyafurones, hyapyrones, hyapyrrolidines

The Hyafurones are of certain interest in the project of the phenylpyruvate dehydrogenase complex as they are the third group of myxobacterial compounds which show the phenylacetate starter unit and genes for the assumed phenyl pyruvate dehydrogenase complex. The structure and purification of the *Hyalangium minutum* polyketides including hyafurone has been published by Okanya et al..[17]

The hyafurone cluster was identified in silico from *Hyalangium minutum* MCy2730 (NOCb10), but can be also found in the sequence of *Hyalangium minutum* MCy2721 (NOCb2) and *Hyalangium minutum* MCy4189 (Hym3). The cluster was split onto two scaffolds, but by using primers NOCB10_hya1_fwd and NOCB10_hya1_rev an amplicon of approximately 5 kbp could be amplified, isolated and was cloned in the pJet vector. The insert was sequenced by primer walking. Homology of the 3´end and the 5´end with the corresponding known sequence suggests the correct amplicon. The scaffolds were conjugated with the respective amplicon to complete the sequence of the putative hyafurone cluster. (Figure **56**).

Though the polyketide assembly line of hyafurones was identified, the elucidation of the biosynthesis will need additional investigations. Beside the hyafurones, also the hyapyrones and hyapyrrolidines are produced. As all three groups exhibit the same polyketide backbone, but only differences in the terminal cyclic reorganization, it is assumed that all of these polyketides are generated from the enzymatic product of the hyafurone PKS. However, due to their chemical variety and the sophisticated genetic module organization the biosynthesis could not be finalized.

Nevertheless, the hyafurones show an interesting chemical composition, as the left part of the molecule with its phenylacetate starter, shows high similarity to phenalamide A, while the right end with its furon ring is similar to aurafurone A[186] (**Figure 55**).

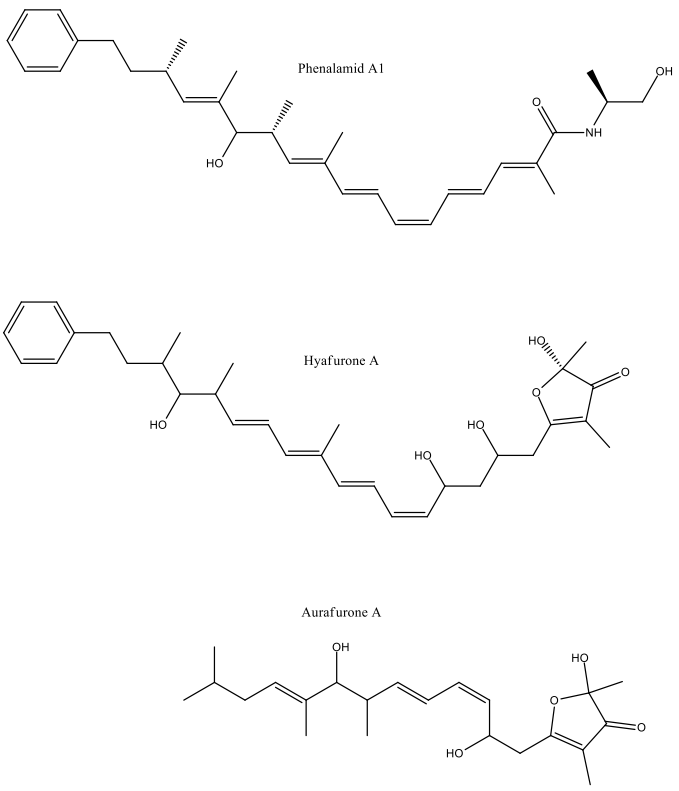

Figure 55: comparison of hyafurone A1 with phenalamid A1 and ripostatin A. The western part of the structure is similar to phenalamid A1, while the

Moreover, with the different molecules in hand and considering the assumption that hyafurones and hyapyrrolines originate from the same assembly line, these molecules might shed light on the biosynthesis of the aurafurones. During the characterization of the aurafurone biosynthesis it could not be finally clarified, if the formation reaction of the furanone ring undergoes Baeyer-villiger reaction like lacton formation with a pyrroline intermediate after PKS release or a PKS bound multistep reaction either with chain extension or without.[187] Due to the pyrone intermediate, which would lead in few steps to hyapyrone B this pathway seems to be most likely, as it explains the origin of hyapyrone B as well as the hyafurones.

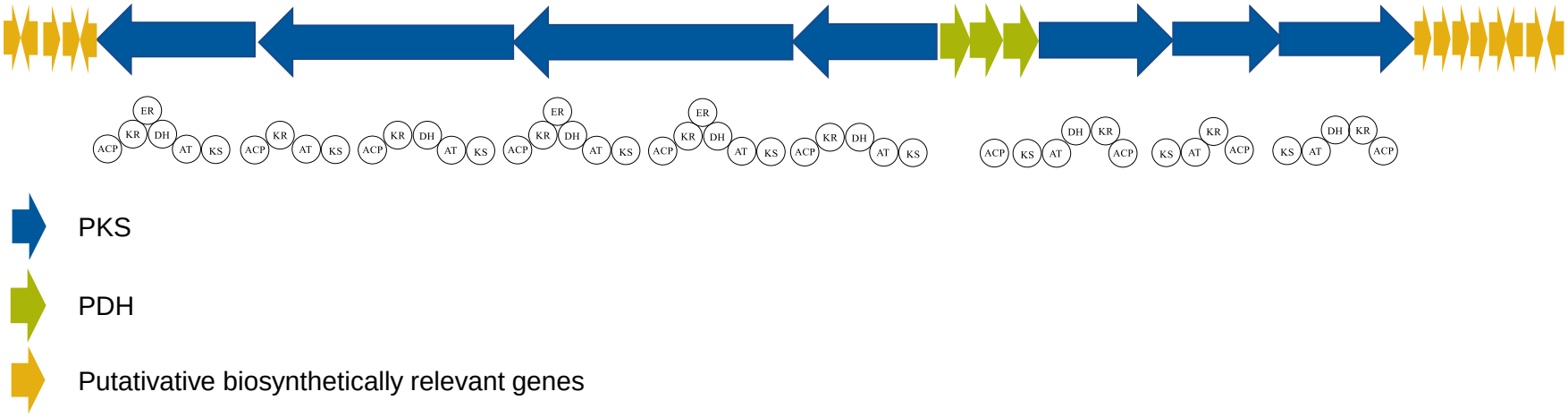

Figure 56: putative Hyafurone biosynthesis cluster from *Hyalangium minutum MCy2730* . Seven PKS genes encode 9 PKS modules. The genes of the phenyl pyruvate dehydrogenase complex (PDH) are located between the PKS genes. Several ORFs with putative functions in the biosynthesis of the diverse heterocyclic metabolites are adjoined upstream and downstream of the assembly line. The respective functions and a hypothesis for the polyketide backbone, heterocyclization and modification have been proposed in the last report.

4.5.9 SNAC Feeding

In order to use the precursor biosynthesis of the phenyl pyruvate dehydrogenase complex for precursor-directed biosynthesis and mutasynthesis, a set of SNAC derivatives of phenyl-pyruvate was used for feeding experiments (Figure 58).

A knockout mutant of the PDH complex in the Myxovalargin producter MCy6431 by disruption of genes *phaA* could be achieved, which led to a loss of the phenalamid production.

Feeding of SNAC esters of phenyl acetate derivatives did not lead to an incorporation in the phenalamides, neither in the wildtype, nor in the PDH KO mutant. Peaks of the precursors can be found in the chromatogram (Figure 60), demonstrating the physicochemical stability. On the other hand the occurrence of the SNAC ester in the extract might be a sign of a missing incorporation. Therefore, addition of 1 % DMSO to the cell broth was carried out in order to enhance membrane penetration. The supplementation did not yield production restoration, though sufficient cell growth could be observed.

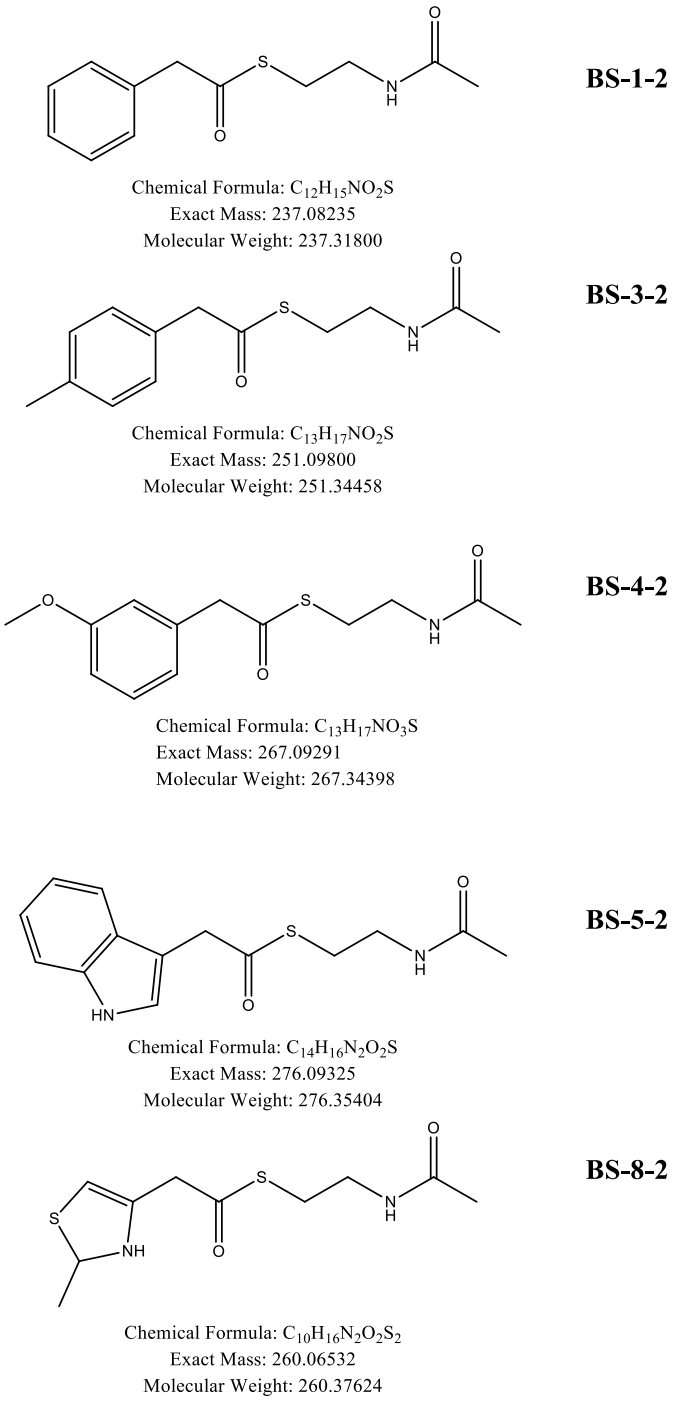

Figure 57: SNAC ester of different phenyl pyruvate derived compounds.

Though incorporation of the chemically related SNAC esters in the wildtype did not yield the expected derivatives indicating that the deficiency was not caused by the knockout itself, the knockout was repeated by insertion of the consecutive tn5 promotor. Also this did not support incorporation.

The SNAC ester feeding was also carried out in the ripostatin producer MSr7234. Also here an incorporation in the ripostatin molecule could not be observed.

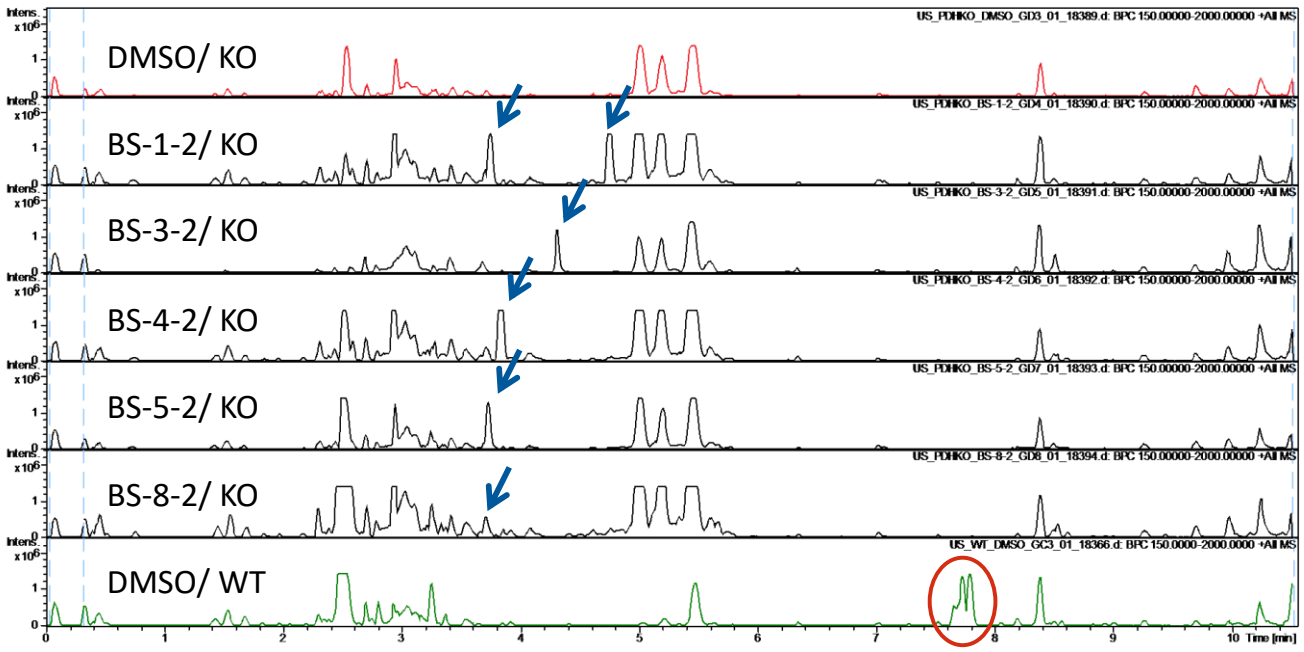

Figure 59 Feeding of phenyl acetate SNAC derivatives. The pyruvate dehydrogenase complex mutant of Ccc1071 was fed with 0.2 mM mutasynthon dissolved in DMSO. As reference the mutant was fed with DMSO. The same experiment was done in parallel with the wildtype (only DMSO reference shown here). An incorporation of the SNAC ester into phenalamid (red circle) could not be detected, neither in the mutant, nor in the wildtype, whereas the free SNAC esters show peaks in the chromatogram (blue arrow) in mutant and wildtype.

5. Discussion

The urgent need for new antibacterial compounds is an issue, which grows more acute every year. The uprising of resistant pathogens - especially multiresistent pathogens - has become a central challenge in antiinfective therapy and has also gained public interest beyond the borders of research and clinical application. A clear presentation of the alarming levels of antimicrobial resistance, was highlighted by the WHO in their global report on surveillance[188]. Updates in regulatory laws[12] or guidance [189,190] try to reduce the unjustified use of antibiotics for human use and in veterinary medicine. International expert teams like the Transatlantic Task Force on Antimicrobial Resistance (TATFAR) [191] were already agreed on by the then-US president and then-President of EU ministers in 2009. However, the recent case of the last-resort drug colisitin, which should be withhold for urgent lifesaving cases of multi drug resistance, has shown how fast a worldwide resistance can spread. The enzym mcr-1 leading to colisitin resistance [192] has been identified worldwide within the last years. [193,194] Colistin is just another example of the continuing identification of drug resistances against final therapy options. Already the resistance against the last resort drug vancomycin of enterococci and staphylococci [195] was a throwback for global health. However, dedicated work of research institutes over the world, continuously have followed up the work on identifying new antibiotics from various sources[196], optimizing known compounds as for example happened for the above mentioned vancomycin[197] or tetracyclines[198] or identifying new targets like demonstrated for myxobacterial natural products .[199] All efforts require a decent level of basic research, as still most of all antiobiotics are of bacterial origin.[200] Recent advances in biotechnology and increased understanding of genomic information has enabled to advance the identification of natural products, but also to re-evaluate our knowledge about known compounds.[201] The myxovalargins are an applicable example how knowledge and technology at time of discovery were exhausted to their possibilites,[114] but recent technologies and new information has enabled the in-depth characterization, allowed genetic access to investigate biosynthesis on the molecular level, and where necessary triggered revision of initial findings. Results of this thesis build the second step of myxovalargin history. After identification, first structure elucidation and bioactivity screening, the foundation is laid for genetic engineering, metabolic engineering and production enhancement.

5.1 Natural Product Chemistry and Biology – Combining approaches to unravel the full picture

Natural product discovery has been in the focus of anti-infective research since its early applications in traditional medicines and after the historical, well known identification of fungal antibiotic properties.[7] After a period of fruitful identification and characterization of a large variety of natural products for antiinfective use, with the increased upcoming of identification of molecular targets, research focus went from isolation of new natural products to chemically synthesized small molecules, which led to such potent drugs as the fluorochinolons.[202] Nevertheless, undesirable side effects always casted a cloud over the chemically synthesized Gyrase inhibitors.[203]

Though the idea to combine chemical and biological approaches has been early used to develop semisynthetically derived natural products, both disciplines were generally used in separated manufacturing steps rather than a direct interaction at different stages of development. The modification of natural product matrices with the toolbox of chemical reactions in the field of organic chemistry was used to generate groups of closely related semisynthetic compounds. Physicochemical difficulties as stability and solubility were tackled as well as pharmacological issues, but also economical and patent limitations were overcome by this approach. Semisynthesis in drug development has enabled to yield such potent drugs as the last resort antibiotics tigecycline and doxycycline.[204,205]

Just in recent years the understanding of biosynthetic machineries has enabled a directed dovetailing of biological and chemical approaches for in-line biotechnological production of semisynthetic compounds.[206,207] The fast and relatively cheap sequencing of whole genomes by new technologies has facilitated the collection of a variety of genetic information of different eukaryotic and prokaryotic origin.[208,209] On the other hand, since the identification of basic biosynthetic mechanisms and their assignment to distinct genomic sequences in various natural product synthesizing organisms, the intense investigation of these machineries has led to an increasing knowledge and understanding of the origin of the chemically and biologically refined natural products.[210] Beside the numerous published NRPS and PKS gene clusters of bacterial origin, a variety of non-published clusters and partially identified clusters is still in the pipeline of research groups all over the world.

Nevertheless, research on elucidation of biosynthesis pathways of natural products remains a tedious, time- and resource-consuming investigational effort. The benefit for applicational use in the field of antibiotics research - despite the benefit of basic knowledge - is not always obvious. The knowledge about a secondary metabolite's biosynthesis, however, offers several important insights and opportunities to understand (and allow the exploitation of) a group of natural product compounds. The identification and characterization of natural product biosynthesis gives biotechnology the opportunity to discern and take targeted influence on the outcome of natural product manufacturing in the host cell. It is possible to influence the yields by overcoming production bottlenecks as precursor, enzyme regulation or self-resistance, as well as by promotor switches or even total host switch.[211] The structural outcome can be challenged by combined chemical and biosynthetic approaches as precursor directed biosynthesis or mutasynthesis.[212,213] Also the introduction or exchange of enzymes or even intermediate pathways can be helpful. The increasing number of identified clusters, intermediate products and biosynthetic machineries allow comparative analysis and understanding of factors in natural product biosynthesis. For several newly identified natural products it is already common praxis to use the retrobiosynthetic approach to identify the corresponding gene cluster as shown for the myxovalargins in this work. In-silico tools might soon be available to split molecules into their biosynthetic moieties and predict the NRPS/ PKS assembly line as well as the tailoring enzymes and precursor producing enzymes, allowing a fast identification of corresponding genes and compounds coming from each of the two directions. The biotechnological tools and the understanding of the production mechanisms allows us furthermore to fine-tune at various points of the production process. The streptomycetes as origin of a bandwidth of different anti-infectives are well characterized and the toolbox available for this producer group is filled with precise straight forward techniques as well as sophisticated approaches.[214] Though for myxobacteria not all tools are available or well characterized, promising results and compounds were already achieved. Therefore, it is a major goal of the natural products groups at the Helmholtz Institute, also reflected in the work presented here, to increase this knowledge in various ways to strengthen the biotechnological framework around the platform 'myxobacteria' and to elevate the accessibility of their natural products.

While on one hand the approach to isolate compounds, identify their secondary metabolite gene cluster and to use that knowledge to achieve targeted manipulation of its biosynthesis, on the other hand the reverse direction also allows a variety of applications to draw information of a secondary metabolite gene cluste[156]r to identify or characterize the corresponding compound.

Especially in the fields of discovery of new natural product the terms metabolome mining[127] and genome mining[215] describe these bi-directional route to yield a common goal. One side is mainly driven by increasing capabilities of analytical techniques [216], the other side draws advantage of the steadily advancing sequencing and biotechnological tools[217] and the contributions of each newly identified biosynthesis feature or assembly line. But the genomic information not only allows the discovery of new natural products, moreover it supports the identification and structure elucidation of entire compound families. The myxovalargin project is an example how the elucidation of secondary metabolite biosynthesis allowed to shed new light on the stereochemistry of this compound class. Though prediction of chemical moieties solely based on domain order and functional alignments can be misleading especially in context of PKS gene clusters, the linear NRPS-type gene cluster of the myxovalargin compound class allowed to question the initial chiral assignments. The distinct correlation of epimerization domain occurrence with the assigned stereochemical properties except of the two mismatching stereocenters lead to challenging the previously established structural properties. As the assignment of stereocenters by chemical approaches did not offer straight forward techniques, (furthermore the identification of coeluting myxovalargins with identical masses, thus different stereochemistry, were identified in the same fraction), a combined approach of biosynthetic prediction and chemical-analytical techniques was pursued. Thus, in the end it was possible to resolve stereochemistry allowing to timely benefit of this knowledge in the parallel workstream of the chemical synthesis of myxovalargin A avoiding synthesis research in vain.

Though such cases are dependent on the reliability of genetic predictions, which often does not fit textbook biosynthetic logic,[127] knowledge and prediction accurateness is increasing as well as available tools for that purpose. In some cases the biosynthesis hypothesis may be dependent on the analytical structure elucidation as e.g. in case of the pyxipyrrolones [218] in other cases the structural elucidation is dependent on genetic analysis and subsequent confirmation as shown for myxovalargins. Finally, in the future analytic and genetic approaches need to work increasingly hand in hand to unravel the challenges in natural product research.

5.3 Future of the myxovalargin project and fate of cytotoxic antibiotics

The crux of natural products – making natural products accessible for drug developement

The search for new bioactive antibiotics has resulted in a variety of natural products from different biological origin. Nevertheless, most of these compounds fail to be accessible for chemical in-depth characterization, or producing organisms fail to be biotechnologically accessible or sustainable. Even if these requirements are fulfilled, a lot of organisms are microbiologically and biotechnologically tough to handle and thus prevent feasible follow-up work. A major aim of the myxovalargin project was to tackle some of these issues to establish the basis for a long-term sustainable project. Though for a lot of molecules of bacterial origin total synthesis has been established despite their chemical challenges [219,220], the myxovalargins show an intriguing stereochemical complexity despite of their polypeptide skeletal structure. Their chiral organization and their unusual, non-proteinogenic building blocks hinder a feasible synthetic approach by now.[221] Therefore, it is of major interest to access chemical as well as biological means to develop a potential antibacterial compound, but also to establish a stable biological system. As part of this work it was possible to identify a strain, which offers a variety of chances to apply biotechnological and microbiological tools. MCy6431 shows optimal growth conditions and a high production of the myxovalargin compound class. Furthermore, alternative producers which might serve as potential alternate candidates - like MCy9171 and MCy5730 - are available. Basic upscaling steps were successfully implemented as well as a downstream purification process to yield enough material from a variety of biotechnological approaches. Furthermore, the strain can be reliably accessed by single-crossover mutagenesis. Nevertheless, additional tools should be applied to the strain, which are increasingly developed for other bacterial families,[222] but also specifically adapted for myxobacteria. An attempt of double-crossover mutation was conducted during this project, but could not be studied into detail. Though the experiment failed, it has to be noted that it was only applied on a single location with a single construct. Double crossover mutation might shed additional lights on the biosynthetic properties of some genes e.g. the *mxvB* gene, with its CP domain of unkown function including a scaffold of an A domain like sequence. A second tool, which has to be studied in detail is the promotor insertion. A commonly used promotor (tn5) was employed during this project that was shown to function in myxobacteria [223] and even to be used to increase production of myxobacterial metabolites in other strains like the Thuggacins. [224] The strength of this promotor in comparison to the natural promotor of myxovalargin biosynthesis is unclear. An in depth analysis of different native and engineered promotors and their activity

as intensively investigated for Streptomycetes[225,226] might lead to the identification of potential strong promoters, which could be used to increase production levels or widen specific bottlenecks in biosynthesis. The identification of myxobacterial promotors and a thorough comparison of those of myxobacterial, as well as other origin might open up a toolbox for a variety of applications. Another approach to overcome potential bottlenecks in biosynthesis could be a gene duplication or insertion of complete gene cassettes in the genome via e.g. attB sites.[227] This attempt was considered and respective plasmids cloned, however it could not be finalized. The insertion of a gene cassette from *mxvI* to *mxvK* could reduce the influence of potential bottlenecks in the production, as well as improve the self-resistance (ABC transporter) or the precursor or tailoring reactions (MxvG, MxvH, MxvJ). The gene cassette *mxvI* to *mxvK* is of central importance, as it encodes the gene for β -tyrosine production, as well as the self-resistance ABC transporter, the putative hydroxylase and the *Mbt*H-like protein, which belongs to a group of enzymes, which were demonstrated to have an impact on production yields.[228] Though it was tried to overcome a putative limitation of β -tyrosine by feeding of the synthetic molecule, the overexpression by duplication or promotor insertion might influence production due to improved intracellular supply.

The hypothetical heterologous expression of the myxovalargin gene cluster as shown for other myxobacterial compounds[229] is assumed to be likely not superior to the original producer, as MCy6431 has a high yield production of myxovalargins combined with strong self-resistance mechanisms against this group of broad spectrum antibiotics. Furthermore, the demonstrated suitability for large scale fermentation implies an eligible candidate for further production. Nevertheless the development of a heterologous host system could be used to identify and clarify still not completely elucidated steps of the biosynthesis, since in a heterologous expression system additional mutagenesis techniques can be applied or distinct mutations introduced. [230,231] The project has also shown, that the myxovalargin producer MCy6431 can be further manipulated by environmental conditions to alter its myxovalargin production. Beside production optimization using altered media composition, it can be pursued to narrow down the variability of natural derivatives. Due to the promiscuity for valine and isoleucine incorporation, the availability of the respective amino acids might be optimized to reduce unwanted broad myxovalargin derivative production, which impedes the downstream purification process. On the other hand an oversupply other than valine, the most prominent short chain amino acid in the myxovalargins, might lead to an increase of certain derivatives or even to the occurrence of completely new myxovalargin derivatives. The natural diversity as well as the mutasynthesis studies demonstrate how the promiscuous steps in myxovalargin

biosynthesis can be exploited. The knowledge of this susceptibility can be used to either try to steer the biosynthesis in a certain direction, to achieve few or particular members of the myxovalargin family, or to widen the incorporation yielding new compounds for bioactivity screenings. Though we were not able to increase the biological activity nor to decrease the cytotoxic effects of Myxovalargin A, a step forward was made to bring Myxovalargin towards a pharmaceutically usable lead structure.

Facing pharmacological challenges with multidisciplinary approaches

In the biosynthesis studies myxovalaring demonstrated beside its biofilm destruction, als cytotoxic effects. Cytotoxicity often is a knockout criterion for interesting antibacterial compounds. Despite of a strong pharmaceutical potential of the myxovalargins as demonstrated in vitro and in vivo on biofilms, the risk to fail for use in humans due to critical side effects is a major drawback and impedes further research activities. Although this approach is well understandable from an economic perspective, the increasing resistance against established drugs and the slow progress in new marketed antibiotics should engage a focus on neglected compounds, where common textbook rules for lead structures do not apply or pharmacological and toxicological doubts discourage further research. Such compounds in fact need dedicated long-term projects to really evaluate their pharmaceutical potential. The complexity of natural products for drug developement, the urgency of arising resistance, and the often-close correlation of effects and side effects of anti-infectives, requires a comprehensive multidisciplinary approach and farsighted projects.

Possibilities to overcome certain problems of promising compounds, which offer high potential, but have reached dead end in further chemical modification, require coordinated interaction of different scientific fields. At this point galenical techniques and pharmacological considerations need to be applied to overcome the toxicological disadvantages. Vehicles for drug administration transporting the active pharmaceutical ingredient (API) to the respective target in the organism is an ongoing focus of galenical research. For the myxovalargins, this does not necessarily mean to access the bacterial cells with its challenging barrier of cellular membrane, transporters and enzymes but to achieve release in or at the biofilm matrix. The matrix as target itself might open a variety of opportunities and specific targets for galenic carriers with their exopolysaccharides, proteins and nucleic acid composition. Biofilm specific targets might reduce interaction of the API with other cells or tissue, therefore reducing side effects and enabling use of cytotoxic compounds. Moreover, the vehicles can protect the unwanted release

of the compound other than at the required target. However, this approach is depending on the understanding of the composition of bacterial biofilms.

Further thoughts to evaluate the potential of myxovalargin could pursue a synergic approach with other antibiotics like ciprofloxacin. As ciprofloxacin acts against planktonic cells, while unable to destroy biofilms, its combination with myxovalargin could be a promising combination. In such constellation a dose reduction of both antibiotics can be evaluated, to maintain biofilm destruction and antibiotic activity, but to reduce cytotoxic or other side effects and thus enable local as well as systemic applications.

Furthermore, the local application of myxovalargin might offer another potential indication. Since biofilm formation appears on surfaces a local application can be the preferred treatment in various infections like the application as aerosols in bacterial lung infections. A topic approach was presented for application of gaseous nitric oxide by a controlled release dressing against *P. aeruginosa*.[232] Similar approaches could be pursued for myxovalargin, with its demonstrated destruction of bacterial biofilms. Generally, the approach of embedding the compound in a matrix with a controlled release could overcome cytotoxic disadvantages, especially when applied in a synergistic composition. Implants are of high medicinal importance but are also source of a large number of nosocomial infections of opportunistic bacteria.[233] Implant infections often include colonization in biofilm leading to therapeutic as well as immune system resistance and ultimately to replacement of the implant, if necessary by surgical intervention.[234] Biofilm formation of implants is an issue for almost all fields of implant application, including therapeutical use in vascular or coronar indication, as well as urinary implants[233] or orthopaedics[235] and others. [236] Coupling or embedding antibacterial compounds in a matrix or on the surface could prevent such complications.[237] However, since nosocomial infections often are caused by multi resistant strains like *S. aureus* or *P. aeruginosa* the bacteria may not respond to several antibiotics and as soon as a biofilm is formed, the enclosed bacterial cells itself are tough to medicate. Evaluating the therapeutical use of myxovalargin alone or in combination, might overcome this central issue.

The cytotoxic effect could even be of advantage for local applications, where a cellular overgrowth or clotting appears as additional problem like e.g. for stents. Stent infections are relatively seldom, but are severe with high mortality and were often associated with multiresistent *S. aureus* infection or *P. aeruginosa* infection. [238] Infections of immunomodulating and antiproliferative drug eluting stents were observed and even considered to abet such infections.[239,240] Such cases might allow to make use of the proclaimed disadvantage.

Though in the end, it might fail to balance the advantages and disadvantages of the compound for several applications, others might raise hope to find a therapeutic indication. The global situation of resistance expansion demands to ponder different options. First steps would include a dose dependency correlation between cytotoxicity, antibacterial effect and biofilm disruption for the most prominent myxovalargins. Moreover, the synergism with antibiotics like Ciprofloxacin, but also antiproliferative compounds like Paclitaxel should be evaluated on the aboved mentioned parameter. Based on that, the different options can be weighed and a suitable strategy defined.

Lastly, the mode of action of myxovalargin should be further investigated. Studies on ribosome binding are ongoing; nevertheless, its biofilm activity must be caused by a different mode of action. Whether this is based on unspecific cell destruction or a specific disruption of the biofilm needs to be evaluated. It might offer further insights into biofilms as well as understanding and identification of putative targets.

5.5 The phenyl pyruvate dehydrogenase complex

The phenyl pyruvate dehydrogenase complex is an interesting example on how enzymatic processes of primary metabolism are adapted and used in secondary metabolism to specifically yield modified precursors for natural product biosynthesis, without interfering with primary metabolism. By encoding the ACP moiety in the gene of *ripH* the bridge was made from primary to secondary metabolism. There are other examples found in secondary metabolism, which show how pathways and precursors are used to amend the secondary metabolite machineries in order to generate the chemical diversity of natural products. Knowing this, it could be a feasible approach to search for such genes conjoining the genes for PKS moieties as well as enzymes of known metabolic pathways in order to elucidate and manipulate precursors of bacterial biosynthesis.

After finalization of the practical work for this thesis, two publications touching this project were published. A phenalamid gene cluster from *Myxococcus stipitatus* DSM 14675 was published in 2016.[185] The reported gene cluster and the general understanding of the biosynthesis is in accordance with the experiments and results for MCy6431, which were generated several years before the publication. The comparison with the structurally similar myxalamids was performed, but the bridge to the myxobacterial compounds ripostatin and the *Hyalangium* compounds was not captured by the authors.

Furthermore, the phenyl pyruvate dehydrogenase complex project was continued by Dr. Chengzhang Fu and Dr. David Auerbach at MINS to elucidate the biochemical details of this enzymae complex. Dr. Fu could confirm the biosynthetic reactions in an in vitro stepwise approach with the respective enzymes. He was able to generate the intermediates as well as the final product of the phenyl pyruvate dehydrogenase complex, thus proving the proposed role in secondary metabolism and solving the question of the carbon loss in ripostatin.[169]

The identification and publication of this biosynthetic feature enables different applicational use. The substrate specific enzymatic reaction, which could be restored in vitro by heterologously expressed enzymes, allows to be refined for application e.g. in industrial synthesis or chemical synthesis with enzymatic reaction steps. Furthermore, the precursor and its corresponding genes allow a precise prediction in in-silico tools. Such understanding of specialized functions in biosynthetic machineries allows to relatively quickly identify putative gene clusters corresponding to identified compounds, or even to identify other producers by

screening across scattered genetic information of single strains. This way, the BGC of the *Hyalangium* metabolites as well as other producers of ripostatins and phenalamids were identified.

Beside the phenyl pyruvate dehydrogenase complex, those three compound classes of myxobacterial origin are of particular interest, due to their close chemical relationship with other myxobacterial compounds. In this context these groups apparently demonstrate how every single identified secondary metabolite and its connected biosynthesis constitutes a value in itself that is beneficial to the natural product community. These compounds shed light on still unsolved issues. The similar chemical moieties present in the hyafurones and the aurafurones for example allows to support the hypothesis of the furanone formation via a Baeyer-Villiger oxidation, which was one of three previously proposed putative pathways to form this moiety.[186] The hyapyrones are the link between the PKS assembly line and the furone formation.

Furthermore, interesting is the close relationship of phenalamide to other myxobacterial compounds like the myxalamids and the hyafurones. In case of the myxalamids an approach of module swapping might be interesting in terms of future genetic engineering. The close relationship of the hyafurones with the aurafurones might allow different applications for interchange of genetic scaffolds in order to substitute scaffolds of the assembly line. Besides the aspect of genetic engeneering, these close relationships of compounds are interesting from a microbiological and evolutionary point of view. Distinct mechanisms and biosynthesis aspects of chemical moieties, which are exclusive for those myxobacterial strains could be a result of horizontal gene transfer. This is in particular interesting, since all three strains producing the phenyl pyruvate moiety in ripostatin, phenalamide and the *Hyalangium* derivatives originate from strains of different suborders. Moreover, the additional cross-links to myxalamids and aurafurones broaden the perspective of horizontal relations. Evolutionary investigation of the combination of different secondary metabolite genes can give hints on the evolution of diversity and thereby advance our understanding of biosynthetic assembly lines in myxobacteria.

7. References

(1) Brachman, P. S. Infectious diseases--past, present, and future. *International Journal of Epidemiology* **2003**, *32* (5), 684–686. DOI: 10.1093/ije/dyg282.

(2) Fears, J. R. The plague under Marcus Aurelius and the decline and fall of the Roman Empire. *Infectious disease clinics of North America* **2004**, *18* (1), 65–77. DOI: 10.1016/S0891-5520(03)00089-8.

(3) Semmelweis, I. P. *Offener Brief an sämmtliche Professoren der Geburtshilfe*; Königl. ungar. Universitäts-Buchdr, 1862.

(4) Plotkin, S. A. Vaccines: past, present and future. *Nature medicine* **2005**, *11* (4 Suppl), 11. DOI: 10.1038/nm1209.

(5) Koch, R. *Die Ätiologie der Tuberkulose - (Nach, einem in der Physiologischen Gesellschaft zu Berlin am 24. März 1882 gehaltenen Vortrage)*; Gesammelte Werke von Robert Koch; Robert Koch-Institut.

(6) Ehrlich, P.; Bertheim, A. Über das salzsaure 3.3′-Diamino-4.4′-dioxy-arsenobenzol und seine nächsten Verwandten. *Ber. Dtsch. Chem. Ges.* **1912**, *45* (1), 756–766. DOI: 10.1002/cber.191204501110.

(7) Fleming, A. On the Antibacterial Action of Cultures of a Penicillium, with Special Reference to their Use in the Isolation of B. influenzæ. *British journal of experimental pathology* **1929**, *10* (3), 226–236.

(8) Coates, Anthony R M; Halls, G.; Hu, Y. Novel classes of antibiotics or more of the same? *British journal of pharmacology* **2011**, *163* (1), 184–194. DOI: 10.1111/j.1476-5381.2011.01250.x.

(9) Neu, H. C. The Crisis in Antibiotic Resistance. *Science* **1992**, *257* (5073), 1064–1073. DOI: 10.1126/science.257.5073.1064.

(10) Spellberg, B.; Guidos, R.; Gilbert, D.; Bradley, J.; Boucher, H. W.; Scheld, W. M.; Bartlett, J. G.; Edwards, J., JR. The epidemic of antibiotic-resistant infections: a call to action

for the medical community from the Infectious Diseases Society of America. *Clinical infectious diseases : an official publication of the Infectious Diseases Society of America* **2008**, *46* (2), 155–164. DOI: 10.1086/524891.

(11) Tennille Tracy and Thomas Burton. FDA Clears Way for New Curbs on Antibiotics Given to Farm Animals:Obama administration pursues ways to fight so-called superbugs. *The Wall Street Journal,* June 2.

(12) *AMG § 58d Verringerung der Behandlung mit antibakteriell wirksamen Stoffen*, 2014.

(13) Anderson, J. Declaration_of_Support_for_Combating_AMR_Jan_2016.

(14) Hede, K. Antibiotic resistance: An infectious arms race. *Nature* **2014**, *509* (7498), S2-S3.

(15) Davies, J.; Davies, D. Origins and evolution of antibiotic resistance. *Microbiology and molecular biology reviews : MMBR* **2010**, *74* (3), 417–433. DOI: 10.1128/MMBR.00016-10.

(16) Blair, J. M. A.; Webber, M. A.; Baylay, A. J.; Ogbolu, D. O.; Piddock, L. J. V. Molecular mechanisms of antibiotic resistance. *Nature reviews. Microbiology* **2015**, *13* (1), 42–51. DOI: 10.1038/nrmicro3380.

(17) Lemmen, S. Mono- versus Kombinationstherapie bei Antibiotika. *Krankenh.hyg. up2date* **2009**, *4* (01), 65–74. DOI: 10.1055/s-0028-1119610.

(18) Ball, P.; Geddes, A.; Rolinson, G. Amoxycillin Clavulanate: an Assessment after 15 Years of Clinical Application. *Journal of Chemotherapy* **1997**, *9* (3), 167–198. DOI: 10.1179/joc.1997.9.3.167.

(19) Malfertheiner, P.; Megraud, F.; O'Morain, C. A.; Gisbert, J. P.; Kuipers, E. J.; Axon, A. T.; Bazzoli, F.; Gasbarrini, A.; Atherton, J.; Graham, D. Y.; Hunt, R.; Moayyedi, P.; Rokkas, T.; Rugge, M.; Selgrad, M.; Suerbaum, S.; Sugano, K.; El-Omar, E. M. Management of Helicobacter pylori infection-the Maastricht V/Florence Consensus Report. *Gut* **2017**, *66* (1), 6–30. DOI: 10.1136/gutjnl-2016-312288.

(20) Schwank S. Impact of Bacterial Biofilm Formation on In Vitro and In Vivo Activities of Antibiotics. *Antimicrob. Agents Chemother.*- **1998** (42), 895–898.

(21) Stewart, P. S.; William Costerton, J. Antibiotic resistance of bacteria in biofilms. *The Lancet*, *358* (9276), 135–138. DOI: 10.1016/S0140-6736(01)05321-1.

(22) Zhao, G.; Usui, M. L.; Lippman, S. I.; James, G. A.; Stewart, P. S.; Fleckman, P.; Olerud, J. E. Biofilms and Inflammation in Chronic Wounds. *Advances in Wound Care* **2013**, *2* (7), 389–399. DOI: 10.1089/wound.2012.0381.

(23) Lübbert, C.; Wendt, K.; Feisthammel, J.; Moter, A.; Lippmann, N.; Busch, T.; Mössner, J.; Hoffmeister, A.; Rodloff, A. C. Epidemiology and Resistance Patterns of Bacterial and Fungal Colonization of Biliary Plastic Stents: A Prospective Cohort Study. *PLoS ONE* **2016**, *11* (5), e0155479. DOI: 10.1371/journal.pone.0155479.

(24) Branda, S. S.; Vik, å.; Friedman, L.; Kolter, R. Biofilms: the matrix revisited. *Trends in Microbiology*, *13* (1), 20–26. DOI: 10.1016/j.tim.2004.11.006.

(25) Lee, J.; Wu, J.; Deng, Y.; Wang, J.; Wang, C.; Wang, J.; Chang, C.; Dong, Y.; Williams, P.; Zhang, L.-H. A cell-cell communication signal integrates quorum sensing and stress response. *Nat Chem Biol* **2013**, *9* (5), 339–343.

(26) Zender, M.; Witzgall, F.; Drees, S. L.; Weidel, E.; Maurer, C. K.; Fetzner, S.; Blankenfeldt, W.; Empting, M.; Hartmann, R. W. Dissecting the Multiple Roles of PqsE in Pseudomonas aeruginosa Virulence by Discovery of Small Tool Compounds. *ACS Chem. Biol.* **2016**, *11* (6), 1755–1763. DOI: 10.1021/acschembio.6b00156.

(27) Steinbach, A.; Maurer, C. K.; Weidel, E.; Henn, C.; Brengel, C.; Hartmann, R. W.; Negri, M. Molecular basis of HHQ biosynthesis: molecular dynamics simulations, enzyme kinetic and surface plasmon resonance studies. *BMC Biophysics* **2013**, *6*, 10. DOI: 10.1186/2046-1682-6-10.

(28) Foxley, M. A.; Friedline, A. W.; Jensen, J. M.; Nimmo, S. L.; Scull, E. M.; King, J. B.; Strange, S.; Xiao, M. T.; Smith, B. E.; Thomas Iii, K. J.; Glatzhofer, D. T.; Cichewicz, R. H.; Rice, C. V. Efficacy of ampicillin against methicillin-resistant Staphylococcus aureus restored through synergy with branched poly(ethylenimine). *J Antibiot* **2016**.

(29) Katz, L.; Baltz, R. H. Natural product discovery: past, present, and future. *Journal of industrial microbiology & biotechnology* **2016**, *43* (2-3), 155–176. DOI: 10.1007/s10295-015-1723-5.

(30) Felnagle, E. A.; Jackson, E. E.; Chan, Y. A.; Podevels, A. M.; Berti, A. D.; McMahon, M. D.; Thomas, M. G. Nonribosomal Peptide Synthetases Involved in the Production of Medically Relevant Natural Products. *Mol. Pharmaceutics* **2008**, *5* (2), 191–211. DOI: 10.1021/mp700137g.

(31) Butler, M. S.; Buss, A. D. Natural products--the future scaffolds for novel antibiotics? *Biochemical pharmacology* **2006**, *71* (7), 919–929. DOI: 10.1016/j.bcp.2005.10.012.

(32) Ganesan, A. The impact of natural products upon modern drug discovery. *Current opinion in chemical biology* **2008**, *12* (3), 306–317. DOI: 10.1016/j.cbpa.2008.03.016.

(33) Cragg, G. M.; Newman, D. J. Natural products: a continuing source of novel drug leads. *Biochimica et biophysica acta* **2013**, *1830* (6), 3670–3695. DOI: 10.1016/j.bbagen.2013.02.008.

(34) Dias, D. A.; Urban, S.; Roessner, U. A historical overview of natural products in drug discovery. *Metabolites* **2012**, *2* (2), 303–336. DOI: 10.3390/metabo2020303.

(35) Baumann, S.; Herrmann, J.; Raju, R.; Steinmetz, H.; Mohr, K. I.; Hüttel, S.; Harmrolfs, K.; Stadler, M.; Müller, R. Cystobactamids: myxobacterial topoisomerase inhibitors exhibiting potent antibacterial activity. *Angewandte Chemie (International ed. in English)* **2014**, *53* (52), 14605–14609. DOI: 10.1002/anie.201409964.

(36) Johnston, C. W.; Magarvey, N. A. Natural products: Untwisting the antibiotic'ome. *Nature chemical biology* **2015**, *11* (3), 177–178. DOI: 10.1038/nchembio.1757.

(37) Braine, T. Race against time to develop new antibiotics. *Bulletin of the World Health Organization* **2011**, *89* (2), 88–89. DOI: 10.2471/BLT.11.030211.

(38) Kesselheim, A. S.; Outterson, K. Fighting antibiotic resistance: marrying new financial incentives to meeting public health goals. *Health affairs (Project Hope)* **2010**, *29* (9), 1689–1696. DOI: 10.1377/hlthaff.2009.0439.

(39) Ganesan, A. Natural products as a hunting ground for combinatorial chemistry. *Current opinion in biotechnology* **2004**, *15* (6), 584–590. DOI: 10.1016/j.copbio.2004.09.002.

(40) Genilloud, O. The re-emerging role of microbial natural products in antibiotic discovery. *Antonie van Leeuwenhoek* **2014**, *106* (1), 173–188. DOI: 10.1007/s10482-014-0204-6.

(41) Demain, A. L.; Sanchez, S. Microbial drug discovery: 80 years of progress. *The Journal of antibiotics* **2009**, *62* (1), 5–16. DOI: 10.1038/ja.2008.16;

(42) Bauernfeind, A. Classification of beta-lactamases. *Reviews of infectious diseases* **1986**, *8 Suppl 5*, 81.

(43) Srivastava, A.; Talaue, M.; Liu, S.; Degen, D.; Ebright, R. Y.; Sineva, E.; Chakraborty, A.; Druzhinin, S. Y.; Chatterjee, S.; Mukhopadhyay, J.; Ebright, Y. W.; Zozula, A.; Shen, J.; Sengupta, S.; Niedfeldt, R. R.; Xin, C.; Kaneko, T.; Irschik, H.; Jansen, R.; Donadio, S.; Connell, N.; Ebright, R. H. New target for inhibition of bacterial RNA polymerase: 'switch region'. *Current Opinion in Microbiology* **2011**, *14* (5), 532–543. DOI: 10.1016/j.mib.2011.07.030.

(44) Campbell, E. A.; Korzheva, N.; Mustaev, A.; Murakami, K.; Nair, S.; Goldfarb, A.; Darst, S. A. Structural mechanism for rifampicin inhibition of bacterial rna polymerase. *Cell* **2001**, *104* (6), 901–912.

(45) Mukhopadhyay, J.; Das, K.; Ismail, S.; Koppstein, D.; Jang, M.; Hudson, B.; Sarafianos, S.; Tuske, S.; Patel, J.; Jansen, R.; Irschik, H.; Arnold, E.; Ebright, R. H. The RNA polymerase "switch region" is a target for inhibitors. *Cell* **2008**, *135* (2), 295–307. DOI: 10.1016/j.cell.2008.09.033.

(46) Darst, S. A. New inhibitors targeting bacterial RNA polymerase. *Trends Biochem. Sci.* **2004**, *29* (4), 159–160.

(47) Donadio, S.; Staver, M.; McAlpine, J.; Swanson, S.; Katz, L. Modular organization of genes required for complex polyketide biosynthesis. *Science* **1991**, *252* (5006), 675–679. DOI: 10.1126/science.2024119.

(48) Walsh, C. T.; Fischbach, M. A. Natural products version 2.0: connecting genes to molecules. *Journal of the American Chemical Society* **2010**, *132* (8), 2469–2493. DOI: 10.1021/ja909118a.

(49) Finking, R.; Marahiel, M. A. Biosynthesis of nonribosomal peptides1. *Annual review of microbiology* **2004**, *58*, 453–488. DOI: 10.1146/annurev.micro.58.030603.123615.

(50) Gao, X.; Haynes, S. W.; Ames, B. D.; Wang, P.; Vien, L. P.; Walsh, C. T.; Tang, Y. Cyclization of fungal nonribosomal peptides by a terminal condensation-like domain. *Nature chemical biology* **2012**, *8* (10), 823–830. DOI: 10.1038/nchembio.1047.

(51) Müller, S.; Rachid, S.; Hoffmann, T.; Surup, F.; Volz, C.; Zaburannyi, N.; Müller, R. Biosynthesis of crocacin involves an unusual hydrolytic release domain showing similarity to condensation domains. *Chemistry & biology* **2014**, *21* (7), 855–865. DOI: 10.1016/j.chembiol.2014.05.012.

(52) Sundaram, S.; Hertweck, C. On-line enzymatic tailoring of polyketides and peptides in thiotemplate systems. *Current opinion in chemical biology* **2016**, *31*, 82–94. DOI: 10.1016/j.cbpa.2016.01.012.

(53) Crawford, J. M.; Portmann, C.; Kontnik, R.; Walsh, C. T.; Clardy, J. NRPS substrate promiscuity diversifies the xenematides. *Organic letters* **2011**, *13* (19), 5144–5147. DOI: 10.1021/ol2020237.

(54) Li, Y.; Weissman, K. J.; Muller, R. Myxochelin biosynthesis: direct evidence for two- and four-electron reduction of a carrier protein-bound thioester. *Journal of the American Chemical Society* **2008**, *130* (24), 7554–7555. DOI: 10.1021/ja8025278.

(55) Weber, T. In silico tools for the analysis of antibiotic biosynthetic pathways. *International journal of medical microbiology : IJMM* **2014**, *304* (3-4), 230–235. DOI: 10.1016/j.ijmm.2014.02.001.

(56) Medema, M. H.; Blin, K.; Cimermancic, P.; Jager, V. de; Zakrzewski, P.; Fischbach, M. A.; Weber, T.; Takano, E.; Breitling, R. antiSMASH: rapid identification, annotation and analysis of secondary metabolite biosynthesis gene clusters in bacterial and fungal genome sequences. *Nucleic acids research* **2011**, *39* (Web Server issue), W339-46. DOI: 10.1093/nar/gkr466.

(57) Finn, R. D.; Clements, J.; Eddy, S. R. HMMER web server: interactive sequence similarity searching. *Nucleic acids research* **2011**, *39* (Web Server issue), W29-37. DOI: 10.1093/nar/gkr367.

(58) Boddy, C. N. Bioinformatics tools for genome mining of polyketide and non-ribosomal peptides. *J. Ind. Microbiol. Biotechnol.* **2014**, *42* (2), 443–450. DOI: 10.1007/s10295-013-1368-1.

(59) Yadav, G.; Gokhale, R. S.; Mohanty, D. Computational Approach for Prediction of Domain Organization and Substrate Specificity of Modular Polyketide Synthases. *Journal of Molecular Biology* **2003**, *328* (2), 335–363. DOI: 10.1016/S0022-2836(03)00232-8.

(60) Weber, T.; Blin, K.; Duddela, S.; Krug, D.; Kim, H. U.; Bruccoleri, R.; Lee, S. Y.; Fischbach, M. A.; Müller, R.; Wohlleben, W.; Breitling, R.; Takano, E.; Medema, M. H. antiSMASH 3.0 – a comprehensive resource for the genome mining of biosynthetic gene clusters. *Nucleic Acids Res.* **2015**, in press. DOI: 10.1093/nar/gkv437.

(61) Duddela; Srikanth. *A bioinformatics approach for conceptual genome mining*.

(62) Medema, M. H.; Kottmann, R.; Yilmaz, P.; Cummings, M.; Biggins, J. B.; Blin, K.; Bruijn, I. de; Chooi, Y. H.; Claesen, J.; Coates, R. C.; Cruz-Morales, P.; Duddela, S.; Düsterhus, S.; Edwards, D. J.; Fewer, D. P.; Garg, N.; Geiger, C.; Gomez-Escribano, J. P.; Greule, A.; Hadjithomas, M.; Haines, A. S.; Helfrich, Eric J N; Hillwig, M. L.; Ishida, K.; Jones, A. C.; Jones, C. S.; Jungmann, K.; Kegler, C.; Kim, H. U.; Kötter, P.; Krug, D.; Masschelein, J.; Melnik, A. V.; Mantovani, s. M.; Monroe, E. A.; Moore, M.; Moss, N.; Nützmann, H.-W.; Pan, G.; Pati, A.; Petras, D.; Reen, F. J.; Rosconi, F.; Rui, Z.; Tian, Z.; Tobias, N. J.; Tsunematsu, Y.; Wiemann, P.; Wyckoff, E.; Yan, X.; yim, G.; Yu, F.; Xie, Y.; Aigle, B.; Apel, A. K.; Balibar, C. J.; Balskus, E. P.; Barona-Gómez, F.; Bechthold, A.; Bode, H. B.; Borriss, R.; Brady, S. F.; Brakhage, A. A.; Caffrey, P.; Cheng, Y.-Q.; Clardy, J.; Cox, R. J.; Mot, R. de; Donadio, S.; Donia, M. S.; van der Donk, Wilfred A; Dorrestein, P. C.; Doyle, S.; Driessen, Arnold J M; Ehling-Schulz, M.; Entian, K.-D.; Fischbach, M. A.; Gerwick, L.; Gerwick, W. H.; Gross, H.; Gust, B.; Hertweck, C.; Höfte, M.; Jensen, S. E.; Ju, J.; Katz, L.; Kaysser, L.; Klassen, J. L.; Keller, N. P.; Kormanec, J.; Kuipers, O. P.; Kuzuyama, T.; Kyrpides, N. C.; Kwon, H.-J.; Lautru, S.; Lavigne, R.; Lee, C. Y.; Linquan, B.; Liu, X.; Liu, W.; Luzhetskyy, A.; Mahmud, T.; Mast, Y.; Méndez, C.; Metsä-Ketelä, M.; Micklefield, J.; Mitchell, D. A.; Moore, B. S.; Moreira, L. M.; Müller, R.; Neilan, B. A.; Nett, M.; Nielsen, J.; O'Gara, F.; Oikawa, H.; Osbourn, A.; Osburne, M. S.; Ostash, B.; Payne, S. M.; Pernodet, J.-L.; Petricek, M.; Piel, J.; Ploux, O.; Raaijmakers, J. M.; Salas, J. A.; Schmitt, E. K.; Scott, B.; Seipke, R. F.; Shen, B.; Sherman, D. H.; Sivonen, K.; Smanski, M. J.; Sosio, M.; Stegmann, E.; Süssmuth, R. D.; Tahlan, K.; Thomas, C. M.; Tang, Y.; Truman, A. W.; Viaud, M.; Walton,

J. D.; Walsh, C. T.; Weber, T.; van Wezel, Gilles P; Wilkinson, B.; Willey, J. M.; Wohlleben, W.; Wright, G. D.; Ziemert, N.; Zhang, C.; Zotchev, S. B.; Breitling, R.; Takano, E.; Glöckner, F. O. Minimum Information about a Biosynthetic Gene cluster. *Nat. Chem. Biol.* **2015**, *11* (9), 625–631. DOI: 10.1038/nchembio.1890.

(63) Arnison, P. G.; Bibb, M. J.; Bierbaum, G.; Bowers, A. A.; Bugni, T. S.; Bulaj, G.; Camarero, J. A.; Campopiano, D. J.; Challis, G. L.; Clardy, J.; Cotter, P. D.; Craik, D. J.; Dawson, M.; Dittmann, E.; Donadio, S.; Dorrestein, P. C.; Entian, K. D.; Fischbach, M. A.; Garavelli, J. S.; Göransson, U.; Gruber, C. W.; Haft, D. H.; Hemscheidt, T. K.; Hertweck, C.; Hill, C.; Horswill, A. R.; Jaspars, M.; Kelly, W. L.; Klinman, J. P.; Kuipers, O. P.; Link, A. J.; Liu, W.; Marahiel, M. A.; Mitchell, D. A.; Moll, G. N.; Moore, B. S.; Müller, R.; Nair, S. K.; Nes, I. F.; Norris, G. E.; Olivera, B. M.; Onaka, H.; Patchett, M. L.; Piel, J.; Reaney, M. J. T.; Rebuffat, S.; Ross, R. P.; Sahl, H. G.; Schmidt, E. W.; Selsted, M. E.; Severinov, K.; Shen, B.; Sivonen, K.; Smith, L.; Stein, T.; Süssmuth, R. E.; Tagg, J. R.; Tang, G. L.; Truman, A. W.; Vederas, J. C.; Walsh, C. T.; Walton, J. D.; Wenzel, S. C.; Willey, J. M.; van der Donk, W. Ribosomally synthesized and post-translationally modified peptide natural products: overview and recommendations for a universal nomenclature. *Nat. Prod. Rep.* **2013**, *30* (1), 108–160. DOI: 10.1039/C2NP20085F.

(64) Ortega, M. A.; Hao, Y.; Zhang, Q.; Walker, M. C.; van der Donk, Wilfred A; Nair, S. K. Structure and mechanism of the tRNA-dependent lantibiotic dehydratase NisB. *Nature* **2015**, *517* (7535), 509–512. DOI: 10.1038/nature13888.

(65) Cotter, P. D.; Ross, R. P.; Hill, C. Bacteriocins - a viable alternative to antibiotics? *Nature reviews. Microbiology* **2013**, *11* (2), 95–105. DOI: 10.1038/nrmicro2937.

(66) Tholl, D. Biosynthesis and biological functions of terpenoids in plants. *Advances in biochemical engineering/biotechnology* **2015**, *148*, 63–106. DOI: 10.1007/10_2014_295.

(67) Zwenger, S.; Basu, C. Plant terpenoids: applications and future potentials. *Biotechnology and Molecular Biology Reviews* **2008**, *3* (1), 1.

(68) SIREESHA, B.; REDDY, B. V.; BASHA, S.K.; CHANDRA, K.; ANASUYA, D. A REVIEW ON PHARMACOLOGICAL ACTIVITIES OF ALKALOIDS. *WJCMPR* **2019**, *01* (06), 230–234. DOI: 10.37022/WJCMPR.2019.01068.

(69) Stachelhaus, T.; Mootz, H. D.; Marahiel, M. A. The specificity-conferring code of adenylation domains in nonribosomal peptide synthetases. *Chemistry & biology* **1999**, *6* (8), 493–505. DOI: 10.1016/S1074-5521(99)80082-9.

(70) Röttig, M.; Medema, M. H.; Blin, K.; Weber, T.; Rausch, C.; Kohlbacher, O. NRPSpredictor2--a web server for predicting NRPS adenylation domain specificity. *Nucleic acids research* **2011**, *39* (Web Server issue), W362-7. DOI: 10.1093/nar/gkr323.

(71) Rausch, C.; Hoof, I.; Weber, T.; Wohlleben, W.; Huson, D. H. Phylogenetic analysis of condensation domains in NRPS sheds light on their functional evolution. *BMC Evol. Biol.* **2007**, *7*, 78–92.

(72) Christiansen, G.; Philmus, B.; Hemscheidt, T.; Kurmayer, R. Genetic variation of adenylation domains of the anabaenopeptin synthesis operon and evolution of substrate promiscuity. *Journal of bacteriology* **2011**, *193* (15), 3822–3831. DOI: 10.1128/JB.00360-11.

(73) Cortina, N. S.; Krug, D.; Plaza, A.; Revermann, O.; Müller, R. Myxoprincomid: Entdeckung eines Naturstoffs mithilfe einer umfassenden Analyse des sekundären Metaboloms von Myxococcusxanthus. *Angew. Chem.* **2012**, *124* (3), 836–841. DOI: 10.1002/ange.201106305.

(74) Crawford, J. M.; Portmann, C.; Kontnik, R.; Walsh, C. T.; Clardy, J. NRPS substrate promiscuity diversifies the xenematides. *Organic letters* **2011**, *13* (19), 5144–5147. DOI: 10.1021/ol2020237.

(75) Villiers, Benoit R M; Hollfelder, F. Mapping the limits of substrate specificity of the adenylation domain of TycA. *Chembiochem : a European journal of chemical biology* **2009**, *10* (4), 671–682. DOI: 10.1002/cbic.200800553.

(76) Fischbach, M. A.; Walsh, C. T. Assembly-line enzymology for polyketide and nonribosomal Peptide antibiotics: logic, machinery, and mechanisms. *Chemical reviews* **2006**, *106* (8), 3468–3496. DOI: 10.1021/cr0503097.

(77) Cortes, J.; Haydock, S. F.; Roberts, G. A.; Bevitt, D. J.; Leadlay, P. F. An unusually large multifunctional polypeptide in the erythromycin-producing polyketide synthase of Saccharopolyspora erythraea. *Nature* **1990**, *348* (6297), 176–178. DOI: 10.1038/348176a0.

(78) Pickens, L. B.; Tang, Y. Decoding and engineering tetracycline biosynthesis. *Metabolic engineering* **2009**, *11* (2), 69–75. DOI: 10.1016/j.ymben.2008.10.001.

(79) Molnár, I.; Schupp, T.; Ono, M.; Zirkle, R. E.; Milnamow, M.; Nowak-Thompson, B.; Engel, N.; Toupet, C.; Stratmann, A.; Cyr, D. D.; Gorlach, J.; Mayo, J. M.; Hu, A.; Goff, S.; Schmid, J.; Ligon, J. M. The biosynthetic gene cluster for the microtubule-stabilizing agents epothilones A and B from Sorangium cellulosum So ce90. *Chemistry & biology* **2000**, *7* (2), 97–109. DOI: 10.1016/S1074-5521(00)00075-2.

(80) Till, M.; Race, P. R. The Assembly Line Enzymology of Polyketide Biosynthesis. *Methods in molecular biology (Clifton, N.J.)* **2016**, *1401*, 31–49. DOI: 10.1007/978-1-4939-3375-4_2.

(81) Hertweck, C.; Luzhetskyy, A.; Rebets, Y.; Bechthold, A. Type II polyketide synthases: gaining a deeper insight into enzymatic teamwork. *Natural product reports* **2007**, *24* (1), 162–190. DOI: 10.1039/B507395M.

(82) Funa, N.; Ohnishi, Y.; Fujii, I.; Shibuya, M.; Ebizuka, Y.; Horinouchi, S. A new pathway for polyketide synthesis in microorganisms. *Nature* **1999**, *400* (6747), 897–899. DOI: 10.1038/23748.

(83) Shimizu, Y.; Ogata, H.; Goto, S. Type III Polyketide Synthases: Functional Classification and Phylogenomics. *Chembiochem : a European journal of chemical biology* **2017**, *18* (1), 50–65. DOI: 10.1002/cbic.201600522.

(84) Khosla, C.; Herschlag, D.; Cane, D. E.; Walsh, C. T. Assembly line polyketide synthases: mechanistic insights and unsolved problems. *Biochemistry* **2014**, *53* (18), 2875–2883. DOI: 10.1021/bi500290t.

(85) Shen, B. Polyketide biosynthesis beyond the type I, II and III polyketide synthase paradigms. *Current opinion in chemical biology* **2003**, *7* (2), 285–295. DOI: 10.1016/S1367-5931(03)00020-6.

(86) Dutta, S.; Whicher, J. R.; Hansen, D. A.; Hale, W. A.; Chemler, J. A.; Congdon, G. R.; Narayan, A. R.; Hakansson, K.; Sherman, D. H.; Smith, J. L.; Skiniotis, G. Structure of a modular polyketide synthase. *Nature* **2014**, *510* (7506), 512–517. DOI: 10.1038/nature13423.

(87) Keatinge-Clay, A. T. A tylosin ketoreductase reveals how chirality is determined in polyketides. *Chemistry & biology* **2007**, *14* (8), 898–908. DOI: 10.1016/j.chembiol.2007.07.009.

(88) Zheng, J.; Taylor, C. A.; Piasecki, S. K.; Keatinge-Clay, A. T. Structural and functional analysis of A-type ketoreductases from the amphotericin modular polyketide synthase. *Structure (London, England : 1993)* **2010**, *18* (8), 913–922. DOI: 10.1016/j.str.2010.04.015.

(89) Keatinge-Clay, A. Crystal structure of the erythromycin polyketide synthase dehydratase. *Journal of Molecular Biology* **2008**, *384* (4), 941–953. DOI: 10.1016/j.jmb.2008.09.084.

(90) Piel, J. Biosynthesis of polyketides by trans-AT polyketide synthases. *Natural product reports* **2010**, *27* (7), 996–1047. DOI: 10.1039/b816430b.

(91) Ridley, C. P.; Lee, H. Y.; Khosla, C. Evolution of polyketide synthases in bacteria. *Proceedings of the National Academy of Sciences of the United States of America* **2008**, *105* (12), 4595–4600. DOI: 10.1073/pnas.0710107105.

(92) Piel, J. Biosynthesis of polyketides by trans-AT polyketide synthases. *Natural product reports* **2010**, *27* (7), 996–1047. DOI: 10.1039/b816430b.

(93) Till, M.; Race, P. R. Progress challenges and opportunities for the re-engineering of trans-AT polyketide synthases. *Biotechnology letters* **2014**, *36* (5), 877–888. DOI: 10.1007/s10529-013-1449-2.

(94) Li, P.-f.; Li, S.-g.; Li, Z.-f.; Zhao, L.; Wang, T.; Pan, H.-w.; Liu, H.; Wu, Z.-h.; Li, Y.-z. Co-cultivation of Sorangium cellulosum strains affects cellular growth and biosynthesis of secondary metabolite epothilones. *FEMS microbiology ecology* **2013**, *85* (2), 358–368. DOI: 10.1111/1574-6941.12125.

(95) Myronovskyi, M.; Tokovenko, B.; Brotz, E.; Ruckert, C.; Kalinowski, J.; Luzhetskyy, A. Genome rearrangements of Streptomyces albus J1074 lead to the carotenoid gene cluster activation. *Applied microbiology and biotechnology* **2014**, *98* (2), 795–806. DOI: 10.1007/s00253-013-5440-6.

(96) Guo, F.; Xiang, S.; Li, L.; Wang, B.; Rajasärkkä, J.; Gröndahl-Yli-Hannuksela, K.; Ai, G.; Metsä-Ketelä, M.; Yang, K. Targeted activation of silent natural product biosynthesis pathways by reporter-guided mutant selection. *Metab. Eng.* **2014**, *28C*, 134–142. DOI: 10.1016/j.ymben.2014.12.006.

(97) Thaxter, R. On a Myxobacteriaceae, a new order of Schizomycetes. *Botanical Gazette* **1892**, *17*, 389–406.

(98) Wenzel, S. C.; Müller, R. Myxobacteria--'microbial factories' for the production of bioactive secondary metabolites. *Molecular bioSystems* **2009**, *5* (6), 567–574. DOI: 10.1039/b901287g.

(99) Han, K.; Li, Z. F.; Peng, R.; Zhu, L. P.; Zhou, T.; Wang, L. G.; Li, S. G.; Zhang, X. B.; Hu, W.; Wu, Z. H.; Qin, N.; Li, Y. Z. Extraordinary expansion of a Sorangium cellulosum genome from an alkaline milieu. *Scientific Reports* **2013**, *3* (2101), 1–7. DOI: 10.1038/srep02101.

(100) Gerth, K.; Pradella, S.; Perlova, O.; Beyer, S.; Müller, R. Myxobacteria: proficient producers of novel natural products with various biological activities—past and future biotechnological aspects with the focus on the genus Sorangium. *Journal of biotechnology* **2003**, *106* (2-3), 233–253. DOI: 10.1016/j.jbiotec.2003.07.015.

(101) Hoffmann, T.; Müller, S.; Nadmid, S.; Garcia, R.; Müller, R. Microsclerodermins from terrestrial myxobacteria: An intriguing biosynthesis likely connected to a sponge symbiont. *J. Am. Chem. Soc.* **2013**, *45* (135), 16904–16911. DOI: 10.1021/ja4054509.

(102) Timmermans, M. L.; Paudel, Y. P.; Ross, A. C. Investigating the Biosynthesis of Natural Products from Marine Proteobacteria: A Survey of Molecules and Strategies. *Marine Drugs* **2017**, *15* (8), 235. DOI: 10.3390/md15080235.

(103) Munoz-Dorado, J.; Marcos-Torres, F. J.; Garcia-Bravo, E.; Moraleda-Munoz, A.; Perez, J. Myxobacteria: Moving, Killing, Feeding, and Surviving Together. *Frontiers in microbiology* **2016**, *7*, 781. DOI: 10.3389/fmicb.2016.00781.

(104) Shimkets, L. J.; Dworkin, M.; Reichenbach, H. The Myxobacteria. In *The Prokaryotes: Volume 7: Proteobacteria: Delta, Epsilon Subclass*; Dworkin, M., Falkow, S., Rosenberg, E.,

Schleifer, K.-H., Stackebrandt, E., Eds.; Springer New York, 2006; pp 31–115. DOI: 10.1007/0-387-30747-8_3.

(105) Gibiansky, M. L.; Hu, W.; Dahmen, K. A.; Shi, W.; Wong, G. C. L. Earthquake-like dynamics in Myxococcus xanthus social motility. *Proceedings of the National Academy of Sciences of the United States of America* **2013**, *110* (6), 2330–2335. DOI: 10.1073/pnas.1215089110.

(106) Herrmann, J.; Fayad, A. A.; Muller, R. Natural products from myxobacteria: novel metabolites and bioactivities. *Natural product reports* **2016.** DOI: 10.1039/C6NP00106H.

(107) Weissman, K. J.; Müller, R. A brief tour of myxobacterial secondary metabolism. *Bioorganic & medicinal chemistry* **2009**, *17* (6), 2121–2136. DOI: 10.1016/j.bmc.2008.11.025.

(108) Kling, A.; Lukat, P.; Almeida, D. V.; Bauer, A.; Fontaine, E.; Sordello, S.; Zaburannyi, N.; Herrmann, J.; Wenzel, S. C.; Konig, C.; Ammerman, N. C.; Barrio, M. B.; Borchers, K.; Bordon-Pallier, F.; Bronstrup, M.; Courtemanche, G.; Gerlitz, M.; Geslin, M.; Hammann, P.; Heinz, D. W.; Hoffmann, H.; Klieber, S.; Kohlmann, M.; Kurz, M.; Lair, C.; Matter, H.; Nuermberger, E.; Tyagi, S.; Fraisse, L.; Grosset, J. H.; Lagrange, S.; Muller, R. Targeting DnaN for tuberculosis therapy using novel griselimycins. *Science* **2015**, *348* (6239), 1106–1112. DOI: 10.1126/science.aaa4690.

(109) Irschik, H.; Augustiniak, H.; Gerth, K.; Höfle, G.; Reichenbach, H. The ripostatins, novel inhibitors of eubacterial RNA polymerase isolated from myxobacteria. *J. Antibiot.* **1995**, *48* (8), 787–792.

(110) Southern, E. Southern blotting. *Nat Protoc* **2006**, *1* (2), 518–525. DOI: 10.1038/nprot.2006.73.

(111) Irschik, H.; Gerth, K.; Kemmer, T.; Steinmetz, H.; Reichenbach, H. The Myxovalargins, new peptide antibiotics from Myxococcus fulvus (Myxobacterales) I. Cultivation, isolation, and some chemical and biological properties. *J. Antibiot.* **1983**, *36* (1), 6–12.

(112) Irschik, H.; Reichenbach, H. The mechanism of action of myxovalargin A, a peptide antibiotic from Myxococcus fulvus. *J. Antibiot.* **1985**, *38* (9), 1237–1245.

(113) Steinmetz, H.; Irschik, H.; Reichenbach, H.; Höfle, G. Structure elucidation of the peptide antibiotics myxovalargin A-D. In *Chemistry of Peptides and Proteins - Proceedings of the Sixth UssR-FRG Symposium on Chemistry of Peptides and Proteins (Hamburg, FRG, Sept 1-5, 1987)*; König, W.A., Voelter, W., Eds.; Attempto Verlag, 1987; pp 13–18.

(114) Schulz, R. Untersuchungen zur Biosynthese von Myxovalargin, einem Antibiotikum aus Myxococcus fulvus (Myxobacterales), Techn. Universität Carolo-Wilhelmina, Braunschweig, 1984.

(115) Herrmann, J.; Lukezic, T.; Kling, A.; Baumann, S.; Huttel, S.; Petkovic, H.; Muller, R. Strategies for the Discovery and Development of New Antibiotics from Natural Products: Three Case Studies. *Current topics in microbiology and immunology* **2016**, *398*, 339–363. DOI: 10.1007/82_2016_498.

(116) Musken, M.; Di Fiore, S.; Romling, U.; Haussler, S. A 96-well-plate-based optical method for the quantitative and qualitative evaluation of Pseudomonas aeruginosa biofilm formation and its application to susceptibility testing. *Nature protocols* **2010**, *5* (8), 1460–1469. DOI: 10.1038/nprot.2010.110.

(117) Musken, M.; Di Fiore, S.; Dotsch, A.; Fischer, R.; Haussler, S. Genetic determinants of Pseudomonas aeruginosa biofilm establishment. *Microbiology (Reading, England)* **2010**, *156* (Pt 2), 431–441. DOI: 10.1099/mic.0.033290-0.

(118) Pawar, V.; Crull, K.; Komor, U.; Kasnitz, N.; Frahm, M.; Kocijancic, D.; Westphal, K.; Leschner, S.; Wolf, K.; Loessner, H.; Rohde, M.; Haussler, S.; Weiss, S. Murine solid tumours as a novel model to study bacterial biofilm formation in vivo. *Journal of internal medicine* **2014**, *276* (2), 130–139. DOI: 10.1111/joim.12258.

(119) Pawar, V.; Komor, U.; Kasnitz, N.; Bielecki, P.; Pils, M. C.; Gocht, B.; Moter, A.; Rohde, M.; Weiss, S.; Haussler, S. In Vivo Efficacy of Antimicrobials against Biofilm-Producing Pseudomonas aeruginosa. *Antimicrobial agents and chemotherapy* **2015**, *59* (8), 4974–4981. DOI: 10.1128/AAC.00194-15.

(120) Garcia, R.; Müller, R. Family Myxococcaceae. In *The Prokaryotes*; Rosenberg, E., DeLong, E.F., Lory, S., Stackebrandt, E., Thompson, F., Eds.; Springer-Verlag, 2014; pp 191–212.

(121) Euzeby, J. List of new names and new combinations previously effectively, but not validly, published. *International journal of systematic and evolutionary microbiology* **2007**, *57* (Pt 5), 893–897. DOI: 10.1099/ijs.0.65207-0.

(122) Metzker, M. L. Sequencing technologies - the next generation. *Nature reviews. Genetics* **2010**, *11* (1), 31–46. DOI: 10.1038/nrg2626.

(123) English, A. C.; Richards, S.; Han, Y.; Wang, M.; Vee, V.; Qu, J.; Qin, X.; Muzny, D. M.; Reid, J. G.; Worley, K. C.; Gibbs, R. A. Mind the gap: upgrading genomes with Pacific Biosciences RS long-read sequencing technology. *PloS one* **2012**, *7* (11), e47768. DOI: 10.1371/journal.pone.0047768.

(124) Ambrosi, H. D.; Hartmann, V.; Pistorius, D.; Reissbrodt, R.; Trowitzsch-Kienast, W. Myxochelins B, C, D, E and F: A new structural principle for powerful siderophores imitating nature. *Eur. J. Org. Chem.* **1998**, 541–551.

(125) Duetz, W. A.; Rüedi, L.; Hermann, R.; O'Connor, K.; Büchs, J.; Witholt, B. Methods for Intense Aeration, Growth, Storage, and Replication of Bacterial Strains in Microtiter Plates. *Applied and environmental microbiology* **2000**, *66* (6), 2641–2646.

(126) Krug, D.; Müller, R. Discovery of additional members of the tyrosine aminomutase enzyme family and the mutational analysis of CmdF. *ChemBioChem* **2009**, *10* (4), 741–750. DOI: 10.1002/cbic.200800748.

(127) Cortina, N. S.; Krug, D.; Plaza, A.; Revermann, O.; Müller, R. Myxoprincomid: Entdeckung eines Naturstoffs mithilfe einer umfassenden Analyse des sekundären Metaboloms von Myxococcusxanthus. *Angew. Chem.* **2012**, *124* (3), 836–841. DOI: 10.1002/ange.201106305.

(128) Rottig, M.; Medema, M. H.; Blin, K.; Weber, T.; Rausch, C.; Kohlbacher, O. NRPSpredictor2--a web server for predicting NRPS adenylation domain specificity. *Nucleic acids research* **2011**, *39* (Web Server issue), W362-7. DOI: 10.1093/nar/gkr323.

(129) Schneider, A.; Marahiel, M. A. Genetic evidence for a role of thioesterase domains, integrated in or associated with peptide synthetases, in non-ribosomal peptide biosynthesis in Bacillus subtilis. *Arch. Microbiol.* **1998**, *169* (5), 404–410.

(130) Buntin, K.; Weissman, K. J.; Müller, R. An unusual thioesterase promotes isochromanone ring formation in ajudazol biosynthesis. *ChemBioChem* **2010**, *11* (8), 1137–1146.

(131) Quadri, L. E.; Sello, J.; Keating, T. A.; Weinreb, P. H.; Walsh, C. T. Identification of a Mycobacterium tuberculosis gene cluster encoding the biosynthetic enzymes for assembly of the virulence-conferring siderophore mycobactin. *Chem. Biol.* **1998**, *5* (11), 631–645.

(132) Boll, B.; Taubitz, T.; Heide, L. Role of MbtH-like proteins in the adenylation of tyrosine during aminocoumarin and vancomycin biosynthesis. *The Journal of biological chemistry* **2011**, *286* (42), 36281–36290. DOI: 10.1074/jbc.M111.288092.

(133) Wolpert, M.; Gust, B.; Kammerer, B.; Heide, L. Effects of deletions of mbtH-like genes on clorobiocin biosynthesis in Streptomyces coelicolor. *Microbiology* **2007**, *153* (5), 1413–1423. DOI: 10.1099/mic.0.2006/002998-0.

(134) Davidsen, J. M.; Bartley, D. M.; Townsend, C. A. Non-ribosomal propeptide precursor in nocardicin A biosynthesis predicted from adenylation domain specificity dependent on the MbtH family protein NocI. *Journal of the American Chemical Society* **2013**, *135* (5), 1749–1759. DOI: 10.1021/ja307710d.

(135) Kelley, L. A.; Mezulis, S.; Yates, C. M.; Wass, M. N.; Sternberg, Michael J E. The Phyre2 web portal for protein modeling, prediction and analysis. *Nature protocols* **2015**, *10* (6), 845–858. DOI: 10.1038/nprot.2015.053.

(136) Makris, T. M.; Knoot, C. J.; Wilmot, C. M.; Lipscomb, J. D. Structure of a dinuclear iron cluster-containing β-hydroxylase active in antibiotic biosynthesis. *Biochemistry* **2013**, *52* (38), 6662–6671. DOI: 10.1021/bi400845b.

(137) Ueoka, R.; Ise, Y.; Ohtsuka, S.; Okada, S.; Yamori, T.; Matsunaga, S. Yaku'amides A and B, cytotoxic linear peptides rich in dehydroamino acids from the marine sponge Ceratopsion sp. *Journal of the American Chemical Society* **2010**, *132* (50), 17692–17694. DOI: 10.1021/ja109275z.

(138) Kuranaga, T.; Sesoko, Y.; Sakata, K.; Maeda, N.; Hayata, A.; Inoue, M. Total synthesis and complete structural assignment of yaku'amide A. *Journal of the American Chemical Society* **2013**, *135* (14), 5467–5474. DOI: 10.1021/ja401457h.

(139) NOBUYOSHI SHIMADA, KAZUSHI MORIMOTO, HIROSHI NAGANAWA, TOMOHISA TAKITA, MASA HAMADA, KENJI MAEDA. ANTRIMYCIN, A NEW PEPTIDE ANTIBIOTIC. *The Journal of antibiotics* **1981**, *34* (12), 1613–1614.

(140) Hartkoorn, R. C.; Sala, C.; Neres, J.; Pojer, F.; Magnet, S.; Mukherjee, R.; Uplekar, S.; Boy-Röttger, S.; Altmann, K.-H.; Cole, S. T. Towards a new tuberculosis drug: pyridomycin - nature's isoniazid. *EMBO molecular medicine* **2012**, *4* (10), 1032–1042. DOI: 10.1002/emmm.201201689.

(141) Tesmar, A. von. *Investigation of bacterial secondary metabolite pathways*.

(142) Rachid, S.; Krug, D.; Kunze, B.; Kochems, I.; Scharfe, M.; Zabriskie, T. M.; Blöcker, H.; Müller, R. Molecular and biochemical studies of chondramide formation-highly cytotoxic natural products from Chondromyces crocatus Cm c5. *Chem. Biol.* **2006**, *13* (6), 667–681. DOI: 10.1016/j.chembiol.2006.06.002.

(143) Rachid, S.; Krug, D.; Weissman, K. J.; Müller, R. Biosynthesis of (R)-beta-tyrosine and its incorporation into the highly cytotoxic chondramides produced by Chondromyces crocatus. *J. Biol. Chem.* **2007**, *282* (30), 21810–21817.

(144) Wu, W. H.; Morris, D. R. Biosynthetic Arginine Decarboxylase from Escherichia coli:PURIFICATION AND PROPERTIES. *Journal of Biological Chemistry* **1973**, *248* (5), 1687–1695.

(145) Rosenfeld, H. J.; Roberts, J. Arginine decarboxylase from a Pseudomonas species. *Journal of bacteriology* **1976**, *125* (2), 601–607.

(146) Ishida, K.; Christiansen, G.; Yoshida, W. Y.; Kurmayer, R.; Welker, M.; Valls, N.; Bonjoch, J.; Hertweck, C.; Börner, T.; Hemscheidt, T.; Dittmann, E. Biosynthesis and structure of aeruginoside 126A and 126B, cyanobacterial peptide glycosides bearing a 2-carboxy-6-hydroxyoctahydroindole moiety. *Chemistry & biology* **2007**, *14* (5), 565–576. DOI: 10.1016/j.chembiol.2007.04.006.

(147) Ishida, K.; Welker, M.; Christiansen, G.; Cadel-Six, S.; Bouchier, C.; Dittmann, E.; Hertweck, C.; Tandeau de Marsac, Nicole. Plasticity and evolution of aeruginosin biosynthesis in cyanobacteria. *Applied and environmental microbiology* **2009**, *75* (7), 2017–2026. DOI: 10.1128/AEM.02258-08.

(148) Fujii, K.; Sivonen, K.; Adachi, K.; Noguchi, K.; Sano, H.; Hirayama, K.; Suzuki, M.; Harada, K.-i. Comparative study of toxic and non-toxic cyanobacterial products: Novel peptides from toxic Nodularia spumigena AV1. *Tetrahedron Letters* **1997**, *38* (31), 5525–5528. DOI: 10.1016/S0040-4039(97)01192-1.

(149) Bitonti, A. J.; Casara, P. J.; McCann, P. P.; Bey, P. Catalytic irreversible inhibition of bacterial and plant arginine decarboxylase activities by novel substrate and product analogues. *Biochemical Journal* **1987**, *242* (1), 69–74.

(150) Krug, D.; Scheid, U.; Barsch, A.; Yates, S.; Zurek, G.; Müller, R.; Beecher, C.; Jong, F. de. *Isotopic Ratio Outlier Analysis (IROA®) coupled with the Bruker maXis 4G QTOF to investigate changes in the secondary metabolite profiles of Myxobacteria*, 2013.

(151) Bode, H. B.; Ring, M. W.; Schwär, G.; Altmeyer, M. O.; Kegler, C.; Jose, I. R.; Singer, M.; Müller, R. Identification of additional players in the alternative biosynthesis pathway to isovaleryl-CoA in the myxobacterium Myxococcus xanthus. *ChemBioChem* **2009**, *10* (1), 128–140.

(152) Mahmud, T.; Wenzel, S. C.; Wan, E.; Wen, K. W.; Bode, H. B.; Gaitatzis, N.; Müller, R. A biosynthetic pathway to isovaleryl-CoA in myxobacteria: the involvement of the mevalonate pathway. *Chembiochem : a European journal of chemical biology* **2005**, *6* (2), 322–330. DOI: 10.1002/cbic.200400261.

(153) Li, Y.; Luxenburger, E.; Müller, R. An alternative isovaleryl CoA biosynthetic pathway involving a previously unknown 3-methylglutaconyl CoA decarboxylase. *Angewandte Chemie (International ed. in English)* **2013**, *52* (4), 1304–1308. DOI: 10.1002/anie.201207984.

(154) Bode, H. B.; Ring, M. W.; Schwär, G.; Kroppenstedt, R. M.; Kaiser, D.; Müller, R. 3-Hydroxy-3-methylglutaryl-coenzyme A (CoA) synthase is involved in the biosynthesis of isovaleryl-CoA in the myxobacterium Myxococcus xanthus during fruiting body formation. *J. Bacteriol.* **2006**, *188* (18), 6524–6528.

(155) Tobias Bock; Eva Luxenburger; Judith Hoffmann; Vlad Schütza; Christian Feiler; Rolf Müller; Wulf Blankenfeldt. AibA/AibB Induces an Intramolecular Decarboxylation in Isovalerate Biosynthesis by Myxococcus xanthus. *Angewandte Chemie International Edition* **2017**, *56* (33), 9986–9989. DOI: 10.1002/anie.201701992.

(156) Bode, H. B.; Meiser, P.; Klefisch, T.; Cortina, Niña Socorro d j; Krug, D.; Göhring, A.; Schwär, G.; Mahmud, T.; Elnakady, Y. A.; Müller, R. Mutasynthesis-derived myxalamids and origin of the isobutyryl-CoA starter unit of myxalamid B. *Chembiochem : a European journal of chemical biology* **2007**, *8* (17), 2139–2144. DOI: 10.1002/cbic.200700401.

(157) Bode, H. B.; Reimer, D.; Fuchs, S. W.; Kirchner, F.; Dauth, C.; Kegler, C.; Lorenzen, W.; Brachmann, A. O.; Grun, P. Determination of the absolute configuration of peptide natural products by using stable isotope labeling and mass spectrometry. *Chemistry (Weinheim an der Bergstrasse, Germany)* **2012**, *18* (8), 2342–2348. DOI: 10.1002/chem.201103479.

(158) Bretscher, A. P.; Kaiser, D. Nutrition of Myxococcus xanthus, a fruiting myxobacterium. *J. Bacteriol.* **1978**, *133* (2), 763–768.

(159) Magarvey, N. A.; Beck, Z. Q.; Golakoti, T.; ing, Y.; Huber, U.; Hemscheidt, T. K.; Abelson, D.; Moore, R. E.; Sherman, D. H. Biosynthetic characterization and chemoenzymatic assembly of the cryptophycins. Potent anticancer agents from Nostoc cyanobionts. *ACS Chem. Biol.* **2006**, *1*, 766–779.

(160) Christiansen, G.; Fastner, J.; Erhard, M.; Borner, T.; Dittmann, E. Microcystin Biosynthesis in Planktothrix: Genes, Evolution, and Manipulation. *Journal of bacteriology* **2003**, *185* (2), 564–572. DOI: 10.1128/JB.185.2.564–572.2003.

(161) Ishida, K.; Lincke, T.; Hertweck, C. Assembly and absolute configuration of short-lived polyketides from Burkholderia thailandensis. *Angew. Chem. Int. Ed. Engl.* **2012**, *51* (22), 5470–5474.

(162) Irschik, H.; Augustiniak, H.; Gerth, K.; Höfle, G.; Reichenbach, H. The ripostatins, novel inhibitors of eubacterial RNA polymerase isolated from myxobacteria. *J. Antibiot.* **1995**, *48* (8), 787–792.

(163) Augustiniak, H.; Irschik, H.; Reichenbach, H.; Hofle, G. Antibiotics from gliding bacteria .78. Ripostatin A, B, and C: Isolation and structure elucidation of novel metabolites from Sorangium cellulosum. *Liebigs Ann. Chem.* **1996** (10), 1657–1663.

(164) Trowitzsch-Kienast, W.; Forche, E.; Wray, V.; Reichenbach, H.; Jurkiewicz, E.; Hunsmann, G.; Höfle, G. Phenalamide, neue HIV-Inhibitoren aus Myxococcus stipitatus Mx s40. Antibiotika aus Gleitenden Bakterien, 45. *Liebigs Ann. Chem.* **1992**, *16*, 659–664.

(165) Okanya, P. W.; Mohr, K. I.; Gerth, K.; Kessler, W.; Jansen, R.; Stadler, M.; Müller, R. Hyafurones, hyapyrrolines, and hyapyrones: polyketides from Hyalangium minutum. *J. Nat. Prod.* **2014**, *77* (6), 1420–1429.

(166) Reed, L. J. Multienzyme Complexes. *Accounts of Chemical Research* **1974** (7), 40–46.

(167) Reed, L. J. Multienzyme Complexes. *Accounts of Chemical Research* **1974** (7), 40–46.

(168) G K Brown, L J Otero, M LeGris, R M Brown. Pyruvate dehydrogenase deficiency. *JMed Genet* **1994;** (31), 875–879.

(169) Fu, C.; Auerbach, D.; Li, Y.; Scheid, U.; Luxenburger, E.; Garcia, R.; Irschik, H.; Muller, R. Solving the Puzzle of One-Carbon Loss in Ripostatin Biosynthesis. *Angewandte Chemie (International ed. in English)* **2017**, *56* (8), 2192–2197. DOI: 10.1002/anie.201609950.

(170) Heath, C.; Jeffries, A. C.; Hough, D. W.; Danson, M. J. Discovery of the catalytic function of a putative 2-oxoacid dehydrogenase multienzyme complex in the thermophilic archaeon Thermoplasma acidophilum. *FEBS letters* **2004**, *577* (3), 523–527. DOI: 10.1016/j.febslet.2004.10.058.

(171) Heath, C.; Posner, M. G.; Aass, H. C.; Upadhyay, A.; Scott, D. J.; Hough, D. W.; Danson, M. J. The 2-oxoacid dehydrogenase multi-enzyme complex of the archaeon Thermoplasma acidophilum − recombinant expression, assembly and characterization. *FEBS Journal* **2007**, *274* (20), 5406–5415. DOI: 10.1111/j.1742-4658.2007.06067.x.

(172) Mitchison, D.; Davies, G. The chemotherapy of tuberculosis: past, present and future. *The international journal of tuberculosis and lung disease : the official journal of the International Union against Tuberculosis and Lung Disease* **2012**, *16* (6), 724–732. DOI: 10.5588/ijtld.12.0083.

(173) O'Neill, A.; Oliva, B.; Storey, C.; Hoyle, A.; Fishwick, C.; Chopra, I. RNA polymerase inhibitors with activity against rifampin-resistant mutants of Staphylococcus aureus. *Antimicrob. Agents Chemother.* **2000**, *44* (11), 3163–3166.

(174) Zumla, A.; Nahid, P.; Cole, S. T. Advances in the development of new tuberculosis drugs and treatment regimens. *Nat Rev Drug Discov* **2013**, *12* (5), 388–404.

(175) Fruth, M.; Plaza, A.; Hinsberger, S.; Sahner, J. H.; Haupenthal, J.; Bischoff, M.; Jansen, R.; Müller, R.; Hartmann, R. W. Binding mode characterization of novel RNA polymerase inhibitors using a combined biochemical and NMR approach. *ACS Chem. Biol.* **2014**, *9* (11), 2656–2663. DOI: 10.1021/cb5005433.

(176) Irschik, H.; Gerth, K.; Höfle, G.; Kohl, W.; Reichenbach, H. The myxopyronins, new inhibitors of bacterial RNA synthesis from Myxococcus fulvus (Myxobacterales). *J. Antibiot.* **1983**, *36* (12), 1651–1658.

(177) Irschik, H.; Jansen, R.; Höfle, G.; Gerth, K.; Reichenbach, H. The corallopyronins, new inhibitors of bacterial RNA synthesis from Myxobacteria. *J. Antibiot.* **1985**, *38* (2), 145–152.

(178) Sucipto, H.; Wenzel, S. C.; Müller, R. Exploring chemical diversity of a-pyrone antibiotics: molecular basis of myxopyronin biosynthesis. *ChemBioChem* **2013**, *14* (13), 1581–1589. DOI: 10.1002/cbic.201300289.

(179) Sahner, J. H.; Sucipto, H.; Wenzel, S. C.; Groh, M.; Hartmann, R. W.; Müller, R. Advanced mutasynthesis studies on the natural α-pyrone antibiotic myxopyronin from Myxococcus fulvus. *ChemBioChem* **2015**, *16*, 946–953. DOI: 10.1002/cbic.201402666.

(180) Sandmann, A.; Frank, B.; Müller, R. A transposon-based strategy to scale up myxothiazol production in myxobacterial cell factories. *Journal of biotechnology* **2008**, *135* (3), 255–261. DOI: 10.1016/j.jbiotec.2008.05.001.

(181) Helfrich, E. J. N.; Piel, J. Biosynthesis of polyketides by trans-AT polyketide synthases. *Natural product reports* **2016**, *33* (2), 231–316. DOI: 10.1039/c5np00125k.

(182) Buchholz, T. J.; Rath, C. M.; Lopanik, N. B.; Gardner, N. P.; Håkansson, K.; Sherman, D. H. Polyketide β-branching in bryostatin biosynthesis: identification of surrogate acetyl-ACP donors for BryR, an HMG-ACP synthase. *Chemistry & biology* **2010**, *17* (10), 1092–1100. DOI: 10.1016/j.chembiol.2010.08.008.

(183) Bumpus, S. B.; Magarvey, N. A.; Kelleher, N. L.; Walsh, C. T.; Calderone, C. T. Polyunsaturated fatty-acid-like trans-enoyl reductases utilized in polyketide biosynthesis. *Journal of the American Chemical Society* **2008**, *130* (35), 11614–11616. DOI: 10.1021/ja8040042.

(184) Mulwa, L. S.; Stadler, M. Antiviral Compounds from Myxobacteria. *Microorganisms* **2018**, *6* (3). DOI: 10.3390/microorganisms6030073.

(185) Park, S.; Hyun, H.; Lee, J. S.; Cho, K. Identification of the phenalamide biosynthetic gene cluster in Myxococcus stipitatus DSM 14675. *Journal of microbiology and biotechnology* **2016.** DOI: 10.4014/jmb.1603.03023.

(186) Kunze, B.; Reichenbach, H.; Müller, R.; Höfle, G. Aurafuron A and B, new bioactive polyketides from Stigmatella aurantiaca and Archangium gephyra (Myxobacteria). Fermentation, isolation, physico-chemical properties, structure and biological activity. *The Journal of antibiotics* **2005**, *58* (4), 244–251. DOI: 10.1038/ja.2005.28.

(187) Frank, B.; Wenzel, S. C.; Bode, H. B.; Scharfe, M.; Blöcker, H.; Müller, R. From genetic diversity to metabolic unity: studies on the biosynthesis of aurafurones and aurafuron-like structures in myxobacteria and streptomycetes. *J. Mol. Biol.* **2007**, *374* (1), 24–38.

(188) Organization, W. H. *Antimicrobial Resistance*:*Global Report on Surveillance*; World Health Organization, 2014.

(189) FDA. Guidance for Industry #209:The Judicious Use of Medically Important Antimicrobial Drugs in Food-Producing Animals, *2012*.

(190) European Medicines Agency. European expert group proposes reduction of use in animals of last resort antibiotic colistin to manage risk of resistance.

(191) CDC. tatfar-progress_report_2014.

(192) Liu, Y.-Y.; Wang, Y.; Walsh, T. R.; Yi, L.-X.; Zhang, R.; Spencer, J.; Doi, Y.; Tian, G.; Dong, B.; Huang, X.; Yu, L.-F.; Gu, D.; Ren, H.; Chen, X.; Lv, L.; He, D.; Zhou, H.; Liang, Z.; Liu, J.-H.; Shen, J. Emergence of plasmid-mediated colistin resistance mechanism MCR-1 in animals and human beings in China:A microbiological and molecular biological study. *The Lancet Infectious Diseases* **2016**, *16* (2), 161–168. DOI: 10.1016/S1473-3099(15)00424-7.

(193) Falgenhauer, L.; Waezsada, S.-E.; Yao, Y.; Imirzalioglu, C.; Käsbohrer, A.; Roesler, U.; Michael, G. B.; Schwarz, S.; Werner, G.; Kreienbrock, L.; Chakraborty, T. Colistin resistance gene mcr-1 in extended-spectrum β-lactamase-producing and carbapenemase-

producing Gram-negative bacteria in Germany. *The Lancet Infectious Diseases*, *16* (3), 282–283. DOI: 10.1016/S1473-3099(16)00009-8.

(194) McGann, P.; Snesrud, E.; Maybank, R.; Corey, B.; Ong, A. C.; Clifford, R.; Hinkle, M.; Whitman, T.; Lesho, E.; Schaecher, K. E. Escherichia coli Harboring mcr-1 and blaCTX-M on a Novel IncF Plasmid: First Report of mcr-1 in the United States. *Antimicrobial agents and chemotherapy* **2016**, *60* (7), 4420–4421. DOI: 10.1128/AAC.01103-16.

(195) Howden, B. P.; Davies, J. K.; Johnson, P. D. R.; Stinear, T. P.; Grayson, M. L. Reduced vancomycin susceptibility in Staphylococcus aureus, including vancomycin-intermediate and heterogeneous vancomycin-intermediate strains: resistance mechanisms, laboratory detection, and clinical implications. *Clinical microbiology reviews* **2010**, *23* (1), 99–139. DOI: 10.1128/CMR.00042-09.

(196) Clardy, J.; Fischbach, M. A.; Walsh, C. T. New antibiotics from bacterial natural products. *Nature biotechnology* **2006**, *24* (12), 1541–1550. DOI: 10.1038/nbt1266.

(197) Okano, A.; Isley, N. A.; Boger, D. L. Peripheral modifications of ΨCH2NHTpg(4)vancomycin with added synergistic mechanisms of action provide durable and potent antibiotics. *Proceedings of the National Academy of Sciences of the United States of America* **2017**, *114* (26), E5052-E5061. DOI: 10.1073/pnas.1704125114.

(198) Lesnik, U.; Lukezic, T.; Podgorsek, A.; Horvat, J.; Polak, T.; Sala, M.; Jenko, B.; Harmrolfs, K.; Ocampo-Sosa, A.; Martinez-Martinez, L.; Herron, P. R.; Fujs, S.; Kosec, G.; Hunter, I. S.; Muller, R.; Petkovic, H. Construction of a new class of tetracycline lead structures with potent antibacterial activity through biosynthetic engineering. *Angewandte Chemie (International ed. in English)* **2015**, *54* (13), 3937–3940. DOI: 10.1002/anie.201411028.

(199) Kling, A.; Lukat, P.; Almeida, D. V.; Bauer, A.; Fontaine, E.; Sordello, S.; Zaburannyi, N.; Herrmann, J.; Wenzel, S. C.; Konig, C.; Ammerman, N. C.; Barrio, M. B.; Borchers, K.; Bordon-Pallier, F.; Bronstrup, M.; Courtemanche, G.; Gerlitz, M.; Geslin, M.; Hammann, P.; Heinz, D. W.; Hoffmann, H.; Klieber, S.; Kohlmann, M.; Kurz, M.; Lair, C.; Matter, H.; Nuermberger, E.; Tyagi, S.; Fraisse, L.; Grosset, J. H.; Lagrange, S.; Muller, R. Targeting DnaN for tuberculosis therapy using novel griselimycins. *Science* **2015**, *348* (6239), 1106–1112. DOI: 10.1126/science.aaa4690.

(200) Newman, D. J.; Cragg, G. M. Natural products as sources of new drugs over the 30 years from 1981 to 2010. *Journal of natural products* **2012**, *75* (3), 311–335. DOI: 10.1021/np200906s.

(201) Moloney, M. G. Natural Products as a Source for Novel Antibiotics. *Trends in pharmacological sciences* **2016**, *37* (8), 689–701. DOI: 10.1016/j.tips.2016.05.001.

(202) LESHER, G. Y.; FROELICH, E. J.; GRUETT, M. D.; BAILEY, J. H.; BRUNDAGE, R. P. 1,8-NAPHTHYRIDINE DERIVATIVES. A NEW CLASS OF CHEMOTHERAPEUTIC AGENTS. *Journal of medicinal and pharmaceutical chemistry* **1962**, *91*, 1063–1065.

(203) Mutschler, E. *Mutschler Arzneimittelwirkungen*:*Pharmakologie - Klinische Pharmakologie - Toxikologie*, 10., vollst. überarb. und erw. Aufl.; Wiss. Verlagsges, 2012.

(204) Nelson, M. L.; Levy, S. B. The history of the tetracyclines. *Annals of the New York Academy of Sciences* **2011**, *1241*, 17–32. DOI: 10.1111/j.1749-6632.2011.06354.x.

(205) Rose, W. E.; Rybak, M. J. Tigecycline: first of a new class of antimicrobial agents. *Pharmacotherapy* **2006**, *26* (8), 1099–1110. DOI: 10.1592/phco.26.8.1099.

(206) Weissman, K. J. Mutasynthesis - uniting chemistry and genetics for drug discovery. *Trends Biotechnol.* **2007**, *25* (4), 139–142.

(207) Weist, S.; Süssmuth, R. D. Mutational biosynthesis-a tool for the generation of structural diversity in the biosynthesis of antibiotics. *Appl. Microbiol. Biotechnol.* **2005**, *68* (2), 141–150.

(208) Waterston, R. H.; Lindblad-Toh, K.; Birney, E.; Rogers, J.; Abril, J. F.; Agarwal, P.; Agarwala, R.; Ainscough, R.; Alexandersson, M.; An, P.; Antonarakis, S. E.; Attwood, J.; Baertsch, R.; Bailey, J.; Barlow, K.; Beck, S.; Berry, E.; Birren, B.; Bloom, T.; Bork, P.; Botcherby, M.; Bray, N.; Brent, M. R.; Brown, D. G.; Brown, S. D.; Bult, C.; Burton, J.; Butler, J.; Campbell, R. D.; Carninci, P.; Cawley, S.; Chiaromonte, F.; Chinwalla, A. T.; Church, D. M.; Clamp, M.; Clee, C.; Collins, F. S.; Cook, L. L.; Copley, R. R.; Coulson, A.; Couronne, O.; Cuff, J.; Curwen, V.; Cutts, T.; Daly, M.; David, R.; Davies, J.; Delehaunty, K. D.; Deri, J.; Dermitzakis, E. T.; Dewey, C.; Dickens, N. J.; Diekhans, M.; Dodge, S.; Dubchak, I.; Dunn, D. M.; Eddy, S. R.; Elnitski, L.; Emes, R. D.; Eswara, P.; Eyras, E.; Felsenfeld, A.; Fewell, G. A.; Flicek, P.; Foley, K.; Frankel, W. N.; Fulton, L. A.; Fulton, R.

S.; Furey, T. S.; Gage, D.; Gibbs, R. A.; Glusman, G.; Gnerre, S.; Goldman, N.; Goodstadt, L.; Grafham, D.; Graves, T. A.; Green, E. D.; Gregory, S.; Guigo, R.; Guyer, M.; Hardison, R. C.; Haussler, D.; Hayashizaki, Y.; Hillier, L. W.; Hinrichs, A.; Hlavina, W.; Holzer, T.; Hsu, F.; Hua, A.; Hubbard, T.; Hunt, A.; Jackson, I.; Jaffe, D. B.; Johnson, L. S.; Jones, M.; Jones, T. A.; Joy, A.; Kamal, M.; Karlsson, E. K.; Karolchik, D.; Kasprzyk, A.; Kawai, J.; Keibler, E.; Kells, C.; Kent, W. J.; Kirby, A.; Kolbe, D. L.; Korf, I.; Kucherlapati, R. S.; Kulbokas, E. J.; Kulp, D.; Landers, T.; Leger, J. P.; Leonard, S.; Letunic, I.; Levine, R.; Li, J.; Li, M.; Lloyd, C.; Lucas, S.; Ma, B.; Maglott, D. R.; Mardis, E. R.; Matthews, L.; Mauceli, E.; Mayer, J. H.; McCarthy, M.; McCombie, W. R.; McLaren, S.; McLay, K.; McPherson, J. D.; Meldrim, J.; Meredith, B.; Mesirov, J. P.; Miller, W.; Miner, T. L.; Mongin, E.; Montgomery, K. T.; Morgan, M.; Mott, R.; Mullikin, J. C.; Muzny, D. M.; Nash, W. E.; Nelson, J. O.; Nhan, M. N.; Nicol, R.; Ning, Z.; Nusbaum, C.; O'Connor, M. J.; Okazaki, Y.; Oliver, K.; Overton-Larty, E.; Pachter, L.; Parra, G.; Pepin, K. H.; Peterson, J.; Pevzner, P.; Plumb, R.; Pohl, C. S.; Poliakov, A.; Ponce, T. C.; Ponting, C. P.; Potter, S.; Quail, M.; Reymond, A.; Roe, B. A.; Roskin, K. M.; Rubin, E. M.; Rust, A. G.; Santos, R.; Sapojnikov, V.; Schultz, B.; Schultz, J.; Schwartz, M. S.; Schwartz, S.; Scott, C.; Seaman, S.; Searle, S.; Sharpe, T.; Sheridan, A.; Shownkeen, R.; Sims, S.; Singer, J. B.; Slater, G.; Smit, A.; Smith, D. R.; Spencer, B.; Stabenau, A.; Stange-Thomann, N.; Sugnet, C.; Suyama, M.; Tesler, G.; Thompson, J.; Torrents, D.; Trevaskis, E.; Tromp, J.; Ucla, C.; Ureta-Vidal, A.; Vinson, J. P.; Niederhausern, A. C. von; Wade, C. M.; Wall, M.; Weber, R. J.; Weiss, R. B.; Wendl, M. C.; West, A. P.; Wetterstrand, K.; Wheeler, R.; Whelan, S.; Wierzbowski, J.; Willey, D.; Williams, S.; Wilson, R. K.; Winter, E.; Worley, K. C.; Wyman, D.; Yang, S.; Yang, S.-P.; Zdobnov, E. M.; Zody, M. C.; Lander, E. S. Initial sequencing and comparative analysis of the mouse genome. *Nature* **2002**, *420* (6915), 520–562. DOI: 10.1038/nature01262.

(209) Hopwood, D. A. The Streptomyces genome--be prepared! *Nature biotechnology* **2003**, *21* (5), 505–506. DOI: 10.1038/nbt0503-505.

(210) Jensen, P. R. Natural Products and the Gene Cluster Revolution. *Trends in Microbiology* **2016**, *24* (12), 968–977. DOI: 10.1016/j.tim.2016.07.006.

(211) Bian, X.; Tang, B.; Yu, Y.; Tu, Q.; Gross, F.; Wang, H.; Li, A.; Fu, J.; Shen, Y.; Li, Y.-z.; Stewart, A. F.; Zhao, G.; Ding, X.; Müller, R.; Zhang, Y. Heterologous Production and Yield Improvement of Epothilones in Burkholderiales Strain DSM 7029. *ACS chemical biology* **2017.** DOI: 10.1021/acschembio.7b00097.

(212) Kirschning, A.; Hahn, F. Merging chemical synthesis and biosynthesis: A new chapter in the total synthesis of natural products and natural product libraries. *Angew. Chem. Int. Ed. Engl.* **2012**, *51* (17), 4012–4022.

(213) Sahner, J. H.; Sucipto, H.; Wenzel, S. C.; Groh, M.; Hartmann, R. W.; Müller, R. Advanced mutasynthesis studies on the natural α-pyrone antibiotic myxopyronin from Myxococcus fulvus. *ChemBioChem* **2015**, *16*, 946–953. DOI: 10.1002/cbic.201402666.

(214) Bilyk, B.; Luzhetskyy, A. Unusual site-specific DNA integration into the highly active pseudo-attB of the Streptomyces albus J1074 genome. *Applied microbiology and biotechnology* **2014**, *98* (11), 5095–5104. DOI: 10.1007/s00253-014-5605-y.

(215) Kersten, R. D.; Yang, Y.-L.; Xu, Y.; Cimermancic, P.; Nam, S.-J.; Fenical, W.; Fischbach, M. A.; Moore, B. S.; Dorrestein, P. C. A mass spectrometry-guided genome mining approach for natural product peptidogenomics. *Nature chemical biology* **2011**, *7* (11), 794–802. DOI: 10.1038/nchembio.684.

(216) Krug, D.; Müller, R. Secondary metabolomics: the impact of mass spectrometry-based approaches on the discovery and characterization of microbial natural products. *Nat. Prod. Rep.* **2014**, *31* (6), 768–783. DOI: 10.1039/c3np70127a.

(217) Fu, J.; Bian, X.; Hu, S.; Wang, H.; Huang, F.; Seibert, P. M.; Plaza, A.; Xia, L.; Müller, R.; Stewart, A. F.; Zhang, Y. Full-length RecE enhances linear-linear homologous recombination and facilitates direct cloning for bioprospecting. *Nature biotechnology* **2012**, *30* (5), 440–446. DOI: 10.1038/nbt.2183.

(218) Kjaerulff, L.; Raju, R.; Panter, F.; Scheid, U.; Garcia, R.; Herrmann, J.; Müller, R. Pyxipyrrolones: Structure Elucidation and Biosynthesis of Cytotoxic Myxobacterial Metabolites. *Angewandte Chemie (International ed. in English)* **2017.** DOI: 10.1002/anie.201704790.

(219) Charest, M. G.; Lerner, C. D.; Brubaker, J. D.; Siegel, D. R.; Myers, A. G. A convergent enantioselective route to structurally diverse 6-deoxytetracycline antibiotics. *Science (New York, N.Y.)* **2005**, *308* (5720), 395–398. DOI: 10.1126/science.1109755.

(220) Balog, A.; Meng, D.; Kamenecka, T.; Bertinato, P.; Su, D.-S.; Sorensen, E. J.; Danishefsky, S. J. Total Synthesis of(?:)-Epothilone A. *Angew. Chem. Int. Ed. Engl.* **1996**, *35* (2324), 2801–2803. DOI: 10.1002/anie.199628011.

(221) Gille, F. Studien zur Total- und Mutasynthese von Myxovalargin und synthetische Untersuchungen zu den Cystobactamiden.

(222) Bilyk, O.; Luzhetskyy, A. Metabolic engineering of natural product biosynthesis in actinobacteria. *Current opinion in biotechnology* **2016**, *42*, 98–107. DOI: 10.1016/j.copbio.2016.03.008.

(223) Saulnier, P.; Hanquier, J.; Jaoua, S.; Reichenbach, H.; Guespin-Michel, J. F. Utilization of IncP-1 plasmids as vectors for transposon mutagenesis in myxobacteria. *Journal of general microbiology* **1988**, *134* (11), 2889–2895. DOI: 10.1099/00221287-134-11-2889.

(224) Buntin, K.; Irschik, H.; Weissman, K. J.; Luxenburger, E.; Blöcker, H.; Müller, R. Biosynthesis of thuggacins in myxobacteria: comparative cluster analysis reveals basis for natural product structural diversity. *Chemistry & biology* **2010**, *17* (4), 342–356. DOI: 10.1016/j.chembiol.2010.02.013.

(225) Siegl, T.; Tokovenko, B.; Myronovskyi, M.; Luzhetskyy, A. Design, construction and characterisation of a synthetic promoter library for fine-tuned gene expression in actinomycetes. *Metabolic engineering* **2013**, *19*, 98–106. DOI: 10.1016/j.ymben.2013.07.006.

(226) Myronovskyi, M.; Luzhetskyy, A. Native and engineered promoters in natural product discovery. *Natural product reports* **2016**, *33* (8), 1006–1019. DOI: 10.1039/c6np00002a.

(227) Combes, P.; Till, R.; Bee, S.; Smith, M. C. M. The streptomyces genome contains multiple pseudo-attB sites for the (phi)C31-encoded site-specific recombination system. *Journal of bacteriology* **2002**, *184* (20), 5746–5752.

(228) Felnagle, E. A.; Barkei, J. J.; Park, H.; Podevels, A. M.; McMahon, M. D.; Drott, D. W.; Thomas, M. G. MbtH-like proteins as integral components of bacterial nonribosomal peptide synthetases. *Biochemistry* **2010**, *49* (41), 8815–8817. DOI: 10.1021/bi1012854.

(229) Tu, Q.; Herrmann, J.; Hu, S.; Raju, R.; Bian, X.; Zhang, Y.; Müller, R. Genetic engineering and heterologous expression of the disorazol biosynthetic gene cluster via Red/ET recombineering. *Scientific Reports* **2016**, *6*, 21066 EP -.

(230) Wang, H.; Li, Z.; Jia, R.; Hou, Y.; Yin, J.; Bian, X.; Li, A.; Müller, R.; Stewart, A. F.; Fu, J.; Zhang, Y. RecET direct cloning and Redαβ recombineering of biosynthetic gene clusters, large operons or single genes for heterologous expression. *Nature protocols* **2016**, *11* (7), 1175–1190. DOI: 10.1038/nprot.2016.054.

(231) Lynd, L. R.; Zhao, H.; Katz, L.; Baltz, R. H.; Bull, A. T.; Junker, B.; Masurekar, P.; Davies, J. E.; Reeves, C. D.; Demain, A. L., Eds. *Manual of Industrial Microbiology and Biotechnology, Third Edition*; American Society of Microbiology, 2010. DOI: 10.1128/9781555816827.

(232) Sulemankhil, I.; Ganopolsky, J. G.; Dieni, C. A.; Dan, A. F.; Jones, M. L.; Prakash, S. Prevention and treatment of virulent bacterial biofilms with an enzymatic nitric oxide-releasing dressing. *Antimicrobial agents and chemotherapy* **2012**, *56* (12), 6095–6103. DOI: 10.1128/AAC.01173-12.

(233) Schierholz, J. M.; Beuth, J. Implant infections: a haven for opportunistic bacteria. *The Journal of hospital infection* **2001**, *49* (2), 87–93. DOI: 10.1053/jhin.2001.1052.

(234) Costerton, J. W.; Montanaro, L.; Arciola, C. R. Biofilm in implant infections: its production and regulation. *The International journal of artificial organs* **2005**, *28* (11), 1062–1068.

(235) Arciola, C. R.; Campoccia, D.; Ehrlich, G. D.; Montanaro, L. Biofilm-based implant infections in orthopaedics. *Advances in experimental medicine and biology* **2015**, *830*, 29–46. DOI: 10.1007/978-3-319-11038-7_2.

(236) Pawlowski, K. S.; Wawro, D.; Roland, P. S. Bacterial biofilm formation on a human cochlear implant. *Otology & neurotology : official publication of the American Otological Society, American Neurotology Society [and] European Academy of Otology and Neurotology* **2005**, *26* (5), 972–975.

(237) Jansen, B.; Peters, G. Modern strategies in the prevention of polymer-associated infections. *Journal of Hospital Infection* **1991**, *19* (2), 83–88. DOI: 10.1016/0195-6701(91)90100-M.

(238) Bosman, W M P F; Borger van der Burg, B L S; Schuttevaer, H. M.; Thoma, S.; Hedeman Joosten, P. P. Infections of intravascular bare metal stents: a case report and review of literature. *European journal of vascular and endovascular surgery : the official journal of the European Society for Vascular Surgery* **2014**, *47* (1), 87–99. DOI: 10.1016/j.ejvs.2013.10.006.

(239) Le, M. Q.; Narins, C. R. Mycotic pseudoaneurysm of the left circumflex coronary artery: a fatal complication following drug-eluting stent implantation. *Catheterization and cardiovascular interventions : official journal of the Society for Cardiac Angiography & Interventions* **2007**, *69* (4), 508–512. DOI: 10.1002/ccd.21014.

(240) Marcu, C. B.; Balf, D. V.; Donohue, T. J. Post-infectious pseudoaneurysm after coronary angioplasty using drug eluting stents. *Heart, lung & circulation* **2005**, *14* (2), 85–86. DOI: 10.1016/j.hlc.2005.03.006.